Novel Bis (Pyrazol-3-yl) Ligands. Their Synthesis and Coordination Chemistry

Emyr D. Davies

A Thesis Submitted for the Degree of Doctor of Philosophy

at

Cardiff University

July 2007

UMI Number: U585072

UMI

Dissertation Publishing

UMI U585072

ProQuest

Acknowledgements

Many people have helped me to this point and it is thanks to them that I am able to offer this thesis for submission.

Thanks first to Kingsley and Mike, without whose guidance and input, this thesis would never have been completed.

I am also extremely grateful to so many of the staff a within the department. To Woody in particular for all his kind advice and even the occasional drink. I would also like all the technical support staff who have contributed both to my work and happy days.

A big shout out to all who served in Lab 2.84, especially the originals: Rhian, Stu, Huw, Dennis and Nick and also Emma J, Mandeep, Deborah, Miss Spain, Frenchie and my Maira, favourite Mexican, to name but a few.

For good teas and good times, the organic tea club cant be missed out with Ian, Jenny, Huw, Cazzy, Jo, Tony Chris, Simon and Stuart among many others providing ample entertainment throughout.

And a special mention to Jenn..... for her love and support x

Yn ola, i fy nheulu. I'n rhieni a'n frawd, am y cymorth a chefnogaeth, rwyn ddiolchgar iawn.

Abstract

This thesis describes studies into the development of new bis(pyrazol-3-yl) ligands including our studies into their coordination chemistry.

Chapter 1 is a brief introduction to chelating ligands based on heterocycles and outlines specifically looks at poly(pyrazole-1-yl) ligands as well as the few bis(pyrazole-3-yl) ligands publishes to date.

Chapter 2 looks at the traditional synthetic routes to bis(pyrazol-3-yl) ligands and describes how we have manipulated these techniques to synthesise some novel ligands of our own.

Chapter 3 includes a study of the transition metal coordination chemistry of our novel ligands. The coordination chemistry has proven to be diverse with the same ligand showing a capability to form monomers, dimers, polymers and form complexes as a neutral or anionic species.

Chapter 4 investigates the potential for our novel ligands to form ternary copper (II) complexes, incorporating some novel tripodal oxygen ligands instead of the traditional acetylacetone (acac) derivatves .

Chapter 5 describes the coordination chemistry of a ligand formed as a by product of those described in chapter 2. 2,3,6,7-tetramethyl-4,5-diazaocta-3,5-diene-2,7-bis-(pyrazol-3-yl) is a flexible pyrazole based ligand and here we desribe some transition metal complexes.

Table of Contents

Abbreviations

Ac	Aetyl
acac	Acetyl acetonate/2,4-Pentanedione
Ar	Aryl
Bipy	2,2'-Bipyridine
Bpyz	Bis pyrazole
COD	1,5-Cyclooctadiene
Cp	Cyclopentadiene
Cp*	1,2,3,4,5-pentamethylcyclopentadiene
DCM	Dicloromethane
DME	1,2-Dimethoxyethane
DMF.DMA	N,N-Dimethylformamide dimethyl acetal
EtOH	Dthanol
IR	Infa red
Me(acac)	3-Methyl-2,4-pentanedione
MeOH	Methanol
MeTAM	Methyl triacetyl methane
MS(ES)	Electrospray Mass Spectrometry
MMAO	Modified methylaluminoxane
NMR	Nuclear Magnetic Resonance
OTf	Trifluoromethyl sulfonate
phen	1,10-Phenanthroline
PMB	Paramethoxy benzyl
PTC	Phase transfer catalysis
pz	Pyrazole
TACN	1,4,7-Triazacyclononane
terpy	2,2':6',2"-Terpyridine
t-Bu	Tertiary butyl
THF	Tetrahydrofuran
TMEN	N,N,N',N'-Tetramethylethane-1,2-diamine
VT NMR	Variable temperature NMR
X	Halide

Chapter 1:

Introduction

Introduction

N-N'-Chelating Bi-Heteroaromatic Ligands

Since the first compound of this nature, 2,2- bipyridine **1**, was prepared by Blau in 1888 and published along with the first transition metal complex of its kind[1], many more compounds have been obtained with a library of ligands and coordination compounds now described[2]. Of all ligands of this kind, along with 2,2-bipyridine (Bipy), 1,10 –phenanthroline (phen) **2** and 2,2',6',2''-terpyridine (terpy) **3** are amongst the most well known, with many applications in analytical and coordination chemistry[3-5].
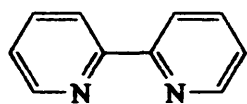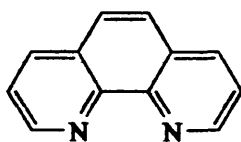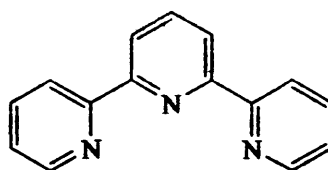
$$\qquad 1 \qquad\qquad\qquad 2 \qquad\qquad\qquad 3$$

The key feature of these pyridine based heterocyclic ligands is their π-electron deficiency. Hence, they behave as excellent π-acceptors[6]. Although substituents in the pyridine rings can significantly modify the physical and chemical properties, much greater changes can result from the replacement of one or both of the pyridine rings by other nitrogen containing heterocycles. Such changes are explained by the very different properties of the various aromatic ringed systems containing nitrogen[6]. In 1987, Reedijk provided a survey of the coordination chemistry of various kinds of nitrogen heterocyclic ligand systems[7].

One of the most common structures used in such substitutions is the pyrazole ring. The ease of synthesis of variously substituted pyrazoles is the most important feature in the incorporation of pyrazole groups in the design of new ligands. This offers the opportunity of both electronic and steric control of the properties of the metal complexes. Similar complexes containing 5 membered N-heterocycles have also been

extensively researched. In these cases, electron rich five–membered heterocycle, pyrazole, is a poorer π-acceptor[7].

Regardless of electronic properties, another factor governs how chelating ligands may be classed. On coordination to a metal centre, a chelating ligand forms a new ringed structure, often providing stability to the newly formed complex. In structurally simple chelating ligands, comprising of two or more heterocycles, the ring tends to be five or six membered. As displayed in figure 1.0, 5-membered rings tend to form when the ligands contain a direct link between two heterocycles [A], where as six membered structures form when the heterocycles are linked by a CH$_2$, CO, NH or S such as in dipyridylamine or pyrazolylmethanes [B]. The size of the ring formed is of course potentially massive with a number of ligands encompassing two heterocycles linked via a long flexible chain [C].
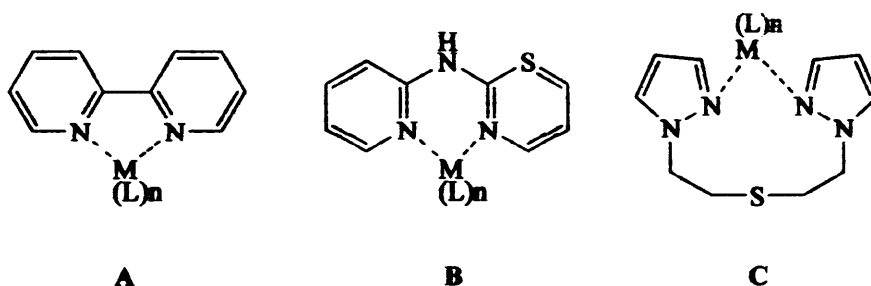
Figure 1.0: Variation in size of chelate rings

N-N'- Chelating Ligands Incorporating the Pyrazole Moiety

The synthesis of chelating ligands incorporating the pyrazole group has generated considerable interest within coordination chemistry, with over a hundred pyrazole based chelating ligands known. Single-crystal X-ray crystallography has revealed various bonding modes for any given ligand system when introduced to different metal centres. Figure 1.1 displays only a few of the simplest examples of chelating ligands containing the pyrazole moiety (4-9)[8-8iv].
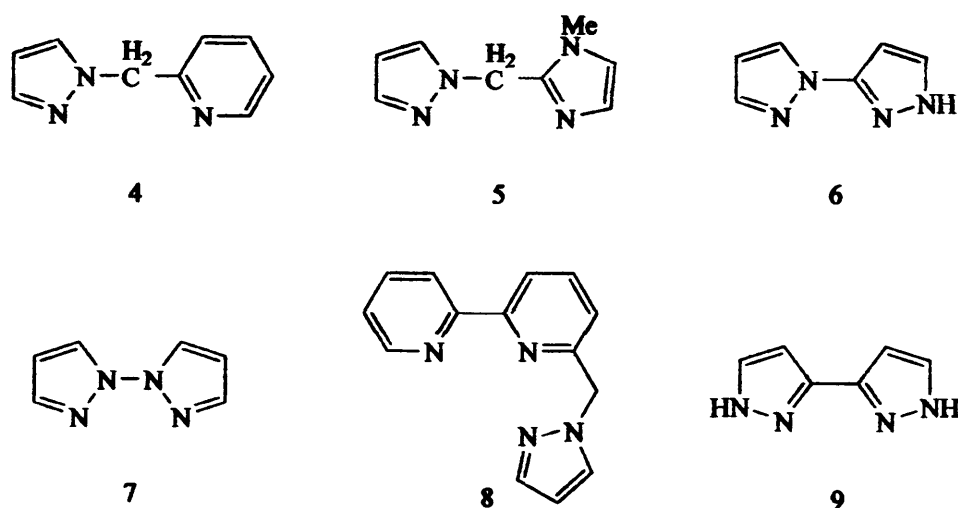
Figure 1.1: Chelating ligands incorporating the pyrazole ring

Of all the chelating ligands systems incorporating the pyrazole unit, among the most successful and researched are the poly (pyrazol-1-yl) borates.

Poly(pyrazol-1-yl) Borate Ligands

Poly (pyrazole-1-yl) borates consist of at least two pyrazole rings, bound via an (N-B-N) link and have the general structure as shown by [D] in figure 1.2.
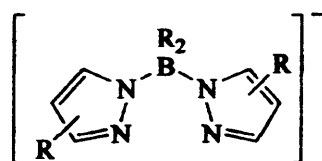
D

R = pz, Alkyl, H, Ar, CO₂H

Figure 1.2: General structure of a Poly(pyrazol-1-yl) Borate.

The process of linking two or more pyrazole rings via a short backbone was popularised by the synthesis of the first (pyrazol-1-yl) borate ligands. The work on this new class of compound was pioneered by Trofimenko in the mid 60's[9] and has gone on to become of huge interest with many applications in chemistry today[10-13].

Poly(pyrazol-1-yl) borates occur primarily in two main forms, illustrated in figure 1.3, with the 'poly' prefix usually a generalisation for the bis [E] and tris [F] substituted analogues. Tetrakis examples are known, but occur less frequently[14].

R = pz, H, Ar, Alkyl, Acid
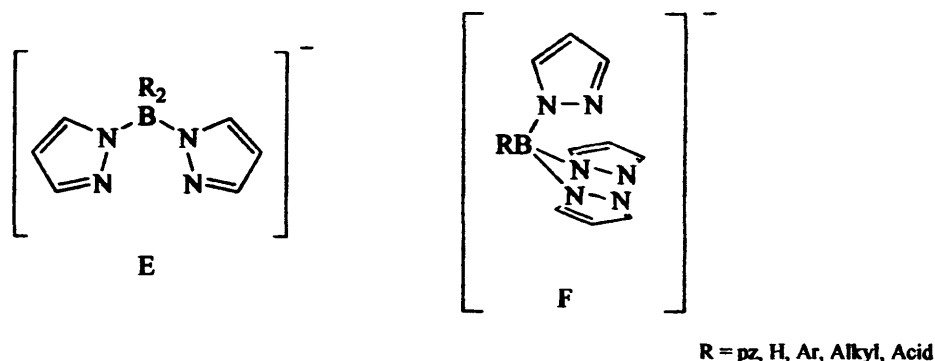
Figure 1.3: General structure for Bis and Tris Poly(pyrazolyl) borate ligands

More specifically, poly(pyrazol-1-yl) compounds are sometimes known as scorpionate ligands, with the bis (pyrazol-1-yl) borates known as heteroscorpionates, and the tris compounds known as homoscorpionates.

Nomenclature

Many reviews and articles published on the topic have their own nomenclature to enable the structures of poly(pyrazol-1-yl) compounds to be simplified, and here some simple rules have been adopted.

- A general pyrazoyl group with unspecified substituents is denoted pz^x.

- A general homoscorpionate ligand $HB(pz^x)_3$, with unspecified substituents is denoted as Tp^x.

- Heteroscorpionates are abbreviated as "Bp", with the non pyrazole substituents attached to the central boron atom denoted before the abbreviation. For instance, a bis (pyrazol-1-yl) borate with methyl groups attached to the boron and unspecified substituents on the (pyrazol-1-yl) rings will be denoted as Me_2Bp^x.

- With regards to the notation of specific substituted (pyrazol-1-yl) compounds, the general Bp or Tp prefix is followed, in superscript, by the group at the 3 position, followed by the 4 and 5 positions, with protons ignored. If any substituents are the same, a 2 or 3 follows the notation, again in superscript. According to this logic, the commonly used ligand hydrotris(3,5-dimethyl pyrazol-1-yl)borate 10 would be systematically abbreviated as Tp^{Me2}, however considering the long historical use of Tp*, introduced by Curtis[15], this tends to be overlooked.
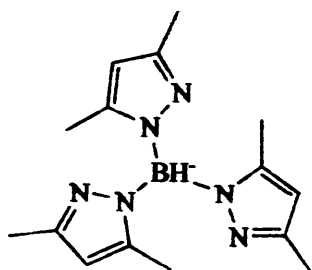
10

- The more complicated and highly substituted compounds of this type have extensive nomenclature of their own. We do not discuss these compounds here and so a discussion of nomenclature is not required.

Properties

Simple poly(pyrazole-1-yl) borates have two or three spectroscopically equivalent (pyrazol-1-yl) rings. The bis complexes resemble enolisable β-dicarbonyl compounds in being uninegative bidentates, while the tris(pyrazol-1-yl) compounds have been compared to Cp,Cp*[12]. These comparisons have been useful only in describing the poly(pyrazol-1-yl) borates in terms of known ligands.

Despite the existence of a large number of substituted pyrazoles[16], most work in the field deals with the unsubsituted pyrazole or the 3,5-dimethyl derivatives. Agrifoglio and co-workers discovered the properties of symmetrical compounds can change dramatically with the introduction of functionalised pyrazoles. This was identified by analysis of the pK_a values at the 2-pyrazole position with varying substitution[17].

Preparation

Many routes to pyrazol-1-yl borates exist. Trofimenko reported their synthesis via the reaction of a heated alkali metal borohydride with an excess of pyrazole[18]. The reaction can be stopped, through careful temperature control, to yield dihydrobis-, hydrotris- and tetrakis(pyrazol-1-yl) borates, a process displayed in **figure 1.4**. Trofimenko reported the dihydrobis compound **11**, was obtained after stirring a molten mixture of potassium borohydride and pyrazole at 90°C. This was kept below 125°C as tris substitution became appreciable above this point. The progress of the vigorous reaction was measured via the evolution of hydrogen in an upturned measuring cylinder, filled with water. The Tri substituted product, **12**, was obtained in much the same way, at an increased temperature of 190°C. Again, the progress of the reaction was monitored by the evolution of hydrogen gas. Trofimenko managed to obtain the tetrakis derivative **13** by stirring at 220-230°C over a much longer time scale. In this case, he reported an 85% yield after 24 hours. The resulting compounds tended to be water soluble and stable to storage.
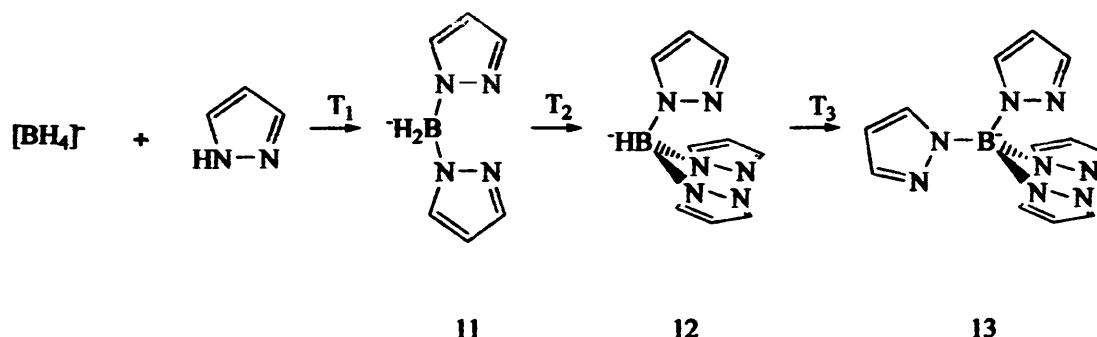
Figue 1.4: Synthesis of multidentate poly(pyrazole-1-yl) borates
via the melt method

Alternative and more specific synthesese have been developed with R_2Bp^x type liagands being prepared form trialkyl boranes, triarylboranes or tetraphenylborate ion. A typical reaction of an R_3B or Ar_3B species with pyrazole is preceded by the formation of an anionic species $[R_3Bpz^x]^-$, through the reaction of R_3B with a pyrazolate ion, $[pz^x]^-$. The R group in $[R_3B \ (pz^x)]^-$ can be replaced by a pz^x group upon the reaction with excess pyrazole.

$$R_3B + [pz^x]^- \longrightarrow [R_3B(pz^x)]^- \xrightarrow{Hpz^x} [R_2B(pz^x)_2]^- + RH$$

More specific reactions are also known in the formation of tris(pyrazol-1-yl) compounds. The boron substituted ligands RTp^x, where R is alkyl or aryl, are generally prepared from the reaction of RBX$_2$ or ArBX$_2$[17,19], (X = halogen or a leaving group such as tosylate) with the pyrazolate ion and excess pyrazole.

$$RBX_2 + 3[pz^x]^- \longrightarrow [RB(pz^x)_3]^- + 2X^+$$
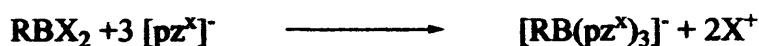
A different route employs organoborohydrides RBH$_2$ or LiRBH$_3$[20], obtained from the reaction of the corresponding boronic acids RB(OH)$_2$ with LiAH$_4$[21], in the reaction with pyrazolate ion and excess pyrazole[22].

$$RBH_2 + [pz^x]^- + 2Hpz^x \longrightarrow [RB(pz^x)_3]^- + 2H^+$$
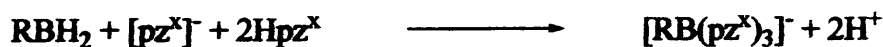
Alternatively, the [RB(pz^x)$_3$]$^-$ ligands may be prepared from the reaction of alkyl or aryl boronic acids[16,23] or RB(OH)$_2$ ester[24-25] with the pyrazolate ion and excess pyrazole.

$$RB(OH)_2 + 2Hpz^x + [pz^x]^- \longrightarrow [RB(pz^x)_3]^- + 2H_2O$$
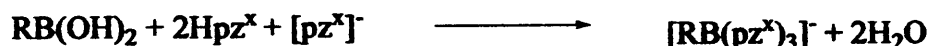
Asymmetric Poly(pyrazol-1-yl) Borates

The synthesis of the first asymmetric ligand 14^{26} opened up a massive potential for investigation. This incorporated two different pyrazole units into one chelating ligand, providing the potential for tuning ligands to specific requirements in the future.

14
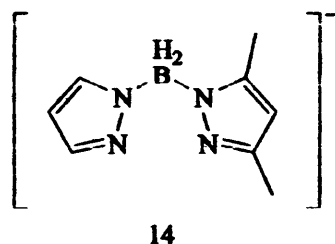
Although a landmark in ligand design, the synthesis of asymmetric poly(pyrazol-1-yl) borates required a new approach due to low yield and selectivity from the developed route. In 1992, Agrifoglio published yields in the region of 90% for compound **15** (i-iv)[17,27,28]. **Figure 1.5** displays the high yielding synthetic route. The convenient synthesis involved the reaction of 3,5-dimethylpyrazole with BH_3.THF complex to form the pyrazole borane. Reaction with iodine at $-30°C$ formed the reactive species and subsequent addition of the appropriate pyrazoles afforded the synthesis of compounds **15** (i-iv)

15
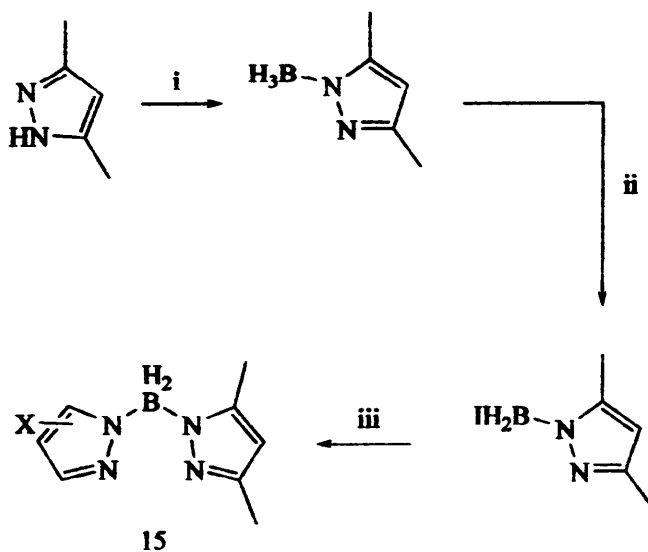
i = BH_3.THF, ii = Iodine, iii = Pyrazole

[15i - X= 3,5-Me], [15ii – X = H], [15iii - X = 3,5-Ph], [15iv – X = 4-Me]

Figure 1.5: Synthesis of the first asymmetric bis(pyrazole-1-yl)borate (15)

Poly(pyrazol-1-yl) Alkane Ligands

Also discovered by Trofimenko[29], poly(pyrazol-1-yl) alkanes represent a structurally similar, but electronically neutral analogue of the poly(pyrazol-1-yl) borates. In this case, the BR_2 bridging fragment has been replaced by a carbon based alternative. The general structure is shown in **figure 1.6**.

G   H
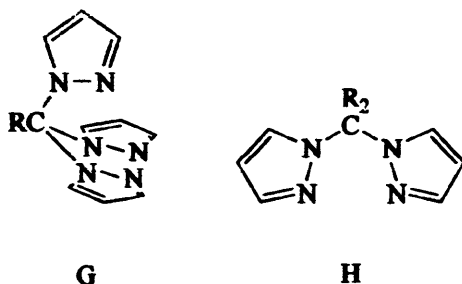
R = pz, H, Ar, Alkyl, Acid

Figure 1.6: General structure of Poly(pyrazol-1-yl) Alkanes.

Again, the synthesis of bi (H) and tris (G) substituted compounds is most common, and as for the pyrazole borates, the same potential for substitution of the pyrazole protons exists, of which structural and electronic diversity is a consequence.

Nomenclature

- Compounds of this nature are not abbreviated as their borate cousins. Here, the pyrazol-1-yl alkanes will be simply recorded with the carbon backbone fragment listed before the pyrazol-1-yl groups. The substitution on the pyrazol-1-yl fragment will be recorded as in the poly(pyrazol-1-yl) borates. According to these rules, Compound **16** will be recorded as $Me_2C(pz^{Me2})_2$, and further abbreviated to $CMe_2(pz^*)_2$. Compound **17** would be recorded as $MeC(pz^*)(pz^{iPr2})$.

16   17
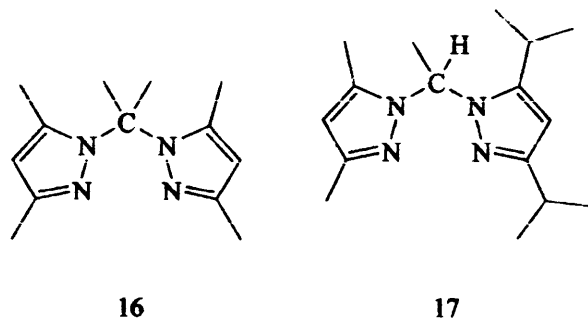
Preparation of bis(pyrazol-1-yl) alkanes

The first compound, published by Trofimenko[29], was the synthesis of $H_2C(pz)_2$, by the reaction of Hpz with CH_2Cl_2 in an autoclave at 150°C. Many other methods have been published[30-32], including the use of phase transfer catalysis in the reaction between azoles and dichloromethane[33]. This method, pioneered by Eluguero and co-workers improved, with regards to percentage yield in particular, on the method published by Trofimenko. Eluergo also described a convenient method for the synthesis of unsymmetrical bis(pyrazol-1-yl) alkanes[34] (figure 1.7). The unsubstituted Hpz is first converted to its 1-hydroxymethyl derivative via by reaction with formaldehyde. Treatment with thionyl chloride yields the 1-chloromethyl compound which is isolated as its hydrochloride salt. Under PTC (phase transfer catalysis) conditions, the 1-chloromethyl pyrazole reacts with equimolar quantities of a substituted pyrazole to selectively produce the asymmetric bis (pyrazol-1-yl) methane.

18
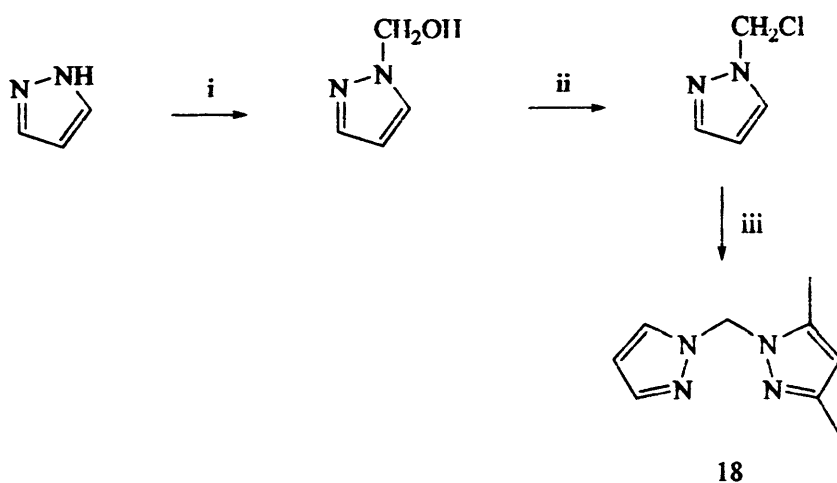
i = HCOH, ii = $SOCl_2$, iii = 3,5 dimethyl pyrazole PTC Conditions

Figure 1.7: Stoichiometric synthesis of Asymmetric Ligand (21) in 3 Steps

Preparation of Tris(pyrazol-1-yl)alkanes

The simplest member of this family, tris(pyrazol-1-yl)methane HC(pz)₃ was first prepared by the reaction of sodium pyrazolate with chloroform in benzene[35]. Although this was not the work of Trofimnko, he is universally regarded as the father of this branch of chemistry on account of his work in expanding the topic[12,36-38]. Elguero developed a general method to synthesise symmetrical compounds involving the liquid/liquid phase transfer method involving the heating of a mixture of the appropriate pyrazole, chloroform, potassium carbonate, and tetrabutylammonium hydrogen sulfate[31]. The synthesis of unsymmetrical HC(pz^x)₃ ligands has also been developed, and occur in the form of HC(pz)₂(pz') and HC(pz)(pz')(pz'') systems.

Coordination Compounds

The coordination chemistry of the poly(pyrazol-1-yl) compounds is an extremely large area with these ligands having the potential to form complexes with main group and transition metals. However, the coordinating behaviour is defined by the formation of the 6-membered ring $RR'B(pz^*)_2M$, (where M may contain additional ligands) and where R, R' can be a number of different groups including H, alkyl, aryl, NR_2 ArS or pz^* (pz^* = 1-(pyrazol-1-yl) or substituted 1-(pyrazol-1-yl)). Because of the bond angles and distances involved, the ring has almost always a boat structure of varying depth. In such a structure, generalised in **figure 1.8**, the pseudo axial group R is curled towards M and may bond to it, interact with it or just screen it.
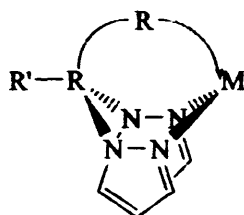
I

Figure 1.8: Coordination mode of a poly(pyrazol-1-yl) ligand

Trofimenko himself drew comparisons between this bonding model and nature, stating that the closest analogy encompassing these features was the scorpion.

"the creature grabs its prey with two identical claws (pz^*_2) and then may proceed to sting it with the sharp point of the curving tail (pseudoaxial R). Therefore I found it appropriate to coin the term scorpionate ligands".

Swiatoslaw Trofimenko

Scorpionates

Although obvious in the case of the tris (pyrazol-1-yl) borates and alkanes, the bis compounds do not immediately seem to have the 'sting in the tail' necessary to be classed as scorpionates. However, the R groups on the carbon/boron backbone can be manipulated to allow such an interaction.
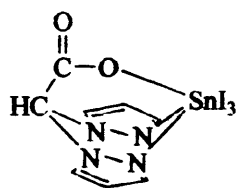
19

A well known class of scorpionate is represented by compound **19**. Bis pyrazole-1-yl acetates are closely related to both neutral tris (pyrazol-1-yl) methane and anionic poly(pyrazol-1-yl) borates with one of the pyrazol-1-yl groups being replaced by a carboxylate moiety. This change introduces a small degree of steric hindrance and considerable coordinative ligand flexibility. As shown by compound **19**, bis(pyrazol-1-yl)acetates can be easily deprotonated encouraging anionic behaviour as an N,N,O-tripodal donor, similar to the tris(pyrazol-1-yl)borates. Alternatively they may react in the neutral form like tris(pyrazol-1-yl)alkanes. Complexes containing the anionic ligand are well known in the literature[39-41], but the neutral complexes are far more rare, the first being synthesised by Pettinari and co-workers in 2005[42]. Bis(pyrazol-1-yl) compounds may also be regarded as scorpionates when the axial R group is a short alkyl fragment or even a proton. This is due to the potential, in the correct conditions, for a hydrogen bond to bridge to the metal centre, a so called agostic interaction[43].

The Agostic Interaction

An agostic interaction is known generally in coordination chemistry as an interaction between a C-*H* proton, and the metal centre. Bis (pyrazol-1-yl) borates and alkanes are sometimes classed as scorpionates due to the interaction between a proton located on the carbon atom bridging the pyrazole structures. This interaction may be between a proton bound directly to the bridge, or a proton as a component of a short alkyl fragment as demonstrated in **figure 1.9**.
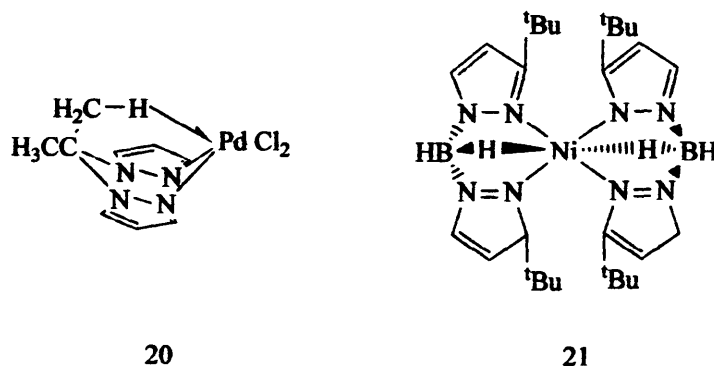
Figure 1.9: The Agostic Interaction

In compound **20**, the interaction is aided by the axial methyl orientation[44], while in compound **21**, the agostic interaction is attributed to the deep boat configuration adopted which minimises non bonding ᵗButyl interactions and brings the proton in question in close proximity to the nickel atom, allowing an interaction[45].

Although Trofimenko is known as a contributor above all others in the field of scorpionates, the coordination chemistry and its applications is an area in which he has not played a large role. He prefers to synthesise the ligands and allow others to explore the chemistry that can be done with them.

"I consider myself a gunsmith rather than a hunter."

Swiatoslaw Trofimenko

Poly(pyrazol-1-yl)borate/scorpionate chemistry is an area of chemistry still growing with complexes of more than seventy elements having been reported. The known ability to form complexes with a number of metal centres ranging from lithium to tin makes this class of ligand one of the most diverse ligand systems in chemistry.

Bonding Modes

The main reason for the diverse coordination chemistry known is the number of different bonding modes available. The agnostic interaction in bis(pyrazol-1-yl) compounds has already been discussed. Some of the most common modes of coordination are depicted in **figure 1.10** and include: tridentate (I), bidentate with a third donor group above the metal but uncoordinated (II). Metalation of the tris(pyrazole-1-yl) can occur with $Pt(II)^{46}$ and $Ir(III)^{47}$ complexes known (III). Alternatively, the third pyrazole may be directed away from the metal centre leaving the final group in the pseudoaxial position (IV). With reference to the unsymmetrical compounds e.g. the bis (pyrazol-1-yl) acetates, (V) is known. Complexes are known to exhibit a number of different coordination geometries and can be monomeric, dimeric, halogen bridged and polymeric.
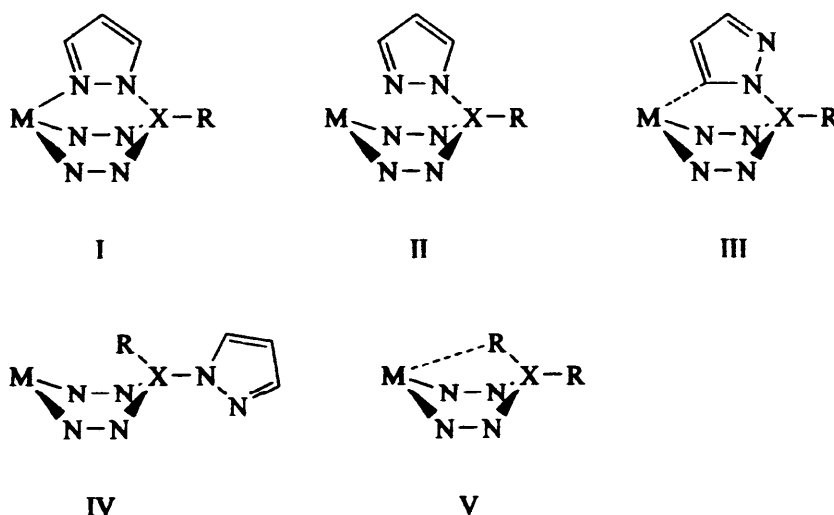
(Pyrazol-1-yl) rings have been omitted for clarity

Figure 1.10: Bonding Modes

Bis (Pyrazol-3-yl) Ligands

Although poly(pyrazol-1-yl) compounds are by far the largest class of ligands incorporating the pyrazole unit into a chelating centre, others are known. A small family of ligands has grown over the last 50 years with a close similarity to the bis (pyrazol-1-yl)alkanes. These compounds show a structural difference in that the point of attachment of the carbon bridge spanning the pyrazole rings lies at the 3 position, leaving the non chelating nitrogen atom free to play a coordinative role. The general structure of a bis(pyrazole-3-yl) compound in shown in **figure 1.11**.
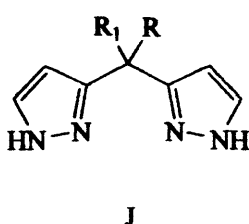
R = H, Me, CO, NOMe

Fig 1.11: General Structure of a Bis(pyrazol-3-yl) Ligand

Little is known about this particular class of compound. Few are known in the literature and their coordination chemistry is virtually non existent. The first bis(pyrazole-3-yl) ligand **22** was published in the late 50's[48]. Although fully characterised, it has not been exploited for coordination chemistry, or as far as we are aware for any other purpose, since its discovery.
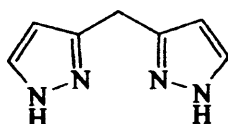
22

The reaction to synthesise **22** (**figure 1.12**) utilised the known chemistry, in which diazomethane reacts with acetylene in a concerted [3 + 2] cycloaddition. In this case, Reimlinger used a bis diazo methane resulting in a double cyclisation, recovering the desired product, **22** in a yield of 85%.
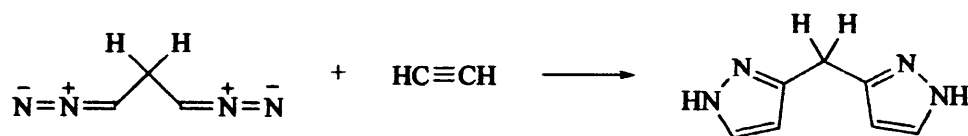
Figure 1.12: Cycloaddition Reaction to form Bis(pyrazol-3-yl) 22

Reimlinger went on to synthesise more compounds of this type, 23[8iv] and 24[48], with varying degrees of separation between the pyrazole rings. We are not aware of any coordination chemistry involving compound 24, however Jones and collaborators did acknowledge the fact that 23, 3,3'-bipyrazole (bpyz), had been largely overlooked. They reported the first complex to incorporate the ligand as [(bpyz)Ru(Phen)$_2$]$^{2+}$, which was isolated as the hexafluorophospate salt [49].

23   24
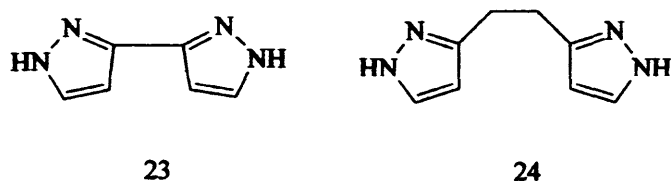
Functionalised bis(pyrazol-3-yl) compounds

Bis(pyrazole-3-yl) compounds were again in the spotlight during the late 1960's. This time however, the aim of the research was to create different properties within the bis pyrazol-3-yl system by functionalisation of the carbon bridge between the two pyrazole units. Two groups submitted different routes to the same compound[50,8iv], which substituted a carbonyl group at the position in question (25).

25
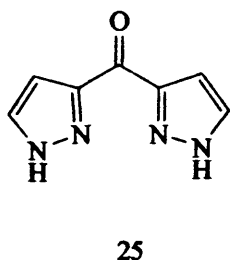
The method submitted by Manecke and Schenck utilised similar chemistry to that of Reimlinger in the synthesis of the unfunctionalised bis(pyrazol-3-yl) compound 22,

utilising a bis acetylene ketone in conjunction with diazomethane[50]. Reimlinger himself preferred the manipulation of compound **22** involving the reaction with chromium trioxide in concentrated acid[8iv].

Due to its requirement in the preparation of neuroprotective agents for the treatment of stroke, a new route to this ketone bridged bis pyrazole was published by Subramanyam[51]. The author was concerned over the use of the highly toxic reagent, diazomethane, in the synthesis published by others and hence set out to develop a route of his own. During his work on the regiospecific C-5 (C-3) functionalisation of N-1 protected pyrazoles he discovered the PMB (para-methoxybenzyl) protecting group was extremely effective. **Figure 1.13** displays the route taken to furnish the desired product in 50% yield.

i = n-BuLi. ii = MeONMeCOOEt. iii = TFA/Δ
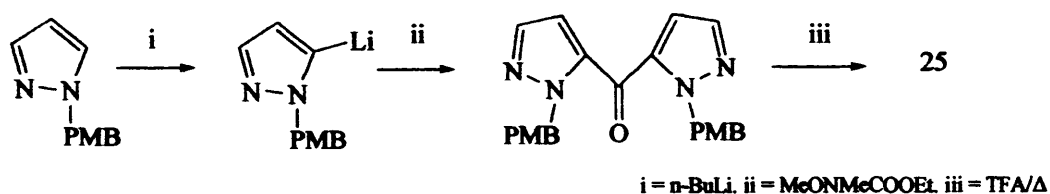
Figure 1.13: Synthesis of 25

In 1982, although the general synthetic method had been used many times in the synthesis of pyrazole rings in organic synthesis, Plescia and collaborators published a new synthetic route to bis(pyrazol-3-yl) compounds[52]. The conditions were mild and took place over two steps from a β-dicarbonyl starting material. The process, displayed in **figure 1.14**, involved the treatment of the β-dicarbonyl with dimethylformamide dimethylacetal (DMF.DMA). The enaminone product was treated with hydrazine hydrate, again under mild conditions to create the cyclisation step required to form the pyrazole rings.

i = DMF.DMA, ii = N₂H₄
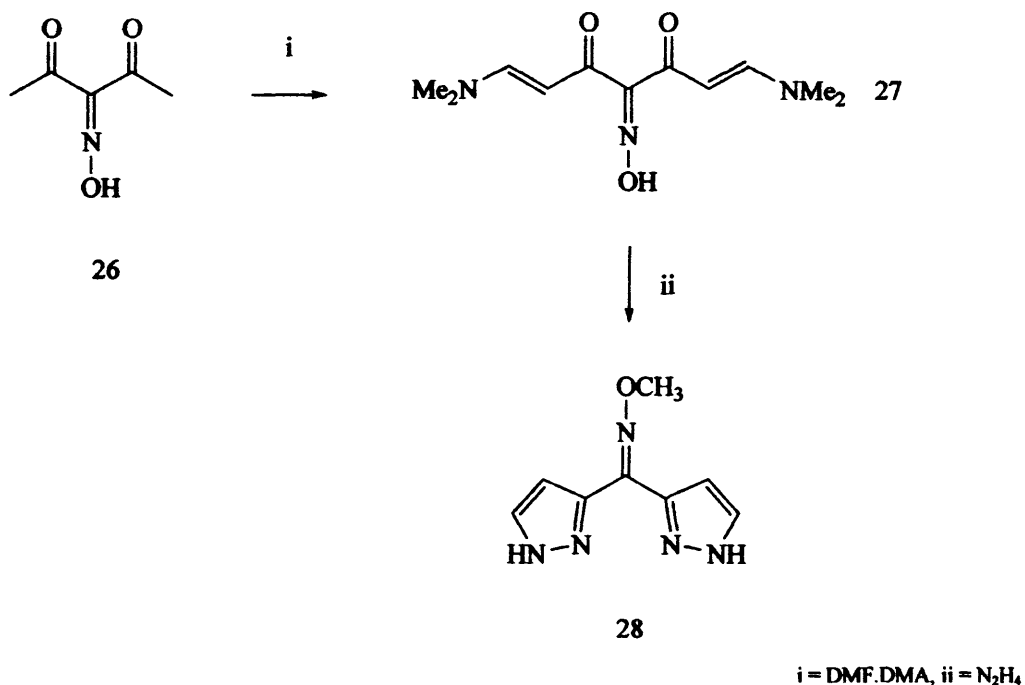
Figure 1.14: Synthesis of bis(pyrazole-3-yl) compound 32

Chiral Spiro Bis Pyrazolyl Ligands

More recently, bis(pyrazol-3-yl) ligands were reported by Sasai and collaborators in 2003[53]. This publication detailed the synthesis of the first chiral spiro bis pyrazole ligands **29** and **30** and the application of new bis pyrazole ligands to asymmetric catalysis.

29   30
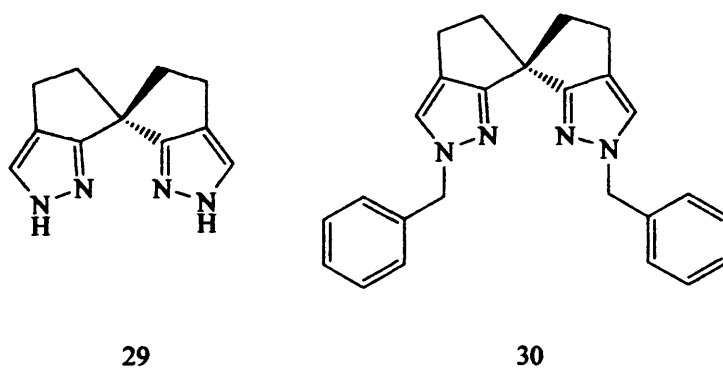
The authors, expanding on their work with bis isoxazolines, succeeded in developing new chiral ligands and reported copper (II) complexes which exhibited catalytic activity in the asymmetric ene reaction. However, isolation of the copper (II) species was not achieved, instead it was synthesised in situ via a 1:1 reaction with Cu(OTf)₂.

The stereochemistry of the ligands reported (29 and 30) displays the coordinating nitrogen atoms pointing in opposite directions, questioning the possibility of a monomeric metal complex of the ligand in a chelating fashion. No complexes have been fully characterised and so the nature of the catalytic species is not known. However, during the work mentioned on bis isoxazolines containing the same stereochemistry, complexes were obtained in which the ligand twisted in order to chelate to the metal centre, unexpectedly in a hexa-coordinated copper (II) complex 31[54].

i = Cu(OTF)₂
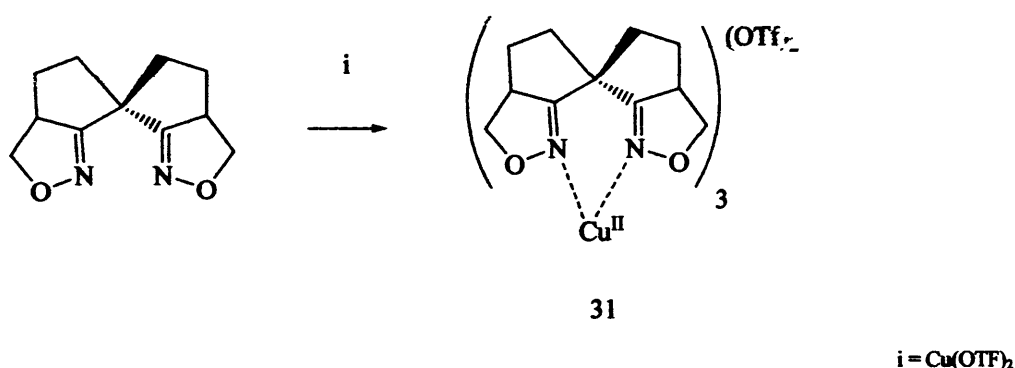
Figure 1.15: Synthesis of the hexa-coordinated copper (II) complex 31

The synthetic route to the new bis(pyrazole-3-yl) ligands was as the previous example, where a β-dicarbonyl was treated with DMF.DMA to produce an enaminone intermediate (figure 1.16). Cyclisation with hydrazine hydrarate produced compound 29. Reaction of the same intermediate with a functionalised hydrazine analogue allowed the synthesis of 30.

i = DMF.DMA, ii = N₂H₄, iii = H₂N-NH(CH₂Ph)
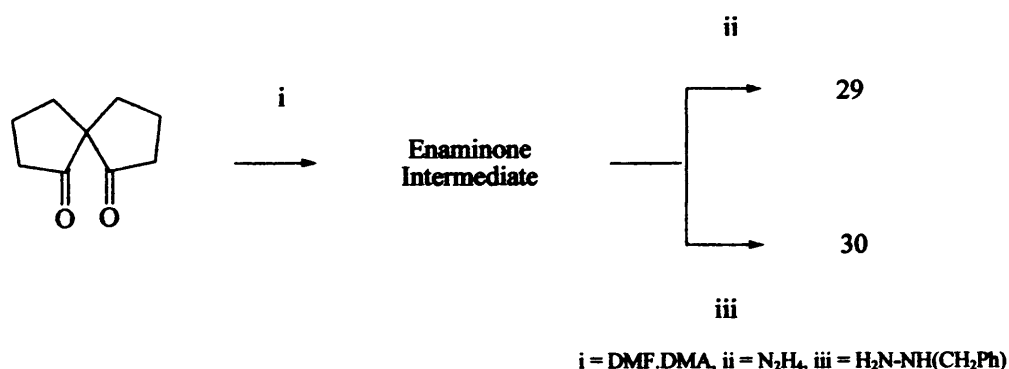
Figure 1.16: Synthesis of ligands 29 and 30

Project Outline

The success of the poly(pyrazol-1-yl) compounds as ligands is undisputable, and in bis(pyrazol-3-yl) compounds we see the potential to open up an equally interesting field of coordination chemistry. Although the ease of interchangability with regards to the steric and electronic properties is not immediately apparent, the range of different acac (acetyl acetone) and substituted hydrazine reagents which are commercially available is certainly a good starting point. In the following chapters we discuss our attempts to synthesise some new bis(pyrazol-3-yl) compounds, and their coordination chemistry.

References

[1]   F. Blau, *Rer. Dtsch.Chem. Ges.*, **27**,1888, 1077

[2]   E. C. Contstable, P. J. Steel, *Coord. Chem. Rev.*, **93**, 1989, 205

[3]   W. R. McWhinnie, J. D. Miller, *Adv. Inorg. Chem. Radiochem.*, **12**, 1969, 135

[4]   L. A. Summers, *Adv. Heterocycl. Chem.*, **35**, 1984, 281

[5]   E. C. Constable, *Adv. Inorg. Chem. Radiochem.*, **30**, 1986, 69

[6]   V. P. Manaev, O. P. Shkurko, S. G. Baram, *Adv. Heterocycl. Chem.*, **42**, 1987,
        1

[7]   J. Reedijk, *Comprehensive Coordination Chemistry. Vol. 2, Pergamon,
        Oxford.*, 1987, 73

[8]   P. K Byers, *Organometallics.*, **9**, 1990, 210

[8i]   J. Fifani, A. Ramdam, G. Tarrago, *New. J. Chem.*, **1**, 1977, 521

[8ii]   J. D. Perez, G. I. Yranzo, M. A. Ferraris, R. M. Claramunt, C. Lopez, J.
        Elguero, *Tetrahedron.*, **44**, 1988, 6429

[8iii] A. J. Downard, G. E. Honey, P. J. Steel., *Inorg. Chem.*, **30**, 1990, 3733

[8iv]   H. Reimlinger, J Vandewalle, A. Van Overstraten, *Ann. Chem.*, **720**, 1968, 124

[9]   S. Trofimenko, *J. Am. Chem. Soc.*, 1966, 1842

[10]   K. Niedenzu, S. Trofimenko, *Top. Curr. Chem.*, **131**, 1986, 1

[11]   S. Trofimenko, *Prog. Inorg. Chem.*, **34**, 1986, 115

[12]   S. Trofimenko, *Chem. Rev.*, **93**, 1993, 943

[13]   N. Kiatjima, W. B. Tolman, *Prog. Inorg. Chem.*, **43**, 1995, 419

[14]   H. Adams, S. R. Batten, G. M. Davies, M. B. Duriska, J. C. Jeffrey, P. Jensen,
        J. Lu, G. R. Moston, S. J. Coles, M. B. Hursthouse, M. D. Ward, *Dalton
        Trans.*, 2005, 1910

[15]   M. D. Curtis, K. B. Shiu, W. M. Butler, *J. Am. Chem. Soc.*, **108**, 1986, 1550

[16]   S. Trofimenko, *J. Am. Chem. Soc.*, **89**, 1967, 6288

[17]   G. Agrifoglio, *Inorg. Chim. Acta.*, **197**, 1992, 159

[18]   S. Trofimenko, *Inorg. Synth.*, **12**, 1970, 99

[19]   F. Jakle, K. Polborn, M. Wagner, *Chem. Ber.*, **129**, 1996, 603

[20]   R. Garcia, A. Paulo, A. Domingos, I. Santos, *J. Organometal. Chem.*, **632**,
        2001, 41

[21]   B. Singaram, T. E. Cole, C. H. Brown, *Organometallics.*, **3**, 1984, 774

[22]   J. L. Aubagnac, R. M. Claramunt, J. Elguero, I. Gilles, D. Sanz, S. Trofimenko, A. Virgili, *Bull. Chem. Soc. Belg.*, **104**, 1995, 473

[23]   D. L. Reger, M. E. Tarquini, *Inorg. Chem.*, **21**, 1982, 840

[24]   U. E. Bucher, T. F. Fassier, M. Hunzicker, R. Nesper, H. Riiegger, L. M. Venazi, *Gazz. Chim. Ital.*, **125**, 1995, 181

[25]   C. Kimblin. T. Hascall, G. Parkin, *Inorg. Chem.*, **36**, 1997, 5680

[26]   S. J. Chiou, P. Ge, C. G. Riordan, L. M. Liable-Sands, A. L. Reingold, *Chem Commun.*, 1999, 159

[27]   G. Agrifoglio, E. Frauendorfer, *Inorg. Chem.*, **21**, 1982, 4122

[28]   M. Caparelli, G Agrifoglio, *J. Crystallogr. Spectrosc. Res.*, **6**, 1992, 651

[29]   S. Trofimenko, *J. Am. Chem. Soc.*, **70**, 1970, 5118

[30]   R. M. Claramunt, H. Hernandez, J. Elguero, S. Julia, *Bull. Chem. Soc. Fr.*, 1983, 5

[31]   S. Julia, J. del Mazo, L. Avila, J. Elguero, *Org. Prep. Proced. Int.*, **16**, 1984 229

[32]   A. Katritzky, A. Abdel-Rahman, D. Leahy, O. Shwarz, *Tetrahedron.*, **24**, 1983, 4133

[33]   S. Julia, P. Sala, J. del Mazo, M. Sancho, C. Ochoa, J. Elguero, *J. Heterocyclic. Chem.*, **19**, 1982, 1141

[34]   S. Julia, C. Martinez-Martorell, J. Elguero, *Heterocycles.*, **24**, 1986, 2233

[35]   W. Hückel, H. Bretschneider, *Ber. Dtsch. Chem. Ges.*, **70**, 1937, 2024

[36]   S. Trofimenko, *J. Am. Chem. Soc.*, **89**, 1967, 3170

[37]   S. Trofimenko, *Acc. Chem. Res.*, **4**, 1971, 17

[38]   S. Trofimenko, *Chem. Rev.*, **72**, 1972, 497

[39]   A. Otero, J. Fernandez-Baeza, A. Antinolo, F. Carello-Hermosila, J. Tejeda, E. Diez-Barra, A. Lara-Sanchez, L. Sanshez-Barba, I. Lopez-Solera, *Organometallics.*, **20**, 2001, 2428

[40]   R. Mueller, E. Heubner, N. Burzlaff, *Eur. J. Inorg. Chem.*, 2004, 2151

[41]   A. Otero, J. Fernandez-Baeza, A. Antinolo, J. Tejeda, E. Diez-Barra, A. Lara-Sanchez, L. Sanshez-Barba, I. Lopez-Solera, *Inorg. Chem.*, **43**, 2004, 1350

[42]   F. Marchetti, M. Pellei, C. Pettinari, R. Pettinari, E. Rivarola, C. Santini, B. W. Skelton, A. H. White, *J. Organomet. Chem.*, **690**, 2005, 1878

[43]   M. Brookhart, M. L. H. Green, *J. Organomet Chem.*, **250**, 1983, 395

[44]   G. Minghetti, M. A. Cinellu, A. L. Bandini, G. Banditelli, F. DeMartin, M. Manaserro, *J. Organomet. Chem.*, **315**, 1986, 387

[45]   E. Carmona, E. Gutferrez-Puebla, A. Monge, C. Nicasio, M. Paneque, T. R. Belderrain, C. Ruiz-Valero, *Book of abstracts, 202nd national meeting of the American Chemical Society.* 1991

[46]   A. J. Canty, N. J. Minchin, J. M. Patrick, A. H. White, *Dalton Trans.*, 1983. 1253

[47]   D. Heinekey, W. Oldham, J. Wiley, *J. Am. Chem. Soc.*, **118**, 1996, 12842

[48]   H. Reimlinger, *Chem. Ber.*, **92**, 1959, 970

[49]   H. Jones, M. Newell, C. Metcalfe, S. E. Spey, H. Adams, J. A. Thomas, *Inorg. Chem. Comm.*, **4**, 2001, 475

[50]   G. Manecke, H. U. Schenck, *Tet. Lett.*, **8**, 1969, 617

[51]   C. Subramanyam, *Synth. Comm.*, **25**, 1995, 761

[52]   S. Plescia, G. Diadone, V. Spiro, *J. Heterocyclic. Chem.*, **19**, 1982, 1385

[53]   S. Takizawa, Y. Honda, M. A. Arai, T. Kato, H Sasai, *Heterocycles.*, **60**, 2003, 2551

[54]   M. A. Arai, T. Arai, H. Sasai, *Org. Lett.*, **11**, 1999, 1795

Chapter 2:

Novel Bis(pyrazol-3-yl) Ligands

Introduction

Synthesis of bis(pyrazol-3-yl) ligands

As described in Chapter 1, the modern and preferred method of synthesis of bis pyrazole compounds is the reaction of a bis ketone with DMF.DMA to form an enaminone intermediate, before reacting with hydrazine hydrate to form the desired product. DMF. acetals have been used in many other areas of heterocyclic syntheses, under many different conditions. They react with a number of different acidic protons in accordance with **figure 2.1** to form the enamine product. DMF.DMA has found the widest application amongst these compounds, playing a significant role in the synthesis of heterocycles[1-3].

$$R-CH_3 \quad + \quad + \quad \begin{array}{c} -O \\ \diagup \\ -O \end{array} N \diagdown \quad \longrightarrow \quad R \diagdown \diagup N \diagdown$$
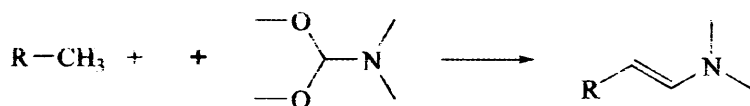
Figure 2.1: Condensation Reaction between Acidic Protons and DMF.DMA

The cyclisation reaction to form the heterocycle can follow many paths, and ultimately, the ring size, as well as nature, number and placement of the heteroatoms within the ring rely on this process. The main factors governing the outcome of the reaction are:

1. Presence of other functional groups within the compound.

2. The reagents used to induce cyclisation.

Synthesis of Heterocycles from Enamines

The following section describes the synthesis of well known heterocycles from enamines, produced through the reaction of the relevant starting materials with DMF.DMA. The elimination of dimethyl amine is the driving factor behind each cyclisation (**figure 2.2**).

i = Ring closing step
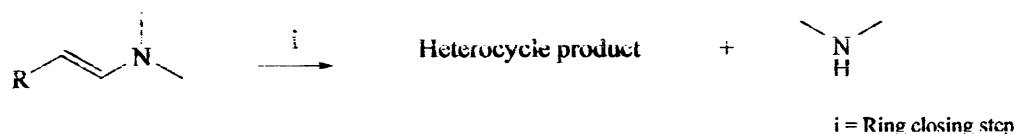
Figure 2.2: General synthesis of heterocycles from enaminones

Indoles - Bachto-Leimgruber Synthesis

The Bachto-Leimgruber synthesis (**figure 2.3**) involves the condensation of 0-nitrotoluene derivatives with formamide acetals followed by the reduction of trans-β-dimethylamino-2-nitrostyrene which results to furnish indole derivatives.
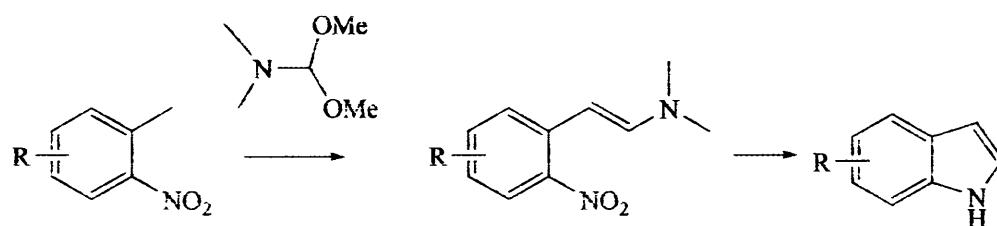
Figure 2.3: The Bachto-Leimgruber Indole Synthesis

The reductive cyclisation reaction occurs with the loss of a molecule of dimethyl amine, forming the 5-membered indole ring. Many methods have been employed for the reductive cyclisation of diakylamino-2-nitrostyrenes to the appropriate indoles. These methods include H_2/Pd on carbon, H_2/Ni, $Fe/AcOH$, $Na_2S_2O_4$, $FeSO_4/NH_4OH$ among others[4].

Isoxazoles

Isoxazoles have been synthesised in much the same way. In 1976 Y. Lin and S. Lang synthesised a bis oxazoline from para-diacetyl benzene[5]. The process involved the reaction of the bis-acetylene aromatic with DMF.DMA to form the familiar enaminone intermediate. The oxazoline 1 was formed through reaction with

hydroxylamine hydrochloride, initiating the loss of dimethylamine and subsequent cyclisation (**figure 2.4**).

i = DMF Acetal, ii = NH₂OH
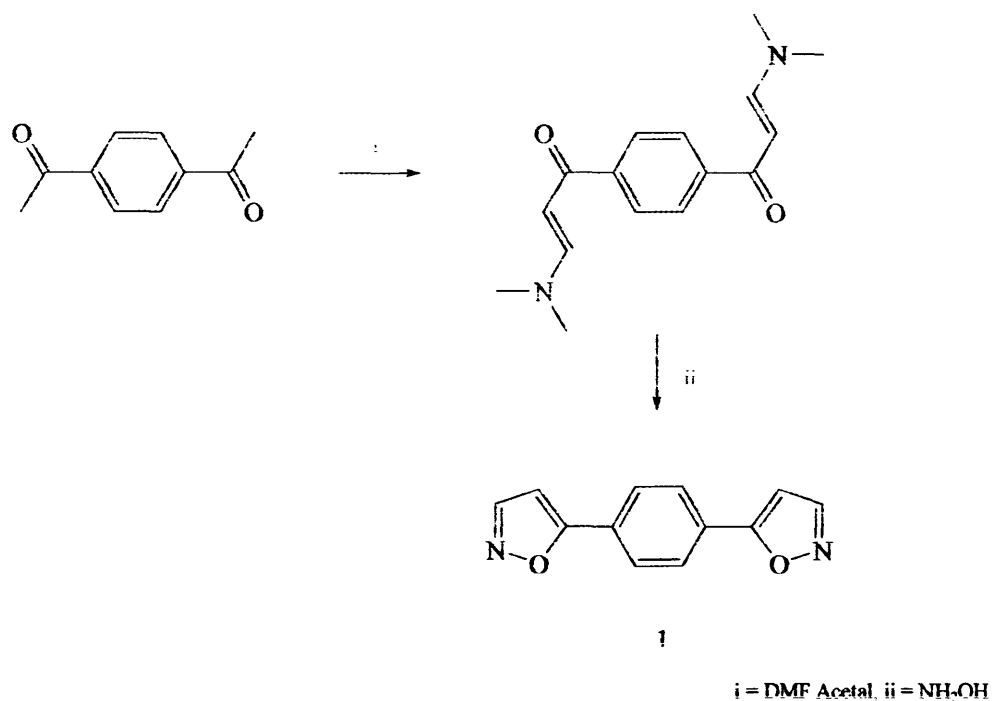
Figure 2.4: Isoxaole Synthesis

6-membered rings

Compounds of this type are also accessible from this chemistry with a range of mono and bis nitrogen substituted rings being synthesised by Keshk in 2003[6]. **Figure 2.5** shows how the utilisation of different starting materials can give a number of 6-membered ring systems from a simple starting point.
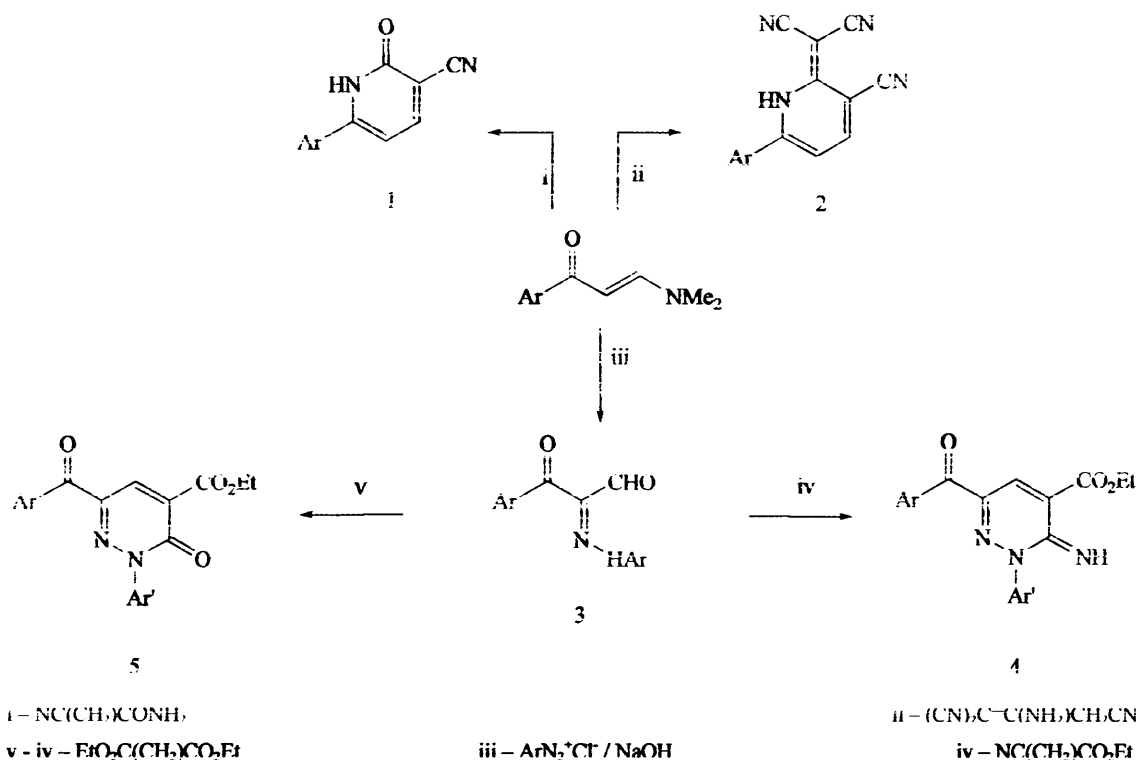
Figure 2.5: Synthesis of 6 membered Rings

Microwave Synthesis

The utility of microwaves in the ring closing step of heterocyclic synthesis has been subject to considerable attention[7-10]. Microwave technology has also been used in the formation of enaminones from carbonyl compounds (**figure 2.6**)[11]. Compound 6 was obtained in a higher yield (96%) than the route published by Elnagdi and co-workers, who reacted the same materials in the presence of a solvent, dioxane, under traditional reflux conditions (75%)[12]. In both cases, the crude product was recrystallised from ethanol.
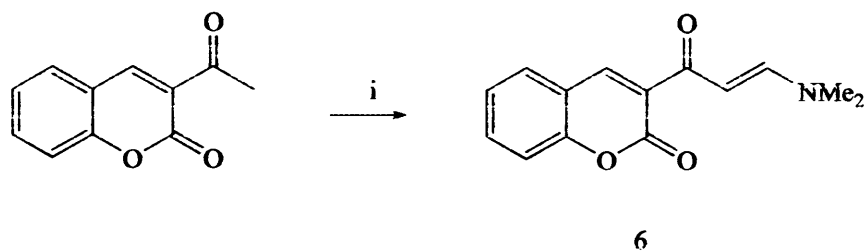
i = DMF.DMA, 5 Mins, M.W.

Figure 2.6: Synthesis of 6 via the microwave method

The enaminone product was reacted under microwave conditions with acetic acid and ammonium acetate to furnish a product of molecular formula $C_{22}H_{13}NO_4$ for which 8 is suggested. It is assumed that the pyrrole derivative 7 initially formed and subsequently underwent a Nenitzescu like cyclisation and decarbonylation, thus yielding 8 (figure 2.7).
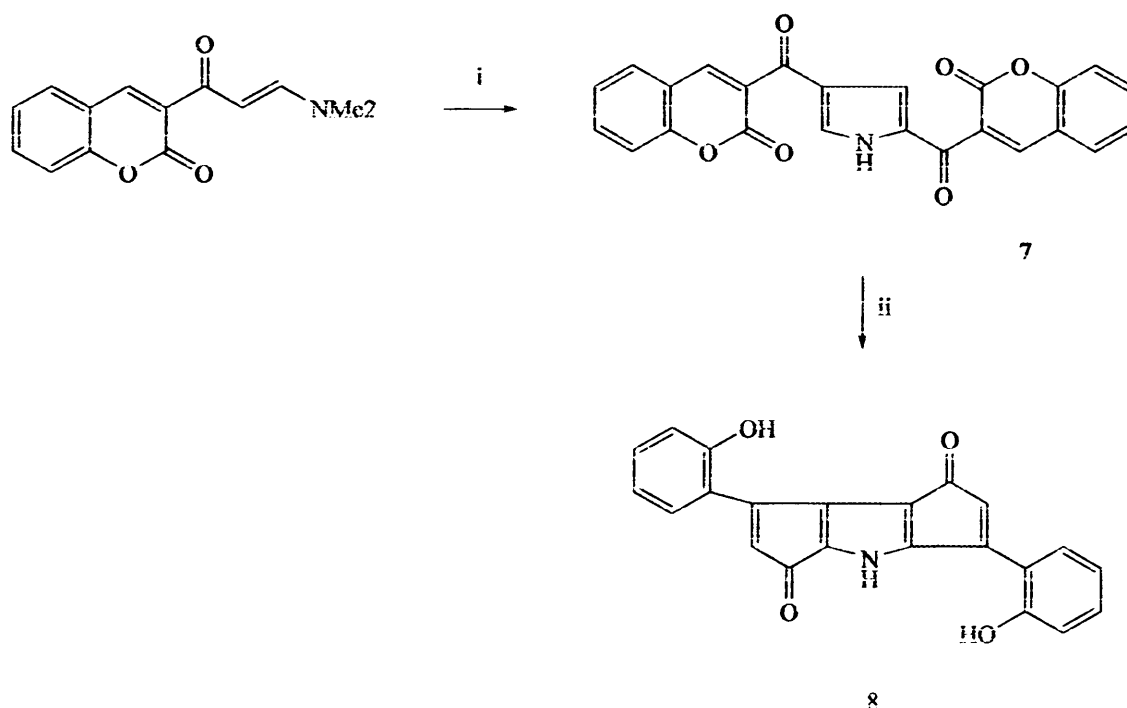
i = AcOH/AcONH₄/ M W/ 5 mins   ii = Cyclisation/Decarbonlation Step

Figure 2.7: Synthesis of (8) via the Microwave Method

Also under microwave conditions, flavones have been synthesised[13]. **Figure 2.8** shows the synthesis in which the formation of the enaminone and subsequent Michael addition of the phenolic compound 9 and dehydrogenation to furnish the flavone 10,

occurs in one step. The crude product is washed with ethanol and obtained in a yield of 71%.

i =DMF.DMA/ THF/ M.W 2 Mins
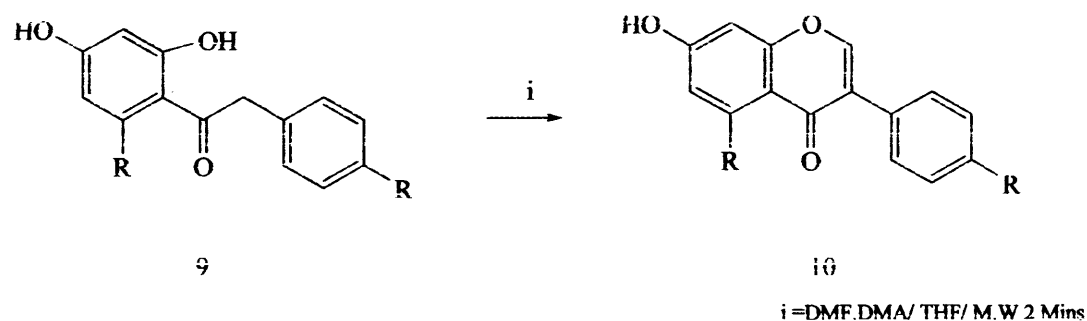
Figure 2.8: Synthesis of 10 via the Microwave Method

Chapter Outline

The following sections of this chapter describe the synthesis of three novel ligands, achieved through manipulation of the known routes described above. Carbonyl compounds in the form of substituted acac compounds were treated with DMF.DMA to form novel enaminone intermediates, and subsequently cyclised by the addition of hydrazine hydrate to form new N^N chelating compounds containing the pyrazole unit.

Synthesis and Discussion

We attempted the synthesis of novel bis enaminone compounds according to the general reaction figure set out by Plescia[14]. We took commercially available, substituted acac derivatives and treated them with DMF.DMA. The novel bis enaminone compounds obtained were subsequently characterised by NMR, IR, and MS. These compounds were treated with hydrazine hydrate and the resulting orange solids obtained on work up were found to be the desired products.

Attempt to Synthesise 26 (Chapter 1) via Modern Methods

Initially we explored the synthesis of the original member of this family of compounds via the modern method. To synthesise the carbon bridged bis pyrazole 26 (Chapter 1) reported by Reimlinger[15], via the modern method, acac must be reacted with DMF.DMA to produce a bis substituted intermediate (figure 2.9). Unfortunately, the reaction is not viable due to the acidity of the protons at the 3 position[16]. This behaviour has also been described in reactions with a number of Acac compounds with varying substitution at the 1 and 5 positions[17].

i = DMF.DMA
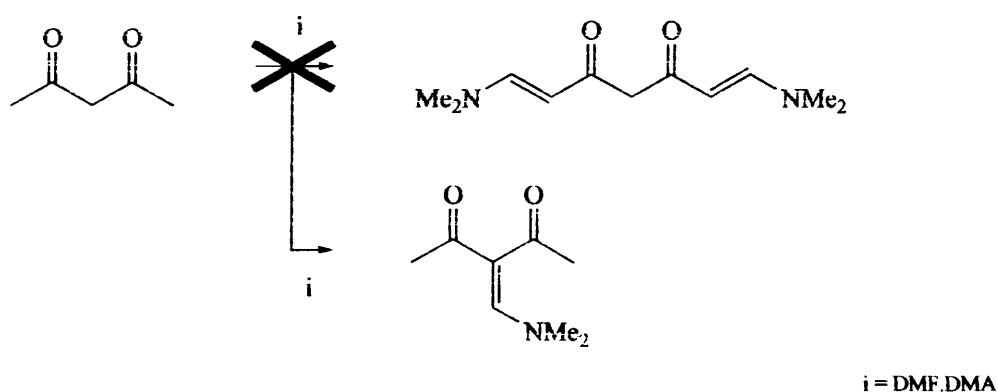
Figure 2.9: Attempted synthesis of bis(pyrazol-3-yl)methane

The reaction proceeds in this way due to the localisation of the negative charge between the two carbonyl centres at position 3. Consequently, the enamine reacts mainly at this point, allowing little opportunity for the synthesis of the bis pyrazole via cyclisation with hydrazine hydrate.

Synthesis of Novel Enaminones

The simple acac derivatives chosen to carry out this work were 3,3-dimethyl 2,4-pentanedione (11) and 3-methyl 2,4-pentanedione (12).
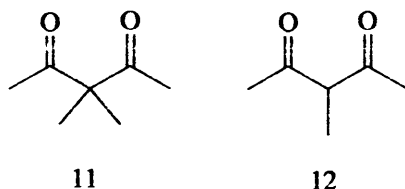
Compounds 11 and 12 were treated with an excess of neat DMF.DMA according to figure 2.10. Volatiles were removed from the brown viscous liquid obtained in both cases under reduced pressure. Unreacted starting material was removed from the crude product via repeated precipitation from diethyl ether and hexanes. The disubstituted enaminone compounds 2a and 2b were obtained.

i = DMF.DMA, 100°C

R= Me (2a), H (2b)
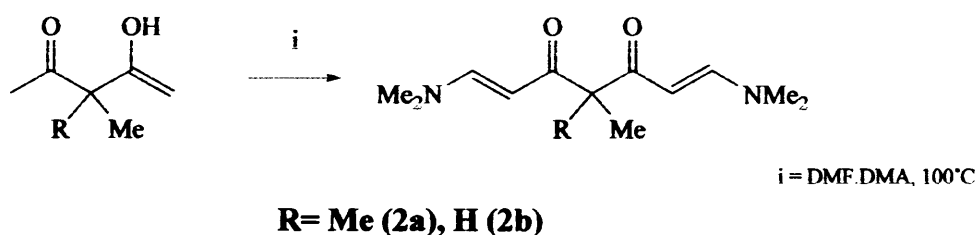
Figure 2.10: Enaminone Formation Reaction

Analysis of the brown solids obtained revealed the presence of by-products in both cases. NMR and MS(ES) data suggested the solids were a mixtre containing the desired product and the monosubstituted compounds 2c/2d

R = Me (2c), H (2d)
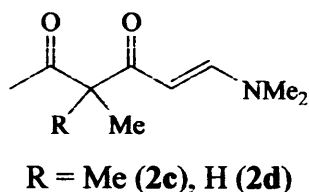
It was noticed that the solubility of the mono substituted analogues was greatly enhanced in hot hexanes verses that of the bis substituted enaminones. Consequently, pure samples of the desired bis enaminone products were obtained via repeated

washes with hot hexanes. **2c** was also isolated and like **2a** and **2b**, characterised by NMR, MS, and IR. Compound **2d** is yet to be isolated. Where as the solubilities of **2a** and **2c** in hot hexanes were clearly distinct, allowing the efficient recovery of both, the isolation of **2d** from a mixture via this method was achieved at a yield of 48%. Unlike **2a**, the bis enaminone **2b** was slightly soluble in hot hexanes. The mother liquor from the hot hexane wash yielded a mixed product.

^{1}H NMR

The three similar compounds, **2a**, **2b**, and **2c**, have the same functionality outside the diketone unit from the starting material. The enamine fragment formed is identical in the compounds and therefore comparisons can easily be made (**figure 2.11**). **Table 2.1** contains selected peaks positions from all three enaminones and the starting materials used in their synthesis respectively.
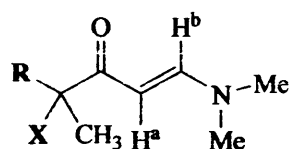
	2a	2b	2c
R			
X	Me	H	Me

Figure 2.11: Enaminone Derivatives

35

Table 2.1: Chemical shifts of starting material and product protons

(All measurements taken in $CDCl_3$)

Compound	H[a]	H[b]	CH_3	X
12 - acac			1.20	1.20
2a	7.51	5.00	1.25	1.25
2c	7.60	4.90	1.25	1.25
11 - acac			2.35	3.70
2b	7.40	4.95	1.20	3.35

From the data obtained on the products, we can determine that the reaction has not significantly affected the peaks at the position bridging the two carbonyl groups in relation to their respective positions in the starting materials. Further inspection of the spectra revealed the two N-nethyl fragments to be distinct in all cases, suggesting a delocalisation of the nitrogen lone pair across the molecule. This suggests the presence of an iminium ion, hence a C-N double bond possessing two different methyl groups. However on manipulation with VT-NMR, the peaks converge. The general trend is represented in **figure 2.12**, a VT ^{1}H NMR spectrum of **2a**.
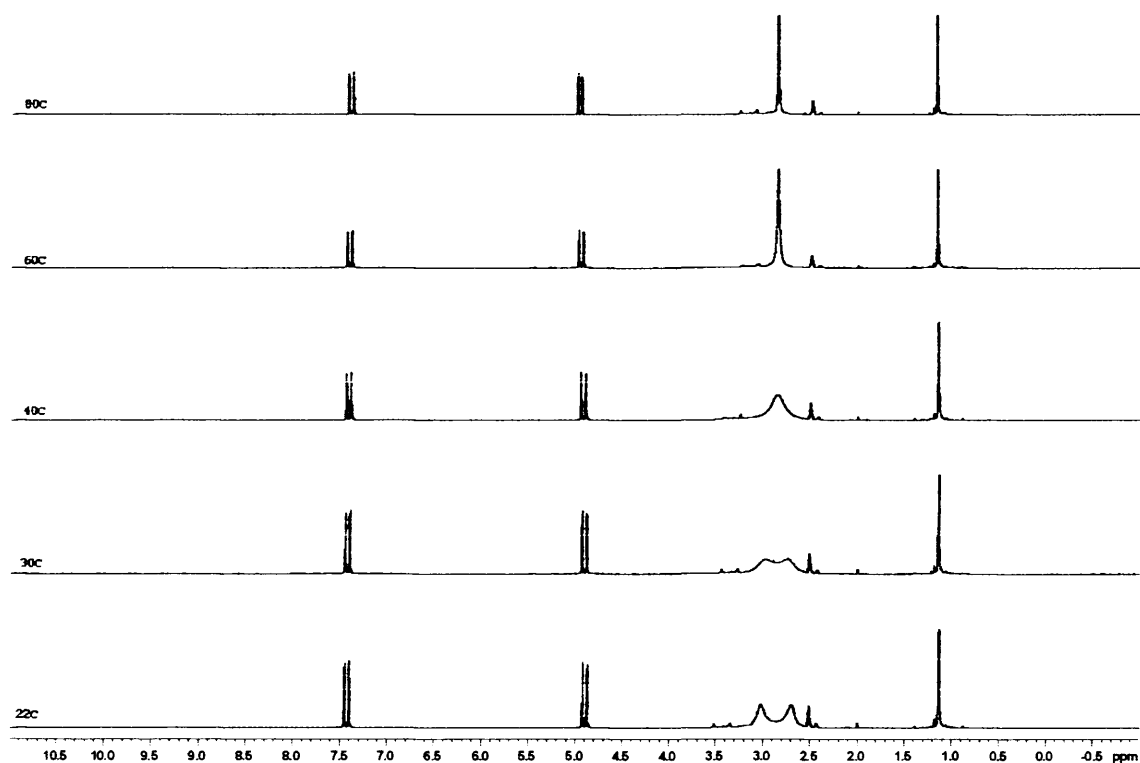
Fig 2.12: VT NMR of **2a**

The spectrum, performed in deuterated toluene and recorded on a 250MHz spectrometer, clearly shows the presence of two distinct and broad methyl peaks (3.05 and 2.70) at ambient temperature. The two peaks begin to merge at only a few degrees higher and a single sharp peak is achieved at 80°C. The $\Delta G^{\ddagger}$ value was measured by taking an average of the readings between 30°C and 40°C at an average of 67 KJ mol^{-1}, according to the equation below. The value given is typical of similar systems investigated by Clayden et al[18] in their work on barriers to rotation on tertiary amides:

$$\Delta G = 8.31 \ Tc[22.96 + \ln(Tc/\Delta V)]$$

Tc - Temperature at which coalescence into a broad peak occurs

ΔV - Difference in Hertz between the two peaks at the slow exchange limit (6.74 Hz)

On isolation of the two targets **2a** and **2b**, it was decided to progress with the next step and attempt to synthesise the desired bis pyrazole chelating ligands by the reaction with hydrazine hydrate.

2e   **2f**
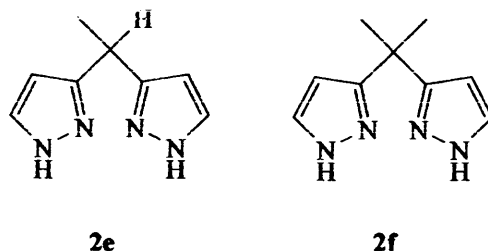
Synthesis of bis pyrazole ligands 2e and 2f

The transformations were attempted via the standard method mentioned previously. Early reactions in mild conditions (room temperature stir) yielded mixed results and so due to the lack of complexity in the molecule and need for a double cyclisation reaction to occur, the reactions were performed under slightly forcing conditions. A methanol solution of the appropriate enaminone was stirred under reflux with an excess of hydrazine hydrate. All volatiles were removed from the resulting orange liquid under reduced pressure and the resulting brown oil precipitated from ethyl

acetate and hexane. Further purification via precipitation from ethyl acetate and hexanes allowed us to obtain the desired products **2e** and **2f**.

^{1}H NMR

The structurally simple bis pyrazole compounds synthesised provided simple NMR spectra as expected. Each displayed two characteristic doublets between 6 and 7.5 ppm with coupling constants between 1.5 and 2.0 Hz, typical of these heteroaromatic systems. Due to the simplicity of the spectra, these features were the only ones distinctive to the products.

Reaction of 2c with Hydrazine Hydrate

The unexpected isolation of **2c** was the gateway to a novel ligand system. The molecule contained two possibilities for the formation of a pyrazole, **(figure 2.13)**, when reacted with hydrazine hydrate. Route A represents the product of a reaction similar to that of the synthesis of **2e** and **2f**. The hydrazine hydrate reacts and a cyclisation is performed with the elimination of diethyl amine. Route B represents the standard reaction of a 1,3- diketone with hydrazine hydrate.
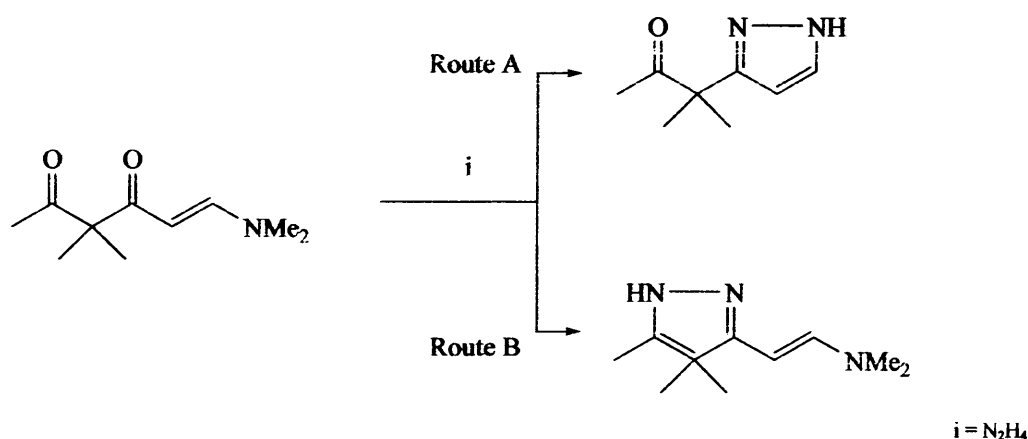
Figure 2.13: Possible products from the Reaction of 2c
with Hydrazine Hydrate

The reaction with a stoichiometric amount of hydrazine hydrate would almost certainly lead to a mixture of products. Instead, we decided to use an excess of

hydrazine hydrate and forcing conditions in an attempt to reach a conclusive result. A sample of **2c** dissolved in methanol was treated with an excess of hydrazine hydrate, and subjected to reflux conditions. The orange solution obtained was reduced in volume under vacuum and the brown oil precipitated from ethyl acetate and hexanes. This furnished a brown solid.

Analysis

The first piece of evidence obtained was an MS(ES). This provided us with excellent data in that a single peak was found at m/z 301. A clean ^{1}H NMR revealed a structural similarity to the bis pyrazole ligand **2c** with two doublets between 6 and 8 ppm with couplings of 2.08 and 2.07 Hz respectively, confirming the synthesis of a pyrazole ring. The presence of a singlet between 1 and 2 ppm in a 1:6 ratio with respect to the pyrazole protons was expected and represents the two methyl groups on the bridging carbon atom. The final peak in the spectrum, again a singlet between 1 and 2 ppm, has an integration half the size of that representing the two identical methyl protons on the pyrazolyl ring.

On the surface, it seems that the reaction according to Route A has occurred, and to a degree, this is correct. However, the position of the ^{1}H NMR signal representing a potential COCH_3 fragment is too low and with no carbonyl peak in the IR spectrum, this outcome was ruled out. If we accept that the cyclisation step has occurred, the molecular ion of mass 301 and ^{1}H NMR spectrum with only a few features suggests a symmetrical compound. The MS(ES) data supported the synthesis of compound **2g** via a double dehydration reaction between two molecules of the product of Route A. The double cyclisation was possible due to the excess of hydrazine present in the reaction mixture (**figure 2.14**).

2g

i = N$_2$H$_4$
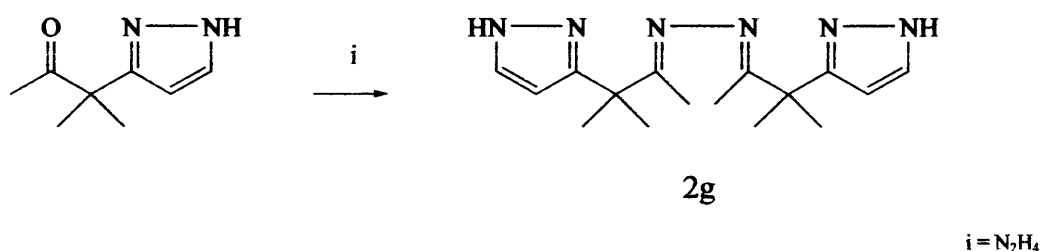
Figure 2.14: Synthesis of **2g**

Compound **2g** is, to our knowledge, unknown in the literature and, with no references to similar compounds found, a new class of ligand. It has the potential to chelate two metal centres and form metal complexes across the periodic table as has been described in chapter 5.

Attempted synthesis of Functionalised Bis Pyrazoles

As earlier mentioned, the synthesis of bis pyrazoles containing functionalised pyrazole rings is possible through two main routes.

1. Initial use of a substituted acac.

2. Use of a functionalised hydrazine derivative in the ring closing step.

Due to the isolation of the enaminone intermediate **2b**, it was decided to react this with phenyl hydrazine in similar conditions to previous reactions (**figure 2.15**).

i = N₂H₃(Ph)
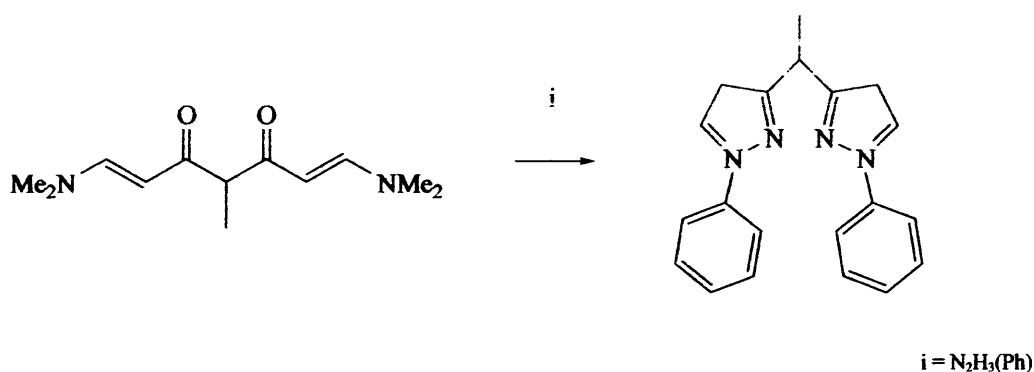
Figure 2.15: Possible route to functionalised bis pyrazol-3-yl ligands

The diketone and phenyl hydrazine were refluxed in ethanol overnight. The reaction resulted in the isolation of a brown oil on removal of solvent, and extraction of an aqueous solution of the product with DCM. The ^{1}H NMR of the material obtained clearly contained more than one compound. The presence of multiple doublets in the aromatic region suggests a mixture of products from these reactions and as yet we have been unable to separate these compounds to obtain conclusive results.

40

Conclusion

We have synthesised three new ligands, from simple starting materials, and in good yield under relatively mild reaction conditions. There is scope to expand the family further and they have the potential to form chelate complexes with a wide range of metal centres.

Experimental

General Comments

All NMR data are quoted in δ/ppm. The ^1H NMR and ^{13}C NMR spectra were recorded on a Bruker AM-400 spectrometer and referenced to $SiMe_4$ ($\delta = 0$ ppm).

MS(ES) was preformed on a VG visions Platform II instrument by the Department of Chemistry, Cardiff Universty.

Infa red spectra were recorded on a Nicolet 500 FT-IR spectrometer, each compound was measured as a solution in DCM unless otherwise stated.

All manipulations were carried out using standard Schlenk techniques under dinitrogen. Diethyl ether (Et_2O) and n-hexane were dried and degassed by refluxing under dinitrogen over sodium wire and benzophenone. DCM, MeOH and MeCN were dried over calcium hydride and distilled prior to use.

Dry DMF.DMA was purchased from Aldrich Chemicals and immediately transferred from a Sureseal container to a dry Schenk tube under an atmosphere of dinitrogen.

All starting materials were obtained from Aldrich Chemicals unless otherwise stated.

4,4-dimethyl-1,7-dimethylamino-3,5-hept-1,7-ene dione (2a)
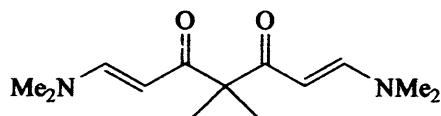
3,3-dimethyl-2,4-pentanedione (3.0g, 23.4 mmol) and DMF.DMA (70.2mmol) were placed in a Schlenk and stirred under reflux for 16 hours. The solution was cooled and excess solvent removed under reduced pressure. The brown oil was recrystallised from ethyl acetate and hexane to yield a brown crystalline solid. This material was triturated with hot hexane and filtered. The filtrate was collected and washed with hot hexanes (2x20mL) to yield the desired product as a brown solid. Yield (1.97g, 10.75 mmol, 47%). MS(ES) m/z: 239.1748 $[M+H]^+$. ^{1}H NMR (CDCl$_3$, δ): 7.51 (d, J = 12.49, 2H, Ar), 5.00 (d, J = 12.49, 2H, Ar), 2.98 (s, br, 6H, NCH 3), 2.70 (s, br, 6H, NCH_3), 1.25 (s, 6H, 2xCH_3). ^{13}C NMR (CDCl$_3$, δ): 196.16(2 CO), 152.48(2 CHN), 92.45 (COCH), 58.33 ((CO)$_2$$C$), 44.7 (2 N$CH_3$), 37.11 (2 N$CH_3$), 22.96 (2 C($CH_3$). IR (DCM, cm^{-1}): 2995 (C-H), 1659 (C=O), 1127 (C-N)

4-methyl-1,7-dimethylamino-3,5-hept-1,7-ene dione (2b)

Procedure according to 2a, with 3-methyl-2,4-pentanedione (5g, 43.8 mmol) and DMF.DMA (131.4 mmol). The desired product was obtained as a brown solid. Yield (3.9g, 17.5 mmol, 48%). MS(ES): m/z: 224.1548 $[M+H]^+$. ^{1}H NMR (CDCl$_3$, δ): 7.40 (d, J = 12.62, 2H, pz), 4.95 (d, J = 12.61, 2H, pz), 3.35 (q, J = 6.45, H), 2.90 (s, br, 2 x NCH 3), 2.60 (s, br, 2 x NCH 3), 1.20 (d, J = 6.98, 3H, CH_3). ^{13}C NMR (CDCl$_3$, δ): 194.02 (2 CO), 153.71 (2 CHN), 108.78 (COCH), 68.11 ((CO)$_2$$C$), 45.00 (2 N$CH_3$), 37.08 (2 N$CH_3$), 14.36 ($CH_3$). IR (DCM, cm^{-1}) 1646 (C=O)
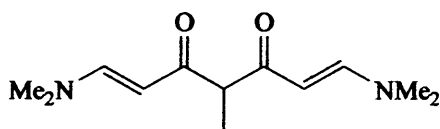
1 – Dimethylamino-4,4-dimethyl-3,5-hex -2-ene dione (2c)
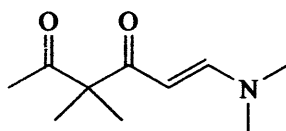
3,3-Dimethyl acac (3.0g, 23.4 mmol) and DMF.DMA (70.2mmol) were placed in a Schlenk and stirred under reflux for 16 hours. The solution was cooled and excess solvent removed under reduced pressure. The brown oil was recrystallised from ethyl acetate and hexane to yield a brown crystalline solid. This material was triturated with hot hexane and filtered. The eluent was cooled to yield the desired product as a yellow solid. Yield (2.13g, 11.63 mmol, 49.7%). MS(ES) m/z: 206.1163 [M+Na]$^+$. ^{1}H NMR (CDCl$_3$, δ): 7.60 (d, J = 12.27, H, Ar), 4.90 (d, J = 12.24, H, Ar), 3.10 (s, 3H, NCH_3), 2.75 (s, 3H, NCH_3), 2.05 (s, 3H, CH_3), 1.25 (s, 6H, 2 x CH_3). ^{13}C NMR (CDCl$_3$, δ): 209.80 (CH$_3$$C$O), 195.62 ($C$O), 153.61 (2 CHN), 90.94 (2 COCH), 60.59 (CMe$_2$), 45.06 (2 NMe$_2$), 37.16 (2 NMe$_2$), 26.14 (CH$_3$CO), 21.83 (2 CCH$_3$). IR (nujol, cm^{-1}): 2901 (C-H) 1712, 1666 (C=O)

1,1-Bis(pyrazol-3-yl)ethane (2e)
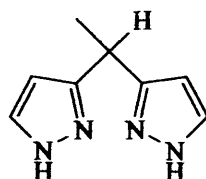
To a solution of 2.4(2.0g, 9.02mmol) in ethanol (20mL) was added hydrazine hydrate (1.29mL, 27.08mmol). The yellow solution was allowed to stir under reflux for 16 hours. The solution was cooled and the volatiles removed under reduced pressure. The resulting brown solid was washed with hexanes (2 x 1mL) and precipitated from ethyl acetate/petroleum ether (40-60). The ppt was dried under vacuum and the solid product recovered as an orange hydrosgopic solid. (1.06g, 6.54 mmol, 73%). MS(ES) m/z: 163.097 [M+H]$^+$. ^{1}H NMR (CDCl$_3$, δ): 7.38 (d, J = 1.58, 2H, pz), 6.05(d, J = 1.56, 2H, pz), 4.25 (q, J = 7.23, H), 1.60(d, J = 7.30, 3H, CH_3). ^{13}C NMR (CD$_3$OD, δ): 157.32 (2C, pz-3), 134.02 (2C, pz-5) 103.40 (2C, pz-4), 32.15 (C(pz)$_2$), 20.96 (CH_3). IR (DCM, cm^{-1}): 3310 (NH)

2,2-bis(pyrazol-3-yl)propane (2f)
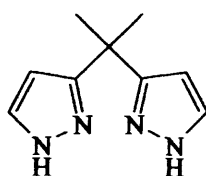
Procedure according to 2e with 2a (6.16g, 48.12 mmol) in ethanol (20mL) and hydrazine hydrate (19.17mL, 144mmol). The desired product was obtained as an orange solid. Yield (6.93g, 39.37 mmol, 82%). MS(ES) m/z: 177.1134 [M+H]$^+$. ^{1}H NMR (CDCl$_3$, δ): 7.40 (d, J = 2.00, H, pz), 6.10 (d, J = 1.98, H, pz), 1.75 (s, 6H, 2 x CH_3). ^{13}C NMR (CDCl$_3$, δ): 142.73 (2C, pz-3), 130.10 (2C, pz-5) 101.45 (2C, pz-4), 36.15 (C(pz)$_2$), 20.15 (CH_3). IR (DCM, cm^{-1}): 3319 (NH)

2,3,6,7-tetramethyl-4,5-diazaocta-3,5-diene-2,7-bis-(pyrazol-3-yl) (2g)

HN——N   N——N   N——NH
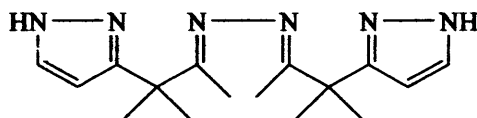
To a solution of 2c (3.00g, 10mmol) in ethanol (20mL) was added hydrazine hydrate (1.45mL, 30mmol). The yellow solution was allowed to stir under reflux for 16 hours. The solution was cooled and the volatiles removed under reduced pressure. The resulting brown solid was washed with hexanes (2 x 20mL) and precipitated from ethyl acetate/petroleum ether 40-60. The ppt was dried under vacuum and the product recovered as an orange solid. (2.37g, 7.9 mmol, 79%). MS(ES) m/z: 301.2147 [M+H]$^+$. ^{1}H NMR (CD$_2$Cl$_2$, δ): 7.40 (d, J = 2.08, 2H, pz), 6.10 (d, J = 2.07, 2H, pz), 1.49 (s, 6H, 2 x CH_3), 1.45 (s, 12H, 4 x CH_3). ^{13}C NMR (CD$_3$OD, δ): 165.63 (2C, immine), 143.98 (2C, pz-3), 134.20 (2C, pz-5), 104.14 (2C, pz-4), 44.43 (2C, C(CH$_3$)$_2$), 27.01 (4C, CH_3), 14.80 (2C, NCCH_3).

References

[1]   Aldrich Chemical Company, *Technical Information Bulletin "DMF.Acetals".*, 1973

[2]   H. Meerwein, W. Florian, N. Schon, G. Stopp, *Ann. Chem.*, **641**, 1961, 1

[3]   E. Barcelo-Barachins, F. J. Santos, L. Pingou, M. T. Galaceran, *Analytica Chimicta Acta.*, **545**, 2005, 209

[4]   J-J. Li, *Named Reactions In Heterocyclic Chemistry, Wiley.*, 2004, 104

[5]   Y. Lin, S. A. Lang Jr, *J. Heterocyclic Chem.*, **14**, 1977, 345

[6]   E. M. Keshk, *Heteroatom Chem.*, **15**, 1, 2004

[7]   S. Caddick, *Tetrahedron.*, **51**, 1995, 10403

[8]   A Loupy, A. Petit, J. Hamelin, F. Texier-Boullet, P. Jacqnault, D. Mathe, *Synthesis.*, **9**, 1998, 1213

[9]   L. Perreux, A. Loupy, *Tetrahedron.*, **57**, 2001, 9199

[10] P. Lidstrom, J. Tierny, B. Wathey, J. Westman, *Tetrahedron.*, **57**, 2001, 9225

[11] K. M. Al-Zaydi, *Molecules.*, **8**, 2003, 541

[12] F. M. A. A. El-Taweel, M. H. Elnagdi, *J. Het. Chem.*, **38**, 2001, 981

[13] Y. Chang, M. G. Nair, R. C. Satnell, W. G. Helferich, *J. Agric. Food Chem.*, **42**, 1994, 1869

[14] S. Plescia, G. Daidone, V. Spiro, *J. Hetrocyclic. Chem.*, **19**, 1982, 1385

[15] H. Reimlinger, *Chem. Ber.*, **92**, 1959, 970

[16] P. Schenone, L. Mosti, G. Menozzi, *J. Heterocyclic. Chem.*, **19**, 1982, 1355

[17] G. Menozzi, L. Merello, P. Fossa, S. Schenone, A. Ranise, L Mosti, F. Bondavalli, R. Loddo, C. Murgioni, V. Mascala, P. La Colla, E. Tamburni, *Bioorg. Med. Chem.*, **12**, 2004, 5465

[18] A Ahmed, R. A. Bragg, J. Clayden, L. W. Lai, C. McCarthy, J. H. Pink, N. Westlund, S. A. Yasin, *Tetrahedron.*, **54**, 1998, 13277

Chapter 3:

Bis (pyrazol-3-yl) Coordination Chemistry

Introduction

On obtaining two new ligands it was difficult to know where to begin with no complexes which were potentially available to us known. As with the development of the ligands, the structural similarity to scorpionate ligands was the main source of reference as we set out to open a new chapter in coordination chemistry. We also reviewed the coordination chemistry of monodentate pyrazole complexes. Scorpionate complexes can occur as monomers, dimers (directly bound to the same metal centre or bridged by another atom or polymers[1-4], and represent one of the most widely used classes of ligands in transition metal chemistry. The ligands produced by us show a clear structural similarity to the bis(pyrazol-3-yl) alkanes in particular as neutral species, and there lay the basis for our initial predictions as to what may be achievable with regards to the coordination behaviour of our new compounds. Although bis(pyrazol-3-yl) alkanes are known to react extensively with Group (I) metals[5], along with the lower end of the transition series[6], we chose to investigate coordination chemistry of the softer metals in the series as defined by the HSAB principle.

As mentioned previously, the general characteristic shown by a large majority of scorpionate complexes is the six membered ring formed on complexation[7]. While bipy or phen metal adducts are likely to form an approximately planar five membered M-N-C-C-N moiety, upon coordination of $R_2C(pz^x)_2$ to a metal centre, a six membered cycle is formed for which a boat conformation is forecast. Studies have shown the internal and external angles of these compounds, along with the majority of their scorpionate ligand counterparts are known to undergo wide variations reliant on the nature of the metal centre and the substituents on the pyrazole rings[8]. Deviations away from the boat structure are known with some complexes adopting a distorted chair conformation as in the dimeric titanium adduct [bis(cyclopentadienyltitanium)(μ-pyrazolato-N,N)]$_2$[9], and the molybdenum complex dihydrobis(3,5-dimethylpyrazolyl)borate(η^3-allyl)dicarbonyl molybdenum[10]. Related studies with pyrazoboles have shown that the energy differences between chair, boat or planar confirmations with regards to the six membered rings formed on

complexation are small, with the solid state configuration mainly determined by packing effects.

In general, the 6-membered metallocyclic moieties usually adopt a boat conformation due to the fact that the metal and central backbone atom of the ligand, carbon or boron in these cases, have to be coplanar with both pyrazole rings, which in turn are not parallel. **Figure 3.1** displays the rings formed with the pyrazole atoms not involved in the boat structure omitted for clarity. The flat plane N-N-N-N, acts as a base for the boat with the M and Linker atom raised out of this plane by varying degree depending on the atoms involved. [A] is the representation for a general pyrazolyl alkane, while [B] represents what may be possible with our ligands.
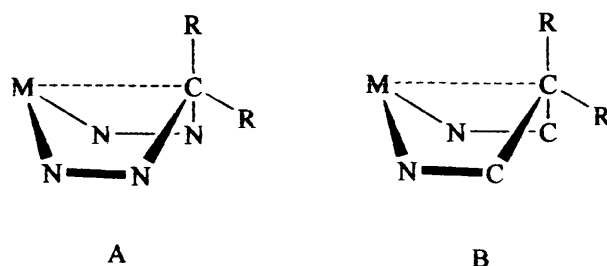
Figure 3.1: 6-membered Boat Conformations

The angle of intersection between the two pyrazolyl rings can provide a measure of the depth of the boat and depends on the nature of both the M, and R group, which is axially bound to the backbone atom which may interact with the metal. Put simply, studies to date suggest the planes of the two pyrazole rings are also planar with the imaginary line between the metal and the point opposite in the six membered ring, Boron or Carbon. Therefore, the planes from two separate pyrazole rings from the same ligand intersect at the distance M-C or M-B as appropriate. **Figure 3.2** represents a "head on view" from the point of view of the metal atom. The visible nitrogen and carbon atoms represent the plane of the pyrazole rings which in turn are in the same plane as the M-Pyrazole linker atom distance. The angle between the two planes, θ, is an indicator for the depth of the potential boat.
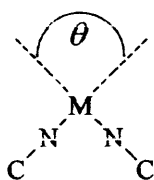
Figure 3.2: Angle between the plane of two pyrazole rings on coordination

As the value of θ approaches 180°, and the pyrazole rings become planar with each other, the depth of the boat decreases with the metallocycle formed approaching planarity as in the 5 membered bipy moieties. As the angle decreases, the metal atom is lifted out of the N-N-N-N plane, and in extreme cases where the angle approaches 100°, the potential for agostic bonds increases[11].

Synthesis and Characterisation

The bis pyrazole ligands prepared in chapter 2 have been chosen due to the lack of knowledge with regards to these structurally simple molecules. The results of investigations into the coordination behaviour of these ligands with some transition metals in the (+II) state are now presented.

Palladium Complexes

Preparation and Characterisation of Pd(II) Complexes With Bis Pyrazoles **2e** and **2f**

Mixing MeCN solutions of either the compounds **2e** or **2f** with palladium dichloride bis acetonitrile [PdCl$_2$(MeCN)$_2$] in MeCN resulted in the immediate formation of the N^N chelated dichloropalladium complexes **3a** and **3b** respectively (**figure 3.3**).

2e/2f $\xrightarrow{\text{ i }}$

i – PdCl$_2$(MeCN)$_2$,MeCN, RT

R = H – **3a**, R=Me – **3b**
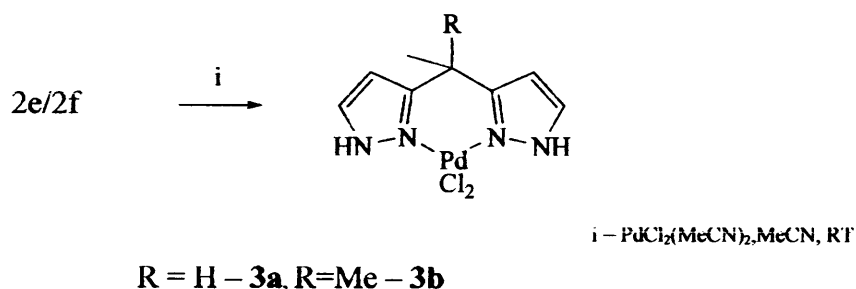
Figure 3.3: Formation of palladium complexes 3a and 3b

Complexes **3a** and **3b** are red, air stable solids and have been characterised by microanalysis, IR, ^{1}H NMR, MS as well as an X-ray crystal structure determination.

^{1}H NMR

The chelation of the symmetrical donor was apparent from the appearance of the NH protons as a broad peak at 11.75 (**3a**) and 11.80 (**3b**) respectively, a feature not present in the ^{1}H NMR of the free ligand. **Table 3.1** shows the ^{1}H NMR peak positions for both complexes. The presence of the NH protons is suggested by the sharp IR peaks at 3323 cm^{-1} (**3a**) and 3317 cm^{-1} (**3b**)

Table 3.1: ^{1}H NMR peak positions for 3a and 3b (ppm)

Complex	Hpz	Hpz	Me	R	NH
3a	m 7.58	m 6.32	d 1.61	q (H) 4.35	br 11.75
3b	m 7.55	m 6.35	s 1.70	s (CH₃) 1.70	br 11.80

The values obtained show a small downfield shift on complexation. The existence of boat -to- boat interconversions is known in structurally similar (bis pyrazole-1-yl complexes of palladium) complexes[12]. The boat -to- boat interconversions which may be present in our complexes is represented in **figure 3.4**, and shows how different signals may be obtained due to the equatorial or axial position of the R substituents. This may in turn be responsible for the slightly distorted nature of the expected pyrazole doublets in the ^{1}H NMR's of **3a** and **3b**. The paper also describes how steric bulk is a hindrance to this process, thus showing a higher population of one state over the other in some cases. We are unable to present our findings regarding the fluctional behaviour of **3a** and **3b**, however similar complexes have shown two distinct pyrazole rings under VT NMR conditions at low temperature[13].
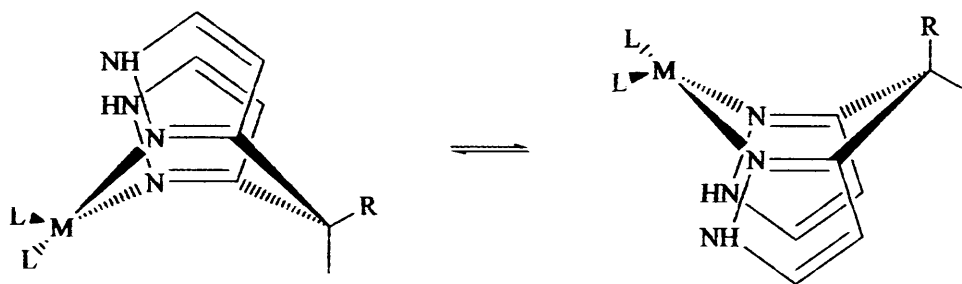
Figure 3.4: Boat-to-Boat Interconversions

X-Ray Analysis

Crystals of both **3a** and **3b** were grown by slow evaporation of MeCN solutions. X ray crystal structure determinations were carried out by Dr Liling Ooi at Cardiff University.

X Ray analysis of 3a

The X ray structure of **3a** is shown in **figure 3.5** and clearly confirms the N^N chelation mode on coordination of ligand **2e**. The palladium centre has a slightly distorted square planar geometry. Selected bond lengths and angles are shown in **table 3.2** (see appendix A for the completed data, collection and refinement details together with atomic coordinates).
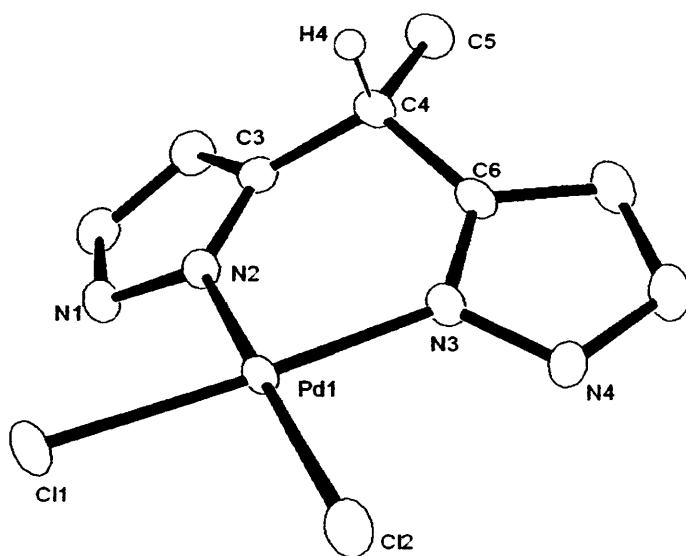
Majority of protons have been omitted for clarity

Fig 3.5: X Ray Structure of 3a

Table 3.2: Selected Bonds and Bond Angles 3a

Bond Lengths Å		Bond Angles°	
N(2)-Pd(1)	2.005(2)	N(2)-Pd(1)-N(3)	86.54(10)
N(3)-Pd(1)	2.005(2)	Cl(1)-Pd-Cl(2)	90.98(3)
Pd(1)-Cl(1)	2.2834(7)	C(3)-C(4)-C(6)	113.3(2)
Pd(1)-Cl(2)	2.2929(8)	N(3)-Pd(1)-Cl(1)	177.05(7)
		N(2)-Pd(1)-Cl(2)	175.82(7)

As seen in **table 3.2**, the bite angle is 86.54(10)°. The Pd-Cl distances are within normal limits and there is no agostic interaction between the proton on the ring

bridging proton and the palladium centre. This is reflected in the shallow boat configuration as expected and the axial position of the proton.
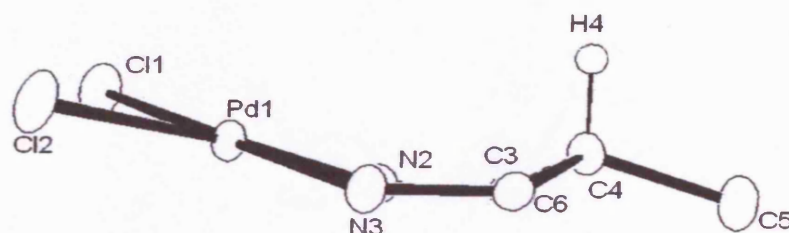
Fig 3.5: Boat conformation displayed by 3a

Calculation and Comparison of the Boat Angles

Many methods for comparing the relationship between the depth of the boat formed and the angle between the pyrazole planes have been discussed in previous work. In 1985, Brock, Niedenzu and collaborators published a paper on symmetrical pyrazoboles, relating the angles between the N-N-N-N plane and (i) a plane defined by N-B-N, and (ii) a plane define by that of the pyrazole ring[14]. In contrast, Capparelli and Agrifoglio published their findings regarding some zinc complexes produced in 1992 by comparing the dihedral angles between the points N-M-B-N' where N is the nitrogen atom involved in the N-M Bond, and N', the nitrogen atom on the other pyrazole ring, bound to the bridging boron atom, and the deviation in Å of the M and B atoms away from the N-N-N-N plane[15].
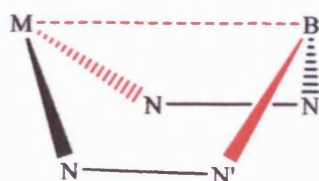
Figure 3.6: Calculation of the boat angles by Capparelli and Agrifoglio

We have taken a far simpler approach to this aspect of the analysis. Due to the structural difference in our ligands, the base of our boat structures is denoted N-C-C-

N. Using the package ORTEP-3, we have drawn centroids at the point N-N and C-C respectively. The angle between the metal atom and the N-C-C-N plane via centroid N-N has been denoted boat angle B1, and the angle between the basal plane and carbon linker atom via centroid C-C, B2.
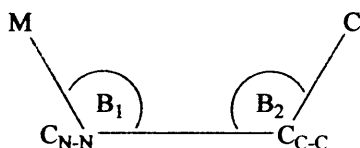
Figure 3.7: Our evaluation of the boat angle

The average of these two values is obtained and used to compare the angles between the two pyrazole ring planes. The angles B1 and B2 are not similar in the palladium complex displayed in **figure 3.7**, however we feel an average of B1 and B2 will reflect the depth of any boat structure reported, as this will be a relatively constant feature of any metallocycles produced.

In this case, the angle between the two pyrazole planes, θ, is 144.96°. The boat angles for this compound are 163.41° and 147.91°, representing angles B1 and B2 respectively at an average of 155.66°.

Hydrogen Bonding

The hydrogen bonding network displayed here (**figure 3.8**) shows an association between N(1) and Cl(2) of neighbouring complex units. The hydrogen bond is 3.279Å in length and produces a 'zig zag' effect in the arrangement of palladium centres at a Pd-Pd'-Pd" angle of 109.92° at a Pd-Pd' distance of 6.912Å. No hydrogen bonding is apparent to link neighbouring 2-D sheets. No hydrogen bonding is present between adjacent zig-zag strands.
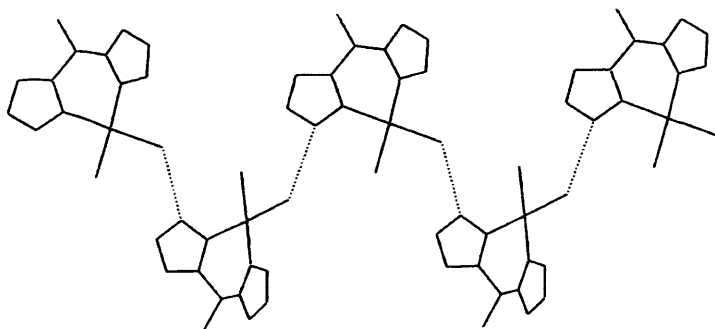
Figure 3.8: Hydrogen bonding within **3a**

X Ray Analysis of palladium (II) complex 3b

Similar to the previous complex, the X-ray crystal determination confirms the N^N chelation mode of ligand 2f. The structure obtained by Dr L. Ooi at Cardiff University is shown in **figure 3.9**. Selected distances and angles are shown in **Table 3.3**, and full data in Appendix A.
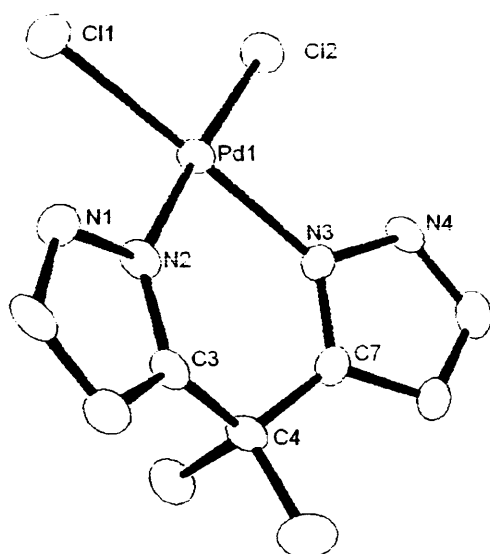
Fig 3.9: X Ray Structure of **3b**

Table 3.3: Bond angles and distances in **3b**

Bond Lengths Å		Bond Angles°	
N(2)-Pd(1)	2.009(4)	N(2)-Pd(1)-N(3)	86.72(18)
N(3)-Pd(1)	2.101(4)	Cl(1)-Pd-Cl(2)	91.92(5)
Pd(1)-Cl(1)	2.2947(14)	C(3)-C(4)-C(7)	115.00(2)
Pd(1)-Cl(2)	2.2993(15)	N(3)-Pd(1)-Cl(1)	177.40(7)
		N(2)-Pd(1)-Cl(2)	176.83(14)

The bite angle displayed by this complex is 86.72(18)° with Pd-Cl bonds relating to normal values for N-Pd Chelating compounds. The angle between the pyrazole planes is 28.04° with an average boat depth angle of 160.85° obtained from the values 170.01° (B1) and 151.69° (B2) respectively.
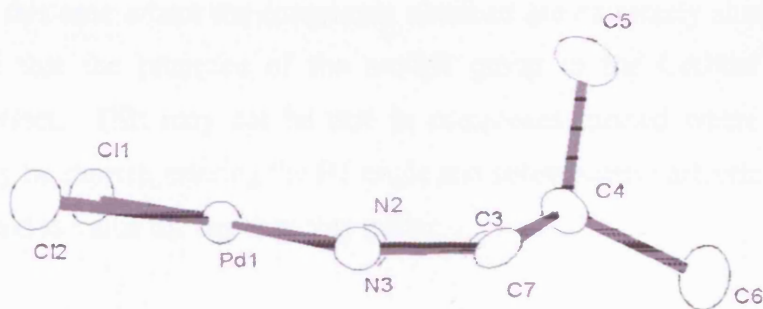
Fig 3.10: Shallow boat configuration displayed by 3b

Hydrogen bonding

No such interactions exist within this compound. The packing arrangement is displayed in **figure 3.11**.
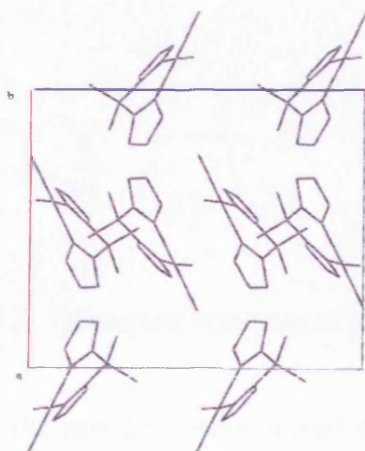
Fig 3.11: Packing arrangement as viewed along crystallographic b axis

Comparison of the Boat Formations Displayed by Complexes 3a and 3b

On visual comparison it is clear that complex **3a** has adopted a deeper boat configuration. The significant difference in the angle of pyrazole plane intersection in the two complexes, with the angle in complex **3a**, 7.00° less than in complex **3b**, has upheld the work already proposed and confirmed in this case that the lesser the angle of intersection between the two pyrazole planes, the deeper the boat.

It is clear in this case where the complexes obtained are extremely similar with only one variable that the presence of the methyl group in the Carbon linker has a substantial effect. This may not be true in complexes formed where the N-Metal distances may be shorter, altering the B1 angle and subsequently affecting the average boat angle used to value the depth in this study.

Attempted synthesis of [(2f)PdMeCl]

On successful isolation of the palladium complexes described above, we felt confident in our ability to produce unsymmetrical Methyl palladium chloride analogues. Many similar complexes are known and usually synthesised via the reaction of a bidentate nitrogen donor with the common reagent [MePd(COD)Cl]. **Figure 3.12** displays the reaction attempted.

i – [MePd(COD)Cl]
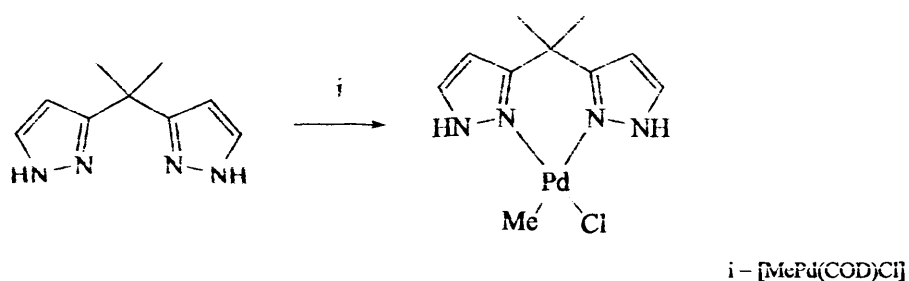
Figure 3.12: Attempted synthesis of [LPdMeCl]

Stoichiometric quantities of the reactants were stirred in acetonitrile (MeCN) for 1 hour. The opaque white solution was filtered and excess solvent removed under reduced pressure. The white solid obtained was dried under reduced pressure, re-dissolved in DCM and precipitated out of solution with diethyl ether. The resulting white solid was triturated with hexane and filtered. Initial H^{1}NMR analysis, conducted in dry, deuterated dichloromethane, suggests the desired complex was formed. **Fig 3.13** shows the initial spectrum obtained.
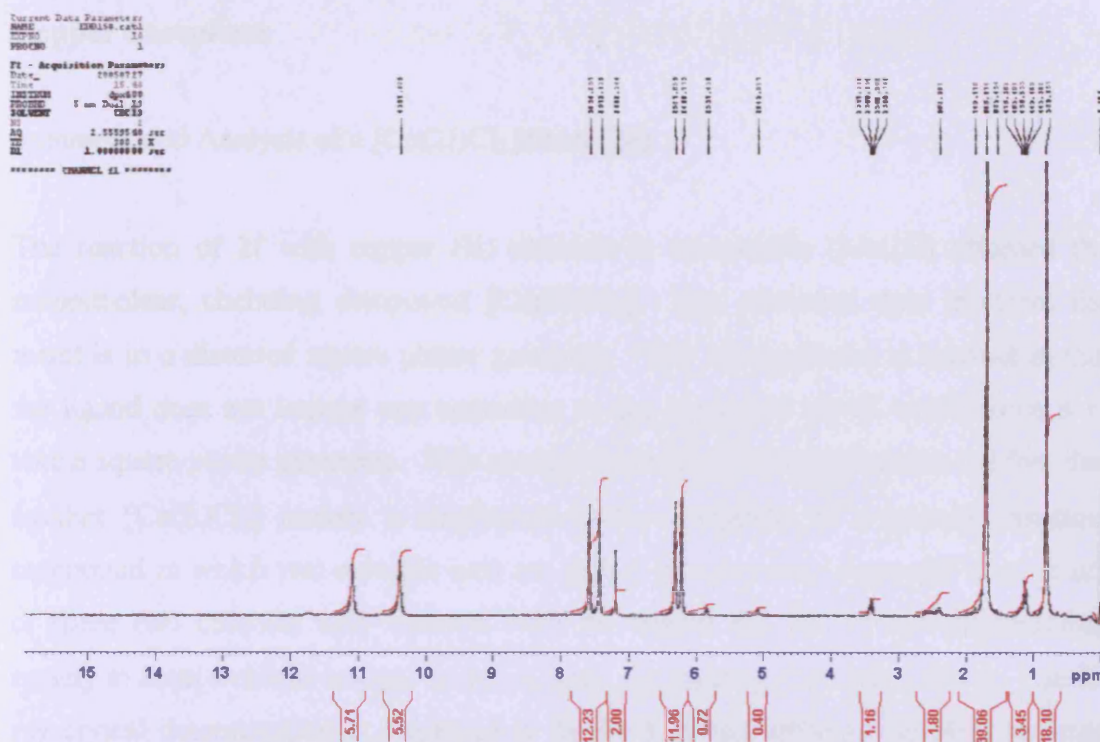
Figure 3.13: ¹H NMR of a crude sample of [(3b)PdMeCl]

The presence of four individual multiplets at 6.28ppm, 6.35ppm, 7.45ppm and 7.60 ppm respectively in the aromatic region, each integrating to a single proton is strong evidence for the formation of the complex. Also, as in the palladium dichloride analogues the NH peaks are now visible where as they were not present in the starting matrial. Again, as the complex formed is not symmetrical, the resulting broad peaks at 10.35ppm and 11.10ppm represent single NH groups with each integrating to one proton apiece. As expected, broad multiplets between 2 and 3 ppm are not present, suggesting the COD has been removed. The remaining peak present in both starting material and product is the M-Me which has shifted up field by a significant amount from 0.95ppm to 0.70ppm in the product. However, attempts to purify the compound by precipitation were unsuccessful due to the unstable nature of the complex.

We were unable to obtain analogous results for the coordination of ligand 2e. We have found this hygroscopic ligand to be awkward to handle with little quality material obtained when reacted with simple metal salts. At this point it was decided to concentrate on the coordination chemistry of ligand 2f for the time being.

Copper Complexes

Synthesis and Analysis of a [Cu(2f)Cl₂]dimer (3c)

The reaction of **2f** with copper (II) chloride in acetonitrile (MeCN) afforded the mononuclear, chelating compound $[Cu(2f)Cl_2]$. The structural data indicates the metal is in a distorted square planar geometry. This configuration is unusual in that the ligand does not impose any constraint on the metal ion which would force it to take a square planar geometry. This configuration could be explained by the fact that another $[Cu(L)Cl_2]$ moiety is implicated in the formation of a pseudo dinuclear compound in which two chloride ions are shared between two copper(II) ions. Each of these two chloride ions interacts with the copper (II) ion of the neighbouring moiety to form a chloro-bridge. In this system, the distance Cu-Cu is 3.938Å. The X-ray crystal determination is displayed in **figure 3.14** and **table 3.4** displays selected angles and bond lengths. X Ray analysis was carried out by Elenna Rowan Mapp at Cardiff University. Full data is contained in Appendix A.
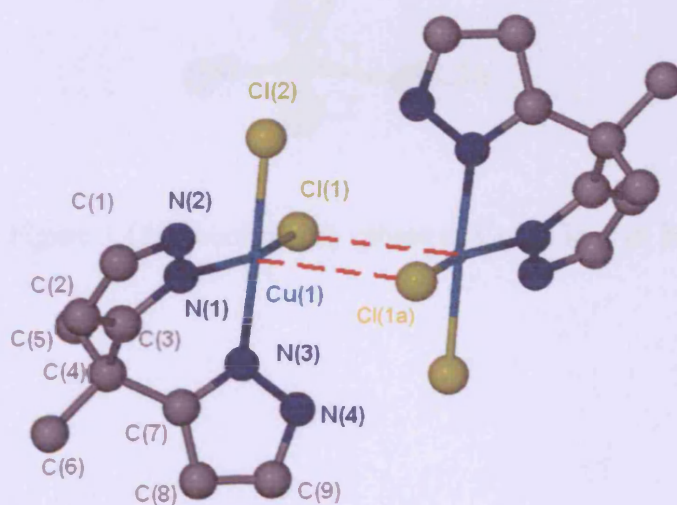
Fig 3.14: X ray structure of the dinuclear Cu(II) complex 3c

Table 3.4: Selected distances and angles of [Cu(2f)Cl$_2$]$_2$

Bond Lengths Å		Bond Angles°	
Cu(1)-Cl(1)	2.31(17)	N(1)-Cu(1)-Cl(1)	157.71(15)
Cu(1)-Cl(2)	2.26(18)	N(3)-Cu(1)-Cl(2)	172.50(15)
Cu(1)-Cl(1a)	2.88	Cl(1a)-Cu(1)-Cl(1)	82.14
N(1)-Cu(1)	2.00(5)	N(1)-Cu(1)-Cl(1a)	119.30(5)
N(3)-Cu(1)	1.98(5)	N(1)-Cu(1)-N(3)	84.00(2)

Each copper (II) atom in pentacoordinated and has a distorted square pyramidal arrangement. Work by Reedijk and collaborators has allowed us to quantify the distortion of pentacoordinate Cu(II) complexes[10]. Via a simple formula, the range between the square-pyramidal and trigonal-bipyramidal extremities possible in a five membered complex can be gauged.
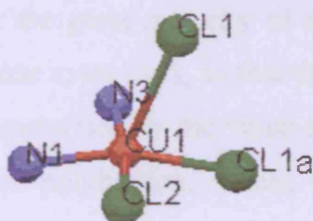
Figure 3.15: Coordination sphere of Cu(II) ions in 3c

Structural Index Parameter

In a five co-ordinate system such as the one represented in **figure 3.16**, ideally square-pyramidal geometry is associated with $\alpha = \beta = 180°$, where β is the greater of the angles between any two atoms and α is the second largest. In this case α and β are the identical angles between opposing moieties on the basal plane.

A
B———M———C
D   F
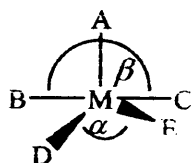
Fig 3.16: Calculation of the structural index parameter

For perfectly trigonal-bipyramidal geometry, β is again 180°, measured between the axial moieties via the metal centre. α is 120° and is a measure of the three identical angles in the basal plane. In the great majority of square-pyramidal systems, M is displaced out of the BCDE plane towards A, so that these C_{4v} geometries usually have $\alpha = \beta < 180°$, and can be characterised by the value of (β α), which is 0° for a C_{4v}, and 60 for a D_{3h} coordination polyhedron. Thus, the geometric parameter τ was defined where:

$$\tau = (\beta \quad \alpha)/60$$

This formula is applicable to five co-ordinate structures as an index of the degree of trigonality, within the extremities of square-pyramidal and trigonal-bipyramidal geometries where a value of 1 represents a pure trigonal bi-pyramidal geometry and a value of 0 represent a perfect square pyramid.

With regards to our complex, $[Cu_2(2f)_2Cl_4]$, A is defined as atom Cl(1a) due to the fact it does not represent one of the points defining the two largest angles. Therefore, the angles required to complete the calculation in this case are N(3)-Cu(1)-(Cl2)

172.57 (β) and N(1)-Cu(1)-Cl(1) 157.81 (α). The value τ = 0.24 obtained shows a significant distortion from the perfect square-pyramid geometry.

Boat angles

The boat structure displayed in **figure 3.17** appears to be deep in this case with the average of boat angles B1 (155.68°) and B2 (140.02°) at a value of 147.85° and a pyrazole plane intersection angle at 132.20°. The boat obtained is significantly deeper than the previous complexes and has comparable M-N distances.
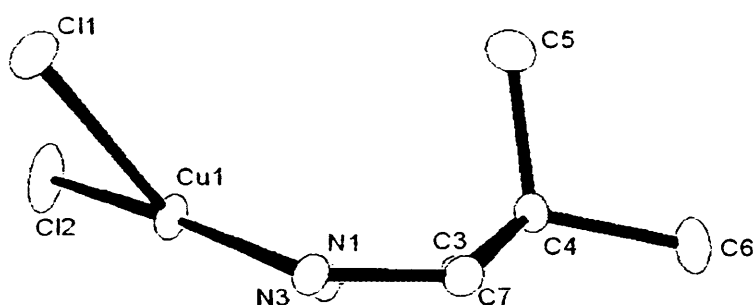
Fig 3.17: Boat configuration displayed by 3c

Hydrogen Bonding

The hydrogen bond network present in this complex forms a one dimensional polymer, with interactions between Cl(1) and N(2) of neighbouring dimers at 3.299Å (**figure 3.18**). An internal interaction also exists between Cl(2) and N(4) of each dimer(2 on each dimer as structure was formed via reflection of the asymmetric unit. This interaction is measured at 3.129Å. Again no hydrogen bonding to link strands and form a 3-D network exists.
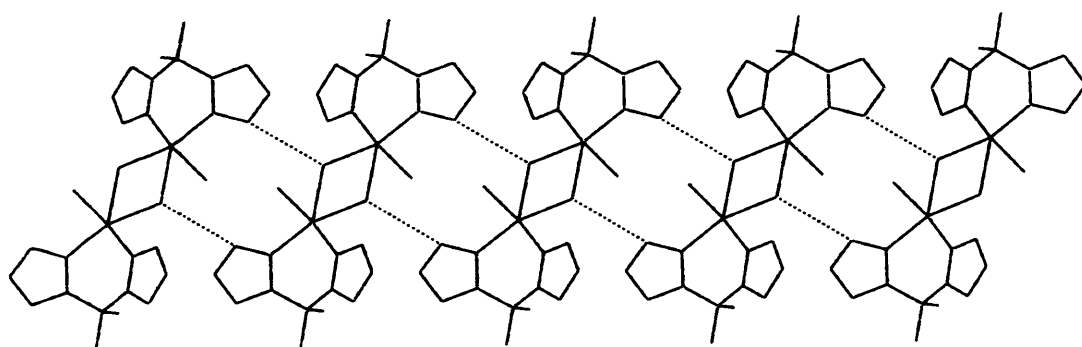
Fig 3.18: Representation of the hydrogen bonding in 3c.

(Image generated by Mercury 1.4.1)

Synthesis and Analysis of [Cu(2f)₂(3d)](OTf)₂

The reaction of copper (II) trifluoromethylsulfonate and **2f** in an acetonitrile solvent system resulted in the percipitation of a brown solid after stirring for 16 hours. The removal of the solvent under reduced pressure and subsequent slow recrystallisation form dichloromethane and hexane produced brown block crystals suitable for X-ray analysis within one month. X ray analysis was carried out at Cardiff University by Dr Andreas Stasch. The crystals were also analysed by IR and microanalysis and here we report our findings.

X Ray Analysis

The data reveals copper atoms in two slightly different environments. Both are in a distorted square planar geometry with two ligands chelating to each (**figure 3.19**). The structural difference between the two structures is marginal as seen in **table 3.5** with full data available in appendix A). The asymmetric unit also contained a $[CF_3SO_3]^-$ moiety and half a molecule of dichloromethane. The counter ion in this case is not involved in coordination to the metal centre, but acts as a bridge, linking the two slightly different copper environments in a repeating fashion via hydrogen bonds.
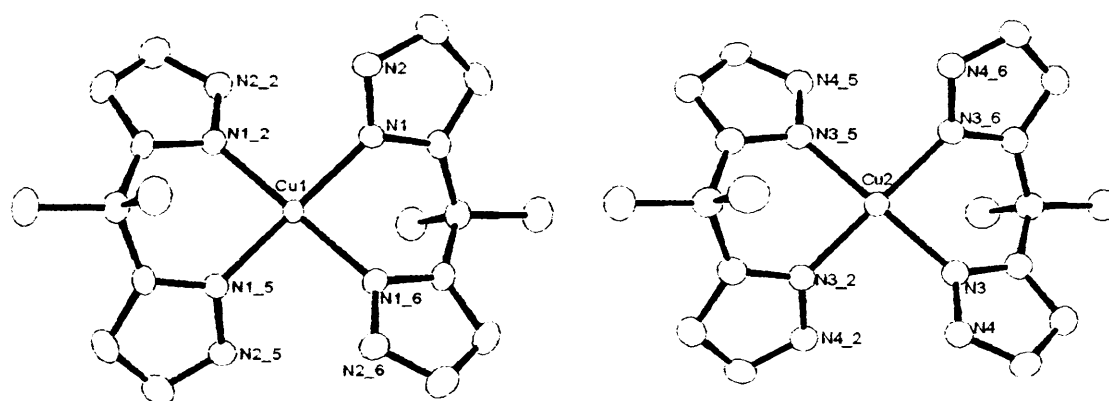
Fig 3.19: X Ray Structure of 3d, comprising two slightly different copper (II) units

67

Table 3.5: Selected angles and distances from **3d**

Cu(1)		Cu(2)	
Atoms	Angle °	Atoms	Angle°
N(1)-Cu(1)-N(1_6)	86.18(13)	N(3)-Cu(2)-N(3_6)	87.17(14)
N(1)-Cu(1)-N(1_2)	93.82(13)	N(3)-Cu(2)-N(3_2)	92.83(14)
N(1)-Cu(1)-N(1_5)	180.00(19)	N(3)-Cu(2)-N(3_5)	180.0(19)

Cu(1)		Cu(2)	
Atoms	Distance Å	Atoms	Distance Å
N(1)-Cu(1)	1.951(2)	N(3)-Cu(2)	1.972(2)
O(3)-Cu(1)	2.803	O(1)-Cu(2)	2.803

The Bite angles displayed by the ligands are 86.18(13)° and 87.17(14)°, with identical N(1) atoms on opposite sides of the complex at exactly 180°.

A two dimensional hydrogen bond network links the two types of CuL_2 unit via triflate ions. The Cu(1) unit is bound to $O(3)_{triflate}$ via N(2) at a distance of 2.769 Å. The same triflate ion is associated with N(4) of the Cu(2) unit via O(1) at a distance of 2.803 Å. The pattern is repeated along the lattice in the x and y directions to form a sheet. No hydrogen bonding occurs in the z direction to link the sheets. In total, each Cu unit is bound to four triflate anions, allowing the charge to be shared and providing each copper centre with a (+II) charge. The main difference between the two copper units is the orientation with respect to each other. Figure **3.20** displays the distribution of atoms in which each Cu(1) unit is flanked by four Cu(2) ions, via the triflate anions. The hanging contacts have been removed for clarity, but the potential to build a 2-D sheet is clear.
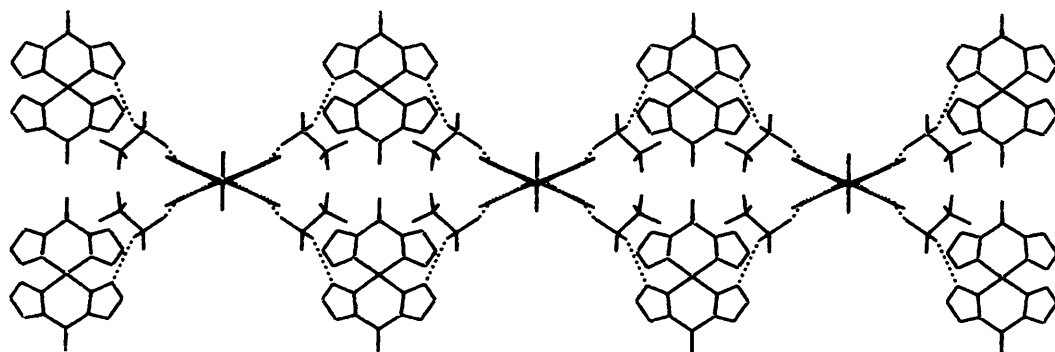
Fig 3.20: Mercury representation of the hydrogen bonding in 3d

Boat Angles

The two boat metallocycles formed are very similar as expected. However, they do not follow the expected rule with respect to the comparison of average boat angle vs pyrazole plan intersection angle.

The boat formed around Cu(1), displayed in **figure 3.21** as the symmetrical dimer with identical boat and plane angles for both metallocycles formed, has values of 152.96° (B1), and 137.76° (B2) at an average of 145.36°. The angle of planar intersection, θ, is 129.10°. The corresponding boat angles of 157.07° (B1) and 135.09° (B2) around Cu(2), as expected, provide a similar average at 146.08° (**Figure 3.22**).
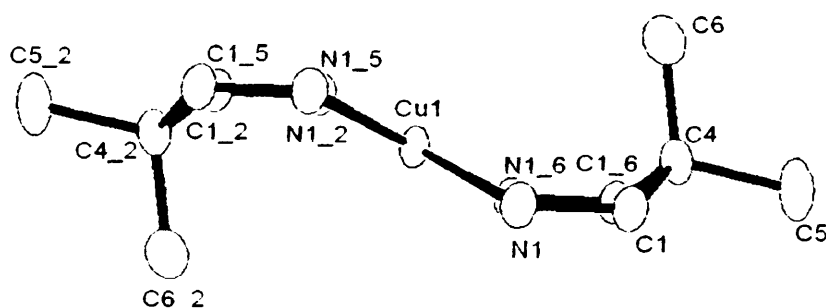
Fig 3.21: Boat structure displayed by the interaction of ligands around Cu(1)
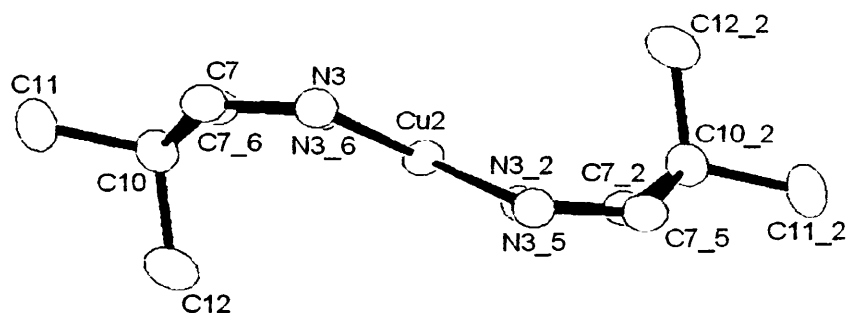
Fig 3.22: Boat structure displayed by the interaction of ligands around Cu(2)

However, the similarity in average boat angle has not provided a similar result in the comparison of pyrazole plane intersection angles. The expected result here with a slight increase in average boat angle from Cu(1) to Cu(2) was a comparable decrease in the angle between the pyrazole planes. This trend was predicted and is due to the increased boat angles around Cu(2), showing the copper and bridging carbon atom are less displaced from the N-C-C-N basal plane. In actuality a significant decrease in the planar intersection angle around Cu(2) was observed, 120.59°, suggesting the boat is less pronounced than in the metallocycles containing Cu(1), however the 'butterfly effect' of the pyrazole rings is increased around Cu(2), with more downward folding. At present we are unclear over the cause of this discrepancy in the trend, but see the packing arrangement as a possible cause.

Cobalt Complexes

Preparation of Cobalt (II) Complexes with Bis Pyrazole 2f

The reaction of cobalt (II) chloride with ligand **2f** (1:2) in acetonitrile solution produced a clear blue solution overnight. The solvent was reduced in volume to encourage the crystallisation of any potential products, and green blocks were recovered within 1 week. This material was suitable for X-ray analysis and the procedure performed at Cardiff University by Dr Andreas Stasch. The compound was also characterised by IR and microanalysis. Within two weeks, a pink material had formed within the same flask. Some crystals suitable for X-ray were collected, and here we describe the data gathered on both complexes.

Analysis of $[Co_2(2f)_2(\mu\text{-OH})]Cl.[CoCl_4]$ (**3e**)

X Ray Analysis

The X-ray crystal structure of the green material obtained is displayed in **figure 3.23**. The structure consists of two cobalt (II) centres separated by 3.108 Å in similar octahedral environments. Five of the six donors around each cobalt atom are nitrogen atoms supplied by the bis pyrazole ligands which occur in two different forms (half ionic, supplying three nitrogen donors and half neutral, supplying two nitrogen donors apiece). There are four ligands in total within each dimer. The final coordination site in both metal centres is filled via a hydroxide ion which bridges the two cobalt atoms. Figure 3.23 displays how two of the ligands contribute to the coordination sphere of both cobalt atoms.
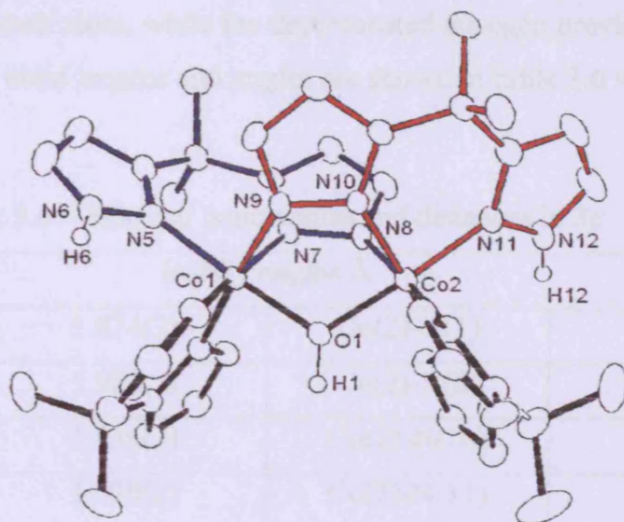
Fig 3.23: X Ray Structure of the cation in 3e

This structure is similar to that hypothesised by Akita and collaborators in 2005 (**figure 3.24**)[17]. In this complex, two nickel centres are bound by one anionic tris(pyrazol-1-yl) borate ligand each with a hydroxyl bridge spanning the two metal centres. The Ni-Ni centre is also spanned by a single deprotonated pyrazole moiety, supplying one nitrogen donor to each of the metal centres. Unfortunately, full data does not exist and we are unable to compare.
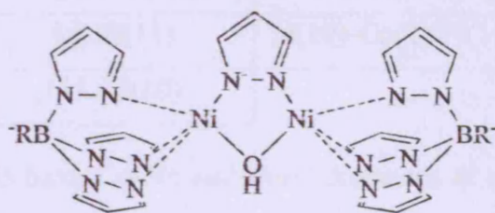
Figure 3.24: Complex similar to 3e, hypothesised by Akita

In our novel complex, the four ligands are present in two different forms, with two in each. Firstly, the ligand acts as we have already seen, a neutral chelating ligand and provides each of the metal centres with two nitrogen donors. Secondly, the ligand is present in an anionic form, with one of the pyrazole rings being deprotonated and therefore allowing the ligand to provide three avenues for metal coordination. In the case of the anionic ligands, the nitrogen atoms usually utilised for coordination are

associated with one cobalt atom, while the deprotonated nitrogen provides an N donor to the other. Selected bond lengths and angles are shown in **table 3.6** with full data in appendix A.

Table 3.6: Selected bond angles and distances in **3e**

Bond Lengths Å			
Co(1)-O(1)	1.874(2)	Co(2)-O(1)	1.880(2)
Co(1)-N(7)	1.907(3)	Co(2)-N(8)	1.910(3)
Co(1)-N(3)	1.930(3)	Co(2)-N(10)	1.914(3)
Co(1)-N(9)	1.930(2)	Co(2)-N(11)	1.920(3)
Co(1)-N(1)	1.934(3)	Co(2)-N(13)	1.933(3)
Co(1)-N(5)	1.936(3)	Co(2)-N(15)	1.948(3)
Bond Angles °			
N(1)-Co(1)-N(7)	177.06(11)	N(8)-Co(2)-N(15)	176.18(11)
N(3)-Co(1)-N(9)	176.01(11)	N(10)-Co(2)-N(13)	176.86(11)
N(5)-Co(1)-O(1)	176.45(10)	N(11)-Co(2)-O(1)	175.85(10)
N(1)-Co(1)-N(3)	88.41(11)	N(13)-Co(2)-N(15)	87.62(12)
N(1)-Co(1)-N(9)	93.22(11)	N(10)-Co(2)-N(15)	94.40(11)
N(3)-Co(1)-N(7)	93.61(11)	N(8)-Co(2)-N(13)	94.00(10)
N(7)-Co(1)-N(9)	84.62(11)	N(8)-Co(2)-N(10)	83.84(11)
N(7)-Co(1)-N(5)	89.30(11)	N(10)-Co(2)-N(11)	89.50(11)
Co(1)-O(1)-Co(2)	111.77(10)		

The two neutral ligands have Co-N$_{(Ligand)}$ bond distances at an average of 1.932 and 1.9405 Å, with the longest average distance around Co(2). The bite angles concerning the two neutral components are also slightly different with values of 88.41(11)° Co(1) and 87.62(12)° Co(2). The CMe$_2$ linker in both cases is lifted out of the plane NNCC as expected, however, the shallow boat structure present in all complexes discussed thus far is almost invisible with the metal raised only slightly. **Figure 3.25** displays the environment around both cobalt centres, showing the planarity of the newly formed six membered rings. Both show little of the expected boat like character with Co(2) in particular raised out of the NNCC plane by only 3.15°.
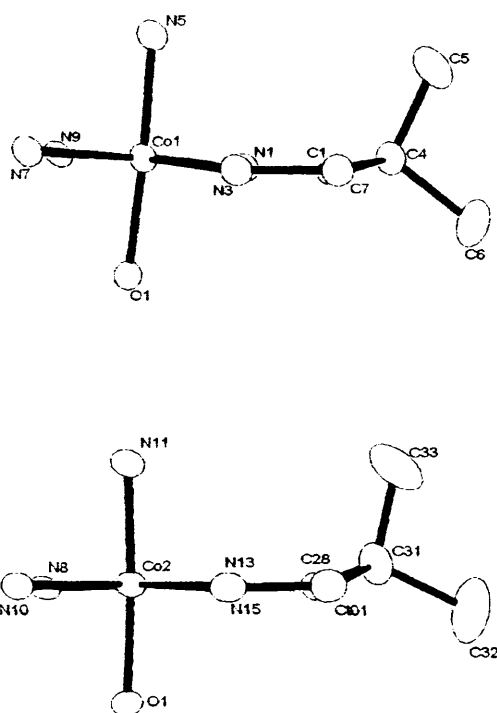
Fig 3.25: Shallow boat configuration displayed by 3e around both Co centres

The respective angles between the two pyrazole planes are 159.35° (B1, 174.49 and B2, 163.53) around Co(1) and 151.35° (B1, 176.85 and B2, 155.63) in Co(2). This significant difference is attributed to the position of the Carbon linker atom in the ring incorporating Co(2). Here, the carbon atom is raised out of the NNCC plane at an angle of 24.37°, compared to 16.47° in the Co(1) ring. As predicted, this increased angle, and the small but significant effect on the average boat angle has incurred an increase in the inter pyrazole plane angle in the metallocycle incorporating Co(1). The two anionic bis pyrazole ligands, in which one half functions 'normally' as a single N donor to the Co centre and the other is able to bond to two sites via two different nitrogen atoms due to its deprotonation, show no significant structural differences to their neutral counterparts, with the bond lengths and angles in the 5 membered pyrazole rings relatively similar. The constraint imposed by the rigidity of the anionic bond to the other cobalt centre has brought the ligands closer to the metal to which the ligand has chelated to with average Co-N(ligand) distances of 1.9215Å Co(1) and 1.917Å Co(2) respectively, confirmed by a slightly larger bite angle at the chelating centre, measured at an average of 89.4°. It is not appropriate to measure the

effect of these extra bonds on the boat angles as the environments of the pyrazole rings are no longer symmetrical due to them being fixed to the bulk of the complex.

The hydroxy bridge between the two metals, confirmed by the broad IR peak at 3590 cm^{-1} is at an average of 1.877 Å (Co(1)-O(1) – 1.874(2) Å, Co(2)-O(1) – 1.880(2) Å), and is slightly shorter than some relatively similar complexes containing two cobalt centres and N donor ligands. [Tp^{iPr2}Co]$_2$(μ-OH)(μ-OBz) - 1.938 Å[18] and Co$_2$L1(μ-OH)(CH$_3$CN)$_4$]$^{3+}$ - 1.999 Å[19] where L1 is the acyclic pyridazine based Schiff base ligand 1.
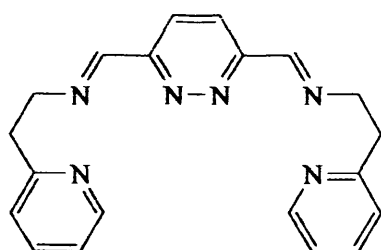
1

Both Incarvito[20] and Buchler[21] among others have also published OH bridged metal centres. In these cases the ligands utilised are capable of bimetallic bonding, and consist of two flexible arms attached to a central 5 membered heterocycle. In addition to the OH bridge, the M-M distance is also spanned by the complexation to one of the nitrogen atoms provided by the central 5 membered ring to each metal atom, forming a new metallocycle, N-Co-O-Co-N.
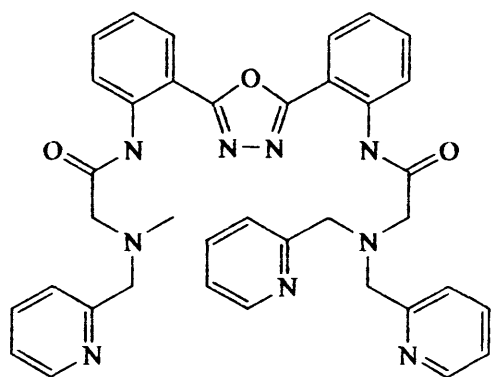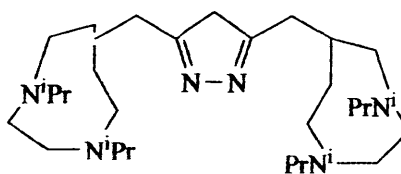
2   3

The complex of 2, [Co(μ-OH)(oxapyme)CoN₃](PF₆)₂, described by Incarvito and collaborators has an average Co-O distance at 1.942 Å while a dinickel complex of the TACN/pyrazolate ligand above (3) shows average M-O value of 1.9925°.

Hydrogen bonding

Hydrogen bonds play a significant role here as two as also included in the asymmetric unit are a chloride ion and a $[CoCl_4]^{2-}$ moiety. Reflection and growth of the asymmetric unit reveals two chloride ions, bridging two units of the system described in **figure 3.26** which are arranged in 'head to toe' fashion. Also found, the two $[CoCl_4]^{2-}$ are required to provide a (+111) environment for both cobalt atoms. The two chloride ions are associated with three nitrogen atoms each. Two are from the neutral ligands on one side of the dimer (N(4) an N(14)) and the other from an anionc ligand on the opposite side of the dimer (N(12), at distances of 3.134Å, 3.098Å and 3.137Å respectively. The $[CoCl_4]^{2-}$ fragments are set at a distance N(16)-Cl(2) – 3.063Å.
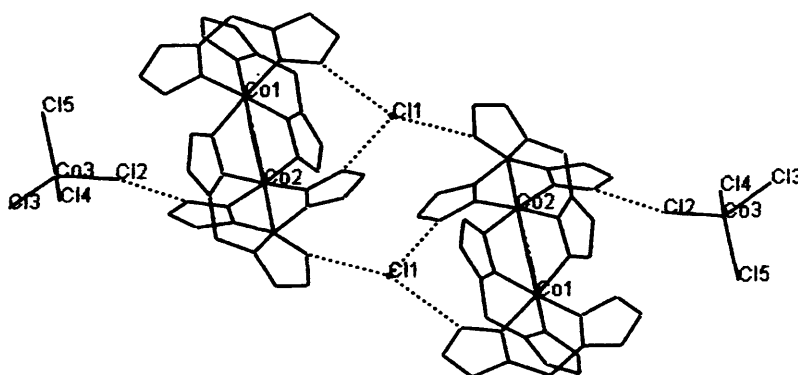
Figure 3.26: Hydrogen bonding linking two bimetallic moieties via a chloride bridge

In addition, three molecules of acetonitrile are present in the asymmetric unit. Two are associated with the dimeric structure with interaction between N(6) and a molecule of acetonitrile, at a length of 2.804Å, and an interaction between the bridging oxygen and acetonitrile is also measured at 3.990Å.

Analysis of $([(2f)_2Co](Cl)_2)_n$ **(3f)**

The X-ray crystal structure of the highly insoluble pink material obtained from the same flask shows the formation of a coordination polymer (**figure 3.27**), with cobalt (II) chloride units bridged by double stranded loops of ligand **2f** in a 1-dimensional repeating fashion where the metal sites are in the crystallographic inversion centre.
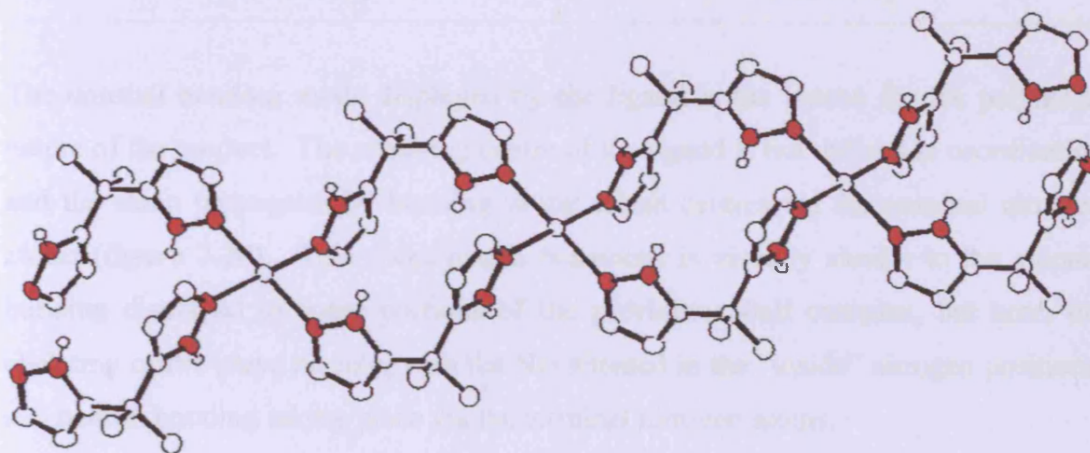
Nitrogen atoms are depicted in colour, chlorine and majority of hydrogen atoms removed for clarity

Figure 3.27: X Ray Structure of polymeric structure **3f**

One dimensional coordination complexes are known, and this novel compound resembles the general structure exhibited by several others published including the Co(II) complex reported by Zhao and collaborators in 2002 utilising the ligand 1,3-bis(triazol-1-yl)propane[22] and the Co, Fe, and Ni 1-D complexes synthesised by Hernandez and collaborators in 1999 with the ligand 1,2-bis(4-pyridyl)ethane[23]. The asymmetric unit for the structure consists of one half of the repeating unit, with the other half generated by reflection. A single molecule of acetonitrile is also present. The near perfect octahedral cobalt centres, (see selected bond angles in **table 3.7**) are spaced at 7.879 Å and are arranged in a linear fashion (Co-Co-Co = 180°). The equatorial plane is occupied by four nitrogen atoms from separate pyrazole rings and the axial positions are occupied by chloride ions. The average Co-N(ligand) bond distance of 2.133 Å is considerably longer than the values obtained in the previous cobalt complex reported (1.907-1.948 Å), with the chloride ions equidistant at Co-Cl distances of 2.48(8) Å.

Table 3.7: Selected bond angles within **3f**

Bond Angles°	
Cl(1)-Co-Cl(1')	180.0(4)
N(1)-Co-N(1')	180.0(1)
Cl(1)-Co-N(1)	89.60(7)
Cl(1)-Co-N(3)	90.26(10)

The unusual bonding mode displayed by the ligand is the reason for the polymeric nature of the product. The chelating centre of the ligand is not utilised in coordination and the chain propagates by bonding to the cobalt centres via the terminal nitrogen atoms (**figure 3.28**). This coordination behaviour is visually similar to the anionic bonding displayed in some portions of the previous cobalt complex, but here, the chelating centre plays no role, with the NH situated in the "inside" nitrogen positions, and neutral bonding taking place via the terminal nitrogen atoms.
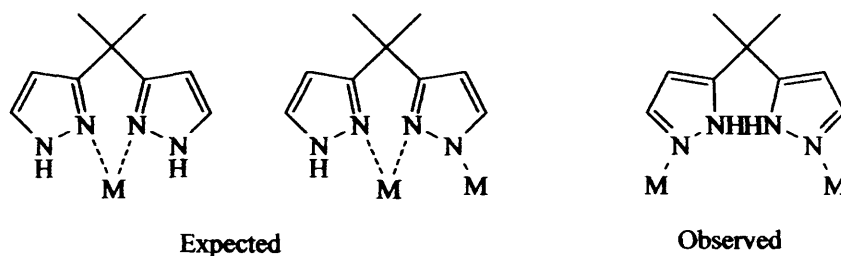
Expected   Observed

Figure 3.28: Expected and observed bonding modes for **3f**

In order to form the 16 membered rings, the ligands loops are formed via "head to toe" arrangement, accounting for the linear structure observed (**figure 3.29**). The ligand is twisted with the plane of each azole ring at almost 90° (dihedral angle between the two azole planes N(4)-C(9)-C(3)-N(2) measured as 88.34°) to its partner (**figure 3.30**). The resulting distorted square cavity has dimensions of ca. 5.5 x 5.5Å (**figure 3.31**).
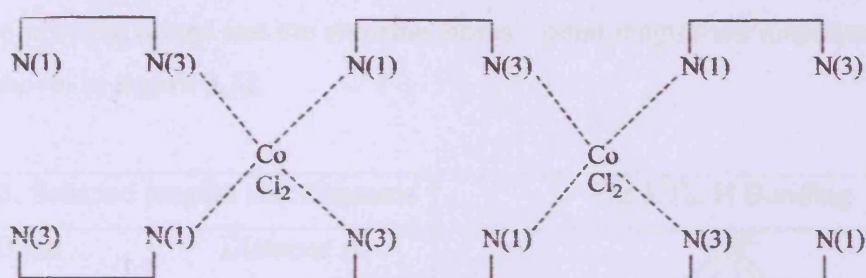
Figure 3.29: Head to toe arrangement of ligands in complex **3f**
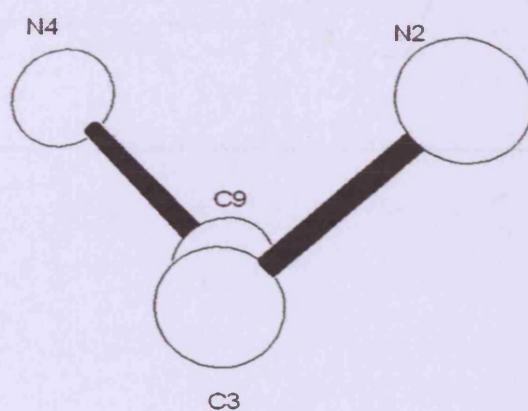
Fig 3.30: Dihedral angle between pyrazole planes in **3f**
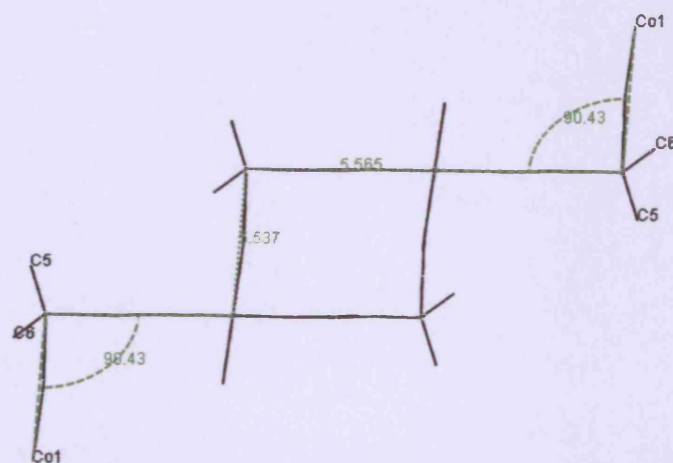
Figure 3.31: Intermetallic distances and angles in **3f**

The hydrogen bond network present in this polymeric complex is one dimensional, and does not provide a link between adjacent strands. Most interactions are between

the ligand nitrogen atoms and the chlorine atoms. Bond lengths are displayed in **table 3.8** and shown in **figure 3.32**.

Table 3.8: Selected lengths and distances		Fig 3.32: H Bonding
H-Bond	Distance Å	
N(1)-Cl(1)	3.283	
N(1)-N(3)	3.024	
N(2)-Cl(1)	3.140	
N(3)-Cl(1)	3.195	
N(4)-Cl(1)	3.098	

Fig 3.32: H Bonding

Microanalysis suggested this was not the case, and we proceeded to investigate the complex further (Found C: 39.1, H: 4.15, N: 20.65). An infared study confirmed no μ-OH bridge was present with the only absorption around 3500 cm⁻ being a sharp at 3497.3 cm⁻ coresponding to the NH displayed in the crystal structure.

X Ray Analysis

From the X-ray structure (figure 3.34) it is clear that the complex obtained is similar in many respects to the building block of the cobalt (iii) dimer discussed earlier. The complex contains an oxo bridged dimetallic core and the ligand is present in both the

neutral and deprotonated form. The asymmetric unit contains seven molecules of acetonitrile and an acetate moiety, probably from the hydrolysis of a molecule of solvent. Selected bond angles and distances are displayed in **table 3.9**.
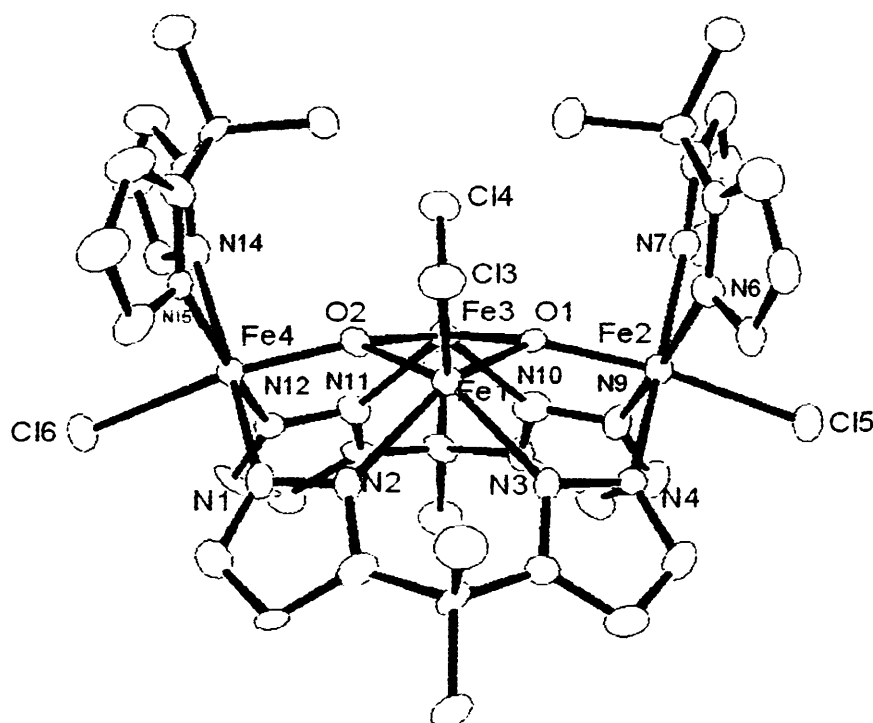
Hydrogen atoms have been omitted for clarity

Fig 3.34: X Ray structure of [(2f)₄(Fe)₂(μ-OFe)₂Cl₄] (3g)

Four iron centres are present in this complex, with two having distorted octahedral geometries, and the other half in a distorted square pyramidal environment (τ = 0.0105 Fe(1) and 0.0125 Fe(3)). At the core of this 1:1 iron to ligand cluster are two μ₃-O bridges, displayed in **figure 3.35**. A single chloride ion is also associated with each iron atom at an average distance of 2.372 Å(octahedral) and 2.2215 Å(square pyramidal).
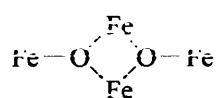
Figure 3.35: Iron core of 3g

Table 3.9: Selected angles and distances from 3g

Bond Lengths Å			
Fe(1)-N(2)	2.0490(8)	Fe(3)-N(10)	2.0557(8)
Fe(1)-N(3)	2.0670(7)	Fe(3)-N(11)	2.050(8)
Fe(1)-O(1)	1.930(5)	Fe(3)-O(1)	1.927(5)
Fe(1)-O(2)	1.938(5)	Fe(3)-O(2)	2.219(3)
Fe(1)-Cl(3)	2.224(3)	Fe(3)-Cl(4)	1.942(5)
Fe(2)-N(4)	2.103(7)	Fe(4)-N(1)	2.114(8)
Fe(2)-N(6)	2.142(8)	Fe(4)-N(12)	2.114(8)
Fe(2)-N(7)	2.133(8)	Fe(4)-N(14)	2.170(8)
Fe(2)-N(9)	2.076(8)	Fe(4)-N(15)	2.165(7)
Fe(2)-O(1)	1.887(5)	Fe(4)-O(2)	1.871(6)
Fe(2)-Cl(5)	2.377(3)	Fe(4)-Cl(6)	2.367(3)
Bond Angles °			
O(2)-Fe(1)-N(3)	142.0(3)	O(1)-Fe(3)-N(3)	141.2(3)
O(1)-Fe(1)-N(2)	142.6(3)	O(2)-Fe(3)-N(10)	141.9(3)
N(4)-Fe(2)-N(7)	168.0(3)	O(2)-Fe(4)-Cl(6)	170.7(2)
N(9)-Fe(2)-N(6)	171.4(3)	N(1)-Fe(4)-N(14)	168.4(3)
O(1)-Fe(2)-Cl(5)	172.6(2)	N(12)-Fe(4)-N(15)	167.3(3)
Fe(2)-O(1)-Fe(3)	127.1(3)	Fe(1)-O(2)-Fe(3)	95.9(2)
Fe(2)-O(1)-Fe(1)	127.3(3)	Fe(4)-O(2)-Fe(1)	127.5(3)
Fe(3)-O(1)-Fe(1)	96.7(2)	Fe(4)-O(2)-Fe(3)	127.8(3)

As seen in **figure 3.34**, the ligand, similarly to complex **3e**, is present here in two different forms. As expected, the ligand acts as a neutral donor of two nitrogen atoms, but it also plays a role not seen in any other complex synthesised by us. The presence of a doubly anionic ligand again increases the number of coordination modes seen displayed by this ligand. Here, the two anionic ligands are associated with three of the metal centres each, via four $N_{(ligand)}$-Fe bonds. **Figure 3.36** displays one of the doubly anionic ligands and its association with three out of the four iron centres.
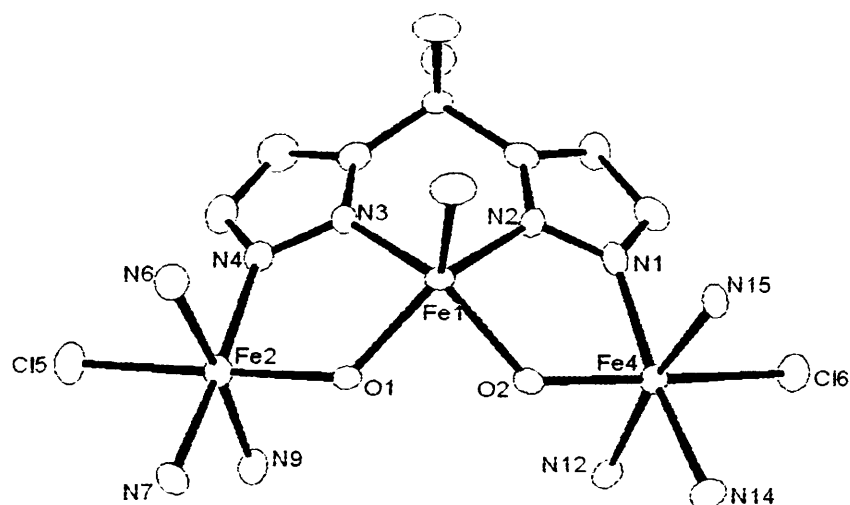
Figure 3.36: Ability of a single ligand to interact with 3 metal centres

The non equivalent iron centres i.e. Fe(1)-Fe(2) or Fe(1)-Fe(4) as shown above, are linked via 5 membered rings created through the sharing of an oxygen and nitrogen atom between the two relevant metal atoms.

Boat Angles

The 6 membered metallocycles displayed in the formation of this complex have a shallow boat geometry. The metallocycles containing no restrictions from the ligand bonding to more than one metal are those containing Fe(2) and Fe(4). The metallocycle incorporating Fe(2) (**figure 3.37**) has an average boat angle of 156.38° (B1, 165.90° and B2, 147.48°). The corresponding angle of pyrazole plane intersection is 139.68°.
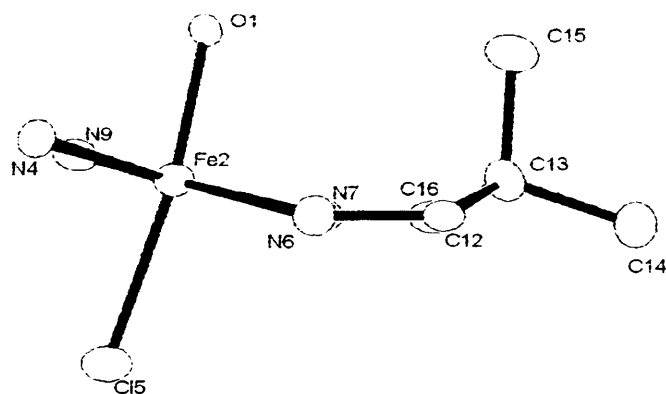
Fig 3.37: Boat configuration around Fe(2)

Figure 3.38 shows the metallocycle formed around Fe(4) and displays a structure considerably different to that previously described. The average boat angle of 152.48° shows a slight decrease, indicating the boat to be more planar than the previous example. However, the angle of pyrazole plane intersection is considerably lower (approximately 11.5° lower) at 128.10°. This result is surprising and does not fit with the hypothesis that with an increase in boat depth comes a decrease in the inter plane angle.
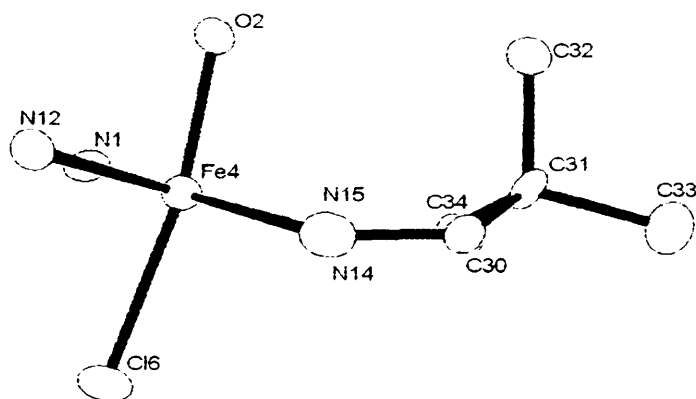
Figure 3.38: Boat configuration around Fe(4)

This may possibly be explained by stereochemical factors, with the axial methyl groups C(1) and C(32) pointing directly towards each other (**figure 3.34**).

While we were unable to compare the boat structure obtained by the intervention of the anionic portion of the cobalt structure described previously, here, the structures

obtained are symmetrical due to the ligands being presented in a doubly anionic form. The respective angles are displayed in **table 3.10** and obey the general rule in which the depth of the metallocycle formed increases as the pyrazole rings are folded back.

Table 3.10: Boat angles within **3g**

Metal Centre	B1 °	B2 °	Average °	Pyr/Pyr °
Fe(1)	165.60	144.03	154.81	137.52
Fe(3)	166.20	141.71	153.95	135.30

Hyrogen bonding

The packing within this molecule is based upon the interaction between adjacent complex molecules and a common acetate moiety. The interactons between N(13) from one complex molecule and N(16) from its neighbouring to the acetate moiety O(3) are measured at 2.779Å and 2.719Å respectively. The alternating Iron clusters are roughly at right angles to their neighbour, a feature shown in **figure 3.38**.
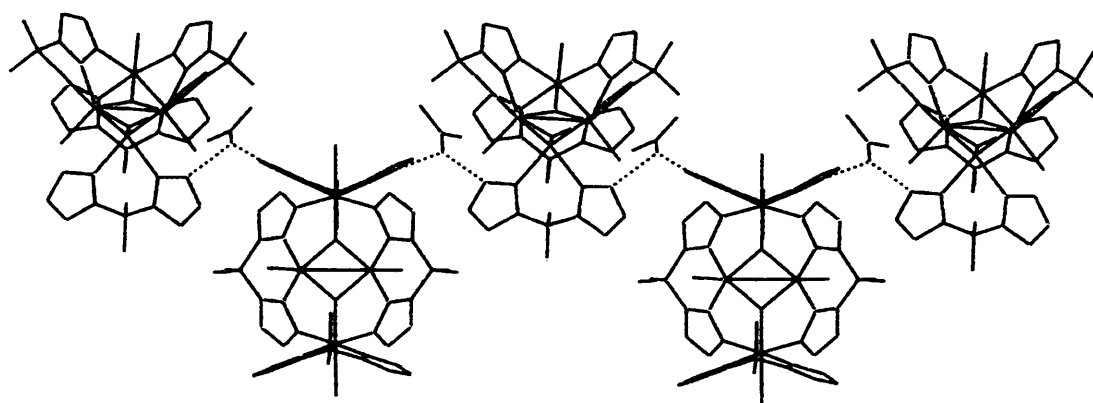
Fig 3.39: Hydrogen bonding within **3g**

Future Work

Described here will be a small list of compounds currently under development.

Reaction of 2f with rhodium

Reaction of 2f with [Rh(COD)₂]BF₄⁻ in dry dichloromehane according to figure 3.40, yielded a yellow solid on elimination of excess solvent. Our initial investigations lead us to believe that we have produced a [Rh(2f)(COD)]BF₄ adduct. Our initial ^{1}H NMR data, displayed in figure 3.41 shows what we believe to be an impure sample of the desired compound.

i = [Rh(COD)₂]BF₄
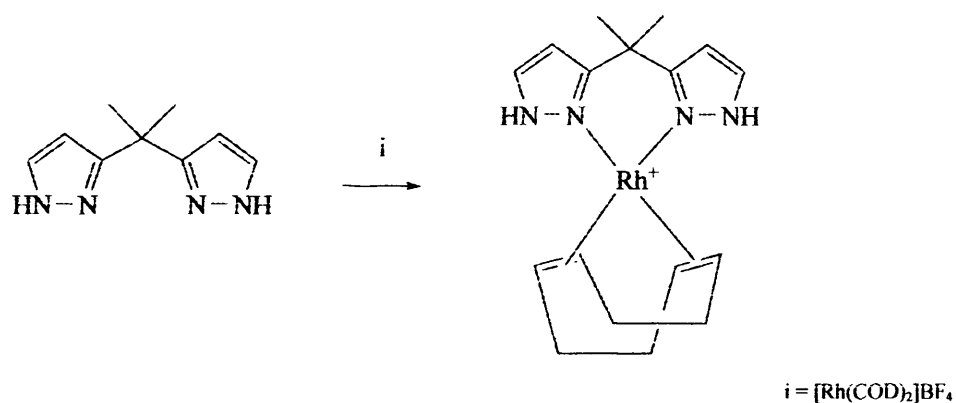
Figure 3.40: Potential Synthesis of [(2f)Rh(COD)]BF₄ (3h)

In our experience, the appearance of an NH peak in the spectrum is a sign that coordination has occurred. The spectrum obtained by us clearly shows this feature at 11.30 ppm.
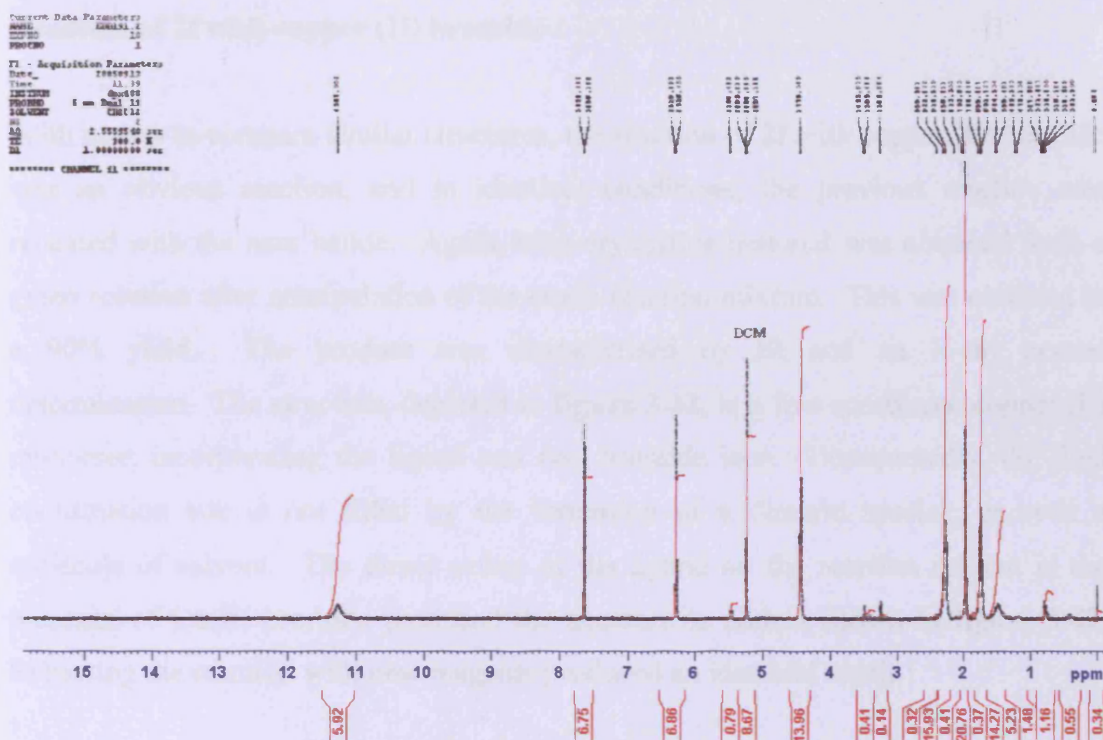
Figure 3.41: ^{1}H NMR Spectrum of product suspected to be (**3h**)

Also, the peaks representing the pyrazole protons are clear, sharp doublets at 7.65 and 6.30 ppm with coupling constants at an average of 2.635 Hz (2.63 and 2.64). A single peak to represent the Rh-Olefin protons is located at 4.45 ppm suggesting a symmetrical molecule. The non aromatic COD protons found at 2.25ppm and 1.75 ppm, with both peaks representing 4 protons are within the limits for similar compounds[25].

We have been unable to obtain a pure sample in order to collect X Ray data or elemental analysis.

Reaction of 2f with copper (II) bromide

With a view to compare similar structures, the reaction of 2f with copper (II) bromide was an obvious reaction, and in identical conditions, the previous reaction was repeated with the new halide. Again, blue crystalline material was obtained from a green solution after manipulation of the crude reaction mixture. This was obtained in a 90% yield. The product was characterised by IR and an X-ray crystal determination. The structure, depicted in **figure 3.42**, is a five coordinate copper (II) monomer, incorporating the ligand and two bromide ions. Unexpectedly, the final coordination site is not filled by the formation of a dimeric species, or even a molecule of solvent. The direct action of the ligand on the reaction solvent in the presence of Cu(II) bromide produced the acetonitrile adduct shown in **figure 3.42**. Repeating the reaction with new reagents produced an identical result.
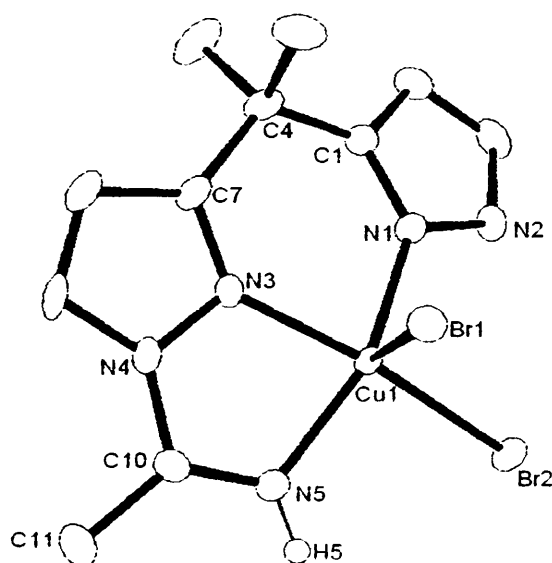
Fig 3.42: X Ray structure of 3i

The monomeric structure obtained has a distorted square pyramidal geometry (τ = 0.070). With the synthesis of a five membered ring on complexation Cu-N(5)-C(10)-N(4)-N(3) in addition to the expected six membered metallocycle Cu-N(1)-C(3)-C(4)-C(7)-N(3), the structure is under considerable constraint with C(7) lifted out of the usually flat plane displayed by all complexes described thus far, occupied by N(1)-

N(3)-C(1)-C(7) or the equivalent. **Table 3.11** lists selected distances and angles with the complete data including collection and refinement details together with the atomic coordinates to be found in appendix A.

Table 3.11: Selected bond lengths and angles within 3i

Bond Lengths Å		Bond Angles°	
Cu(1)-Br(1)	2.6976(18)	N(1)-Cu(1)-N(3)	84.17(10)
Cu(1)-Br(2)	2.4046(13)	N(1)-Cu(1)-N(5)	158.22(10)
Cu(1)-N(1)	1.990(2)	N(3)-Cu(1)-Br(2)	162.47(7)
Cu(1)-N(3)	1.959(3)	N(3)-Cu(1)-N(5)	79.28(10)
Cu(1)-N(5)	1.991(3)	Br(1)-Cu(1)-Br(2)	107.13(2)

By taking the relevant values contained in the table above, 162.46° β and 158.22° α, the structural parameter index, τ, is calculated at 0.07, a value reflecting its primarily square pyramidal structural system. Our initial investigations show this is the most likely product with the same result obtained on repetition of the experiment. IR data shows a peak at 1654 cm^{-1}, probably corresponding to the C=N bond formed. The formation of the complex is predicted to be as a result of the hydrolysis of a molecule of acetonitrile, associated to the metal centre on complexation. Further work is required, first investigating the reaction when performed in a non coordinating solvent.

Reaction of 2f and Nickel (II) Chloride

We have isolated a small amount of crystalline material, suitable for X Ray analysis from the reaction between **2f** and nickel (II) chloride hexahydrate. We expected a similar result to those obtained from the reaction of the same ligand in identical conditions with cobalt (II) chloride hexahydrate. However, for the small amount of material obtained, this was not the case. The initial results show the formation of a triangulo-pentahalo trimetal complex similar to those described by Gambrotta and collaborators[20] and more specifically, the nickel derivative published by Handley $[Ni_3Cl_4(OH)(tmen)_3]^+$ [27], which incorporated the diamine compound N,N,N',N'-tetramethylethane-1,2-dimaine (tmen).

The X ray determination, calculated by Dr Andreas Stasch at Cardiff University shows a triangulo Ni_3 unit with three bridging chlorides but no apparent metal – metal bond. One ligand molecule is bound to each metal atom with the CCNN plane used as the base of the boat in previous calculations at an angle of 85.88° to the M-M-M plane.
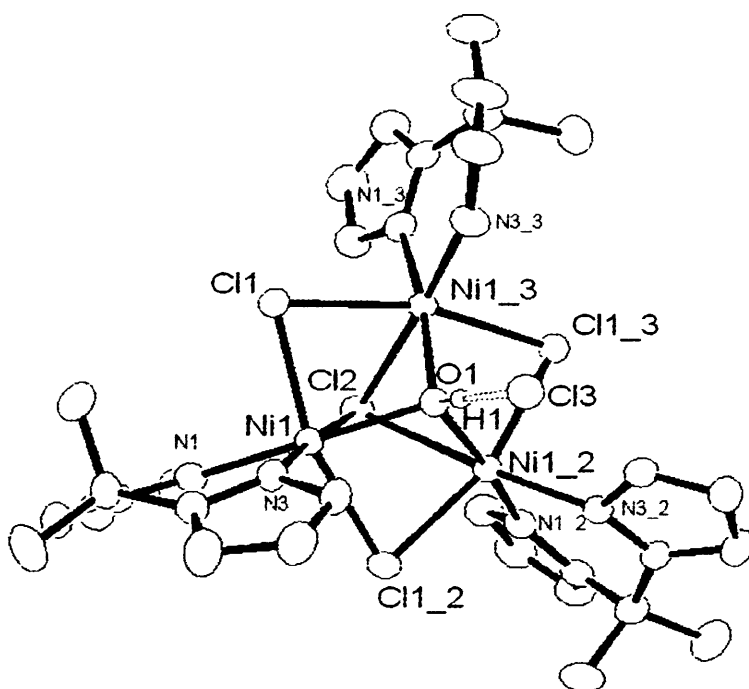
Figure 3.43: X Ray of 3j

As with the previous complexes, the structure contains a hydroxide group in the axial position above the M-M-M plane which is hydrogen bonded to a chlorine atom. Directly opposite, the final chloride ion sits below the M-M-M plane to complete the structure. Some bond angles and distances are listed in **table 3.12** with full data contained in appendix A.

Table 3.12: Selected bonds and angles within complex 3j

Atoms	Distance Å	Atoms	Angle °
Ni(1)-Cl(1)	2.4266(8)	N(3)-Ni(1)-Cl(2)	176.11(7)
Ni(1)-O(1)	2.0143(16)	N(1)-Ni(1)-O(1)	169.23(11)
Ni(1)-Cl(2)	2.5964(9)	Cl(1)-Ni(1)-Cl(1_2)	162.66(2)
Ni(1)-N(3)	2.0340(2)	N(1)-Ni(1)-N(3)	87.05(9)
Ni(1)-N(1)	2.0340(2)	Ni(1)-Cl(2)-Ni(1_2)	72.06(3)
O(1)-H(1)	0.925	Ni(1)-Cl(1)-Ni(1_3)	77.24(2)
H(1)-Cl(1)	2.128	Ni(1)-O(1)-Ni(1_3	98.60(10)

Each metal centre is in a distorted octahedral environment with the two pyrazole nitrogen atoms, the non hydrogen bonded chloride atom sitting below the M_3Cl_3 plane and the oxygen atom occupying the basal plane. The axial coordination sites are filled by two further chloride ions, supplied by the atoms within the M_3Cl_3 plane. These values compare closely with the structure published by Handley *et al* (**Table 3.13**).

Table 3.13: Bond Angles and Distances from $[Ni_3Cl_4(OH)(tmen)_3]Cl$

Atoms	Distance Å	Atoms	Angle °
Ni-X$_{eq}$	2.436(4)	Ni-Cl$_{eq}$-Ni	76.60(5)
Ni-N$_{ligand}$	2.127(9)	Ni-Cl$_{ax}$-Ni	73.57(11)
Ni-Cl$_{ax}$	2.530(3)	Ni-O-Ni	95.80(4)
Ni-O$_{ax}$	2.043(3)		
Ni-Ni	3.026(3)		

Boat angles

Due to the unsymmetrical nature of this compound about the Ni_3Cl_3 axis, the boat displayed is not uniform and shows the significant displacement of one pyrazole nitrogen out of the usually flat NNCC plane due to its proximity to the oxygen atom (**Figure 3.44**). Consequently, we are unable to compare the boat angles and the pyrazole plane intersection angles.
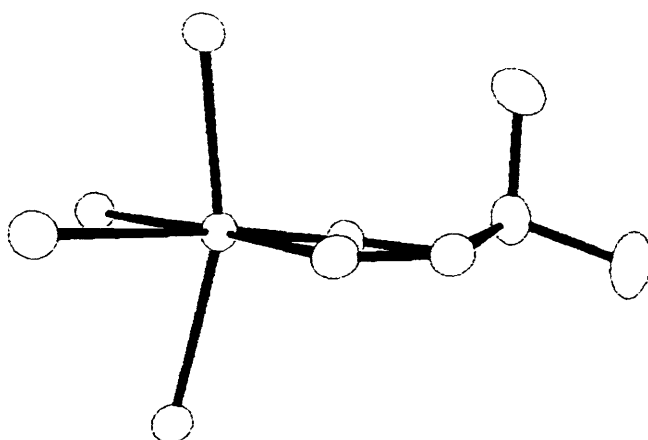
Fig 3.44: X ray diagram showing the unsymmetrical boat structure displayed by 3j

Conclusions

We have synthesised a number of novel complexes, mostly by the utilisation of the novel ligand **2f**. We have shown the ligand is extremely versatile and can form complexes by coordinating to metal centres in a number of different ways:

1. Neutrally through chelating centre
2. Mono-anionically
3. Di-anionically
4. Neutrally via outside nitrogen atoms in polymeric fashion.

We have also discovered that these new ligands are capable of forming complexes in a number of different ways:

1. Monomers
2. Halo bridged metal centres
3. Heteroatom bridged dimers
4. Polymers
5. Clusters

We have shown that this ligand shows similar coordination behaviour to bidentate scorpionate ligands in the formation of boat shaped metallocycles on coordination. **Table 3.14** shows our combined findings with regards to this particular property. The table shows how the depth of the boat shaped metallocycles formed on synthesis of complexes with our ligand is related to the angle of pyrazole plane intersection θ. The table also displays the expected trend with few exceptions (highlighted entries) and also that the dimensions of these boat shaped structures seem to be dependant on the characteristics of the metal as opposed to the nature of the complex obtained. Unfortunately, the feature of boat depth, although mentioned in almost every review of praozol-1-yl chemistry, is rarely measured, and as a consequence we are unable to provide a detailed comparison to the literature. Capparelli and Agrifolgio did provide some measurements in relation to their complex [Zn{H$_2$B(3,5-Me$_2$Pz)(3,5-

Ph$_2$Pz)}$_2$]^{15}, however the dihedral angles have been measured in a different way to us. The Zinc complex is described as having a shallow boat conformation although we have not been able to view the structure in 3D in order to compare. It is difficult to predict the mechanism behind the boat formation complex from the data we have collected as we have information on complexes which all display a different coordination mode to the next. The highlighted entries show that our complexes do not conform to the theory that as the dihedral angle between the pyrazole planes approaches 180°, the depth of the boat formed decreases. However, the entries that do not conform seem to show a steric influence could be causing this effect. Without a far more comprehensive library to measure and a detailed investigation of the electronic influences contained within the complexes, we will be unable to accurately predict the orientation of future complexes, however the data we have collected is an excellent starting point. Fortunately, the structurally similar complexes 3a and 3b do allow us to look at the effect of substitution at the bridging carbon position on the depth of the boat formed. As described earlier, there is a significant difference between the two complexes with the less bulk complex 3a showing a depth some 5° deeper than 3b at an average of 155.60°. It is reasonable to assume that the lack of bulk around the ring bridging carbon in 3a is allowing the boat to become deeper, probably leading to tighter packing. We have seen previously that the agostic interaction is more common in complexes displaying a deep boat, however it is not the case here as no interaction between the axial proton and the palladium centre. However, with a wider application of ligand 3a, we may be able to see the first agostic interaction between a metal centre and a pyrazoly-3-yl ligand. This may be observed by replicating the coordination chemistry of complex 3c (our novel copper complex showing the deepest boat configuration) with the ligand 2a in order to design the best conditions to encourage boat depth.

Table 3.14: Boat configuration trends

Complex	Metal Atom	Mean Boat	Increasing boat depth	θ	Decreasing θ
3e	Co(1)	169.01		159.35	
3e	Co(2)	166.24		151.35	
3b	Pd(1)	160.85		151.96	
3j	Ni(1)	160.08		147.26	
3g	Fe(2)	156.38		139.68	
3g	Fe(4)	152.48		128.10	
3c	Cu(1)	147.85		132.30	
3d	Cu(2)	146.08		120.57	
3d	Cu(1)	145.35		129.10	

Experimental

General Comments

Standard equipment and techniques were used as in chapter 2. In addition:

Crystals were diffracted in a Bruker Nonius Kappa CCD area detector using graphite monochromtised MoKα radiation, I = 0.71073Å.

All elemental analyses were kindly carried out by the Warwick Analytical Service Ltd.

All starting materials were obtained from Aldrich Chemicals unless otherwise stated.

[Pd(MeCN)$_2$Cl$_2$] and [Pd(COD)Cl$_2$] were kindly donated by Johnson Matthey

[MePd(COD)Cl] was prepared via an adapted literature method[28].

[Rh(COD)$_2$]BF$_4$ was prepared via an adapted literature method.

Preparation of Complexes

General Method for the Synthesis of complexes (3a - 3b)

To an acetonitrile solution of PdCl$_2$(MeCN)$_2$ a stoichiometric solution of ligand in acetonitrile was added and stirred at room temperature. After 1 hour, the solution was reduced in volume and the resulting red/orange solid washed with Et$_2$O, hexanes and dried under vacuum.

[Pd(2f)]Cl$_2$ (3a)
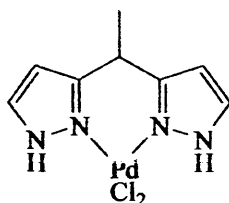
Palladium complex 3a was prepared according to the general method using ligand 2f (0.5g, 3.0 mmol) and PdCl$_2$(MeCN)$_2$ (0.78g, 3.0 mmol). Yield (0.619g, 75%). Anal. Calcd for C$_8$H$_{10}$N$_4$PdCl$_2$: C, 28.30; H, 2.97; N, 16.50. Found: C, 28.31; H, 2.88; N, 16.42. H^{i}NMR (CDCl$_3$, δ) 11.75 (s (br), 2H, NH) 7.58 (m, 2H, Pyr HPz) 6.32 (m, 2H, HPz) 4.35 (q, J = 7.47, 1H, CH) 1.61 (d, J = 7.31, 3H, CH_3). MS (ES) m/z: 163.1 ([2f]$^+$), 268 ([2f + Pd]$^+$), 305 ([2f Pd Cl]$^+$)

[Pd(2f]Cl₂ (3b)
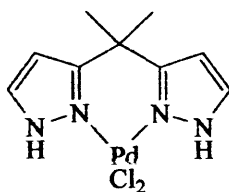
Palladium complex 3b was prepared according to the general method using ligand 2f (0.5g, 2.8 mmol) and PdCl$_2$(MeCN)$_2$ (0.74g, 2.8mmol). Yield (0.619g, 84%). Anal. Calcd for C$_9$H$_{12}$N$_4$PdCl$_2$: C, 30.58; H, 3.42; N, 15.85. Found: C, 30.52; H, 3.28; N, 15.78. H^{i}NMR (CDCl$_3$, δ): 11.8 (s (br), 2H, NH) 7.55 (m, 2H, HPz) 6.35 (m, 2H, HPz) 1.70 (s, 6H, CH_3). IR (KBr, cm^{-1}): 3317, 3116, 2956, 1649, 1513, 1443, 1358.

General Method for the Synthesis of complexes 3c – 3g

To an acetonitrile solution of the appropriate metal salt (2 equiv) in MeCN, a solution of 2f (1 equiv.) in acetonitrile was added and stirred at room temperature. After 1-24 hours, the solution was filtered through celite and reduced in volume. The desired products were recovered 1 day-1 month later as described.

([Cu(2f)]Cl₂)₂ 3c

Copper (II) complex 3c was prepared according to the general method using ligand 2f and copper (II) chloride. The reaction mixture was allowed to stir for 24 hours before filtration. Yield(0.14g, 80%). Anal. Calcd for $C_{19}H_{24}N_8CuCl_4$: C, 234.79; H, 3.89; N, 18.03. Found: C, 34.69; H, 3.84; N, 17.79. IR (KBr cm^{-1}): 3357, 3206, 2945, 2363, 1764, 1503, 1363.

[Cu(2f)₂](OTf)₂ (3d)

Copper complex **3d** was prepared according to the general method using ligand **2f** (0.20g, 1.13 mmol) and coper (II) triflate (0.20g 0.57 mmol). The reaction mixture was allowed to stir for 16 hours before filtration. No crystals were obtained when the filtered and reduced reaction mixture was allowed to stand. Material suitable for X Ray was obtained from slow diffusion of hexanes into a concentrated sample of the complex into dichloromethane (DCM). Yield (0.25g, 62%) Anal. Calc For $[C_{18}H_{24}N_8Cu](CF_3SO_3).1.5$ MeCN C: 35.61, H: 3.70, N 17.15, Found C: 35.67, H: 3.57, N: 17.90.

[Co₂(2f)₂(μ-OH)]Cl.[CoCl₄] (3e)

$[Co_2(2f)_2(\mu\text{-}OH)]Cl.[CoCl_4]$ (3e)

Cobalt complex 3e was prepared according to the general method using ligand 2f (0.20g, 1.13 mmol) and coper (II) triflate (0.20g 0.57 mmol). The reaction mixture was allowed to stir for 16 hours before filtration. No crystals were obtained when the filtered and reduced reaction mixture was allowed to stand. Material suitable for X Ray was obtained from slow diffusion of hexanes into a concentrated sample of the complex into dichloromethane (DCM). Yield (0.2g, 33%) Anal Calcd for [$C_{36}H_{47}$ $N_{16}Co_2O$]Cl.[CoCl₄] C: 40.26, H:4.41, N 20.87. Found C: 40.00, H: 5.48, N: 20.87

([Co(2f)₂]Cl₂)ₙ (3f)

The polymeric cobalt complex **3f** was prepared according to the general method using ligand **2f** (0.20g, 1.13 mmol) and copper (II) triflate (0.20g 0.57 mmol). The reaction mixture was allowed to stir for 16 hours before filtration. No crystals were obtained when the filtered and reduced reaction mixture was allowed to stand. Material suitable for X Ray was obtained from slow diffusion of hexanes into a concentrated sample of the complex into dichloromethane (DCM). Yield (0.1g, 37%) Anal Calcd for C: 44.83, H: 5.02, N: 23.23. Found C: 44.45, H: 4.88, N: 23.01. IR (3226, 2950, 1600, 1543)

[(2f)₄(Fe)₂(μ-OFe)₂]Cl₄ (3g)

Iron complex **3g** was prepared according to the general method using ligand **2f** (0.75g, 4.26 mmol) and iron (II) chloride (anhydrous) (0.138g 8.5mmol). The reaction mixture was allowed to stir for 24 hours before filtration. Yield (0.218g, 47%). Anal. Calc for $C_{36}H_{44}Cl_4Fe_4N_{16}O_2$ C: 39.38, H: 4.04, N: 20.41, Found C: 39.01, H: 4.15, N: 20.65. IR (KBr, cm⁻¹) 3407, 3106, 2965, 2865, 1508

References

[1] D. L. Reger, J. R. Gardinier, P. J. Pellecchia, M. D. Smith, K. J. Brown, *Inorg Chem.*, **42**, 2003, 1469

[2] P. Wehman, G. C. Dol, E. R. Morman, P. C. J. Kamer, P. W. N. Van Leuwen, *Organometallics.*, **13**, 1994, 4856

[3] J. C. Jansen, H. Van Koningsveld, J. A. C. van Ooijen, J. Reedijk, *Inorg Chem.*, **19**, 1980, 170

[4] L. Tang, L. Zang, L. Li, P. Cheng, Z. Wang, J. Wang, *Inorg Chem.*, **38**, 1999, 6326

[5] D. L. Reger, J. E. Collins, M. A. Mathews, A. L. Rheingold, L. M. Liable-Sands, I. A. Guzei, *Inorg. Chem.*, **36**, 1997, 6266

[6] A. Otero, J. Fernandez-Beza, A. Anitolo, J. Tejeda, A. Lara-Sanchez, L. F. Sanchez-Barba, I. Opez-Solera A. M =. Rodriguez, *Inorg Chem.*, **46**, 2007, 1760

[7] A. Shaver, *Organomet. Chem. Rev.*, **3**, 1977, 157

[8] K. Niedenzu, H. Noeth, *Chem. Ber.*, **116**, 1983, 1132

[9] B. F. Fieselmann, D. N. Hendrickson, G. D. Stucky, *Inorg. Chem.*, **17**, 1978, 2047

[10] C. A. Kosky, P. Ganis, G. Avitabile, *Acta Cryst.*, **27**, 1971, 1859

[11] F. A. Cotton, M. Jeremic, A. Shaver, *Inorg. Chim. Acta.*, **6**, 1972, 543-551

[12] N. Arroyo, F. Gomez de la Torre, F. A. Jalon, B. R. Manzano, B. Moreno-Lara, A. M. Rodriguez, *J. Organomet. Chem.*, **603**, 2000, 174

[13] F. A. Jalon, B. R. Manzano, A. Otero, C. M. Rodriguz-Perez, J. Organomet Chem., **494**, 1995, 179

[14] C. P. Brock, N. Niedenzu, E. Hanecker, H. Noeth, *Acta Cryst.*, **10**, 1985, 1458

[15] M. V. Capparelli, G. Agrifoglio, *J. Cryst. Spec. Res.*, **22**, 1992, 651

[16] A. W. Addison, T. N. Rao, J. Reeijk, J. van Ruin, G. C. Verschoor, *Dalton Trans.*, 1984, 1349

[17] K. Uehara, S. Hikichi, A Inagaki, M. Akita, *Chem. Eur. J.*, **9**, 2005, 2788

[18] U. P. Singh, P. Babbar, A. K. Sharma, *Inorg. Chim. Acta.*, **358**, 2005, 271

[19] P. G. Plieger, A. J. Downard, B. Moubrakai, K. S. Murray, S. Brooker, *Dalton Trans.*, 2004, 2157

[20]   C. Incarvito, A. L. Rhiengold, A. L. Gavrilova, C. Jin Quin, B. Bosnich, *Inorg. Chem.*, **40**, 2001, 4101

[21]   S. Buchler, F. Meyer, E. Kenifer, H. Pritzkow, *Inorg. Chim. Acta.*, **337**, 2002, 371

[22]   Q. Zhao, H. Li, X. Wang, Z. Chen, *New. J. Chem.*, **26**, 2002, 1709

[23]   M. L. Hernandez, M. Gotzone Barandika, M. Karmele Urtiaga, R. Cortes, L. Lezama, M. Isabel Arriortura, T. Rojo, *Dalton Trans.*, 1999, 1401

[24]   L. D. Field, B. A. Messerle, L. P. Soler, T. W. Hambley, P. Turner, *J. Organomet. Chem.*, **655**, 2002, 146

[25]   D. Schott, P. Pregosin. Organometallics 25, 2006, 1974

[26]   J. J. Edema, W. Stauthamer, F. Van Bolhius, S. Gambarotta, W. J. J. Smeets, A. L. Spek, *Inrog. Chem.*, **29**, 1990, 1981

[27]   D. A. Handley, P. B. Hitchcock, G. J. Leigh, *Inorg Chim Acta.*, **314**, 2001, 1

[28]   M. Barbra, A. Marson, A. Sacarel, G. Mestrioni, J. Eernsting, C. Elsevier, *Organometallics.*, **23**, 2004, 1974

Chapter 4:

Ternary Copper (II) Complexes

Introduction

The synthesis of mixed ligand complexes containing anionic acac derivatives and an N,N' chelating nitrogen ligand are among the most researched areas in this field. Many examples exist, incorporating phen 1, bipy 2 and bis imines 3 among others, with a range of counter ions in order to resolve the necessary structural and electronic needs of the metal.

| 1 | 2 | 3 |
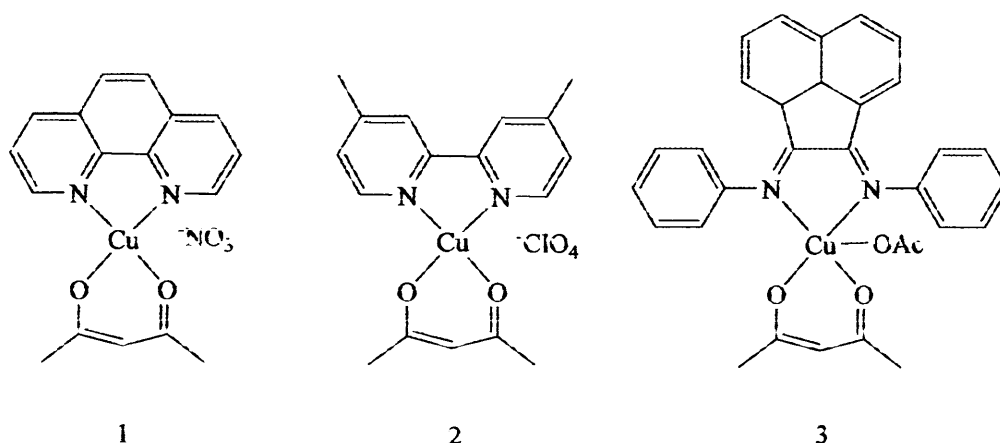
Compounds of this nature are extremely stable and their potential to display unusual spectroscopic, photochemical and electrochemical properties has attracted a wide range of interest. Our aim was to introduce a new dimension into the field, due to our knowledge of a little known compound, methyl triacetyl methane (MeTAM) 4.

4
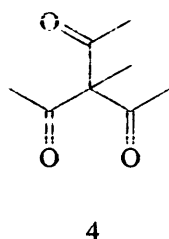
First synthesised in 1968, this potentially facially capping OO'O" chelating ligand had been left unresearched by the coordination chemistry community until its utilisation by Cavell and collaborators in the synthesis of a Cr^{iii} complex and its subsequent use in catalytic studies. Here we detail our attempt to synthesise mixed

ligand copper (II) complexes to incorporate our novel bis pyrazole-3-yl ligand 2f and MeTAM.
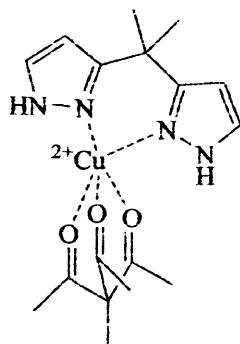
Fig 4.1: Potentially available mixed ligand complex

Chapter outline

The following chapter describes our attempts to synthesise a new family of triketone ligands, based on the ligand MeTAM, via a novel method. Our attempts to produce new ternary complexes incorporating these ligands is described, together with a section detailing the coordination chemistry of MeTAM as a separate ligand.

Synthesis of MeTAM

First synthesised by McKillop and collaborators[a], this compound was discovered while the authors were investigating the alkylation reactions of β-dicarbonyl compounds. They found excellent reaction yields of 90% and above for the reaction of the desired alkyl iodide with the thallium (I) salts of the required dicarbonyl. On development of this research, McKillop found that acylations were also possible via similar reactions. It was found that the acylation reactions could be controlled to give O- or C-acylation. McKillop discovered that reactions at -78°C, utilising acetyl chloride resulted in O-acylation at yields > 90%. However, reactions at room temperature with acetyl fluoride resulted is almost exclusive C-acylation as displayed in figure 4.2. Both reactions were conducted in diethyl ether.
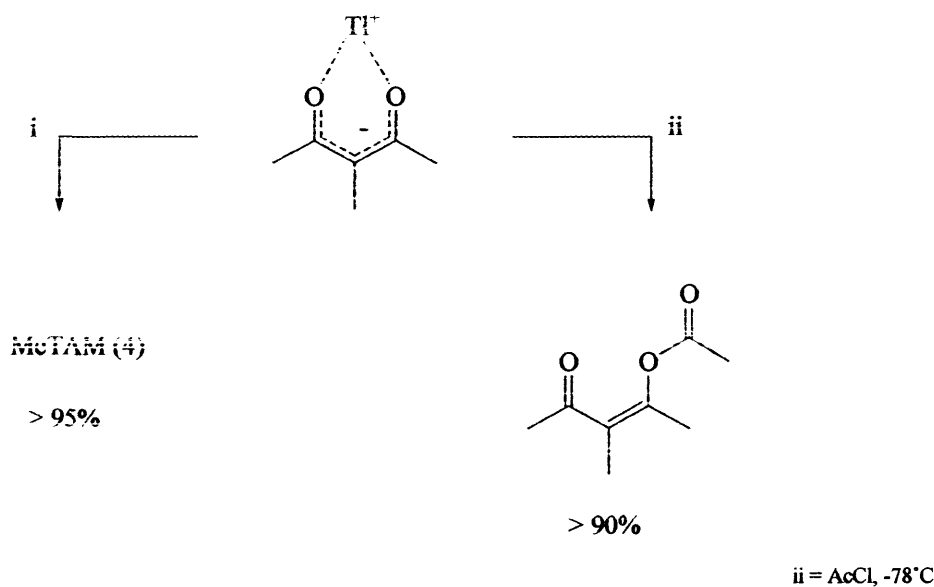
Figure 4.2: Reaction of thallium acac salts with acetyl halides

Other Tri-ketone Ligands

To our knowledge, the only other tripodal ligand of this type was synthesised by Gal and collaborators in 1982[b]. The synthetic route to the compound was relatively simple, starting from 3-methyl-2,4-pentanedione. The reaction, summarised in figure 4.3, proceeded via the deprotonation of the acac by magnesium powder and subsequent addition of the acid chloride allowed the synthesis to proceed. The

reaction was conducted in a 50/50 solution of toluene and benzene and the product was recovered in 25% yield.
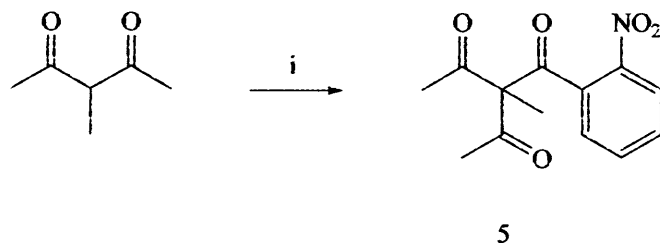
i = p-NO₂ArCl, Mg powder

Fig 4.3: Synthesis of 5

The authors did not investigate the potential of this compound as a coordination ligand however. The molecule was designed in order to create a new route to functionalised pyrazoles.
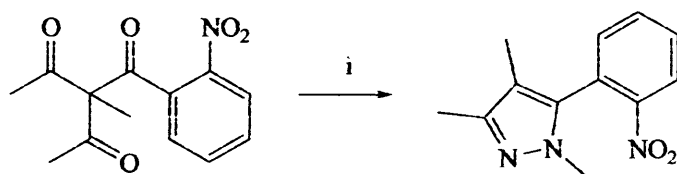
i = N₂H₄, TsOMe, H₂/Pd

Figure 4.4: Synthesis of functionalised pyrazole rings from 5

Coordination Chemistry of MeTAM

In 2002, Cavell and collaborators reported the synthesis of the first complex of MeTAM⁻. The Cr³⁻ complex, a green moisture sensitive solid, was obtained via the reaction of MeTAM with CrCl₃(THF)₃ under an inert atmosphere (figure 4.5) and was characterised by MS and microanalysis.
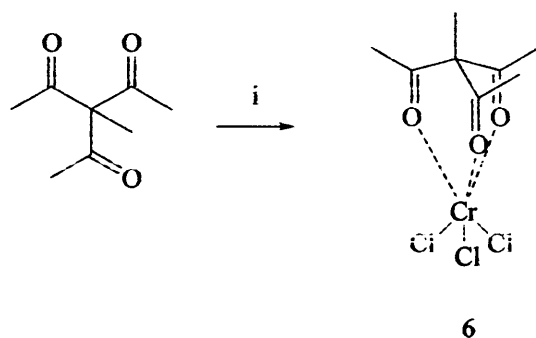
i = CrCl₃(THF)₃, CH₂Cl₂, 24 Hrs. 65%

Figure 4.5: Synthesis of the first complex of MeTAM (6)

Application of the ligand in catalysis (MMAO and ethylene) resulted in the highly selective conversion of ethylene into 1-alkenes.

Chapter Outline

The established methods of synthesis for MeTAM and similar compounds either involve undesirable starting materials, in the case of McKillop with highly toxic thallium, or have resulted in low yielding reactions. We have synthesised a number of new triketone compounds via a novel, high yielding method, and here we report the synthetic detail. In addition, we have attempted some simple co-ordination chemistry with these ligands and also attempted to utilise them in the synthesis of ternary copper (II) complexes incorporating the bis pyrazolyl ligands described earlier.

Results and Discussion

Novel MeTAM Synthesis

The desired compound (MeTAM) was synthesised in one step from 3-methyl-2,4-petanedione via a method similar to that of Gal. The reaction proceeded according to **scheme 4.6**. It is suspected that the addition of the Grignard serves two purposes. Firstly as a base to effectively remove the acidic proton at the 3-position, and secondly, to provide an effective protecting group, guarding against electrophilic attack.
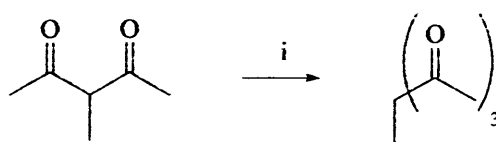
i = MeMgBr, AcCl, DME

Figure 4.6: Synthesis of 4 via a novel method

Solvent Effects

Initial studies by Coogan[*] highlighted the importance of the solvent selection for this reaction. The reaction of the magnesium salt of acac did not provide the same result as the thallium reaction conducted by McKillop. A number of inseparable compounds were obtained, certain to be a mixture of O- and C-acylated compounds. However, he reports the overwhelming advantage of using DME over more traditional reaction solvents. A quick overview of the findings by Coogan, generalised in **figure 4.7**, suggests that the presence of a chelating, coordinating solvent is key here, and provides the extra hindrance required so that the reaction proceeds via the anionic centre at the bridging carbon, and not at the nucleophilic carbonyl oxygen atoms. This was suggested due to the fact that on using more common solvents (THF, MeCN, Et$_2$O) the reaction yielded a mixture of products, proving difficult to separate. On utilisation of DME, the reaction returned a pure sample of the desired product in a yield of 80% after an aqueous workup.

* Unpublished
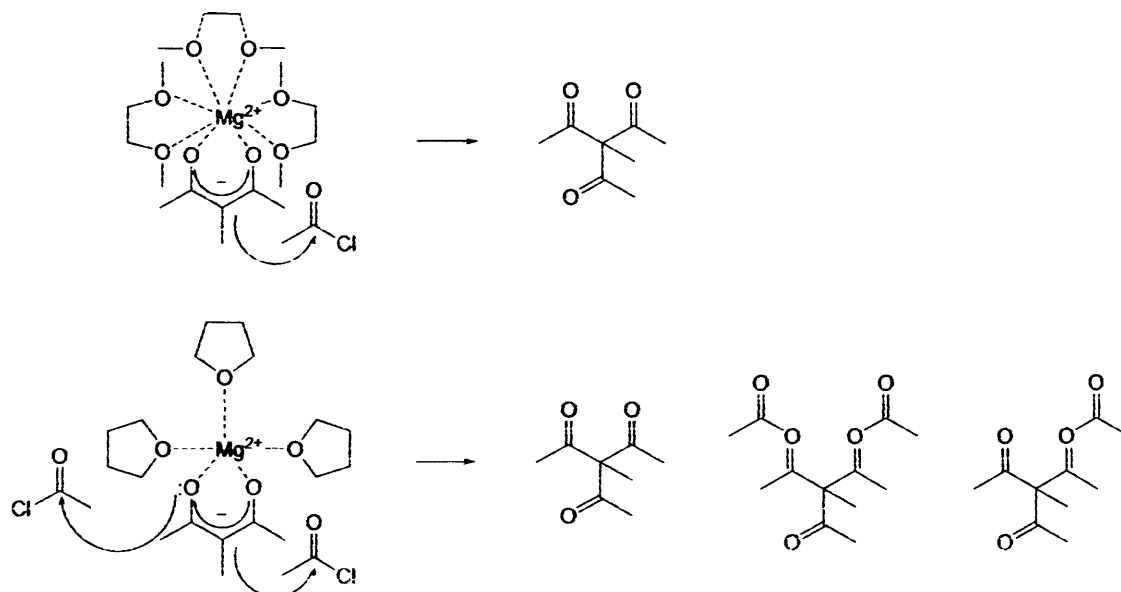
Figure 4.7: DME Vs Non chelating solvents (THF in this case)

On obtaining this result, it was decided to investigate the possibility of building a small library of tri-ketone compounds via an identical method, utilising commercially available acac derivatives to deliver a host of electronic and steric options. Two options were available to us in the exploration of new ligands in this class and eventually we were able to use a combination of both to build a small family of structurally analogous complexes. Firstly, using Me(acac) as a basis, we reacted with varying acid chloride compounds to produce triketones with the same acac backbone, allowing potential to study electronic effect in relation to potential structural differences within complexes. Next, we utilised some commercially available acac derivatives with varied R groups.

Novel Triketone Synthesis

Adhering to the general preparation outlined in **figure 4.6**, the synthesis of all new tri-ketones was achieved in the same way. The appropriate acac derivative was stirred in DMF.DMA at $0^\circ C$ under an inert atmosphere and an equimolar amount of methyl magnesium bromide (3M in diethyl ether) added dropwise. The solution was allowed to react for 1h at $0^\circ C$, and the acid chloride (equimolar) added neat, or as an ethereal solution. The reaction mixture was allowed to return to room temperature. During

the aqueous work up, ammonium chloride (saturated solution) was added to dissolve the mixture and then extracted into dichloromethane. The organic layer was washed with sodium hydrogen carbonate (saturated solution) and water, and then dried over magnesium sulphate. Filtration and removal of the solvent furnished the desired product in yields between 75% and 87% after recrystallisation from hot petroleum ether (40-60%). **Table 4.1** details the variable starting materials and compounds synthesised, quoting the yields obtained. Although compound **4** is not a new ligand, the route described here is yet to be published.

Table 4.1: Novel Tri-ketone Compounds

acac	ROCl	Product		Yield
			4	80%
			4a	75%
			4b	87%
			4c	80%

MeTAM (4)

The high resolution mass spectrum obtained suggests the presence of the molecular ion required, and a simple ^{1}H NMR spectrum obtained shows the methyl protons in

just two chemical environments. A 3:1 ratio of singlets at 2.10 and 1.55 ppm confirms the synthesis. We have also obtained a ^{13}C NMR and IR spectrum.

Synthesis of Compounds **4a-4c**

All compounds are novel and have been characterised by MS(ES), IR, ^{1}H NMR and ^{13}C NMR. Each has been isolated as a pale yellow solid, prone to decomposition over long periods, due to their moisture sensitive nature (**figure 4.8**).
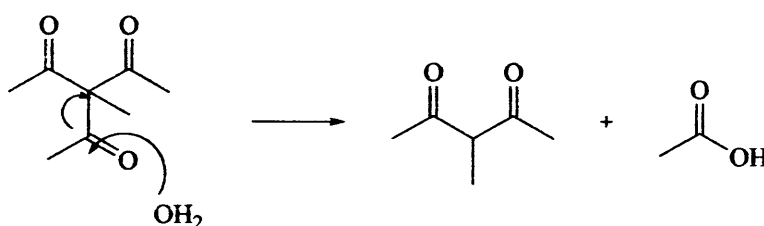
Figure 4.8: Moisture sensitivity of tri-ketones

The initial identification tool used was ^{1}H NMR. The relationship between the acetyl group and central axial methyl group (present in all compounds) being the main source of information and a handle on the expected integrations of all other peaks in the spectrum. **Table 4.2** lists the positions and ratio of the peaks mentioned.

Table 4.2

Compound	Central CH$_3$	Acetyl CH$_3$	Ratio
4a	1.70	2.20, 6H	1:2
4b	1.95	1.95, 3H	1:2
4c	1.80	2.05, 3H	1:1

The ^{1}H NMR spectra are unremarkable and show peaks in the predicted positions. In each case, the acylation at the carbon atom is confirmed by the disappearance of the quartet between 4-5 ppm found in the methyl acac starting materials.

Coordination Chemistry

Here we describe our findings upon the reaction of the selected tri-ketone compounds with copper (II) starting materials in the presence of equimolar amounts of the bis pyrazole-3-yl ligand **2f**.

Reaction of Copper (II) Triflate with equimolar amounts of MeTAM and **2f**.

On mixing acetonitrile solutions of MeTAM, bis pyrazole ligand **2f** and copper (II) trifluorosulfonate, a green solution was obtained after stirring for 3 hours. The solvent was removed to reveal a brown solid. Slow diffusion of hexanes into a concentrated dichloromethane solution revealed a number of blue block crystals, and later, green block crystals also formed. The material was separated, and individually characterised. The green material was found to be the complex **3d**, described in Chapter 3, obtained in 34% yield. The blue material was found to be a mixed ligand complex [Cu(MeAcac)2f(OTf)] **4d**, obtained in 27% yield. The complex was characterised by microanalysis, IR and X-ray crystal structure (**figure 4.10**).
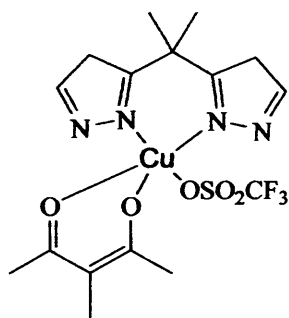
Fig 4.9: Novel ternary Cu(II) complex (**4d**)

The recovery of this decomposite ion product, although not ideal, confirms the ability of **2f** to participate in ternary complexes. No other by-products were recovered, however the decomposition of the MeTAM unit is likely to be due to the moisture sensitivity described earlier. Precautions were taken to ensure the reaction was not contaminated with water, and may go to show the vulnerability of this compound in

solution. The likely by-product is the carboxylic acid as the acetyl group is a poor nucleophile and not likely to have reacted with the triflate ions present.
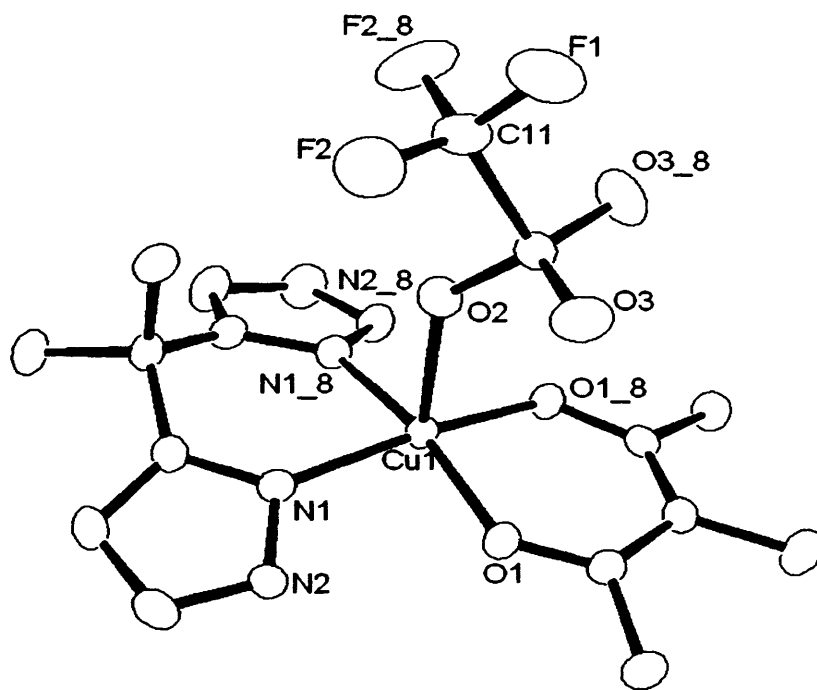
Hydrogen atoms have been omitted for clarity

Figure 4.10: X ray Structure of **4d**

X Ray Analysis

The complex shows a distorted square pyramidal copper (II) unit with two pyrazole nitrogen atoms and two oxygen atoms from acac occupying the basal plane. Although the structural index parameter ($\tau = 0$) suggests perfect square pyramidal geometry, the internal angles clearly show this is not the case. The triflate group in the apical position with a Cu(1)-O(2) distance of 2.356(2) Å. The mean Cu-(N)Pyrazole distance is 1.978 Å and the bite angle N(1)-Cu(1)-N(1_8) 86.7(10)°. Selected distances and angles are shown in **table 4.3**.

Table 4.3: Selected angles and distances from 4d

Bond Lengths Å		Bond Angles °	
Cu(1)-O(1)	1.910(13)	N(1)-Cu(1)-N(1_8)	86.7(10)
Cu(1)-O(1_8)	1.910(13)	N(1)-Cu(1)-O(1)	88.8(6)
Cu(1)-N(1)	1.978(18)	O(1')-Cu(1)-N(1_8)	88.8(6)
Cu(1)-N(1_8)	1.978(18)	O(1)-Cu(1)-O(1_8)	92.5(8)
Cu(1)-O(2)triflate	2.356(2)	N(1)-Cu(1)-O(1_8)	166.4(7)
N(2)-O(3)triflate	2.776	N(1_8)-Cu(1)-O(1)	166.4(7)

As expected, the ring formed on complexation is in a shallow boat conformation. The angle between the two pyrazolyl ring planes is 142.7° giving the symmetrical ringed structure formed with angle B1 at 170.43° and angle B2 at 145.4° at an average of 157.9°.
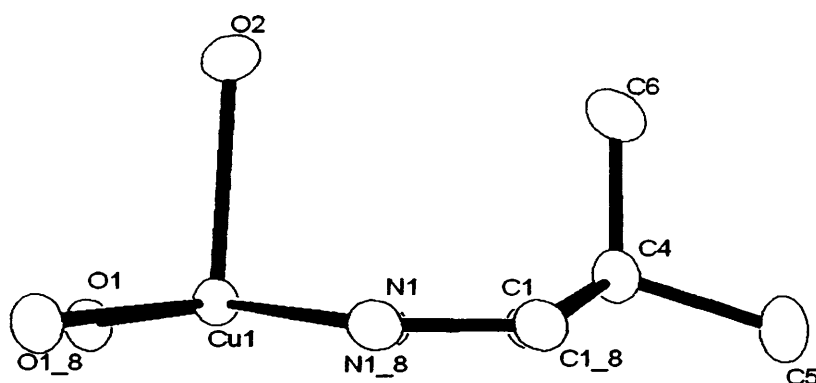
Figure 4.11: Shallow boat structure displayed by 4e

Hydrogen Bonding

The hydrogen bonding network is shown in **figure 4.12**. The complex units are arranged head to toe and are linked via identical interactions of 2.776 Å between O(3) and N(2). The symmetrical nature of the complex allows this in both directions. The Cu-Cu distance is 6.44Å and the zig-zag alignment of the copper centres is at an angle of 131.1°. No interactions between strands were detected.
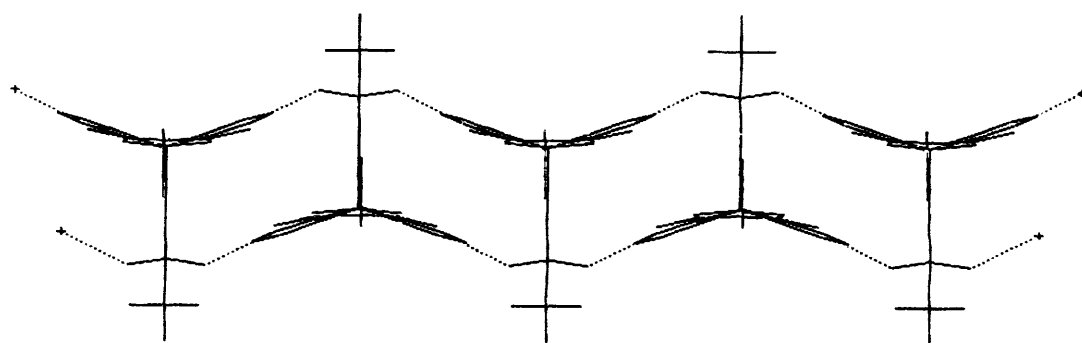
Figure 4.12: Mercury representation of H bonding in 4d

Coordination Chemistry of MeTAM

MeTAM is an oxygen based equivalent of the 3 nitrogen donor of the Tp system. Consequently it is suitable for bonding oxophillic ions such as Cr^{3+} and Zr^{4+}. This section describes our attempt to synthesise such complexes together with those of softer transition metals and some group 1 elements. Here we detail our attempts to replicate the results achieved by Cavell[4] and also the reaction of MeTAM with some transition metal salts.

Results and discussion

Our first intention was to replicate the results of Cavell *et al* in obtaining the $Cr^{III}MeTAM$ complex described. In Cavell's experiment, the product was obtained as a green moisture sensitive solid from the reaction shown previously in **figure 4.5**. Our reaction was identical on observation with an immediate colour change from purple ($CrCl_3(THF)_3$) to green on addition of MeTAM via syringe. The sticky green product obtained after repeat precipitation of the product from hexanes and DCM was difficult to handle and showed no positive product peaks on the application of high resolution mass spectrometry. The unsuccessful result of this experiment was repeated with the other available triketone ligands. Similar experiments were undertaken with iron(II)chloride, zirconium(IV)chloride and $Cr(CO)_3(MeCN)_3$ as substrates in an attempt to form monomeric complexes with the potentially facially capping triketones. The reactions were evaluated initially by ^1H NMR and provided no tenable results. The spectra were not defined nor did they show conclusive evidence of the products or any of the expected by-products of the decomposition of the ligand. The spectra, heavy in detail, were attributed to the potential of the ligands to bind via a number of combinations with three potential sites for coordination.

In conclusion, the tri ketone ligands we have synthesised appear to be extremely vulnerable to decomposition while in solution. Unfortunately they are susceptible to nucleophillic attack from water in particular. Although all efforts were made to avoid this is in our reactions, it is clear that extremely anhydrous conditions are required in order for this family of compounds to succeed as coordinating ligands.

Experimental

MeTAM (4)
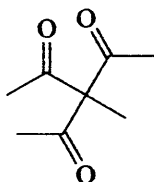
To a solution of Me(acac)(1g, 8.7mmol) in dry degassed DME was added methylmagnesium bromide(3M in Et$_2$O)(2.9mL, 8.7mmol) dropwise at 0°C and stirred for 1h. Acetyl chloride (0.61mL, 8.7mmol) was added dropwise to this solution at 0C and stirred for 16 h. Ammonium chloride(saturated solution)(50mL) was added slowly and the solution stirred. The aqueous layer extracted with dichloromethane (3x30mL). The organic fractions were combined and washed with sodium hydrogen carbonate (2x30mL), water (2x30mL). The solution was dried over magnesium sulphate and concentrated under vacuum. The crude product was recrystallised from petroleum ether 40-60% to yield the product as a white crystalline solid. Yield: (1.08g, 80%). ^{1}H NMR (CDCl$_3$, δ): 2.10 (s, 9H, CH_3) 1.58 (s, 3H, CH_3). ^{13}C NMR (CDCl$_3$, δ): 205.34 (3 CO), 79.71 (C(CO)$_3$), 27.91 (3 COCH$_3$), 17.05 (C(CO)$_3$$CH_3$). IR (KBr, cm^{-1}) 1571 (υ C=O)

3-methyl-3-(4- nitrobenzoyl)-2,4-pentanedione (4a)
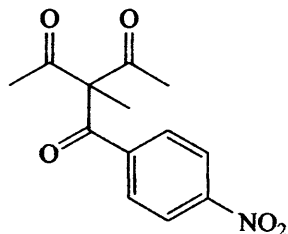
A solution of Me(acac), (1g, 8.70 mmol) was treated with nitrobenzoyl chloride (8.70 mmol) according to the procedure for the synthesis of **4**. The desired product was recovered. Yield (1.73g, 75%). ^{1}H NMR (CDCl$_3$, δ): 8.08 (d, J = 8.15, Ar), 7.70 (t, J = 7.53, Ar), 7.60 (t, J = 7.88, Ar), 7.35 (d, J = 7.61, Ar), 2.23 (6H, s, Ac), 1.65 (3H, s, C*H$_3$). ^{13}C NMR (CDCl$_3$,δ): 201.9 (2 *C*OMe), 195.2 (*C*OPH), 150.0 (*C*(NO)$_2$), 142.8 (Ar), 130.6 (2C, Ar), 120.9 (2C, Ar), 89.4 (*C*(CO)$_3$), 24.9 (2C, CH$_3$CO)`10.7 (*C*H$_3$). IR (KBr, cm^{-1}) 1704 (C=O), 1604 (NO$_2$)

3-Acetyl-3-methyl-1,1-diphenyl pentane-2,4-dione (4b)
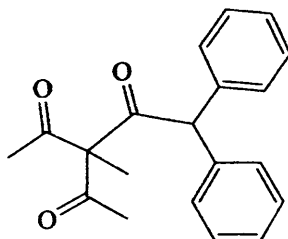
A solution of Me(acac), (1g, 8.70 mmol) was treated with diphenyl acetyl chloride (8.70 mmol) according to the procedure for the synthesis of **4**. The aqueous workup furnished the desired product (0.98g, 87%). ^{1}H NMR (CDCl$_3$, δ) 7.2 (m, 10H, Ar), 5.35 (s, 1H), 1.95 (s, 6H, COC*H$_3$), 1.49 (s, 3H, C(CO)$_3$C*H$_3$). ^{13}C NMR (CDCl$_3$, δ): 205.33 (*C*OPh$_2$), 201.05 (2 *C*O), 142.67 (2 Ar*C*), 128.71 (10 Ar*C*H), 88.92 (*C*(Ac)$_3$), 71.00 (*C*(Ar)$_2$), 26.88 (CO*C*H$_3$), 10.09 (*C*H3C(Ac)$_3$. IR (KBr, cm^{-1}) 1711, 1681 (υ C=O)

2,2,5,5-Tetramethyl-3-methyl-3-acetyl-heptane-3,5-dione (4c)
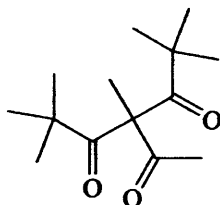
A solution of 2,2,5,5-tetramethyl-3-methyl-heptane-3,5-dione (1g, 5.02mmol) was treated as for compound 4. The desired product was recovered (0.98g, 80%). ^{1}H NMR (CDCl$_3$, δ): 2.10 (s, 3H, CH_3) 1.80 (s, 3H, CH_3) 1.15 (s, 18H, ^{t}Bu). ^{13}C NMR (CDCl$_3$, δ): 213.09 (2 ^{t}BuCO), 202.00 (MeCO), 79.91 (CCH$_3$), 46.26 (2 C(CH$_3$), 28.37 (6 CH$_3$), 27.9 (COCH$_3$), 16.87 (CH_3C(CO)$_3$). IR (KBr cm^{-1}) 1719, 1684 (υ C=O)

[Cu(Me(acac))(2f)]OTf (4d)

Ligand 2f (0.2g, 1.14 mmol) and MeTAM (0.16g, 1.14 mmol) were mixed as solids in a glove box. A solution of Copper Triflate (0.21g, 1.14 mmol) in methanol was added and the reaction stirred for 16 hours. Volatiles were removed from the flask and the brown solid obtained taken into DCM. Slow diffusion of heaxanes into the vessel afforded the synthesis of blue block crystals of the desired product. Yield (0.19g 34%). Anal. Calcd for [C$_{16}$H$_{21}$CuO$_5$SF$_3$].0.5 H$_2$O: C, 37.61; H, 4.34; N, 10.96. Found: C, 37.60; H, 3.97; N, 11.39.

References

[1]   A. M. Madalan, V. C. Kravstov, D. Pajic, K. Zardo, Y. A. Simnov, N Stanica, L. Ouahab, J. Lipkowski, M. Andruh, *Inorg. Chim. Acta.*, **357**, 2004, 415

[2]   A. Paulovicova, U. El-Ayaan, Y. Fukuda, *Inorg. Chim. Acta.*, **321**, 2001, 56

[3]   A. Paulovicova, U. El-Ayaan, K, Shibayama, T. Morita, Y. Fukuda, *Eur. J. Inorg. Chem.*, **10**, 2001, 2641

[4]   T. Rüther, K. J. Cavell, N. Braussaud, B. W. Skelton, A. H. White, *Dalton Trans.*, 2002, 4684

[5]   A. McKillop, E. C. Taylor, G. H. Hawks III, *J. Am. Chem. Soc.*, **90**, 1968, 2421

[6]   M. Gál, O. Feher, E. Tihyani, G. Hovrath and G. Jerkovich, *Tetrahedron.*, **38**, 1982, 2933

Chapter 5:

Coordination Chemistry of our Novel Ligand:

2,3,6,7-tetramethyl-4,5-diazaocta-3,5-diene-2,7-bis-(pyrazol-3-yl)

Introduction

Bi-Coordinating Ligands

The synthesis of a new ligand system was both an exciting and difficult time. We took the potential for this compound **2g** to form bimetallic complexes as a starting point to research similar compounds and discover its potential. This section details the coordination chemistry of some symmetrical ligands with two N,N' chelating centres, joined by a short bridging link.
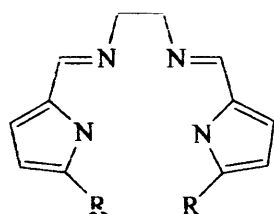
1

The multidentate pyrroylaldiminate ligand **1**, where R = 'Bu, has a structural similarity to our novel ligand. A Schiff base and acyclic derivative of the porphyrins, this ligand is a flexible bis coordinating N,N' ligand. This ligand and some derivatives have been found to be very versatile and able to complex with both transition and earth metals in a number of different coordination modes[i]. **Figure 5.1** displays some of the results published by Lan-Chang and collaborators.

2   3
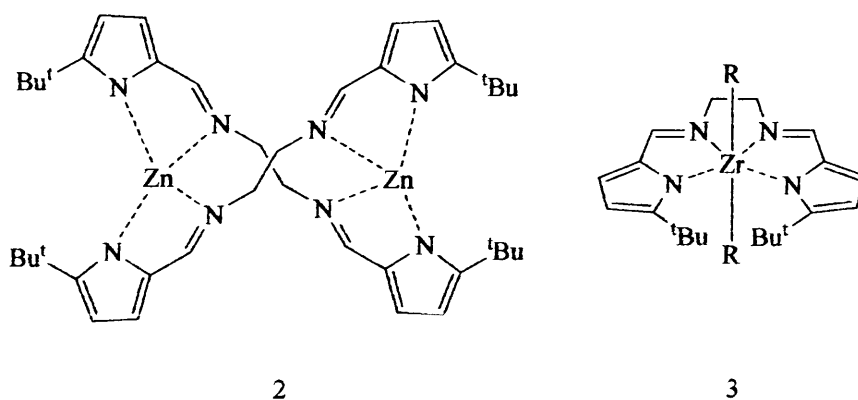
Figure 5.1: Some bonding modes of ligand 1

The complexes displayed are two in a series of known compounds incorporating other transition metals including Copper[2] and Manganese[3] with a derivative of ligand 1 where the 'Butyl moieties are substituted for hydrogen atoms. Although both complexes shown have a distinctive coordination mode, they both fall into the same category. Both can be classed as helicates.

Helicates

This term was coined by Lehn and co-workers for the description of a complex which can contain one or more ligand strands wrapped around a metal centre, in effect, a metal-containing helix[4]. The length of the ligand strand is unlimited, allowing the coordination of several metal centres. Helicates can also incorporate different ligand strands, often leading to constraint and therefore interesting structural characteristics[5]. An excellent review was published by Piguet and collaborators[6], and details all aspects of helicate chemistry not discussed in this brief section.

(A) Single stranded helicates – In this case, the ligand would wrap around a single metal centre, with both coordination sites contributing. Although not considered by everyone as helicates, some single stranded mononuclear helical complexes are important as precursors of double stranded helicates. Compound 2g represents this class of helicate ligand, and **figure 5.2** shows how our ligand may be able to adapt to allow this bonding mode.
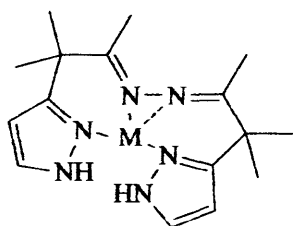
Figure 5.2: Potential of **2g** to acts as a single stranded helicate

(B) Double Stranded Helicates – Here, more than one ligand strand would share, typically two or more metal centres. Compound 2 demonstrates a simple example of this type of complex. Our novel ligand has the potential to display this bonding mode

due to the flexibility around the N-N bond. Twisting around the N-N bond would allow two or more ligands to orientate themselves around a metal centre as shown in compound 2.
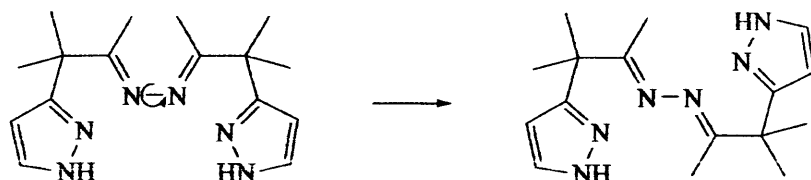
Figure 5.3: Twisting of 2g along N-N bond

Other Potential Bonding Modes

Many other potential bonding modes were considered with only a few mentioned in the following passages. The bis (2-pyridyl) tetrazine ligand 3,6-bis(2-pyridyl)-1,2,4,5-tetrazine shown in **figure 5.4**, forms complexes with many different metal centres[7]. Although the ligand is clearly more rigid than our novel compound, its complexes show the potential for what may be achievable on complexation with a Silver (I) moiety. **Figure 5.4** shows the di-cation of the $[Ag_2L_2](CF_3SO_3)$ complex formed in quantitative yield from a reaction between the ligand and silver triflate. The di-cation is approximately planar with each silver coordinated to a bidentate "bipy" domain of each of the two 3,6-bis(2-pyridyl)-1,2,4,5-tetrazine ligands. The ligand seems to be responsible for imposing the near-planar geometry upon the silver centre.
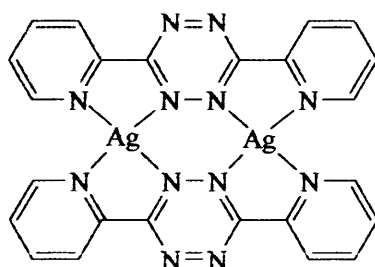
Figure 5.4: Cation of the 3,6-bis(2-pyridyl)-1,2,4,5-tetrazine

complex $[Ag_2L_2](CF_3SO_3)$ (4)

Another ligand showing greater flexibility is **5**. First synthesised by Broker and collaborators, this pyradizine containing two armed grid ligand was synthesised via the reaction of p-anisidine and diformylpyridazine[8].

MeO—⟨benzene⟩—N=⧸ N-N ⧹=N—⟨benzene⟩—OMe
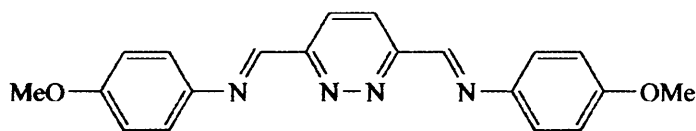
5

The ligand forms complexes with a number of transition metals including nickel and zinc, and displays how a reasonably flexible ligand can show the 2:2 bonding mode as shown by the silver complex, **4**. The complexes are distorted octahedrons with solvent molecules occupying the axial positions. On reaction with Iron Chloride in a 1:1 reaction, the ligand shows an interesting alternative bonding mode. The ligand is not bimetallic on complexation, despite capable of bonding at both chelating centres. The single Iron (II) atom is bound by three bidentate $N_{imine}N_{pyridazine}$ moieties to form three different ligand strands and is in a distorted octahedral environment (**figure 3.5**). The counter ion in the complex is the oxo bridged iron (III) dimer $[Cl_3Fe\text{-}O\text{-}FeCl_3]^{2-}$, formed by the in situ hydrolysis of ferric chloride.
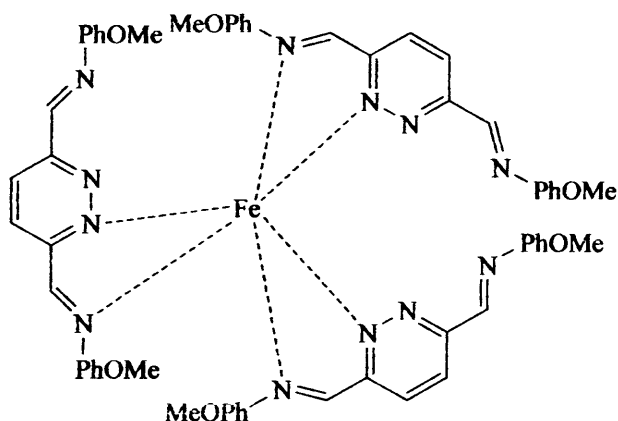
6

Figure 3.5: Cation of the complex $[Fe(5)_3](Cl_3Fe\text{-}O\text{-}FeCl_3)$

Chapter Outline

There are several other ligands and complexes applicable to the previous section, however, instead of studying what may be possible and trying to emulate other results, we found it more interesting to take some suitable substrates and investigate what our ligand was actually capable of. This section details the reaction of our novel ligand with some simple transition metal salts.

Synthesis and Characterisation

Palladium Complex

Reaction of **2g** with palladium dichloride

Mixing McCN solutions of **2g** and palladium dichloride bis acetonitrile [PdCl$_2$(McCN)$_2$] resulted in the formation of the N^N bis chelated dichloropalladium complex **5a** (**figure 5.6**). The orange/red solution obtained was reduced in volume after being allowed to stir for 1 hour and the orange precipitate was recrystallised from hot acetonitrile. **5a** is a red, air stable solid and has been characterised by microanalysis, ^{1}H NMR, IR, MS as well as an X-ray crystal structure determination. The complex produced was expected and confirms the potential of the ligand to chelate bimetalically.

5a

i = PdCl$_2$(McCN)$_2$, RT
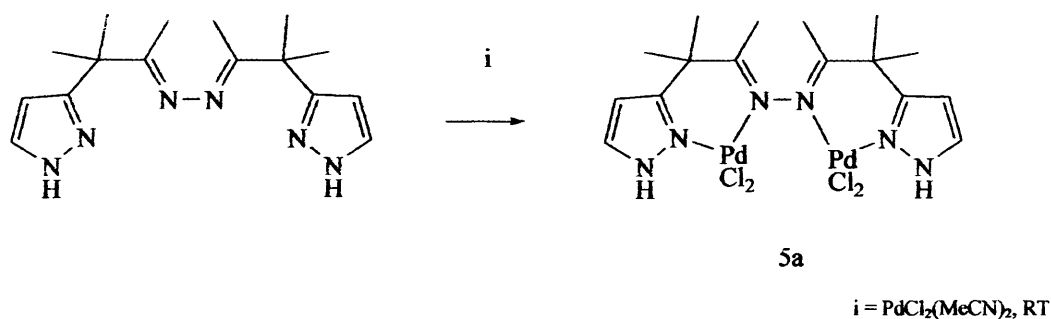
Figure 5.6: Formation of **5a**

^{1}H NMR

The NMR spectrum suggests the two metal centres are spectroscopically equivalent, and shows a small down field shift in the proton peak positions on complexation of the ligand. As in the palladium complexes **3a** and **3b**, the appearance of a broad peak at 11.57 ppm is the best indicator that complexation has occurred as this NH peak is not present in the starting material.

Table 5.1: ^{1}H NMR peak positions comparing Ligand 2g and Complex 5a (ppm)

	NH	pz – H	pz – H	Me	(Me)₂
Ligand	-	7.41	6.10	1.45	1.49
Complex	11.57	7.73	6.45	2.20	2.05

X-Ray Analysis

Crystals of 5a were grown by slow evaporation of a concentrated acetonitrile solution. X ray crystal structure was determined by Dr Liling Ooi at Cardiff University.

The X ray crystal structure as shown in figure 5.7 clearly confirms the N^N chelate mode of coordination of 2g. Each asymmetric unit contains three molecules of acetonitrile. (See appendix C for the completed data, collection and refinement details and atomic coordinates)

Without a crystal structure determination of the free ligand it is difficult to draw conclusions on the structural effects of coordination on this ligand. However, the structure of the complex obtained can allow us to gauge what may be possible with respect to other metal centres. The structure shows that in order to accommodate two metal centres, the ligand, in this case, twists along the N3-N4 bond, linking the two coordination sites (figure 5.8). This action avoids a potential clash between the methyl groups C8 and C9 and also a possible interaction between Cl(2) and Cl(3). Selected bond lengths and angles are shown in tables 5.2 and 5.3. These demonstrate the similarity in the two chelating units around each of the two palladium centres.
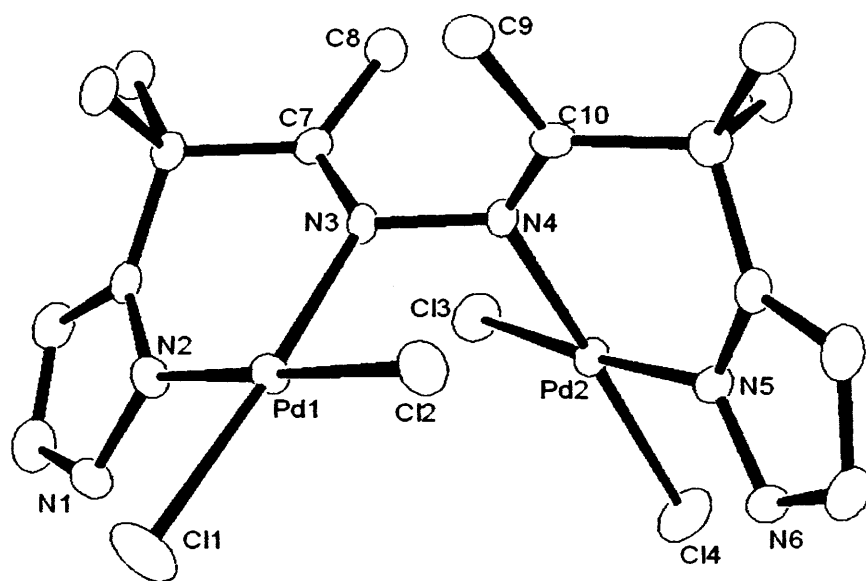
Figure 5.7: X Ray Structure of **5a**
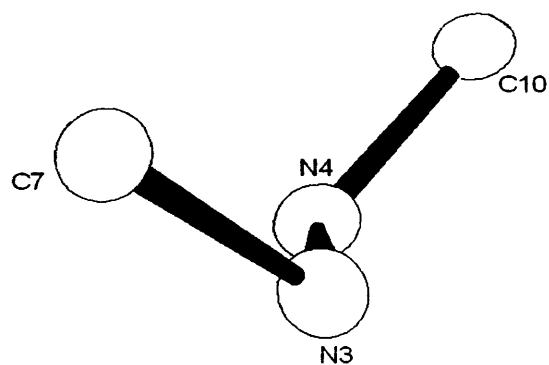
Figure 5.8: 90.9° dihedral angle along the N(3)-N(4) azine bond in **5a**

Table 5.2: Selected Bond Lengths from **5a**

Bond Lengths Around Pd (1) Å		Bond Lengths Around Pd (2) Å	
N(2)-Pd(1)	1.991(3)	N(5)-Pd(2)	1.987(3)
N(3)-Pd(1)	2.062(3)	N(4)-Pd(2)	2.050(3)
Pd(1)-Cl(1)	2.273(10)	Pd(2)-Cl(4)	2.278(11)
Pd(1)-Cl(2)	2.298(10)	Pd(2)-C(l3)	2.300(10)

Table 5.3: Selected Bond Angles from **5a**

Bond Angles Around Pd(1) °		Bond Angles Around Pd(2) °	
N(2)-Pd(1)-N(3)	85.74(5)	N(4)-Pd(1)-N(5)	85.62(13)
N(2)-Pd(1)-Cl(2)	178.91(10)	N(5)Pd(2)-Cl(3)	175.54(10)
N(3)-Pd(1)-Cl(1)	175.20(9)	N(4)-Pd(2)-Cl(4)	172.99(9)
Cl(1)-Pd(1)-Cl(2)	90.15(4)	Cl(3)-Pd(2)-Cl(4)	91.62(4)

Each palladium centre has a distorted square planar geometry, with the effects of chelation rendering the 'bite angles' at Pd(1) and Pd(2), 85.74(5)° and 85.62(13)° respectively. **Table 5.3** demonstrates the chelating centre around the Pd(2) atom is under greater strain, manifested in the increased deviation from the 90° and 180° angles expected.

IR spectroscopy

The infared spectrum shows the NH groups as a sharp peak at 3347 cm^{-1} while the C=N groups are at the lower end of the range at 1589 and 1518 cm^{-1} respectively.

Cobalt Complex

Reaction of **2g** with cobalt (II) chloride

Mixing 1:2 MeCN solutions of **2g** and Cobalt Chloride ($CoCl_2.XH_2O$) resulted in the formation of a lilac precipitate after 1 hour. The highly insoluble solid formed was characterised by crystal structure determination, microanalysis and IR. Crystals of **5b**, suitable for X-Ray analysis were obtained by the slow evaporation of the filtered reaction mixture. The X-ray determination was performed by Dr L. Ooi at Cardiff University.

X-Ray Analysis

The asymmetric unit, consisting of a single metal centre, two ligands bound via the terminal nitrogen positions and two chloride ions is shown in **figure 5.9**. No solvent molecules were detected. Selected bond distances and angles are listed in **tables 5.4** and **5.5**. See appendix C for full data.
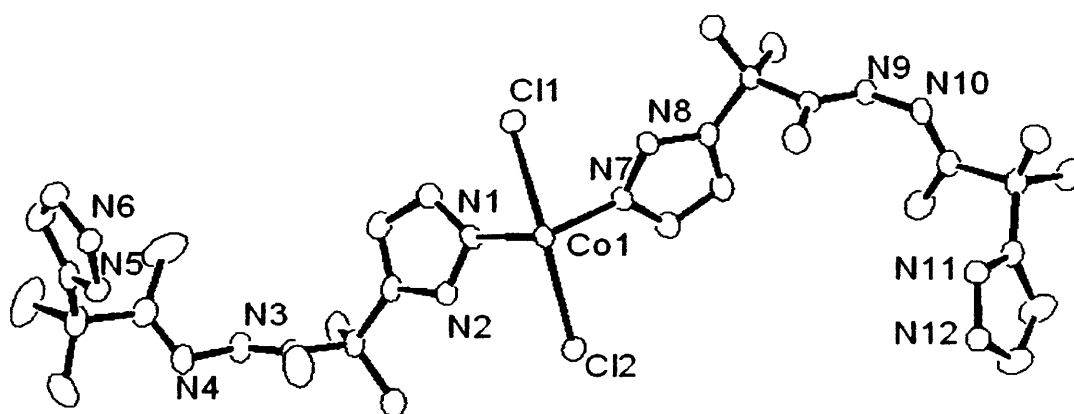
Hydrogen atoms have been omitted for clarity

Figure 5.9: X Ray structure of 5b (Asymmetric Unit)

On reflection of the asymmetric unit, the structure, similar to **3f** (chapter 3), develops into a coordination polymer. The cobalt atoms within the polymer are in a distorted octahedral geometry and are separated by double stranded ligand loops. Two different types of loop exist, each made of an identical pair of one of the two distinct ligands shown in the asymmetric unit.

Better described in figure **5.10**, the blue atoms represent a particular ligand from the asymmetric unit (ligand containing N(1)-N(6)). This forms a symmetrical loop by arranging itself "head to toe" with its identical partner, again similar to the previous coordination polymer reported. The chain grows on the display of identical behaviour by the other ligand (containing N(7)-N(12) from the asymmetric unit (red). The chloride counter ions remain in the axial positions while the propagation of the chain occurs through the terminal nitrogen atoms of the ligand. The pyrazole protons have moved to the inside positions to allow bonding via the terminal nitrogen atoms. The IR spectrum shows a relatively sharp peak corresponding to the NH groups observed in the crystal structure at 3246 cm^{-1}.
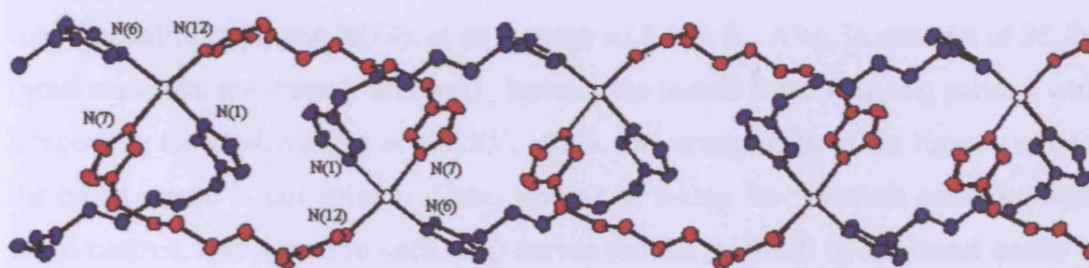
Protons, methyl groups and chlorine atoms emitted for clarity

Figure 5.10: Polymeric X Ray structure of 5b

Table 5.4: Selected bond lengths from 5b

Atoms	Distance Å
Co(1)-Cl(1)	2.534(6)
Co(1)-Cl(2)	2.540(6)
Co(1)-N(1)	2.098(17)
Co(1)-N(6)	2.133(18)
Co(1)-N(7)	2.107(18)
Co(1)-N(12)	2.129(18)

Table 5.5: Selected Bond Angles from 5b

Atoms	Angle $^\circ$
Cl(1)-Co(1)-Cl(2)	179.43(2)
N(1)-Co(1)-N(6)	171.31(7)
N(1)-Co(1)-N(7)	100.41(7)
N(1)-Co(1)-Cl(1)	90.91(5)

The mean Co-N(ligand) distance observed is 2.117 Å, similar to the 2.133 Å displayed in coordination compound 3f. Due to the presence of two slightly different ligands, unlike 3f, the inter metal distances are not equal, instead, they alternate between 8.548 Å (metals bound by loop including N(1) and N(6) and 8.698 Å (metals bound by loops including N(7) and N(12), at an average of 8.623 Å. Also, in contrast to 3f, the metal atoms are not linearly arranged. Instead, the metals form a zig-zag pattern, with a repeating Co-Co-Co angle of 120.85°. Also, the arrangement of the ligands around the metal centre is not simple. Here, instead of taking the "shortest path" between metal centres, one ligand in each loop curves around the back of the metal centre in order to sit trans to its partner. In compound 3f, the ligands are arranged cis to each other (figure 5.11).

(a) Cis arrangement displayed in 3f
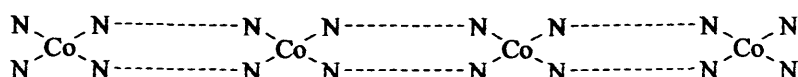
(b) Trans arrangement displayed in 5b
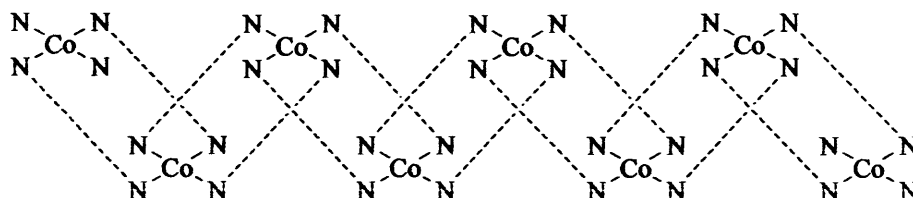
Figure 5.11: Inter metallic bonding in complex 3f (a) and complex 5b (b)

A consequence of this twisting in the ligand is the display of an unusual structural feature. Closer inspection of the polymeric structure revealed that the double stranded ligand loops are at angles approaching perpendicular to each other. The view along

the crystallographic a axis, displayed in **figure 5.12**, shows how a polymeric chain and the orientation of the ligands relate to each other.
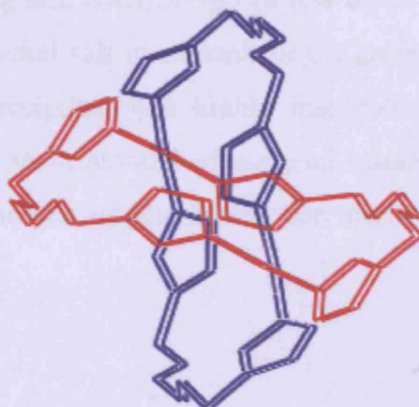
Methyl groups, chlorine atoms and protons omitted for clarity

Fig 5.12: Mercury view along the crystallographic a axis of 5b

Hydrogen Bonding

Again as in **3f,** no hydrogen bond network is in place to link polymeric strands, making this polymer one dimensional. The hydrogen bonding displayed here is concentrated around the octahedral metal centres, with interactions between Cl(1) and the pyrazole nitrogen atoms N(5)-Cl(1) = 3.034 Å and N(6)-Cl(1) = 3.236 Å. Some inter ligand linking between cis orientated pyrazole rings is also evident N(6)-N(8) = 2.947 Å and N(6)-(N12) = 2.817 Å.

Nickel Complex

Reaction of 2g with nickel (II) chloride

A similar result was achieved to the previous reaction involving cobalt. On stirring acetonitrile solutions of **2g** and $NiCl_2.XH_2O$ (a few drops of methanol added due to limited solubility of the nickel salt in acetonitrile), a green precipitate formed within one hour. Again, the precipitate was highly insoluble and was characterised by microanalysis and IR. A small amount of material suitable for X-Ray analysis was obtained by slow evaporation of the filtered reaction mixture.

X-Ray Analysis

As suspected, the crystalline material obtained was isostructural to the cobalt coordination polymer **5b** previously reported, with the asymmetric unit of **5c** is displayed in **figure 5.13**. No solvent molecules were detected.
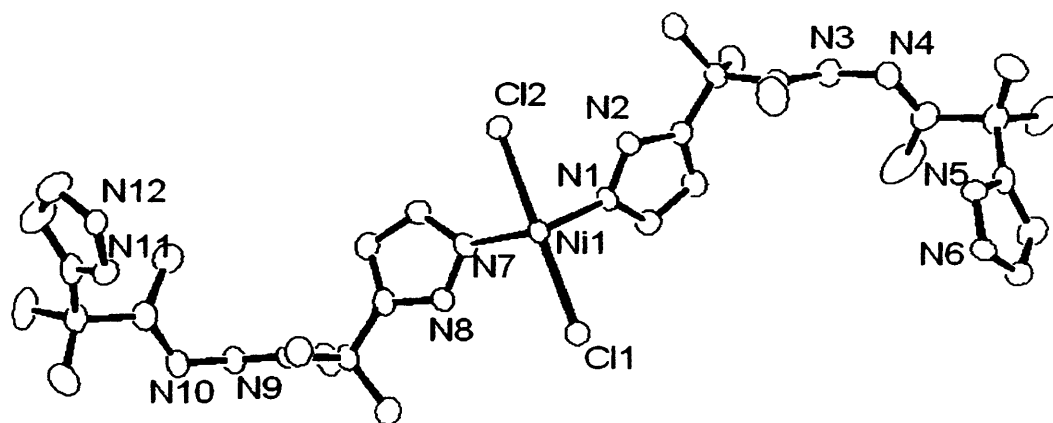
Protons have been omitted for clarity

Fig 5.13: X Ray structure of 5c (Asymmetric Unit)

The general structure of the coordination polymer obtained on reflection is analogous to that displayed in **figure 5.10**. Due to minor deviation in the bond lengths and angles (**tables 5.6** and **5.7**), only small differences exist between the structure displayed by this complex **5c**, and the previously reported **5b**.

Table 5.6: Selected bond lengths in 5c

Bond	Distance Å
Ni(1)-Cl(1)	2.4789(11)
Ni(1)-Cl(2)	2.4900(11)
Ni(1)-N(1)	2.0780(3)
Ni(1)-N(6)	2.0880(3)
Ni(1)-N(7)	2.0870(3)
Ni(1)-N(12)	2.0900(3)

Table 5.7: Selected Bond Angles in 5c

Atoms	Angle°
Cl(1)-Ni(1)-Cl(2)	179.03(4)
N(1)-Ni(1)-N(6)	173.31(13)
N(1)-Ni(1)-N(7)	98.00(13)
N(1)-Ni(1)-Cl(1)	89.02(10)

The inter nickel distances are 8.458 Å (ligand loops including N(1) and N(6), and 8.627 Å (ligand loops containing N(7) and N(12), at an average of 8.542Å. This is significantly shorter than the 8.623 Å average observed in complex **5b**. As a consequence, the Ni-Ni-Ni "zig zag" angle is slightly larger here at 122.45° compared to 120.85° in the cobalt polymer. The Ni-Cl bonds at 2.478(11) Å and 2.490(11) Å are also significantly shorter than the Co-Cl bonds displayed in 5b, at an average of 2.537 Å.
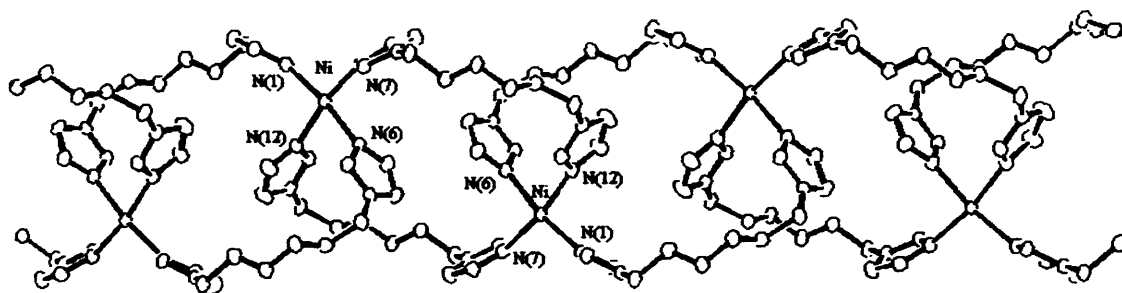
Figure 5.14: Polymeric X Ray structure of 5b

Hydrogen Bonding

The same hydrogen bonding network exists here with the same positions involved. All hydrogen bonds are slightly shorter in the Ni complex N(5)-Cl(1) = 3.017 A, N(6)-Cl(1) = 3.198 A, N(6)-N(7) = 2.915 A (N(7) occupies the same position as N(8) in the Co polymer, but has been labelled differently by the crystallographer) and N(6)-N(12) = 2.794 A.

Summary

We have synthesised three novel complexes of a unique ligand. This section has shown the ligand to be versatile and not only show different bonding modes, but a fundamental change in the behaviour of the ligand, based on the metal centre involved.

Experimental

[(2g)Pd₂Cl₄] (5a)

To a mixture of **2g** (1g, 3.32mmol) and PdCl₂(MeCN)₂(0.86g, 3.32mmol) in a dry schlenk was added MeCN (20mL). The resulting solution was allowed to stir for 1 hour at room temperature. Volatiles were removed under reduced pressure and the resulting brown solid recrystallised from hot MeCN. The desired product was recovered as a red, crystalline solid (Yield 1.26g, 79%). Anal. Calcd for C₁₆H₂₄N₆Pd₂Cl₂: C, 29.34; H, 3.69; N, 12.83. Found: C, 29.45; H, 3.62; N, 12.85. ¹H NMR (400 MHz, CDCl3): δ 11.57 (s (br), 2H, N*H*) 7.73 (m, 2H, *H*Pz) 6.45 (m, 2H, *H*Pz) 2.20 (s, 12H, C*H₃*) 2.05 (s, 6H, C*H₃*). IR (KBr, cm⁻¹): 3548, 3347, 3126, 2965, 1589, 1518, 1420.

([(2g)Co₂Cl₄]ₙ (5b)

To a solution of **2g** (0.07g, 0.23 mmol) in MeCN (20mL) was added CoCl₂.6H₂O (0.027g, 0.11mmol). The blue solution was stirred for 0.5 hours at which point a lilac/pink precipitate appeared. The solution was stirred for a further 16 hours and the solid recovered by filtration. The product was dried under vacuum (0.08g, 95%). Anal. Calcd for (C₁₆H₂₄N₆)₂CoCl₂: C, 52.90; H, 6.10; N, 23.13. Found: C, 52.90; H, 6.31; N, 21.49. IR (KBr, cm⁻¹): 3236, 2965, 1629, 1543, 1468.

([(2g)Ni₂Cl₄]ₙ (5c)

Reaction carried out as far **3b** using NiCl₂.6H₂O (0.39g, 1.66 mmol) and ligand **2g** (1g, 3.32mmol) in MeCN(20mL). MeOH (10mL) was added and the solution allowed to stir for 16 hours. The green precipitate formed was recovered filtration and dried under vacuum (1.15g, >95%). Anal. Calcd for (C₁₆H₂₄N₆)₂NiCl₂: C, 52.91; H, 6.11; N, 23.14. Found: C, 52.90; H, 6.25; N, 22.98. IR (KBr, cm⁻¹): 3246, 2975, 1629, 1543, 1468.

References

[1]   L. C. Liang, P. Y. Lee, W. L. Lan, C. H. Hung, J. Organomet Chem., 689, 2004, 947

[2]   T. Kikuchi, C. Kabuto, H. Yokoi, M. Iwaizumi, W. Mori, J Chem. Soc., Chem. Commun., 1983, 1306

[3]   F. Franceschi, G. Guillemot, E. Solari, C. Floriani, N. Re, H. Birkedal, P. Pattison, Chem. Eur, J., 7, 2001, 1468

[4]   J. M. Lehn, A. Rigault, J. Siegel, J. Harrowfield, B. Chevrier, D. Moras, Proc. Natl. Acad. Sci. U.S.A., 84, 1987, 256

[5]   B. Haskenknopf , J. M. Lehn, G. Baum, D Fenske, Proc. Natl. Acad. Sci. USA., 93, 1996, 1397

[6]   C. Piguet, G. Bernardinelli, G Hopfgartner, Chem. Rev., 97, 1997, 2005

[7]   E. C. Counstable, C. E. Housecroft, B. M. Kariuki, N. Kelly, C. B. Smith, Inorg. Chem. Comm., 5, 2002, 199

[8]   Y. Lan D. Kennepohl, B. Moubaraki, K. Murray, J. Cashion, G. Jameson, S. Broker, Chem. Eur. J., 9, 2003, 3772

Chapter 6:

Concluding Remarks and Future Work

Concluding Remarks and Future Work

Ligand Synthesis

We have isolated and characterised two novel bis pyrazol-3-yl ligands along with along with their bis enaminone precursors (only ligand **2f** shown below). We have also synthesised the bis chelating species **2g**, which is to our knowledge, the first of its kind. Further to our pyrazole based ligands, we have produced 3 novel tri-ketone ligands (**4a-4c**) which were produced in addition to the known compound, **4**, but via a method which was simple and high yielding in comparison with published routes[i].
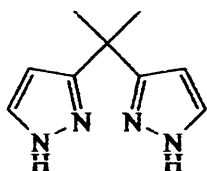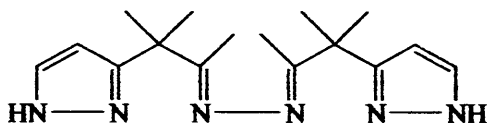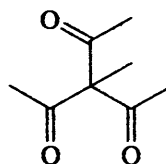
| | 2f | | | 2g | | | 4 | |

The bis pyrazole-3-yl ligands **2d** and **2e** were synthesised in two steps from simple acac precursors with relative ease and in high yields. Their potential for development is wide when the success of the structurally similar bis(pyrazole-1-yl) ligands is considered. Aside from the coordination chemistry to be discussed later, our novel bis pyrazol-3-yl ligands, have an enormous scope to adapt, firstly with the potential substitution of the terminal N-H groups for N-R. Similar ligands are known where the addition of anionic donors can lead to the synthesis of ligands with interesting properties. Compound **1** is known to show photophysical activity[2] and is just one example of how the simple tris(pyrazol-1-yl) structure can be adapted. Similar adaptation of our ligands could produce systems similar to **2**, with the R groups incorporating coordinating nitrogen donors in order to increase the coordination number.

1

2
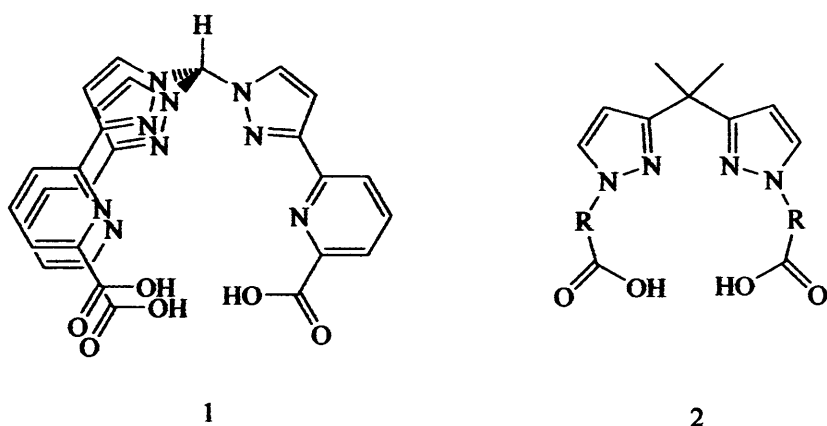
An alternative, and only available in the adaptation of **3d**, is the substitution of the bridging proton via the reaction of **3d** in the presence of pyrazole. This crude reaction could follow the melt method as described in **figure 1.4** and may lead to a potentially hemilabile mixed 1,1-bis-(pyrazol-3-yl)-1-(pyrozol-1-yl) ethane (**4i**) as shown in **figure 6.1**.

4i
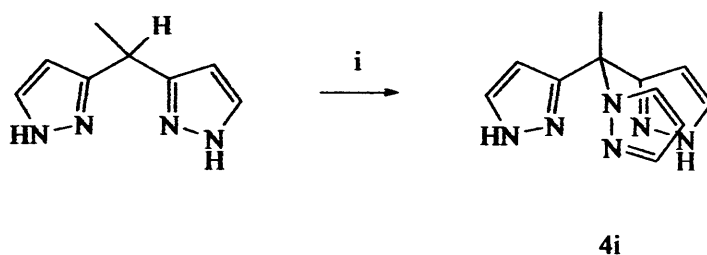
i = High Temperature / Pz

Figure 6.1: Possible access to hemilabile mixed pyrazolyl ligands

The synthesis of **2g**, to our knowledge a novel system, was an unexpected result. Produced from a by-product of the reactions to form **2d** and **2e**, the compound has many attractive features in being flexible and capable of bis-coordination. Potential modifications of this ligand could be made via the utilisation of functionalised hydrazine compounds in the synthesis. Also, the development of the enaminone precursor **2b** (**figure 6.2**) and subsequent reaction with hydrazine would lead to a compound that may be easily adapted as in **figure 6.1** above (**7**). In addition, it may be possible to form a pyrazabole type system (**6**) as is common with the pyrazole-1-yl ligands. Formation of this type of system may allow access to the chemistry of macrocyclic systems.
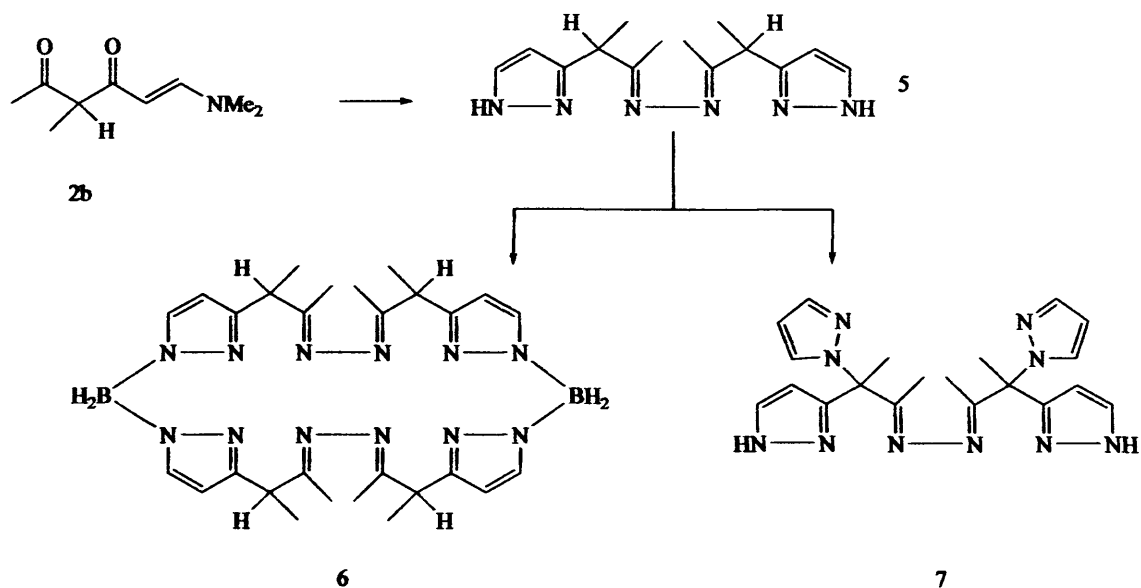
Figure 6.2: Development of enaminone precursor 2b

The novel triketones synthesised were obtained using a high yielding and comparatively simple and low risk method compared to those available in the literature. We have shown adaptation of the simple MeTAM model is possible using commercially available acac's and functionalised acid chlorides. A consequence of this is electronic and steric diversity. However, we have also shown that this system is unstable, a feature attributed to the moisture sensitivity of the ligands. Further investigation is required here and we are confident that a stable version of the tri ketone system will be found. In the meantime, manipulation of the current ligands, or exploration of the triketone concept is ongoing with the two ligands below being potentially attractive targets

8   9
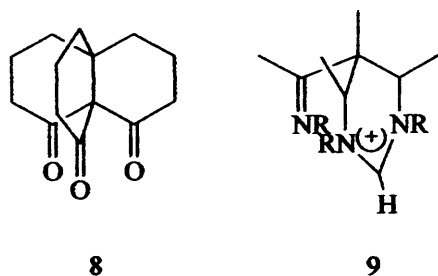
Compund 8, a very robust facially capping ligand, is possibly accessible via the work already done to synthesise the bi-cyclone structure from cyclohexanone[3]. The imidazolium salt with pendant amine 9 is potentially accessible from the tri-ketone

stating material **4**. The tris imine formed via the reaction of **4** with an amine, could be converted into an imidazolium salt using formate and acid[4-5] . **9** could be treated with a base to yield a mixed carbene/imine donor, where carbene complexes are a system known to exhibit catalytic properties[6-8].

Coordination Chemistry

We have produced several novel ligands, three based on the pyrazole ring and several others based on the carbonyl unit. We have shown the pyrazole based compounds **2d** and **2e** have an ability to form complexes with transition metal salts. Compound **2e** in particular has shown it is capable of bonding to metal centres in a number of ways. We have produced complexes that are monomeric, dimeric and polymeric by simple reaction with transition metal salts. **2e** has shown similar behaviour to some scorpionate ligands[9-10] as well as some other nitrogen based chelating ligands[11-12]. Although the complexes produced are an excellent starting point, the possibility of building an extensive library is clear. Also, targeting a possible use and designing specific complexes is an obvious progression. Poly(pyrazol-1-yl) complexes have shown useful properties in many fields including catalysis[13], bioinorganics[14-15] materials[16] and supramolecular[17] chemistry, and we see similar potential for our novel ligands. In relation to polymerisation catalysis via the Ziegler Natta method, the active species (alkyl cations [(L)M-R]$^+$) of complexes like **10** are among the most successful to date, with a significant difference in the polymerisation of alkenes depending on the nature of the R group, which allows tuning of the catalyst. We see a derivative of this complex incorporating our ligands a definite possibility[18].
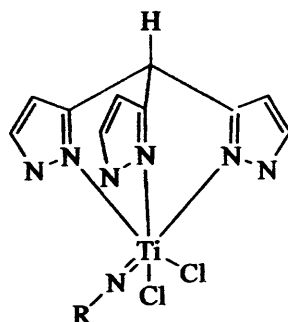
10

The azine linked bis chelating ligand **3f** has also shown an ability to form transition metal complexes. Our palladium complexes formed in the expected way with the two chelating centres binding the metal as expected. The ability to form metal halide linked double stranded polymers was clearly a possibility after the similar result obtained in complex **3f**, and must be attributed a kinetic and not thermodynamic process, characterised by the quick formation of the insoluble product. Again the potential regarding the coordination chemistry here is diverse with the possibility to form helicates and mixed metal complexes.

The potential of the tri ketone ligands to form complexes is clear from the success of the acac unit as a coordination ligand[19]. Although one complex of MeTAM has been published, we were unable to replicate this result. We have discovered that the ligands are unstable in solution, however, we feel that with further investigation into new ligands in addition to the novel ligands already produced, this ligand system will coordinate to a number of metal centres, and as a result have a number applications with catalysis a main objective.

References

[1]   A. McKillop, E. Taylor, G. Hawks (III), *J. Am. Chem, Soc.*, **90**, 1968, 2421

[2]   L. J. Charbonniere, R. Ziessel, *Helv. Chim. Acta.*, **86**, 2003, 3402

[3]   C. L. Hill, M McGrath, T. Hunt, G. Grogan, *Synlett.*, **2**, 2006, 309

[4]   A. A. Gindev, I. M. Mihaltseia, *Synth. Commun.*, **24**, 1994, 1547

[5]   A. J. Arduengo (III), F. P. Genty, P. K. Taverkene, H. E. Simmons, 2001, 6177575, U.S. patent

[6]   W. A. Herrmann, *Agnew. Chem. Int. Ed.*, **41**, 2002, 1290

[7]   K. Ofele, W. A. Herrmann, D. Mihalios, M. Elison, E. Herdtweck, M. Scherer, J. Mink, *J. Organomet. Chem.*, **459**, 1993, 177

[8]   A. C. Hillier, G. A. Grasa, M. S. Viciu, H. M. Lee, C. Yang, S. P. Nolan, *J. Organomet. Chem.*, **653**, 2002, 69

[9]   K. Uehara, S. Hikichi, A Inagaki, M. Akita, *Chem. Eur. J.*, **9**, 2005, 2788

[10]   L. D. Field, B. A. Messerle, L. P. Soler, T. W. Hambley, P. Turner, *J. Organomet. Chem.*, **655**, 2002, 146

[11]   Q. Zhao, H. Li, X. Wang, Z. Chen, *New. J. Chem.*, **26**, 2002, 1709

[12]   D. A. Handley, P. B. Hitchcock, G. J. Leigh, *Inorg. Chim. Acta.*, **314**, 2001, 1

[13]   K. Michuie, R. F. Jordan, *Organometallics.*, **23**, 2004 460

[14]   N. Kitajima, Y. Moro-oka, *Chem. Rev.*, **94**, 1994, 737

[15]   C. G. Young, A. G. Wedd, *Chem. Commun.*, 1997, 1251

[16]   F. Jacle et al. *Chem. Ber.*, **129**, 1996, 603

[17]   N. Kitajima, W. B. Tolman, Prog. *Inorg. Chem.*, **43**, 1995, 419

[18]   H. R. Bigmore, S. R. Dubberley, M. Kranenburg, S. C. Lawrence, A. J. Sealey, J. D. Selby, M. A. Zuideveld, R. A. Cowley, P. Mountfod, *Chem. Commun.*, 2006, 436.

[19]   C. Pettinari, F. Machetti, A. Drozdov, *Comprehensive Coordination Chemisrty (II)*, *Elsevier.*, 1.6, 97

Appendix A

Complex 3a

Identification code	kjc0521
Empirical formula	C8 H10 Cl2 N4 Pd
Formula weight	339.50
Temperature	150(2) K
Wavelength	0.71073 Å
Crystal system	Monoclinic
Space group	P 2(1)/c
Unit cell dimensions	a = 6.5210(2) Å alpha = 90°.
	b = 11.3180(4) Å beta = 91.066(2)°.
	c = 14.9600(5) Å gamma = 90°.
Volume	1103.93(6) Å^3
Z	4
Density (calculated)	2.043 Mg/m^3
Absorption coefficient	2.135 mm^{-1}
F(000)	664
Crystal size	0.50 x 0.30 x 0.10 mm^3
Theta range for data collection	3.12 to 27.48°.
Index ranges	-8<=h<=8, -11<=k<=14, -19<=l<=18
Reflections collected	6680
Independent reflections	2521 [R(int) = 0.0523]
Completeness to theta = 27.48°	99.6 %
Absorption correction	Semi-empirical from equivalents
Max. and min. transmission	0.8148 and 0.4149
Refinement method	Full-matrix least-squares on F^2
Data / restraints / parameters	2521 / 0 / 137
Goodness-of-fit on F^2	1.030
Final R indices [I>2sigma(I)]	R1 = 0.0288, wR2 = 0.0623
R indices (all data)	R1 = 0.0369, wR2 = 0.0677
Largest diff. peak and hole	0.646 and -1.070 e.Å^{-3}

Table 2. Atomic coordinates (x 10^4) and equivalent isotropic displacement parameters (Å^{2}x 10^3) for kjc0521. U(eq) is defined as one third of the trace of the orthogonalized U^{ij} tensor.

	x	y	z	U(eq)
C(1)	3967(5)	5599(3)	2021(2)	22(1)
C(2)	5656(5)	5253(3)	1546(2)	24(1)
C(3)	5345(4)	4052(3)	1343(2)	18(1)
C(4)	6723(4)	3214(3)	862(2)	18(1)
C(5)	8380(5)	3886(3)	356(2)	26(1)
C(6)	5574(5)	2368(3)	249(2)	17(1)
C(7)	6220(5)	1884(3)	-563(2)	24(1)
C(8)	4700(5)	1118(3)	-826(2)	25(1)
N(1)	2741(4)	4658(2)	2088(2)	20(1)
N(2)	3566(4)	3707(2)	1686(2)	17(1)
N(3)	3756(4)	1910(2)	454(2)	18(1)
N(4)	3243(4)	1149(2)	-213(2)	20(1)
Pd(1)	2069(1)	2169(1)	1544(1)	15(1)
Cl(1)	285(1)	2518(1)	2816(1)	24(1)
Cl(2)	256(1)	463(1)	1285(1)	25(1)

Table 3. Bond lengths [Å] and angles [°] for kjc0521.

C(1)-N(1)	1.336(4)
C(1)-C(2)	1.378(4)
C(1)-H(1)	0.9500
C(2)-C(3)	1.406(4)
C(2)-H(2)	0.9500
C(3)-N(2)	1.335(4)
C(3)-C(4)	1.500(4)
C(4)-C(6)	1.514(4)
C(4)-C(5)	1.533(4)
C(4)-H(4)	1.0000
C(5)-H(5A)	0.9800
C(5)-H(5B)	0.9800
C(5)-H(5C)	0.9800
C(6)-N(3)	1.334(4)
C(6)-C(7)	1.405(4)
C(7)-C(8)	1.369(5)
C(7)-H(7)	0.9500
C(8)-N(4)	1.333(4)
C(8)-H(8)	0.9500
N(1)-N(2)	1.350(3)
N(1)-H(1A)	0.8800
N(2)-Pd(1)	2.005(2)
N(3)-N(4)	1.355(3)
N(3)-Pd(1)	2.005(2)
N(4)-H(4)	0.8800
Pd(1)-Cl(1)	2.2834(7)
Pd(1)-Cl(2)	2.2929(8)
N(1)-C(1)-C(2)	107.3(3)
N(1)-C(1)-H(1)	126.4
C(2)-C(1)-H(1)	126.4
C(1)-C(2)-C(3)	105.8(3)
C(1)-C(2)-H(2)	127.1
C(3)-C(2)-H(2)	127.1
N(2)-C(3)-C(2)	108.8(3)
N(2)-C(3)-C(4)	122.1(3)
C(2)-C(3)-C(4)	129.0(3)
C(3)-C(4)-C(6)	113.3(2)
C(3)-C(4)-C(5)	110.9(3)
C(6)-C(4)-C(5)	111.2(2)
C(3)-C(4)-H(4)	107.0
C(6)-C(4)-H(4)	107.0
C(5)-C(4)-H(4)	107.0
C(4)-C(5)-H(5A)	109.5
C(4)-C(5)-H(5B)	109.5
H(5A)-C(5)-H(5B)	109.5
C(4)-C(5)-H(5C)	109.5
H(5A)-C(5)-H(5C)	109.5
H(5B)-C(5)-H(5C)	109.5
N(3)-C(6)-C(7)	109.2(3)
N(3)-C(6)-C(4)	122.6(3)
C(7)-C(6)-C(4)	128.1(3)
C(8)-C(7)-C(6)	105.6(3)

C(8)-C(7)-H(7)	127.2
C(6)-C(7)-H(7)	127.2
N(4)-C(8)-C(7)	107.9(3)
N(4)-C(8)-H(8)	126.1
C(7)-C(8)-H(8)	126.1
C(1)-N(1)-N(2)	111.0(2)
C(1)-N(1)-H(1A)	124.5
N(2)-N(1)-H(1A)	124.5
C(3)-N(2)-N(1)	107.1(2)
C(3)-N(2)-Pd(1)	129.6(2)
N(1)-N(2)-Pd(1)	122.81(19)
C(6)-N(3)-N(4)	106.6(2)
C(6)-N(3)-Pd(1)	129.2(2)
N(4)-N(3)-Pd(1)	124.07(19)
C(8)-N(4)-N(3)	110.7(3)
C(8)-N(4)-H(4)	124.6
N(3)-N(4)-H(4)	124.6
N(2)-Pd(1)-N(3)	86.54(10)
N(2)-Pd(1)-Cl(1)	90.93(7)
N(3)-Pd(1)-Cl(1)	177.05(7)
N(2)-Pd(1)-Cl(2)	175.82(7)
N(3)-Pd(1)-Cl(2)	91.64(8)
Cl(1)-Pd(1)-Cl(2)	90.98(3)

Symmetry transformations used to generate equivalent atoms:

Table 4. Anisotropic displacement parameters (Å^2x 10^3)for kjc0521. The anisotropic displacement factor exponent takes the form: $-2\square^2[\ h^2a^{*2}U^{11} + ... + 2\ h\ k\ a^*\ b^*\ U^{12}\ ]$

	U^{11}	U^{22}	U^{33}	U^{23}	U^{13}	U^{12}
C(1)	31(2)	12(2)	24(2)	-2(1)	-2(1)	-1(1)
C(2)	26(2)	20(2)	26(2)	0(1)	1(1)	-6(1)
C(3)	16(1)	18(2)	19(1)	0(1)	-2(1)	-1(1)
C(4)	14(1)	19(2)	22(1)	0(1)	3(1)	-1(1)
C(5)	20(2)	27(2)	32(2)	0(2)	7(1)	-7(1)
C(6)	16(1)	16(2)	20(1)	4(1)	4(1)	3(1)
C(7)	26(2)	24(2)	22(2)	2(1)	10(1)	0(1)
C(8)	32(2)	24(2)	19(1)	-2(1)	7(1)	0(2)
N(1)	21(1)	19(1)	20(1)	-4(1)	4(1)	1(1)
N(2)	18(1)	14(1)	20(1)	-3(1)	2(1)	-1(1)
N(3)	17(1)	17(1)	20(1)	-2(1)	5(1)	-2(1)
N(4)	21(1)	19(1)	20(1)	-6(1)	3(1)	-4(1)
Pd(1)	13(1)	15(1)	17(1)	-1(1)	5(1)	-1(1)
Cl(1)	24(1)	26(1)	23(1)	-5(1)	12(1)	-3(1)
Cl(2)	28(1)	20(1)	27(1)	-5(1)	11(1)	-10(1)

Table 5. Hydrogen coordinates (x 10^4) and isotropic displacement parameters (Å^2x 10^3) for kjc0521.

	x	y	z	U(eq)
H(1)	3721	6364	2257	27
H(2)	6795	5727	1389	29
H(4)	7442	2725	1328	22
H(5A)	7730	4401	-93	39
H(5B)	9281	3321	60	39
H(5C)	9190	4366	778	39
H(7)	7453	2053	-866	29
H(8)	4685	649	-1352	30
H(1A)	1553	4658	2358	24
H(4)	2105	732	-238	24

Complex 3b

Table 1. Crystal data and structure refinement

Identification code	kjc0514
Empirical formula	C9 H12 Cl2 N4 Pd
Formula weight	353.53
Temperature	150(2) K
Wavelength	0.71073 Å
Crystal system	Orthorhombic
Space group	P bca
Unit cell dimensions	a = 12.4130(7) Å alpha = 90°.
	b = 13.5790(8) Å beta = 90°.
	c = 14.3040(8) Å gamma = 90°.
Volume	2411.0(2) Å^3
Z	8
Density (calculated)	1.948 Mg/m^3
Absorption coefficient	1.959 mm^{-1}
F(000)	1392
Crystal size	0.20 x 0.10 x 0.03 mm^3
Theta range for data collection	3.61 to 26.37°.
Index ranges	-12<=h<=15, -14<=k<=16, -16<=l<=17
Reflections collected	10306
Independent reflections	2454 [R(int) = 0.1080]
Completeness to theta = 26.37°	99.7 %
Absorption correction	Semi-empirical from equivalents
Max. and min. transmission	0.9436 and 0.6953
Refinement method	Full-matrix least-squares on F^2
Data / restraints / parameters	2454 / 0 / 147
Goodness-of-fit on F^2	1.028
Final R indices [I>2sigma(I)]	R1 = 0.0469, wR2 = 0.0744
R indices (all data)	R1 = 0.0975, wR2 = 0.0872
Largest diff. peak and hole	0.632 and -0.623 e.Å^{-3}

Table 2. Atomic coordinates (x 10^4) and equivalent isotropic displacement parameters (Å^{2}x 10^3) for kjc0514. U(eq) is defined as one third of the trace of the orthogonalized U^{ij} tensor.

	x	y	z	U(eq)
C(1)	1268(5)	-1777(4)	1146(4)	25(2)
C(2)	471(5)	-1606(4)	1759(4)	26(2)
C(3)	285(5)	-591(4)	1745(4)	20(1)
C(4)	-456(5)	8(4)	2359(4)	23(1)
C(5)	169(5)	317(4)	3252(4)	33(2)
C(6)	-1420(5)	-650(4)	2657(5)	37(2)
C(7)	-894(4)	919(4)	1919(4)	20(1)
C(8)	-1899(4)	1367(4)	2076(4)	27(2)
C(9)	-1910(5)	2194(4)	1547(4)	27(2)
N(1)	1542(4)	-916(3)	757(3)	22(1)
N(2)	949(4)	-171(3)	1127(3)	20(1)
N(3)	-346(4)	1469(3)	1306(3)	20(1)
N(4)	-974(4)	2251(3)	1089(3)	24(1)
Pd(1)	1081(1)	1227(1)	682(1)	19(1)
Cl(1)	2712(1)	878(1)	-4(1)	30(1)
Cl(2)	1129(1)	2825(1)	164(1)	29(1)

Table 3. Bond lengths [Å] and angles [°] for kjc0514

C(1)-N(1)	1.338(7)
C(1)-C(2)	1.342(8)
C(1)-H(1)	0.9500
C(2)-C(3)	1.398(7)
C(2)-H(2)	0.9500
C(3)-N(2)	1.336(7)
C(3)-C(4)	1.510(8)
C(4)-C(7)	1.491(8)
C(4)-C(5)	1.552(8)
C(4)-C(6)	1.554(8)
C(5)-H(5A)	0.9800
C(5)-H(5B)	0.9800
C(5)-H(5C)	0.9800
C(6)-H(6A)	0.9800
C(6)-H(6B)	0.9800
C(6)-H(6C)	0.9800
C(7)-N(3)	1.338(7)
C(7)-C(8)	1.406(7)
C(8)-C(9)	1.353(8)
C(8)-H(8)	0.9500
C(9)-N(4)	1.336(7)
C(9)-H(9)	0.9500
N(1)-N(2)	1.358(6)
N(1)-H(1A)	0.8800
N(2)-Pd(1)	2.009(4)
N(3)-N(4)	1.353(6)
N(3)-Pd(1)	2.010(4)
N(4)-H(4)	0.8800
Pd(1)-Cl(2)	2.2947(14)
Pd(1)-Cl(1)	2.2993(15)

N(1)-C(1)-C(2)	108.0(5)
N(1)-C(1)-H(1)	126.0
C(2)-C(1)-H(1)	126.0
C(1)-C(2)-C(3)	106.4(5)
C(1)-C(2)-H(2)	126.8
C(3)-C(2)-H(2)	126.8
N(2)-C(3)-C(2)	109.2(5)
N(2)-C(3)-C(4)	122.1(5)
C(2)-C(3)-C(4)	128.6(6)
C(7)-C(4)-C(3)	115.0(5)
C(7)-C(4)-C(5)	107.8(5)
C(3)-C(4)-C(5)	108.7(5)
C(7)-C(4)-C(6)	108.2(5)
C(3)-C(4)-C(6)	108.6(5)
C(5)-C(4)-C(6)	108.4(5)
C(4)-C(5)-H(5A)	109.5
C(4)-C(5)-H(5B)	109.5
H(5A)-C(5)-H(5B)	109.5
C(4)-C(5)-H(5C)	109.5
H(5A)-C(5)-H(5C)	109.5
H(5B)-C(5)-H(5C)	109.5
C(4)-C(6)-H(6A)	109.5

C(4)-C(6)-H(6B)	109.5
H(6A)-C(6)-H(6B)	109.5
C(4)-C(6)-H(6C)	109.5
H(6A)-C(6)-H(6C)	109.5
H(6B)-C(6)-H(6C)	109.5
N(3)-C(7)-C(8)	108.3(5)
N(3)-C(7)-C(4)	123.7(5)
C(8)-C(7)-C(4)	128.0(5)
C(9)-C(8)-C(7)	106.2(5)
C(9)-C(8)-H(8)	126.9
C(7)-C(8)-H(8)	126.9
N(4)-C(9)-C(8)	108.2(5)
N(4)-C(9)-H(9)	125.9
C(8)-C(9)-H(9)	125.9
C(1)-N(1)-N(2)	110.5(5)
C(1)-N(1)-H(1A)	124.7
N(2)-N(1)-H(1A)	124.7
C(3)-N(2)-N(1)	105.9(4)
C(3)-N(2)-Pd(1)	131.5(4)
N(1)-N(2)-Pd(1)	122.4(3)
C(7)-N(3)-N(4)	107.2(4)
C(7)-N(3)-Pd(1)	130.4(4)
N(4)-N(3)-Pd(1)	122.3(4)
C(9)-N(4)-N(3)	110.1(5)
C(9)-N(4)-H(4)	125.0
N(3)-N(4)-H(4)	125.0
N(2)-Pd(1)-N(3)	86.72(18)
N(2)-Pd(1)-Cl(2)	176.83(14)
N(3)-Pd(1)-Cl(2)	90.67(13)
N(2)-Pd(1)-Cl(1)	90.69(14)
N(3)-Pd(1)-Cl(1)	177.40(13)
Cl(2)-Pd(1)-Cl(1)	91.92(5)

Symmetry transformations used to generate equivalent atoms:

Table 4. Anisotropic displacement parameters (A^2x 10^3)for kjc0514. The anisotropic displacement factor exponent takes the form: $-2\square^2[$ $h^2a^{*2}U^{11} + ... + 2$ h k a^* b^* $U^{12}]$

	U^{11}	U^{22}	U^{33}	U^{23}	U^{13}	U^{12}
C(1)	33(4)	18(3)	25(3)	7(3)	-10(3)	-1(3)
C(2)	30(4)	21(3)	28(3)	5(3)	-2(3)	0(3)
C(3)	24(3)	17(3)	19(3)	1(3)	-7(3)	-2(3)
C(4)	29(4)	22(3)	18(3)	3(3)	-2(3)	2(3)
C(5)	40(4)	39(4)	21(3)	-1(3)	-6(3)	6(3)
C(6)	45(4)	26(4)	41(4)	6(3)	7(3)	-10(3)
C(7)	16(3)	21(3)	25(3)	-3(3)	-3(3)	-5(3)
C(8)	18(3)	35(4)	29(3)	2(3)	-3(3)	-1(3)
C(9)	26(4)	28(4)	28(4)	-8(3)	-7(3)	5(3)
N(1)	24(3)	19(3)	21(3)	-6(2)	3(2)	2(2)
N(2)	28(3)	9(2)	22(3)	0(2)	0(2)	2(2)
N(3)	18(3)	22(3)	19(2)	-2(2)	0(2)	0(2)
N(4)	30(3)	17(3)	25(3)	8(2)	-1(2)	7(2)
Pd(1)	22(1)	16(1)	19(1)	1(1)	0(1)	-1(1)
C(1)	27(1)	26(1)	36(1)	5(1)	7(1)	1(1)
C(2)	34(1)	20(1)	35(1)	5(1)	1(1)	-1(1)

Table 5. Hydrogen coordinates (x 10^4) and isotropic displacement parameters (A^2x 10^3) for kjc0514.

	x	y	z	U(eq)
H(1)	1583	-2399	1012	30
H(2)	105	-2081	2129	32
H(5A)	748	774	3082	50
H(5B)	479	-269	3549	50
H(5C)	-325	641	3690	50
H(6A)	-1887	-283	3086	56
H(6B)	-1150	-1242	2971	56
H(6C)	-1833	-842	2102	56
H(8)	-2458	1136	2473	32
H(9)	-2484	2655	1509	33
H(1A)	2037	-843	322	26
H(4)	-793	2727	703	29

Complex 3c

Table 1. Crystal data and structure refinement for mpc0503.

Identification code   c:\xray\mpc050 -1\mpc0503

Empirical formula   C18 H24 Cl4 Cu2 N8

Formula weight   621.33

Temperature   150(2) K

Wavelength   0.71073 A

Crystal system, space group

Unit cell dimensions   a= 7.6321(2)A   alpha= 100.250(2)
     b= 8.7045(2)A   beta= 106.133(2)
     c= 9.9626(3)A   gamma= 105.345(2)

Volume   590.10(3) A^3

Z, Calculated density   1, 1.748 Mg/m^3

Absorption coefficient   2.279 mm^-1

F(000)   314

Crystal size   0.50 x 0.43 x 0.22 mm

Theta range for data collection   2.95 to 27.43 deg.

Limiting indices   -9<=h<=9, -11<=k<=11, -12<=l<=12

Reflections collected / unique   8896 / 2671 [R(int) = 0.1504]

Completeness to theta = 27.43   99.4 %

Max. and min. transmission   0.6280 and 0.3953

Refinement method   Full-matrix least-squares on F^2

Data / restraints / parameters   2671 / 0 / 66

Goodness-of-fit on F^2   2.259

Final R indices [I>2sigma(I)]   R1 = 0.0876, wR2 = 0.2386

R indices (all data)   R1 = 0.0924, wR2 = 0.2434

Extinction coefficient   0.032(9)

Largest diff. peak and hole   4.552 and -2.751 e.A^-3

Table 2. Atomic coordinates (x 10^4) and equivalent isotropic
displacement parameters (A^2 x 10^3) for mpc0503.
U(eq) is defined as one third of the trace of the orthogonalized
Uij tensor.

	x	y	z	U(eq)
C(1)	6811(9)	3126(8)	2798(6)	19(1)
C(2)	5698(8)	2187(8)	3433(6)	18(1)
C(3)	3935(8)	2495(7)	3060(6)	12(1)
C(4)	2186(8)	1828(7)	3466(6)	14(1)
C(5)	2116(9)	3187(8)	4645(6)	20(1)
C(6)	2291(9)	341(8)	4065(7)	21(1)
C(7)	377(8)	1333(7)	2124(6)	14(1)
C(8)	-1233(8)	-114(8)	1575(6)	17(1)
C(9)	-2460(8)	156(7)	388(6)	16(1)
Cl(1)	-268(2)	5916(2)	1577(2)	21(1)
Cl(2)	4343(2)	6901(2)	1697(2)	25(1)
Cu(1)	1971(1)	4590(1)	1512(1)	15(1)
N(1)	3994(7)	3587(6)	2264(5)	14(1)
N(2)	5763(7)	3951(6)	2117(5)	17(1)
N(3)	145(7)	2415(6)	1348(5)	14(1)
N(4)	-1597(7)	1649(6)	275(5)	16(1)

Table 3. Bond lengths [A] and angles [deg] for mpc0503.

C(1)-N(2)   1.339(8)
C(1)-C(2) 1.380(9)
C(1)-H(1) 0.9500
C(2)-C(3) 1.403(8)
C(2)-H(2) 0.9500
C(3)-N(1) 1.342(7)
C(3)-C(4) 1.502(8)
C(4)-C(7) 1.528(7)
C(4)-C(6) 1.530(8)
C(4)-C(5) 1.535(8)
C(5)-H(5A) 0.9800
C(5)-H(5B) 0.9800
C(5)-H(5C) 0.9800
C(6)-H(6A) 0.9800
C(6)-H(6B) 0.9800
C(6)-H(6C) 0.9800
C(7)-N(3) 1.337(8)
C(7)-C(8) 1.399(8)
C(8)-C(9) 1.390(8)
C(8)-H(8) 0.9500
C(9)-N(4) 1.333(8)
C(9)-H(9) 0.9500
Cl(1)-Cu(1) 2.3104(17)
Cl(2)-Cu(1) 2.2613(18)
Cu(1)-N(3) 1.980(5)
Cu(1)-N(1) 2.003(5)
N(1)-N(2) 1.357(7)
N(2)-H(3) 0.8800
N(3)-N(4) 1.357(6)
N(4)-H(4) 0.8800

N(2)-C(1)-C(2)   107.2(5)
N(2)-C(1)-H(1)   126.4
C(2)-C(1)-H(1)   126.4
C(1)-C(2)-C(3)   105.7(5)
C(1)-C(2)-H(2)   127.2
C(3)-C(2)-H(2)   127.2
N(1)-C(3)-C(2)   109.6(5)
N(1)-C(3)-C(4)   121.1(5)
C(2)-C(3)-C(4)   129.3(5)
C(3)-C(4)-C(7)   108.8(4)
C(3)-C(4)-C(6)   110.6(5)
C(7)-C(4)-C(6)   110.5(5)
C(3)-C(4)-C(5)   108.9(5)
C(7)-C(4)-C(5)   109.4(5)
C(6)-C(4)-C(5)   108.6(5)
C(4)-C(5)-H(5A)   109.5
C(4)-C(5)-H(5B)   109.5
H(5A)-C(5)-H(5B)   109.5
C(4)-C(5)-H(5C)   109.5
H(5A)-C(5)-H(5C)   109.5
H(5B)-C(5)-H(5C)   109.5
C(4)-C(6)-H(6A)   109.5
C(4)-C(6)-H(6B)   109.5
H(6A)-C(6)-H(6B)   109.5
C(4)-C(6)-H(6C)   109.5

H(6A)-C(6)-H(6C) 109.5
H(6B)-C(6)-H(6C) 109.5
N(3)-C(7)-C(8)   111.0(5)
N(3)-C(7)-C(4)   119.3(5)
C(8)-C(7)-C(4)   129.6(5)
C(9)-C(8)-C(7)   104.2(5)
C(9)-C(8)-H(8)   127.9
C(7)-C(8)-H(8)   127.9
N(4)-C(9)-C(8)   107.9(5)
N(4)-C(9)-H(9)   126.1
C(8)-C(9)-H(9)   126.1
N(3)-Cu(1)-N(1)   84.0(2)
N(3)-Cu(1)-Cl(2) 172.50(15)
N(1)-Cu(1)-Cl(2) 89.01(15)
N(3)-Cu(1)-Cl(1) 93.02(15)
N(1)-Cu(1)-Cl(1) 157.71(15)
Cl(2)-Cu(1)-Cl(1) 94.47(6)
C(3)-N(1)-N(2)   106.1(5)
C(3)-N(1)-Cu(1)   127.9(4)
N(2)-N(1)-Cu(1)   126.0(4)
C(1)-N(2)-N(1)   111.4(5)
C(1)-N(2)-H(3)   124.3
N(1)-N(2)-H(3)   124.3
C(7)-N(3)-N(4)   105.4(5)
C(7)-N(3)-Cu(1)   129.7(4)
N(4)-N(3)-Cu(1)   124.5(4)
C(9)-N(4)-N(3)   111.4(5)
C(9)-N(4)-H(4)   124.3
N(3)-N(4)-H(4)   124.3

Symmetry transformations used to generate equivalent atoms:

Complex 3d

Table 1. Crystal data and structure refinement

Identification code	asKJC01
Empirical formula	C20.50 H25 Cl0.50 Cu F6 N8 O6 S2
Formula weight	738.87
Temperature	150(2) K
Wavelength	0.71073 A
Crystal system, space group	orthorhombic, Pnnm

Unit cell dimensions
a = 17.784(4) A   alpha = 90 deg.
b = 10.759(2) A   beta = 90 deg.
c = 17.200(3) A   gamma = 90 deg.

Volume	3291.0(11) A^3
Z, Calculated density	4, 1.491 Mg/m^3
Absorption coefficient	0.911 mm^-1
F(000)	1502
Crystal size	0.25 x 0.15 x 0.15 mm
Theta range for data collection	2.97 to 26.00 deg.
Limiting indices	-21<=h<=21, -13<=k<=13, -21<=l<=21
Reflections collected / unique	6073 / 3334 [R(int) = 0.0287]
Completeness to theta = 26.00	99.1 %
Max. and min. transmission	sortav 0.896 and 0.724
Refinement method	Full-matrix least-squares on F^2
Data / restraints / parameters	3334 / 0 / 226
Goodness-of-fit on F^2	1.035
Final R indices [I>2sigma(I)]	R1 = 0.0473, wR2 = 0.1309
R indices (all data)	R1 = 0.0639, wR2 = 0.1413
Largest diff. peak and hole	0.793 and -0.516 e.A^-3

Table 2. Atomic coordinates (x 10^4) and equivalent isotropic
displacement parameters (A^2 x 10^3) for asKJC01.
U(eq) is defined as one third of the trace of the orthogonalized
Uij tensor.

	x	y	z	U(eq)
Cu(1)	0	0	0	21(1)
Cl(1)	1478(4)	4626(7)	826(4)	109(2)
S(1)	3815(1)	7274(1)	2450(1)	35(1)
F(1)	4155(1)	5290(2)	1646(1)	58(1)
O(1)	4486(1)	7860(2)	2136(1)	44(1)
N(1)	655(1)	-761(2)	775(1)	25(1)
C(1)	1400(2)	-936(3)	715(2)	27(1)

Cu(2)	5000	0	0	24(1)
F(2)	3479(1)	6620(2)	1028(1)	64(1)
O(2)	3161(1)	8045(2)	2469(1)	46(1)
N(2)	446(1)	-1239(2)	1469(1)	31(1)
C(2)	1664(2)	-1520(3)	1388(2)	38(1)
F(3)	2984(1)	5457(2)	1903(1)	64(1)
O(3)	3946(1)	6546(2)	3143(1)	42(1)
N(3)	4318(1)	700(2)	791(1)	26(1)
C(3)	1041(2)	-1704(3)	1844(2)	41(1)
N(4)	4108(1)	149(2)	1463(1)	28(1)
C(4)	1806(2)	-480(4)	0	29(1)
C(5)	2626(2)	-959(6)	0	44(1)
C(6)	1802(3)	959(5)	0	39(1)
C(7)	3883(2)	1718(3)	713(2)	27(1)
C(8)	3399(2)	1808(3)	1352(2)	32(1)
C(9)	3556(2)	788(3)	1808(2)	33(1)
C(10)	3967(2)	2534(4)	0	31(1)
C(11)	3353(3)	3536(4)	0	39(1)
C(12)	4747(3)	3156(5)	0	41(1)
C(13)	3596(2)	6102(4)	1723(2)	45(1)
C(14)	1573(11)	5440(16)	0	110(6)

Table 3. Bond lengths [A] and angles [deg] for asKJC01.

Cu(1)-N(1_5)	1.951(2)
Cu(1)-N(1_6)	1.951(2)
Cu(1)-N(1)	1.951(2)
Cu(1)-N(1_5)	1.951(2)
Cl(1)-C(14)	1.678(11)
S(1)-O(2)	1.430(2)
S(1)-O(3)	1.445(2)
S(1)-O(1)	1.454(2)
S(1)-C(13)	1.818(4)
F(1)-C(13)	1.330(4)
N(1)-C(1)	1.342(4)
N(1)-N(2)	1.353(3)
C(1)-C(2)	1.397(4)
C(1)-C(4)	1.508(4)
Cu(2)-N(_6)	1.972(2)
Cu(2)-N(_2)	1.972(2)
Cu(2)-N(_5)	1.972(2)
Cu(2)-N(3)	1.972(2)
F(2)-C(13)	1.335(4)
N(2)-C(3)	1.337(4)
C(2)-C(3)	1.371(5)
F(3)-C(13)	1.327(4)
N(3)-C(7)	1.347(4)
N(3)-N(4)	1.352(3)
N(4)-C(9)	1.337(4)
C(4)-C(1_6)	1.508(4)
C(4)-C(5)	1.547(6)
C(4)-C(6)	1.549(7)
C(7)-C(8)	1.401(4)
C(7)-C(10)	1.515(4)
C(8)-C(9)	1.377(5)
C(10)-C(7_6)	1.515(4)
C(10)-C(11)	1.535(6)
C(10)-C(12)	1.540(6)
C(14)-Cl(1_6)	1.678(11)

N(1_5)-Cu(1)-N(1_6)	93.82(13)
N(1_5)-Cu(1)-N(1)	180.00(19)
N(1_6)-Cu(1)-N(1)	86.18(13)
N(1_5)-Cu(1)-N(1_2)	86.18(13)
N(1_6)-Cu(1)-N(1_2)	180.00(14)
N(1)-Cu(1)-N(1_2)	93.82(13)
O(2)-S(1)-O(3)	115.31(15)
O(2)-S(1)-O(1)	115.10(15)
O(3)-S(1)-O(1)	114.14(14)
O(2)-S(1)-C(13)	104.13(16)
O(3)-S(1)-C(13)	103.08(16)
O(1)-S(1)-C(13)	102.78(16)
C(1)-N(1)-N(2)	106.6(2)
C(1)-N(1)-Cu(1)	126.61(19)
N(2)-N(1)-Cu(1)	126.74(18)
N(1)-C(1)-C(2)	109.3(3)
N(1)-C(1)-C(4)	119.3(3)
C(2)-C(1)-C(4)	131.4(3)
N(3_6)-Cu(2)-N(3_2)	180.00(19)
N(3_6)-Cu(2)-N(3_5)	92.83(14)

N(3_2)-Cu(2)-N(3_5)	87.17(14)
N(3_6)-Cu(2)-N(3)	87.17(14)
N(3_2)-Cu(2)-N(3)	92.83(14)
N(3_5)-Cu(2)-N(3)	180.00(14)
C(3)-N(2)-N(1)	110.5(2)
C(3)-C(2)-C(1)	105.6(3)
C(7)-N(3)-N(4)	106.5(2)
C(7)-N(3)-Cu(2)	126.53(19)
N(4)-N(3)-Cu(2)	126.28(19)
N(2)-C(3)-C(2)	108.1(3)
C(9)-N(4)-N(3)	110.8(2)
C(1_6)-C(4)-C(1)	109.3(3)
C(1_6)-C(4)-C(5)	110.1(2)
C(1)-C(4)-C(5)	110.1(2)
C(1_6)-C(4)-C(6)	108.8(2)
C(1)-C(4)-C(6)	108.8(2)
C(5)-C(4)-C(6)	109.7(4)
N(3)-C(7)-C(8)	109.4(3)
N(3)-C(7)-C(10)	119.7(3)
C(8)-C(7)-C(10)	131.0(3)
C(9)-C(8)-C(7)	105.4(3)
N(4)-C(9)-C(8)	107.9(3)
C(7_6)-C(10)-C(7)	108.0(3)
C(7_6)-C(10)-C(11)	109.7(2)
C(7)-C(10)-C(11)	109.7(2)
C(7_6)-C(10)-C(12)	109.9(2)
C(7)-C(10)-C(12)	109.9(2)
C(11)-C(10)-C(12)	109.6(4)
F(3)-C(13)-F(1)	107.0(3)
F(3)-C(13)-F(2)	107.4(3)
F(1)-C(13)-F(2)	107.6(3)
F(3)-C(13)-S(1)	112.2(3)
F(1)-C(13)-S(1)	111.4(2)
F(2)-C(13)-S(1)	111.1(3)
Cl(1_6)-C(14)-Cl(1)	115.7(11)

Symmetry transformations used to generate equivalent atoms:

(_5) -x,-y,-z   (_6) x,y,-z   (_2) -x,-y,z
(_2) -x+1,-y,z   (_5) -x+1,-y,-z

Table 4. Anisotropic displacement parameters (A^2 x 10^3) for asKJC01.
The anisotropic displacement factor exponent takes the form:
-2 pi^2 [h^2 a*^2 U11 + ... + 2 h k a* b* U12]

	U11	U22	U33	U23	U13	U12
Cu(1)	14(1)	29(1)	19(1)	0	0	4(1)
Cl(1)	123(5)	131(6)	74(4)	-10(4)	6(4)	-8(5)
S(1)	27(1)	41(1)	37(1)	9(1)	-6(1)	2(1)
F(1)	56(1)	57(1)	60(1)	-6(1)	6(1)	14(1)
O(1)	32(1)	46(1)	55(2)	15(1)	-4(1)	-1(1)
N(1)	21(1)	33(1)	21(1)	4(1)	1(1)	3(1)
C(1)	19(1)	33(2)	29(2)	-2(1)	-4(1)	4(1)
Cu(2)	21(1)	27(1)	23(1)	0	0	-1(1)
F(2)	73(2)	81(2)	37(1)	4(1)	-13(1)	8(1)
O(2)	33(1)	52(2)	52(2)	5(1)	-5(1)	12(1)
N(2)	28(1)	43(2)	23(1)	7(1)	3(1)	5(1)
C(2)	30(2)	47(2)	38(2)	2(2)	-10(1)	11(1)
F(3)	49(1)	70(2)	72(2)	-4(1)	-3(1)	-21(1)
O(3)	37(1)	52(2)	38(1)	14(1)	-6(1)	2(1)
N(3)	26(1)	27(1)	24(1)	0(1)	1(1)	-1(1)
C(3)	43(2)	49(2)	31(2)	10(2)	-4(1)	10(2)
N(4)	28(1)	32(1)	25(1)	2(1)	1(1)	1(1)
C(4)	18(2)	37(2)	33(2)	0	0	0(2)
C(5)	19(2)	66(4)	47(3)	0	0	4(2)
C(6)	29(2)	42(3)	46(3)	0	0	-4(2)
C(7)	25(2)	29(2)	28(2)	-4(1)	-2(1)	-4(1)
C(8)	30(2)	35(2)	32(2)	-7(1)	-1(1)	2(1)
C(9)	32(2)	43(2)	24(2)	-6(1)	2(1)	-2(1)
C(10)	35(2)	27(2)	31(2)	0	0	0(2)
C(11)	48(3)	28(2)	41(3)	0	0	8(2)
C(12)	47(3)	33(2)	45(3)	0	0	-11(2)
C(13)	41(2)	53(2)	42(2)	8(2)	-2(2)	0(2)
C(14)	94(13)	68(10)	167(19)	0	0	24(10)

Table 5. Hydrogen coordinates (x 10^4) and isotropic displacement parameters (A^2 x 10^3) for asKJC01.

	x	y	z	U(eq)
H(2)	-17	-1243	1649	37
H(2A)	2168	-1744	1504	46
H(3)	1035	-2093	2339	49
H(4)	4308	-538	1649	34
H(5A)	2634	-1836	-154	66
H(5B)	2840	-873	523	66
H(5C)	2925	-471	-369	66
H(6A)	2028	1265	-483	59
H(6B)	2093	1265	445	59
H(6C)	1283	1258	39	59
H(8)	3038	2440	1451	38
H(9)	3316	576	2282	39
H(11A)	3415	4073	455	58
H(11B)	2857	3138	19	58
H(11C)	3393	4036	-474	58
H(12A)	4836	3548	506	62
H(12B)	4766	3789	-409	62
H(12C)	5134	2528	-97	62
H(14A)	1195	6116	0	132
H(14B)	2077	5834	0	132

Complex 3e

Table 1. Crystal data and structure refinement

Identification code	asKJC03
Empirical formula	C42 H56 Cl5 Co3 N19 O
Formula weight	1197.10
Temperature	150(2) K
Wavelength	0.71069 A
Crystal system, space group	monoclinic, P2(1)/n
Unit cell dimensions	a = 13.623(5) A alpha = 90.000(5) deg.
	b = 23.541(5) A beta = 96.667(5) deg.
	c = 16.645(5) A gamma = 90.000(5) deg.
Volume	5302(3) A^3
Z, Calculated density	4, 1.500 Mg/m^3
Absorption coefficient	1.233 mm^-1
F(000)	2460
Crystal size	0.25 x 0.20 x 0.10 mm
Theta range for data collection	3.00 to 25.00 deg.
Limiting indices	-16<=h<=16, -25<=k<=27, -19<=l<=19
Reflections collected / unique	17305 / 9255 [R(int) = 0.0380]
Completeness to theta = 25.00	99.1 %
Max. and min. transmission	sortav 0.933 and 0.639
Refinement method	Full-matrix least-squares on F^2
Data / restraints / parameters	9255 / 0 / 642
Goodness-of-fit on F^2	1.033
Final R indices [I>2sigma(I)]	R1 = 0.0424, wR2 = 0.0858
R indices (all data)	R1 = 0.0603, wR2 = 0.0919
Largest diff. peak and hole	0.480 and -0.545 e.A^-3

Table 2. Atomic coordinates (x 10^4) and equivalent isotropic
displacement parameters (A^2 x 10^3) for asKJC03.
U(eq) is defined as one third of the trace of the orthogonalized
Uij tensor.

	x	y	z	U(eq)
Co(1)	9132(1)	2529(1)	418(1)	18(1)
Cl(1)	9290(1)	4528(1)	1379(1)	32(1)
O(1)	8858(1)	2933(1)	-553(1)	20(1)
N(1)	8257(2)	1940(1)	-52(2)	21(1)
C(1)	7300(2)	1824(1)	6(2)	23(1)
Co(2)	9990(1)	3298(1)	-849(1)	19(1)
Cl(2)	10435(1)	1326(1)	-1782(1)	33(1)
N(2)	8532(2)	1582(1)	-627(2)	25(1)
C(2)	6993(2)	1382(2)	-529(2)	30(1)
Co(3)	9761(1)	633(1)	-2661(1)	27(1)
Cl(3)	10985(1)	95(1)	-3063(1)	38(1)
N(3)	8015(2)	2869(1)	851(2)	20(1)
C(3)	7794(2)	1244(2)	-918(2)	29(1)
Cl(4)	8873(1)	1002(1)	-3774(1)	49(1)

N(4)	8058(2)	3403(1)	1162(2)	23(1)
C(4)	6693(2)	2112(1)	588(2)	24(1)
Cl(5)	8895(1)	97(1)	-1870(1)	52(1)
N(5)	9491(2)	2098(1)	1398(2)	21(1)
C(5)	6615(3)	1711(2)	1310(2)	37(1)
N(6)	9248(2)	1542(1)	1462(2)	26(1)
C(6)	5647(2)	2210(2)	149(3)	40(1)
N(7)	10021(2)	3114(1)	829(2)	19(1)
C(7)	7086(2)	2687(1)	889(2)	23(1)
N(8)	10349(2)	3481(1)	264(2)	19(1)
C(8)	6556(2)	3109(2)	1237(2)	28(1)
N(9)	10252(2)	2236(1)	-62(2)	19(1)
C(9)	7189(2)	3553(2)	1399(2)	26(1)
N(10)	10674(2)	2603(1)	-568(2)	19(1)
C(10)	10075(2)	2223(1)	2077(2)	24(1)
N(11)	11197(2)	3621(1)	-1132(2)	23(1)
C(11)	10191(3)	1739(2)	2568(2)	35(1)
N(12)	11304(2)	4185(1)	-1251(2)	29(1)
C(12)	9657(3)	1318(2)	2153(2)	36(1)
N(13)	9262(2)	3996(1)	-1080(2)	23(1)
C(13)	10533(2)	2801(1)	2266(2)	25(1)
N(14)	9029(2)	4339(1)	-470(2)	25(1)
C(14)	9884(3)	3139(2)	2800(2)	32(1)
N(15)	9572(2)	3070(1)	-1961(2)	22(1)
C(15)	11563(2)	2706(2)	2735(2)	35(1)
N(16)	9617(2)	2518(1)	-2181(2)	23(1)
C(16)	10650(2)	3141(1)	1511(2)	21(1)
N(17)	6980(2)	3559(1)	-699(2)	36(1)
C(17)	11383(2)	3536(1)	1407(2)	27(1)
N(18)	8908(3)	3950(2)	4568(3)	80(1)
C(18)	11172(2)	3729(1)	626(2)	26(1)
N(19)	8435(3)	562(2)	691(2)	59(1)
C(19)	10945(2)	1862(1)	222(2)	22(1)
C(20)	11816(2)	1973(1)	-96(2)	23(1)
C(21)	11626(2)	2455(1)	-576(2)	20(1)
C(22)	12331(2)	2762(1)	-1058(2)	23(1)
C(23)	12334(3)	2472(2)	-1885(2)	32(1)
C(24)	13380(2)	2715(2)	-591(2)	33(1)
C(25)	12096(2)	3386(1)	-1178(2)	26(1)
C(26)	12745(3)	3816(2)	-1351(3)	41(1)
C(27)	12226(3)	4309(2)	-1383(3)	41(1)
C(28)	8766(2)	4204(1)	-1766(2)	27(1)
C(29)	8221(2)	4680(2)	-1582(2)	32(1)
C(30)	8403(2)	4744(1)	-767(2)	30(1)
C(31)	8844(3)	3963(2)	-2599(2)	33(1)
C(32)	7868(3)	4062(2)	-3143(3)	60(1)
C(33)	9685(3)	4277(2)	-2979(3)	51(1)
C(34)	9061(2)	3335(2)	-2590(2)	26(1)
C(35)	8803(2)	2946(2)	-3202(2)	32(1)
C(36)	9160(2)	2431(2)	-2923(2)	31(1)
C(37)	6467(3)	3909(2)	-529(2)	35(1)
C(38)	5804(3)	4363(2)	-309(3)	62(1)
C(39)	8603(3)	4204(2)	4021(3)	55(1)
C(40)	8183(4)	4522(2)	3319(3)	78(2)
C(41)	8596(3)	126(2)	445(3)	44(1)
C(42)	8798(4)	-425(2)	130(3)	63(1)

Table 3. Bond lengths [A] and angles [deg] for asKJC03.

Co(1)-O(1)	1.874(2)
Co(1)-N(7)	1.907(3)
Co(1)-N(3)	1.930(3)
Co(1)-N(9)	1.930(2)
Co(1)-N(1)	1.934(3)
Co(1)-N(5)	1.936(3)
O(1)-Co(2)	1.880(2)
N(1)-C(1)	1.346(4)
N(1)-N(2)	1.360(4)
C(1)-C(2)	1.401(5)
C(1)-C(4)	1.505(5)
Co(2)-N(8)	1.910(3)
Co(2)-N(10)	1.914(3)
Co(2)-N(11)	1.920(3)
Co(2)-N(13)	1.933(3)
Co(2)-N(15)	1.948(3)
Cl(2)-Co(3)	2.3111(10)
N(2)-C(3)	1.329(4)
C(2)-C(3)	1.371(5)
Co(3)-Cl(5)	2.2535(12)
Co(3)-Cl(3)	2.2557(11)
Co(3)-Cl(4)	2.2648(12)
N(3)-C(7)	1.345(4)
N(3)-N(4)	1.358(4)
N(4)-C(9)	1.339(4)
C(4)-C(7)	1.519(5)
C(4)-C(6)	1.541(4)
C(4)-C(5)	1.542(5)
N(5)-C(10)	1.338(4)
N(5)-N(6)	1.358(3)
N(6)-C(12)	1.328(5)
N(7)-C(16)	1.341(4)
N(7)-N(8)	1.388(3)
C(7)-C(8)	1.392(4)
N(8)-C(18)	1.343(4)
C(8)-C(9)	1.363(5)
N(9)-C(19)	1.337(4)
N(9)-N(10)	1.378(3)
N(10)-C(21)	1.345(4)
C(10)-C(11)	1.400(5)
C(10)-C(13)	1.514(5)
N(11)-N(12)	1.352(4)
N(11)-C(25)	1.354(4)
C(11)-C(12)	1.369(5)
N(12)-C(27)	1.332(4)
N(13)-C(28)	1.349(4)
N(13)-N(14)	1.363(4)
C(13)-C(16)	1.513(5)
C(13)-C(15)	1.541(4)
C(13)-C(14)	1.545(5)
N(14)-C(30)	1.336(4)
N(15)-C(34)	1.342(4)
N(15)-N(16)	1.354(4)

N(16)-C(36)	1.334(4)
C(16)-C(17)	1.390(4)
N(17)-C(37)	1.137(4)
C(17)-C(18)	1.377(5)
N(18)-C(39)	1.129(6)
N(19)-C(41)	1.136(5)
C(19)-C(20)	1.379(4)
C(20)-C(21)	1.394(5)
C(21)-C(22)	1.505(4)
C(22)-C(25)	1.512(5)
C(22)-C(23)	1.537(5)
C(22)-C(24)	1.550(4)
C(25)-C(26)	1.396(5)
C(26)-C(27)	1.357(5)
C(28)-C(29)	1.398(5)
C(28)-C(31)	1.513(5)
C(29)-C(30)	1.359(5)
C(31)-C(34)	1.508(5)
C(31)-C(32)	1.536(5)
C(31)-C(33)	1.558(5)
C(34)-C(35)	1.386(5)
C(35)-C(36)	1.366(5)
C(37)-C(38)	1.473(6)
C(39)-C(40)	1.448(7)
C(41)-C(42)	1.438(6)

O(1)-Co(1)-N(7)	89.90(10)
O(1)-Co(1)-N(3)	91.48(10)
N(7)-Co(1)-N(3)	93.61(11)
O(1)-Co(1)-N(9)	84.95(10)
N(7)-Co(1)-N(9)	84.62(11)
N(3)-Co(1)-N(9)	176.01(11)
O(1)-Co(1)-N(1)	87.91(10)
N(7)-Co(1)-N(1)	177.06(11)
N(3)-Co(1)-N(1)	88.41(11)
N(9)-Co(1)-N(1)	93.22(11)
O(1)-Co(1)-N(5)	176.45(10)
N(7)-Co(1)-N(5)	89.30(11)
N(3)-Co(1)-N(5)	92.02(11)
N(9)-Co(1)-N(5)	91.54(11)
N(1)-Co(1)-N(5)	92.77(11)
Co(1)-O(1)-Co(2)	111.77(10)
C(1)-N(1)-N(2)	105.9(3)
C(1)-N(1)-Co(1)	132.3(2)
N(2)-N(1)-Co(1)	121.43(19)
N(1)-C(1)-C(2)	109.0(3)
N(1)-C(1)-C(4)	124.3(3)
C(2)-C(1)-C(4)	126.7(3)
O(1)-Co(2)-N(8)	88.52(10)
O(1)-Co(2)-N(10)	86.32(10)
N(8)-Co(2)-N(10)	83.84(11)
O(1)-Co(2)-N(11)	175.83(10)
N(8)-Co(2)-N(11)	91.09(11)
N(10)-Co(2)-N(11)	89.50(11)
O(1)-Co(2)-N(13)	91.35(10)
N(8)-Co(2)-N(13)	94.00(11)

N(10)-Co(2)-N(13)	176.86(11)	C(28)-N(13)-N(14)	106.2(3)
N(11)-Co(2)-N(13)	92.82(11)	C(28)-N(13)-Co(2)	132.1(2)
O(1)-Co(2)-N(15)	87.98(10)	N(14)-N(13)-Co(2)	120.8(2)
N(8)-Co(2)-N(15)	176.18(11)	C(16)-C(13)-C(10)	112.5(3)
N(10)-Co(2)-N(15)	94.40(11)	C(16)-C(13)-C(15)	108.6(3)
N(11)-Co(2)-N(15)	92.28(11)	C(10)-C(13)-C(15)	107.7(3)
N(13)-Co(2)-N(15)	87.62(12)	C(16)-C(13)-C(14)	109.2(3)
C(3)-N(2)-N(1)	111.6(3)	C(10)-C(13)-C(14)	109.3(3)
C(3)-C(2)-C(1)	106.3(3)	C(15)-C(13)-C(14)	109.3(3)
Cl(5)-Co(3)-Cl(3)	108.32(5)	C(30)-N(14)-N(13)	109.9(3)
Cl(5)-Co(3)-Cl(4)	115.25(5)	C(34)-N(15)-N(16)	105.7(3)
Cl(3)-Co(3)-Cl(4)	108.46(5)	C(34)-N(15)-Co(2)	133.0(2)
Cl(5)-Co(3)-Cl(2)	102.78(5)	N(16)-N(15)-Co(2)	120.3(2)
Cl(3)-Co(3)-Cl(2)	109.35(4)	C(36)-N(16)-N(15)	111.5(3)
Cl(4)-Co(3)-Cl(2)	112.45(4)	N(7)-C(16)-C(17)	108.9(3)
C(7)-N(3)-N(4)	106.0(2)	N(7)-C(16)-C(13)	124.0(3)
C(7)-N(3)-Co(1)	132.3(2)	C(17)-C(16)-C(13)	127.1(3)
N(4)-N(3)-Co(1)	121.62(19)	C(18)-C(17)-C(16)	105.3(3)
N(2)-C(3)-C(2)	107.2(3)	N(8)-C(18)-C(17)	110.6(3)
C(9)-N(4)-N(3)	110.9(3)	N(9)-C(19)-C(20)	110.0(3)
C(1)-C(4)-C(7)	114.5(3)	C(19)-C(20)-C(21)	105.3(3)
C(1)-C(4)-C(6)	108.0(3)	N(10)-C(21)-C(20)	108.7(3)
C(7)-C(4)-C(6)	107.1(3)	N(10)-C(21)-C(22)	123.8(3)
C(1)-C(4)-C(5)	108.6(3)	C(20)-C(21)-C(22)	127.5(3)
C(7)-C(4)-C(5)	109.9(3)	C(21)-C(22)-C(25)	113.5(3)
C(6)-C(4)-C(5)	108.5(3)	C(21)-C(22)-C(23)	109.4(3)
C(10)-N(5)-N(6)	105.9(3)	C(25)-C(22)-C(23)	109.6(3)
C(10)-N(5)-Co(1)	131.6(2)	C(21)-C(22)-C(24)	107.9(3)
N(6)-N(5)-Co(1)	122.1(2)	C(25)-C(22)-C(24)	107.7(3)
C(12)-N(6)-N(5)	111.6(3)	C(23)-C(22)-C(24)	108.6(3)
C(16)-N(7)-N(8)	108.6(2)	N(11)-C(25)-C(26)	108.3(3)
C(16)-N(7)-Co(1)	130.9(2)	N(11)-C(25)-C(22)	124.7(3)
N(8)-N(7)-Co(1)	116.5(2)	C(26)-C(25)-C(22)	127.0(3)
N(3)-C(7)-C(8)	109.2(3)	C(27)-C(26)-C(25)	106.8(3)
N(3)-C(7)-C(4)	124.5(3)	N(12)-C(27)-C(26)	107.6(3)
C(8)-C(7)-C(4)	126.4(3)	N(13)-C(28)-C(29)	109.4(3)
C(18)-N(8)-N(7)	106.5(3)	N(13)-C(28)-C(31)	124.0(3)
C(18)-N(8)-Co(2)	129.7(2)	C(29)-C(28)-C(31)	126.6(3)
N(7)-N(8)-Co(2)	116.80(19)	C(30)-C(29)-C(28)	105.5(3)
C(9)-C(8)-C(7)	106.5(3)	N(14)-C(30)-C(29)	109.0(3)
C(19)-N(9)-N(10)	107.6(2)	C(34)-C(31)-C(28)	113.1(3)
C(19)-N(9)-Co(1)	130.4(2)	C(34)-C(31)-C(32)	108.1(3)
N(10)-N(9)-Co(1)	115.78(18)	C(28)-C(31)-C(32)	109.6(3)
N(4)-C(9)-C(8)	107.4(3)	C(34)-C(31)-C(33)	108.4(3)
C(21)-N(10)-N(9)	108.3(2)	C(28)-C(31)-C(33)	109.2(3)
C(21)-N(10)-Co(2)	131.5(2)	C(32)-C(31)-C(33)	108.4(3)
N(9)-N(10)-Co(2)	117.34(18)	N(15)-C(34)-C(35)	109.3(3)
N(5)-C(10)-C(11)	109.2(3)	N(15)-C(34)-C(31)	123.2(3)
N(5)-C(10)-C(13)	124.3(3)	C(35)-C(34)-C(31)	127.5(3)
C(11)-C(10)-C(13)	126.5(3)	C(36)-C(35)-C(34)	106.7(3)
N(12)-N(11)-C(25)	106.2(3)	N(16)-C(36)-C(35)	106.8(3)
N(12)-N(11)-Co(2)	122.32(19)	N(17)-C(37)-C(38)	179.9(5)
C(25)-N(11)-Co(2)	131.2(2)	N(18)-C(39)-C(40)	178.3(6)
C(12)-C(11)-C(10)	106.1(3)	N(19)-C(41)-C(42)	179.9(6)
C(27)-N(12)-N(11)	111.0(3)		
N(6)-C(12)-C(11)	107.2(3)		

Symmetry transformations used to generate equivalent atoms:

Table 4. Anisotropic displacement parameters (A^2 x 10^3) for asKJC03.
The anisotropic displacement factor exponent takes the form:
-2 pi^2 [h^2 a*^2 U11 + ... + 2 h k a* b* U12]

	U11	U22	U33	U23	U13	U12
Co(1)	17(1)	19(1)	21(1)	-1(1)	5(1)	0(1)
Cl(1)	38(1)	25(1)	34(1)	-4(1)	12(1)	0(1)
O(1)	17(1)	26(1)	19(1)	0(1)	3(1)	-3(1)
N(1)	21(1)	22(2)	21(2)	-3(1)	5(1)	-2(1)
C(1)	23(2)	24(2)	23(2)	3(2)	2(1)	-1(1)
Co(2)	18(1)	19(1)	22(1)	1(1)	6(1)	1(1)
Cl(2)	37(1)	25(1)	37(1)	-7(1)	-2(1)	-1(1)
N(2)	23(1)	25(2)	27(2)	-5(1)	7(1)	-1(1)
C(2)	26(2)	32(2)	30(2)	-2(2)	-1(2)	-8(2)
Co(3)	23(1)	27(1)	31(1)	-6(1)	7(1)	-1(1)
Cl(3)	33(1)	31(1)	52(1)	-3(1)	16(1)	7(1)
N(3)	20(1)	20(2)	21(2)	0(1)	5(1)	0(1)
C(3)	33(2)	26(2)	28(2)	-8(2)	-1(2)	-5(2)
Cl(4)	48(1)	52(1)	44(1)	-10(1)	-11(1)	19(1)
N(4)	21(1)	23(2)	25(2)	-4(1)	4(1)	-1(1)
C(4)	20(2)	27(2)	25(2)	-2(2)	4(1)	-5(1)
Cl(5)	52(1)	50(1)	59(1)	-10(1)	27(1)	-21(1)
N(5)	22(1)	17(1)	24(2)	0(1)	6(1)	0(1)
C(5)	45(2)	34(2)	36(3)	-2(2)	18(2)	-14(2)
N(6)	29(2)	22(2)	27(2)	1(1)	5(1)	-5(1)
C(6)	19(2)	50(2)	50(3)	-12(2)	4(2)	-1(2)
N(7)	18(1)	18(1)	22(2)	1(1)	7(1)	-2(1)
C(7)	19(2)	27(2)	23(2)	3(2)	5(1)	0(1)
N(8)	22(1)	15(1)	20(2)	-1(1)	8(1)	-3(1)
C(8)	21(2)	34(2)	31(2)	1(2)	10(2)	5(2)
N(9)	21(1)	19(1)	18(2)	1(1)	7(1)	-2(1)
C(9)	27(2)	27(2)	26(2)	-4(2)	9(2)	9(2)
N(10)	19(1)	19(1)	19(2)	2(1)	5(1)	1(1)
C(10)	24(2)	28(2)	23(2)	1(2)	8(2)	-1(1)
N(11)	24(1)	20(2)	26(2)	3(1)	9(1)	2(1)
C(11)	39(2)	38(2)	27(2)	9(2)	-2(2)	-1(2)
N(12)	29(2)	19(2)	41(2)	8(1)	16(1)	2(1)
C(12)	45(2)	28(2)	36(3)	10(2)	5(2)	-2(2)
N(13)	26(1)	21(2)	25(2)	-2(1)	10(1)	3(1)
C(13)	24(2)	28(2)	22(2)	-1(2)	6(1)	-3(2)
N(14)	28(2)	22(2)	28(2)	-1(1)	9(1)	3(1)
C(14)	37(2)	33(2)	27(2)	0(2)	10(2)	0(2)
N(15)	21(1)	24(2)	23(2)	-2(1)	7(1)	1(1)
C(15)	28(2)	41(2)	32(2)	3(2)	-3(2)	-3(2)
N(16)	26(1)	19(2)	27(2)	-2(1)	7(1)	3(1)
C(16)	18(2)	24(2)	23(2)	-4(2)	4(1)	1(1)
N(17)	32(2)	43(2)	32(2)	2(2)	3(1)	6(2)
C(17)	25(2)	29(2)	25(2)	-4(2)	4(2)	-7(2)

N(18)	86(3)	76(3)	78(4)	17(3)	5(3)	17(3)
C(18)	23(2)	24(2)	31(2)	-5(2)	7(2)	-8(1)
N(19)	79(3)	30(2)	64(3)	0(2)	-13(2)	-1(2)
C(19)	31(2)	16(2)	19(2)	0(2)	4(1)	2(1)
C(20)	19(2)	23(2)	28(2)	-1(2)	4(1)	4(1)
C(21)	19(2)	24(2)	18(2)	-4(2)	5(1)	0(1)
C(22)	20(2)	28(2)	23(2)	-1(2)	8(1)	1(1)
C(23)	35(2)	36(2)	29(2)	-1(2)	17(2)	1(2)
C(24)	19(2)	37(2)	44(3)	6(2)	5(2)	-1(2)
C(25)	25(2)	25(2)	28(2)	-2(2)	9(2)	1(1)
C(26)	28(2)	37(2)	61(3)	8(2)	24(2)	-1(2)
C(27)	31(2)	28(2)	69(3)	5(2)	23(2)	-8(2)
C(28)	25(2)	26(2)	30(2)	3(2)	8(2)	3(2)
C(29)	32(2)	26(2)	38(3)	6(2)	9(2)	8(2)
C(30)	32(2)	17(2)	44(3)	-3(2)	13(2)	4(2)
C(31)	42(2)	31(2)	28(2)	5(2)	5(2)	14(2)
C(32)	69(3)	61(3)	45(3)	-9(2)	-17(2)	42(2)
C(33)	81(3)	34(2)	43(3)	7(2)	31(2)	6(2)
C(34)	22(2)	33(2)	23(2)	2(2)	7(1)	5(2)
C(35)	30(2)	40(2)	23(2)	-3(2)	-3(2)	10(2)
C(36)	25(2)	38(2)	28(2)	-9(2)	4(2)	-3(2)
C(37)	34(2)	43(2)	27(2)	5(2)	-2(2)	-3(2)
C(38)	61(3)	64(3)	60(4)	-1(3)	9(2)	26(2)
C(39)	50(3)	60(3)	56(4)	-2(3)	13(2)	8(2)
C(40)	80(4)	108(5)	49(4)	13(3)	17(3)	28(3)
C(41)	60(3)	30(2)	40(3)	10(2)	-4(2)	-7(2)
C(42)	99(4)	36(3)	55(3)	7(2)	12(3)	6(3)

Table 5. Hydrogen coordinates (x 10^4) and isotropic
displacement parameters (A^2 x 10^3) for asKJC03.

	x	y	z	U(eq)
H(1)	8225	2951	-858	24
H(2)	9126	1575	-786	30
H(2A)	6356	1213	-607	36
H(3)	7816	960	-1321	35
H(4)	8587	3620	1202	27
H(5A)	6375	1339	1111	56
H(5B)	6153	1872	1659	56
H(5C)	7268	1668	1620	56
H(6)	8866	1353	1091	31
H(6A)	5684	2465	-312	59
H(6B)	5229	2381	525	59
H(6C)	5362	1845	-44	59
H(8)	5886	3090	1340	34
H(9)	7041	3905	1637	32
H(11)	10565	1710	3085	42
H(12)	10828	4437	-1243	34
H(12A)	9592	937	2327	43
H(14)	9258	4299	44	30
H(14A)	9223	3192	2508	48

H(14B)	10185	3510	2931	48
H(14C)	9831	2928	3301	48
H(15A)	11494	2508	3243	52
H(15B)	11885	3074	2853	52
H(15C)	11966	2477	2407	52
H(16)	9911	2250	-1872	28
H(17)	11916	3648	1793	32
H(18)	11555	4000	377	31
H(19)	10851	1564	590	26
H(20)	12417	1765	-7	28
H(23A)	12485	2068	-1806	49
H(23B)	12836	2650	-2179	49
H(23C)	11682	2514	-2197	49
H(24A)	13388	2897	-61	50
H(24B)	13856	2905	-900	50
H(24C)	13560	2314	-518	50
H(26)	13420	3771	-1432	49
H(27)	12476	4676	-1481	50
H(29)	7809	4910	-1950	38
H(30)	8130	5031	-459	37
H(32A)	7919	3905	-3681	90
H(32B)	7735	4471	-3187	90
H(32C)	7328	3874	-2906	90
H(33A)	10326	4170	-2690	76
H(33B)	9593	4688	-2937	76
H(33C)	9665	4170	-3550	76
H(35)	8446	3021	-3716	38
H(36)	9096	2080	-3204	37
H(38A)	5614	4604	-781	92
H(38B)	6145	4593	128	92
H(38C)	5210	4193	-128	92
H(40A)	7503	4395	3160	117
H(40B)	8579	4458	2872	117
H(40C)	8184	4928	3450	117
H(42A)	8924	-389	-435	95
H(42B)	8228	-674	163	95
H(42C)	9381	-588	449	95

Complex 3f

Table 1. Crystal data and structure refinement

Identification code   asKJC04
Empirical formula   C22 H30 Cl2 Co N10
Formula weight   564.39
Temperature   150(2) K
Wavelength   0.71073 A
Crystal system, space group   orthorhombic, Pbca
Unit cell dimensions   a = 15.189(3) A   alpha = 90 deg.
                                        b = 7.8793(16) A   beta = 90 deg.
                                        c = 22.836(5) A   gamma = 90 deg.
Volume   2733.1(10) A^3
Z, Calculated density   4, 1.372 Mg/m^3
Absorption coefficient   0.854 mm^-1
F(000)   1172
Crystal size   0.20 x 0.12 x 0.08 mm
Theta range for data collection   3.22 to 25.49 deg.
Limiting indices   -18<=h<=18, -9<=k<=9, -27<=l<=27
Reflections collected / unique   4716 / 2537 [R(int) = 0.0298]
Completeness to theta =   25.49   99.6 %
Max. and min. transmission   sortav 0.877 and 0.687
Refinement method   Full-matrix least-squares on F^2
Data / restraints / parameters   2537 / 0 / 163
Goodness-of-fit on F^2   1.107
Final R indices [I>2sigma(I)]   R1 = 0.0476, wR2 = 0.1063
R indices (all data)   R1 = 0.0657, wR2 = 0.1134
Largest diff. peak and hole   0.668 and -0.326 e.A^-3

Table 2. Atomic coordinates (x 10^4) and equivalent isotropic
displacement parameters (A^2 x 10^3) for asKJC04.
U(eq) is defined as one third of the trace of the orthogonalized
Uij tensor.

	x	y	z	U(eq)
Co(1)	0	0	5000	24(1)
Cl(1)	1185(1)	1665(1)	5486(1)	31(1)
N(1)	229(2)	1315(3)	4202(1)	30(1)
C(1)	-30(2)	1146(4)	3651(1)	38(1)
N(2)	736(2)	2730(3)	4195(1)	29(1)
C(2)	295(3)	2443(4)	3300(1)	42(1)
N(3)	890(2)	8048(3)	4725(1)	29(1)
C(3)	789(2)	3450(4)	3660(1)	28(1)
N(4)	709(2)	7161(3)	4234(1)	29(1)
C(4)	1338(2)	5025(4)	3537(1)	28(1)
N(5)	1549(4)	2960(7)	7061(2)	110(2)
C(5)	2277(2)	4487(4)	3368(1)	34(1)
C(6)	924(2)	6010(4)	3024(1)	36(1)
C(7)	1682(2)	7531(4)	4895(1)	32(1)
C(8)	2012(2)	6325(4)	4508(1)	32(1)
C(9)	1374(2)	6119(4)	4084(1)	27(1)

C(10)	1691(3)	4030(7)	6746(2)	67(1)
C(11)	1844(4)	5365(6)	6322(2)	82(2)

Table 3. Bond lengths [A] and angles [deg] for asKJC04.

Co(1)-N(1)	2.125(3)		C(3)-C(4)-C(6)	109.1(2)
Co(1)-N(1_5)	2.125(3)		C(5)-C(4)-C(6)	109.1(3)
Co(1)-N(3_5)	2.141(2)		N(3)-C(7)-C(8)	110.5(3)
Co(1)-N(3)	2.141(2)		C(9)-C(8)-C(7)	105.9(3)
Co(1)-Cl(2)	2.4880(8)		N(4)-C(9)-C(8)	106.0(3)
Co(1)-Cl(1)	2.4880(8)		N(4)-C(9)-C(4)	122.0(3)
N(1)-C(1)	1.326(4)		C(8)-C(9)-C(4)	132.0(3)
N(1)-N(2)	1.355(3)		N(5)-C(10)-C(11)	177.4(6)
C(1)-C(2)	1.389(5)			
N(2)-C(3)	1.349(4)			
C(2)-C(3)	1.367(4)			
N(3)-C(7)	1.329(4)			
N(3)-N(4)	1.350(3)			
N(3)-Co(1)	2.141(2)			
C(3)-C(4)	1.521(4)			
N(4)-C(9)	1.345(4)			
C(4)-C(9)	1.518(4)			
C(4)-C(5)	1.536(4)			
C(4)-C(6)	1.541(4)			
N(5)-C(10)	1.130(6)			
C(7)-C(8)	1.391(4)			
C(8)-C(9)	1.380(4)			
C(10)-C(11)	1.447(7)			

Symmetry transformations used to generate equivalent atoms:
#1 -x,-y,-z+1   #2 -x,-y+1,-z+1   #3 x,y-1,z
#4 x,y+1,z

N(1)-Co(1)-N(1_5)	180.000(1)
N(1)-Co(1)-N(3_5)	90.26(10)
N(1_5)-Co(1)-N(3_5)	89.74(10)
N(1)-Co(1)-N(3)	89.74(10)
N(1_5)-Co(1)-N(3)	90.26(10)
N(3_5)-Co(1)-N(3)	180.00(13)
N(1)-Co(1)-Cl(1)	89.60(7)
N(1_5)-Co(1)-Cl(2)	90.40(7)
N(3_5)-Co(1)-Cl(2)	93.05(7)
N(3)-Co(1)-Cl(2)	86.95(7)
N(1)-Co(1)-Cl(1)	90.40(7)
N(1_5)-Co(1)-Cl(1)	89.60(7)
N(3_5)-Co(1)-Cl(1)	86.95(7)
N(3)-Co(1)-Cl(1)	93.05(7)
Cl(2)-Co(1)-Cl(1)	180.00(4)
C(1)-N(1)-N(2)	103.9(2)
C(1)-N(1)-Co(1)	135.8(2)
N(2)-N(1)-Co(1)	120.31(19)
N(1)-C(1)-C(2)	111.6(3)
C(3)-N(2)-N(1)	113.0(2)
C(3)-C(2)-C(1)	106.0(3)
C(7)-N(3)-N(4)	105.5(2)
C(7)-N(3)-Co(1)	134.9(2)
N(4)-N(3)-Co(1)	119.20(18)
N(2)-C(3)-C(2)	105.5(3)
N(2)-C(3)-C(4)	122.9(3)
C(2)-C(3)-C(4)	131.6(3)
C(9)-N(4)-N(3)	112.1(2)
C(9)-C(4)-C(3)	109.3(2)
C(9)-C(4)-C(5)	109.3(2)
C(3)-C(4)-C(5)	109.2(2)
C(9)-C(4)-C(6)	110.8(2)

Table 4. Anisotropic displacement parameters (A^2 x 10^3) for asKJC04.
The anisotropic displacement factor exponent takes the form:
-2 pi^2 [h^2 a*^2 U11 + ... + 2 h k a* b* U12]

	U11	U22	U33	U23	U13	U12
Co(1)	25(1)	19(1)	29(1)	-2(1)	1(1)	-2(1)
Cl(1)	28(1)	29(1)	36(1)	-4(1)	0(1)	-4(1)
N(1)	36(2)	21(1)	34(1)	-1(1)	2(1)	-6(1)
C(1)	50(2)	30(2)	32(2)	-4(1)	-4(2)	-10(2)
N(2)	32(1)	25(1)	31(1)	-1(1)	-2(1)	-5(1)
C(2)	62(2)	36(2)	28(2)	-2(2)	0(2)	-14(2)
N(3)	32(1)	21(1)	34(1)	-7(1)	-9(1)	3(1)
C(3)	33(2)	23(2)	29(2)	-1(1)	0(1)	0(1)
N(4)	29(1)	26(1)	32(1)	-6(1)	-4(1)	0(1)
C(4)	32(2)	20(2)	32(2)	1(1)	0(1)	2(1)
N(5)	140(5)	125(4)	67(3)	30(3)	30(3)	38(4)
C(5)	36(2)	28(2)	39(2)	0(1)	7(2)	1(1)
C(6)	46(2)	27(2)	36(2)	1(1)	-3(2)	1(2)
C(7)	34(2)	27(2)	34(2)	0(1)	-4(1)	0(1)
C(8)	30(2)	26(2)	39(2)	1(1)	-2(1)	3(1)
C(9)	26(2)	19(1)	35(2)	1(1)	1(1)	-1(1)
C(10)	63(3)	85(3)	53(3)	-8(3)	4(2)	14(3)
C(11)	90(4)	63(3)	94(4)	-10(3)	24(3)	-26(3)

Table 5. Hydrogen coordinates (x 10^4) and isotropic
displacement parameters (A^2 x 10^3) for asKJC04.

	x	y	z	U(eq)
H(1)	-392	249	3513	45
H(2)	1003	3137	4507	35
H(2A)	195	2598	2893	51
H(4)	215	7253	4035	35
H(5A)	2539	3838	3690	51
H(5B)	2633	5499	3291	51
H(5C)	2256	3780	3015	51
H(6A)	937	5305	2670	54
H(6B)	1258	7055	2955	54
H(6C)	313	6296	3119	54
H(7)	1981	7929	5234	38
H(8)	2563	5760	4531	38
H(11A)	1681	4963	5931	124
H(11B)	2468	5679	6326	124
H(11C)	1486	6357	6424	124

Complex 5g

Table 1. Crystal data and structure refinement

Identification code	asKJC04
Empirical formula	C22 H30 Cl2 Co N10
Formula weight	564.39
Temperature	150(2)K
Wavelength	0.71073 A
Crystal system, space group	orthorhombic, Pbca
Unit cell dimensions	a = 15.189(3) A alpha = 90 deg.
	b = 7.8793(16) A beta = 90 deg.
	c = 22.836(5) A gamma = 90 deg.
Volume	2733.1(10) A^3
Z, Calculated density	4, 1.372 Mg/m^3
Absorption coefficient	0.854 mm^-1
F(000)	1172
Crystal size	0.20 x 0.12 x 0.08 mm
Theta range for data collection	3.22 to 25.49 deg.
Limiting indices	-18<=h<=18, -9<=k<=9, -27<=l<=27
Reflections collected / unique	4716 / 2537 [R(int) = 0.0298]
Completeness to theta = 25.49	99.6 %
Max. and min. transmission	sortav 0.877 and 0.687
Refinement method	Full-matrix least-squares on F^2
Data / restraints / parameters	2537 / 0 / 163
Goodness-of-fit on F^2	1.107
Final R indices [I>2sigma(I)]	R1 = 0.0476, wR2 = 0.1063
R indices (all data)	R1 = 0.0657, wR2 = 0.1134
Largest diff. peak and hole	0.668 and -0.326 e.A^-3

Table 2. Atomic coordinates (x 10^4) and equivalent isotropic displacement parameters (A^2x 10^3) for kjc0523. U(eq) is defined as one third of the trace of the orthogonalized U^{ij} tensor.

	x	y	z	U(eq)
C(1)	6322(5)	6314(5)	416(3)	30(3)
C(2)	5809(5)	5810(4)	397(3)	25(2)
C(3)	5854(5)	5520(4)	730(3)	25(2)
C(4)	5416(5)	4948(4)	874(3)	20(2)
C(5)	5054(5)	4599(4)	546(3)	29(3)
C(6)	4770(5)	5176(5)	1131(3)	36(3)
C(7)	5927(5)	4502(4)	1084(3)	21(2)
C(8)	5951(6)	3841(5)	1078(3)	33(3)
C(9)	6497(6)	3680(5)	1333(3)	33(3)
C(10)	5740(6)	4319(5)	2552(3)	32(3)
C(11)	6165(6)	4718(5)	2781(3)	37(3)
C(12)	6868(5)	4805(4)	2603(3)	23(2)
C(13)	7554(5)	5191(4)	2729(3)	27(2)
C(14)	7501(6)	5291(5)	3146(3)	40(3)
C(15)	7537(5)	5859(4)	2541(3)	31(3)
C(16)	8300(5)	4879(4)	2629(3)	26(3)
C(17)	8973(6)	4846(5)	2838(3)	38(3)
C(18)	9487(6)	4531(5)	2634(3)	32(3)
C(19)	8954(6)	3751(5)	1345(3)	34(3)
C(20)	9490(6)	3936(5)	1089(3)	34(3)
C(21)	9473(5)	4603(4)	1096(3)	23(2)

C(22)	9947(5)	5080(5)	891(3)	24(2)
C(23)	10564(5)	5338(5)	1154(3)	36(3)
C(24)	10360(5)	4737(5)	573(3)	35(3)
C(25)	9459(5)	5602(5)	741(3)	25(2)
C(26)	9473(5)	5902(5)	397(3)	30(3)
C(27)	8903(5)	6346(5)	408(3)	25(2)
C(28)	9399(5)	8126(5)	1263(3)	32(3)
C(29)	8950(6)	8274(5)	1555(3)	36(3)
C(30)	8304(5)	7862(4)	1525(3)	22(2)
C(31)	7607(5)	7831(4)	1765(3)	24(2)
C(32)	7619(6)	7235(4)	2016(3)	27(2)
C(33)	7600(6)	8413(4)	2017(3)	33(3)
C(34)	6896(5)	7822(4)	1537(3)	22(2)
C(35)	6221(6)	8171(5)	1587(3)	38(3)
C(36)	5762(6)	8027(5)	1300(3)	38(3)
C(37)	7698(6)	4746(6)	539(3)	51(3)
C(38)	8182(6)	4407(5)	277(4)	40(3)
C(39)	2642(8)	5991(6)	796(4)	65(4)
C(40)	3094(7)	5821(5)	476(4)	46(4)
C(41)	4827(9)	2328(6)	2630(4)	76(5)
C(42)	5111(8)	2722(6)	2335(4)	55(4)
C(43)	3833(8)	3173(6)	1462(4)	73(5)
C(44)	4069(7)	2929(6)	1112(4)	50(4)
C(45)	2454(9)	4210(6)	305(4)	74(4)
C(46)	2632(8)	4233(6)	688(5)	58(4)
C(47)	7430(8)	2959(7)	523(4)	79(5)
C(48)	6896(10)	2445(8)	611(4)	70(5)
C(49)	1428(9)	3093(7)	1609(5)	101(6)
C(50)	869(7)	3475(5)	1804(4)	51(4)
N(1)	6684(4)	6315(3)	736(2)	24(2)
N(2)	6393(4)	5830(3)	938(2)	20(2)
N(3)	6435(4)	4722(3)	1333(2)	19(2)
N(4)	6797(4)	4202(3)	1483(2)	20(2)
N(5)	6163(4)	4192(3)	2254(2)	24(2)
N(6)	6864(4)	4497(3)	2281(2)	23(2)
N(7)	8424(4)	4593(3)	2307(2)	22(2)
N(8)	9166(4)	4393(4)	2311(3)	30(2)
N(9)	8625(4)	4254(4)	1506(2)	26(2)
N(10)	8946(4)	4798(4)	1347(2)	27(2)
N(11)	8907(4)	5875(4)	947(2)	24(2)
N(12)	8565(4)	6348(3)	736(2)	20(2)
N(13)	9061(4)	7665(4)	1066(2)	25(2)
N(14)	8383(4)	7496(4)	1225(2)	25(2)
N(15)	6827(4)	7474(3)	1232(2)	18(2)
N(16)	6123(4)	7604(4)	1077(3)	28(2)
N(17)	8556(6)	4145(5)	78(3)	55(3)
N(18)	3452(6)	5681(5)	228(4)	60(3)
N(19)	5284(6)	3044(5)	2097(4)	68(4)
N(20)	4239(7)	2728(5)	830(4)	73(4)
N(21)	2758(10)	4265(7)	992(4)	111(6)
N(22)	6517(9)	2047(6)	689(5)	109(6)
N(23)	434(6)	3758(5)	1960(3)	54(3)
Fe(1)	6826(1)	5627(1)	1447(1)	16(1)
Fe(2)	7696(1)	4357(1)	1857(1)	20(1)
Fe(3)	8477(1)	5672(1)	1457(1)	16(1)
Fe(4)	7612(1)	6841(1)	953(1)	18(1)

O(1)	7664(3)	5205(2)	1692(2)	14(1)
O(2)	7630(3)	6223(2)	1321(2)	17(1)
Cl(3)	6015(1)	6087(1)	1835(1)	28(1)
Cl(4)	9224(1)	6150(1)	1865(1)	29(1)
Cl(5)	7752(1)	3251(1)	1983(1)	31(1)
Cl(6)	7584(1)	7483(1)	420(1)	29(1)
O(3)	5117(4)	7549(4)	509(2)	38(2)
O(4)	5575(5)	7793(4)	-47(3)	78(3)
C(51)	5089(5)	7471(5)	175(3)	32(3)
C(52)	4546(6)	7015(5)	-9(3)	43(3)

Table 3. Bond lengths [Å] and angles [°] for kjc0523.

C(1)-N(1)	1.328(12)
C(1)-C(2)	1.391(13)
C(1)-H(1)	0.9500
C(2)-C(3)	1.363(14)
C(2)-H(2)	0.9500
C(3)-N(2)	1.375(12)
C(3)-C(4)	1.520(13)
C(4)-C(7)	1.507(13)
C(4)-C(5)	1.539(13)
C(4)-C(6)	1.542(13)
C(5)-H(5A)	0.9800
C(5)-H(5B)	0.9800
C(5)-H(5C)	0.9800
C(6)-H(6A)	0.9800
C(6)-H(6B)	0.9800
C(6)-H(6C)	0.9800
C(7)-N(3)	1.349(11)
C(7)-C(8)	1.394(13)
C(8)-C(9)	1.372(14)
C(8)-H(8)	0.9500
C(9)-N(4)	1.337(12)
C(9)-H(9)	0.9500
C(10)-N(5)	1.342(13)
C(10)-C(11)	1.399(15)
C(10)-H(10)	0.9500
C(11)-C(12)	1.399(13)
C(11)-H(11)	0.9500
C(12)-N(6)	1.341(12)
C(12)-C(13)	1.520(13)
C(13)-C(16)	1.504(13)
C(13)-C(14)	1.536(14)
C(13)-C(15)	1.566(12)
C(14)-H(14A)	0.9800
C(14)-H(14B)	0.9800
C(14)-H(14C)	0.9800
C(15)-H(15A)	0.9800
C(15)-H(15B)	0.9800
C(15)-H(15C)	0.9800
C(16)-N(7)	1.339(13)
C(16)-C(17)	1.400(14)
C(17)-C(18)	1.340(15)
C(17)-H(17)	0.9500
C(18)-N(8)	1.336(13)
C(18)-H(18)	0.9500
C(19)-N(9)	1.341(12)
C(19)-C(20)	1.378(14)
C(19)-H(19)	0.9500
C(20)-C(21)	1.405(13)
C(20)-H(20)	0.9500
C(21)-N(10)	1.360(12)
C(21)-C(22)	1.502(13)

C(22)-C(25)	1.494(14)
C(22)-C(23)	1.541(13)
C(22)-C(24)	1.545(13)
C(23)-H(23A)	0.9800
C(23)-H(23B)	0.9800
C(23)-H(23C)	0.9800
C(24)-H(24A)	0.9800
C(24)-H(24B)	0.9800
C(24)-H(24C)	0.9800
C(25)-N(11)	1.352(12)
C(25)-C(26)	1.405(13)
C(26)-C(27)	1.368(13)
C(26)-H(26)	0.9500
C(27)-N(12)	1.335(11)
C(27)-H(27)	0.9500
C(28)-N(13)	1.345(12)
C(28)-C(29)	1.357(14)
C(28)-H(28)	0.9500
C(29)-C(30)	1.426(13)
C(29)-H(29)	0.9500
C(30)-N(14)	1.344(12)
C(30)-C(31)	1.500(13)
C(31)-C(34)	1.493(13)
C(31)-C(33)	1.534(12)
C(31)-C(32)	1.554(12)
C(32)-H(32A)	0.9800
C(32)-H(32B)	0.9800
C(32)-H(32C)	0.9800
C(33)-H(33A)	0.9800
C(33)-H(33B)	0.9800
C(33)-H(33C)	0.9800
C(34)-N(15)	1.337(12)
C(34)-C(35)	1.399(13)
C(35)-C(36)	1.352(15)
C(35)-H(35)	0.9500
C(36)-N(16)	1.360(13)
C(36)-H(36)	0.9500
C(37)-C(38)	1.462(15)
C(37)-H(37A)	0.9800
C(37)-H(37B)	0.9800
C(37)-H(37C)	0.9800
C(38)-N(17)	1.118(14)
C(39)-C(40)	1.453(18)
C(39)-H(39A)	0.9800
C(39)-H(39B)	0.9800
C(39)-H(39C)	0.9800
C(40)-N(18)	1.140(16)
C(41)-C(42)	1.446(17)
C(41)-H(41A)	0.9800
C(41)-H(41B)	0.9800
C(41)-H(41C)	0.9800
C(42)-N(19)	1.144(16)
C(43)-C(44)	1.439(18)
C(43)-H(43A)	0.9800
C(43)-H(43B)	0.9800

C(43)-H(43C)	0.9800	C(3)-C(2)-H(2)	127.5
C(44)-N(20)	1.150(16)	C(1)-C(2)-H(2)	127.5
C(45)-C(46)	1.434(19)	C(2)-C(3)-N(2)	108.6(8)
C(45)-H(45A)	0.9800	C(2)-C(3)-C(4)	129.4(9)
C(45)-H(45B)	0.9800	N(2)-C(3)-C(4)	122.0(9)
C(45)-H(45C)	0.9800	C(7)-C(4)-C(3)	111.9(7)
C(46)-N(21)	1.131(17)	C(7)-C(4)-C(5)	109.9(7)
C(47)-C(48)	1.47(2)	C(3)-C(4)-C(5)	108.4(8)
C(47)-H(47A)	0.9800	C(7)-C(4)-C(6)	108.5(9)
C(47)-H(47B)	0.9800	C(3)-C(4)-C(6)	109.4(7)
C(47)-H(47C)	0.9800	C(5)-C(4)-C(6)	108.8(7)
C(48)-N(22)	1.104(19)	C(4)-C(5)-H(5A)	109.5
C(49)-C(50)	1.453(18)	C(4)-C(5)-H(5B)	109.5
C(49)-H(49A)	0.9800	H(5A)-C(5)-H(5B)	109.5
C(49)-H(49B)	0.9800	C(4)-C(5)-H(5C)	109.5
C(49)-H(49C)	0.9800	H(5A)-C(5)-H(5C)	109.5
C(50)-N(23)	1.118(14)	H(5B)-C(5)-H(5C)	109.5
N(1)-N(2)	1.359(10)	C(4)-C(6)-H(6A)	109.5
N(1)-Fe(4)	2.114(8)	C(4)-C(6)-H(6B)	109.5
N(2)-Fe(1)	2.049(8)	H(6A)-C(6)-H(6B)	109.5
N(3)-N(4)	1.379(10)	C(4)-C(6)-H(6C)	109.5
N(3)-Fe(1)	2.067(7)	H(6A)-C(6)-H(6C)	109.5
N(4)-Fe(2)	2.103(7)	H(6B)-C(6)-H(6C)	109.5
N(5)-N(6)	1.383(10)	N(3)-C(7)-C(8)	109.6(9)
N(6)-Fe(2)	2.142(8)	N(3)-C(7)-C(4)	121.1(8)
N(7)-N(8)	1.362(10)	C(8)-C(7)-C(4)	129.3(9)
N(7)-Fe(2)	2.133(8)	C(9)-C(8)-C(7)	104.9(9)
N(9)-N(10)	1.401(10)	C(9)-C(8)-H(8)	127.6
N(9)-Fe(2)	2.076(8)	C(7)-C(8)-H(8)	127.6
N(10)-Fe(3)	2.057(8)	N(4)-C(9)-C(8)	110.3(9)
N(11)-N(12)	1.394(10)	N(4)-C(9)-H(9)	124.9
N(11)-Fe(3)	2.050(8)	C(8)-C(9)-H(9)	124.9
N(12)-Fe(4)	2.114(8)	N(5)-C(10)-C(11)	108.1(9)
N(13)-N(14)	1.364(10)	N(5)-C(10)-H(10)	125.9
N(14)-Fe(4)	2.170(8)	C(11)-C(10)-H(10)	125.9
N(15)-N(16)	1.379(10)	C(12)-C(11)-C(10)	105.4(10)
N(15)-Fe(4)	2.165(7)	C(12)-C(11)-H(11)	127.3
Fe(1)-O(1)	1.930(5)	C(10)-C(11)-H(11)	127.3
Fe(1)-O(2)	1.938(5)	N(6)-C(12)-C(11)	109.8(9)
Fe(1)-Cl(3)	2.224(3)	N(6)-C(12)-C(13)	122.0(9)
Fe(1)-Fe(3)	2.8813(15)	C(11)-C(12)-C(13)	128.2(10)
Fe(2)-O(1)	1.887(5)	C(16)-C(13)-C(12)	111.9(7)
Fe(2)-Cl(5)	2.377(3)	C(16)-C(13)-C(14)	110.6(9)
Fe(3)-O(1)	1.927(5)	C(12)-C(13)-C(14)	109.1(8)
Fe(3)-O(2)	1.942(5)	C(16)-C(13)-C(15)	107.6(8)
Fe(3)-Cl(4)	2.219(3)	C(12)-C(13)-C(15)	109.5(8)
Fe(4)-O(2)	1.871(6)	C(14)-C(13)-C(15)	108.0(8)
Fe(4)-Cl(6)	2.367(3)	C(13)-C(14)-H(14A)	109.5
O(3)-C(51)	1.229(12)	C(13)-C(14)-H(14B)	109.5
O(4)-C(51)	1.358(14)	H(14A)-C(14)-H(14B)	109.5
C(51)-C(52)	1.506(15)	C(13)-C(14)-H(14C)	109.5
		H(14A)-C(14)-H(14C)	109.5
N(1)-C(1)-C(2)	110.6(9)	H(14B)-C(14)-H(14C)	109.5
N(1)-C(1)-H(1)	124.7	C(13)-C(15)-H(15A)	109.5
C(2)-C(1)-H(1)	124.7	C(13)-C(15)-H(15B)	109.5
C(3)-C(2)-C(1)	105.1(9)	H(15A)-C(15)-H(15B)	109.5

C(13)-C(15)-H(15C)	109.5	C(29)-C(30)-C(31)	128.5(9)
H(15A)-C(15)-H(15C)	109.5	C(34)-C(31)-C(30)	110.5(8)
H(15B)-C(15)-H(15C)	109.5	C(34)-C(31)-C(33)	109.7(8)
N(7)-C(16)-C(17)	108.7(9)	C(30)-C(31)-C(33)	108.7(7)
N(7)-C(16)-C(13)	123.3(8)	C(34)-C(31)-C(32)	109.3(7)
C(17)-C(16)-C(13)	128.0(11)	C(30)-C(31)-C(32)	111.6(8)
C(18)-C(17)-C(16)	106.5(11)	C(33)-C(31)-C(32)	107.0(8)
C(18)-C(17)-H(17)	126.8	C(31)-C(32)-H(32A)	109.5
C(16)-C(17)-H(17)	126.8	C(31)-C(32)-H(32B)	109.5
N(8)-C(18)-C(17)	108.5(9)	H(32A)-C(32)-H(32B)	109.5
N(8)-C(18)-H(18)	125.8	C(31)-C(32)-H(32C)	109.5
C(17)-C(18)-H(18)	125.8	H(32A)-C(32)-H(32C)	109.5
N(9)-C(19)-C(20)	111.2(9)	H(32B)-C(32)-H(32C)	109.5
N(9)-C(19)-H(19)	124.4	C(31)-C(33)-H(33A)	109.5
C(20)-C(19)-H(19)	124.4	C(31)-C(33)-H(33B)	109.5
C(19)-C(20)-C(21)	105.0(9)	H(33A)-C(33)-H(33B)	109.5
C(19)-C(20)-H(20)	127.5	C(31)-C(33)-H(33C)	109.5
C(21)-C(20)-H(20)	127.5	H(33A)-C(33)-H(33C)	109.5
N(10)-C(21)-C(20)	109.1(8)	H(33B)-C(33)-H(33C)	109.5
N(10)-C(21)-C(22)	120.4(8)	N(15)-C(34)-C(35)	108.8(8)
C(20)-C(21)-C(22)	130.4(9)	N(15)-C(34)-C(31)	122.9(8)
C(25)-C(22)-C(21)	111.1(7)	C(35)-C(34)-C(31)	128.3(9)
C(25)-C(22)-C(23)	111.5(8)	C(36)-C(35)-C(34)	106.2(10)
C(21)-C(22)-C(23)	108.0(9)	C(36)-C(35)-H(35)	126.9
C(25)-C(22)-C(24)	109.6(9)	C(34)-C(35)-H(35)	126.9
C(21)-C(22)-C(24)	108.5(8)	C(35)-C(36)-N(16)	109.6(9)
C(23)-C(22)-C(24)	107.9(8)	C(35)-C(36)-H(36)	125.2
C(22)-C(23)-H(23A)	109.5	N(16)-C(36)-H(36)	125.2
C(22)-C(23)-H(23B)	109.5	C(38)-C(37)-H(37A)	109.5
H(23A)-C(23)-H(23B)	109.5	C(38)-C(37)-H(37B)	109.5
C(22)-C(23)-H(23C)	109.5	H(37A)-C(37)-H(37B)	109.5
H(23A)-C(23)-H(23C)	109.5	C(38)-C(37)-H(37C)	109.5
H(23B)-C(23)-H(23C)	109.5	H(37A)-C(37)-H(37C)	109.5
C(22)-C(24)-H(24A)	109.5	H(37B)-C(37)-H(37C)	109.5
C(22)-C(24)-H(24B)	109.5	N(17)-C(38)-C(37)	179.5(16)
H(24A)-C(24)-H(24B)	109.5	C(40)-C(39)-H(39A)	109.5
C(22)-C(24)-H(24C)	109.5	C(40)-C(39)-H(39B)	109.5
H(24A)-C(24)-H(24C)	109.5	H(39A)-C(39)-H(39B)	109.5
H(24B)-C(24)-H(24C)	109.5	C(40)-C(39)-H(39C)	109.5
N(11)-C(25)-C(26)	108.6(9)	H(39A)-C(39)-H(39C)	109.5
N(11)-C(25)-C(22)	121.0(9)	H(39B)-C(39)-H(39C)	109.5
C(26)-C(25)-C(22)	130.3(9)	N(18)-C(40)-C(39)	179.2(16)
C(27)-C(26)-C(25)	105.6(8)	C(42)-C(41)-H(41A)	109.5
C(27)-C(26)-H(26)	127.2	C(42)-C(41)-H(41B)	109.5
C(25)-C(26)-H(26)	127.2	H(41A)-C(41)-H(41B)	109.5
N(12)-C(27)-C(26)	110.4(9)	C(42)-C(41)-H(41C)	109.5
N(12)-C(27)-H(27)	124.8	H(41A)-C(41)-H(41C)	109.5
C(26)-C(27)-H(27)	124.8	H(41B)-C(41)-H(41C)	109.5
N(13)-C(28)-C(29)	109.4(9)	N(19)-C(42)-C(41)	175.3(16)
N(13)-C(28)-H(28)	125.3	C(44)-C(43)-H(43A)	109.5
C(29)-C(28)-H(28)	125.3	C(44)-C(43)-H(43B)	109.5
C(28)-C(29)-C(30)	104.8(9)	H(43A)-C(43)-H(43B)	109.5
C(28)-C(29)-H(29)	127.6	C(44)-C(43)-H(43C)	109.5
C(30)-C(29)-H(29)	127.6	H(43A)-C(43)-H(43C)	109.5
N(14)-C(30)-C(29)	109.3(9)	H(43B)-C(43)-H(43C)	109.5
N(14)-C(30)-C(31)	122.1(8)	N(20)-C(44)-C(43)	178.2(15)

C(46)-C(45)-H(45A)	109.5	N(13)-N(14)-Fe(4)	120.5(7)
C(46)-C(45)-H(45B)	109.5	C(34)-N(15)-N(16)	108.1(7)
H(45A)-C(45)-H(45B)	109.5	C(34)-N(15)-Fe(4)	132.3(6)
C(46)-C(45)-H(45C)	109.5	N(16)-N(15)-Fe(4)	119.5(6)
H(45A)-C(45)-H(45C)	109.5	C(36)-N(16)-N(15)	107.3(8)
H(45B)-C(45)-H(45C)	109.5	O(1)-Fe(1)-O(2)	82.0(2)
N(21)-C(46)-C(45)	177.9(17)	O(1)-Fe(1)-N(2)	142.6(3)
C(48)-C(47)-H(47A)	109.5	O(2)-Fe(1)-N(2)	85.2(3)
C(48)-C(47)-H(47B)	109.5	O(1)-Fe(1)-N(3)	85.3(3)
H(47A)-C(47)-H(47B)	109.5	O(2)-Fe(1)-N(3)	142.0(3)
C(48)-C(47)-H(47C)	109.5	N(2)-Fe(1)-N(3)	83.6(3)
H(47A)-C(47)-H(47C)	109.5	O(1)-Fe(1)-Cl(3)	112.8(2)
H(47B)-C(47)-H(47C)	109.5	O(2)-Fe(1)-Cl(3)	109.23(18)
N(22)-C(48)-C(47)	177(2)	N(2)-Fe(1)-Cl(3)	104.5(2)
C(50)-C(49)-H(49A)	109.5	N(3)-Fe(1)-Cl(3)	108.7(2)
C(50)-C(49)-H(49B)	109.5	O(1)-Fe(1)-Fe(3)	41.63(16)
H(49A)-C(49)-H(49B)	109.5	O(2)-Fe(1)-Fe(3)	42.11(16)
C(50)-C(49)-H(49C)	109.5	N(2)-Fe(1)-Fe(3)	111.9(2)
H(49A)-C(49)-H(49C)	109.5	N(3)-Fe(1)-Fe(3)	111.3(2)
H(49B)-C(49)-H(49C)	109.5	Cl(3)-Fe(1)-Fe(3)	127.81(9)
N(23)-C(50)-C(49)	178.4(16)	O(1)-Fe(2)-N(9)	85.8(3)
C(1)-N(1)-N(2)	107.3(8)	O(1)-Fe(2)-N(4)	85.3(3)
C(1)-N(1)-Fe(4)	133.9(7)	N(9)-Fe(2)-N(4)	99.6(3)
N(2)-N(1)-Fe(4)	118.5(6)	O(1)-Fe(2)-N(7)	92.4(3)
N(1)-N(2)-C(3)	108.2(8)	N(9)-Fe(2)-N(7)	92.0(3)
N(1)-N(2)-Fe(1)	120.7(6)	N(4)-Fe(2)-N(7)	168.0(3)
C(3)-N(2)-Fe(1)	130.8(7)	O(1)-Fe(2)-N(6)	94.5(3)
C(7)-N(3)-N(4)	107.2(7)	N(9)-Fe(2)-N(6)	171.4(3)
C(7)-N(3)-Fe(1)	132.0(6)	N(4)-Fe(2)-N(6)	89.0(3)
N(4)-N(3)-Fe(1)	120.1(5)	N(7)-Fe(2)-N(6)	79.4(3)
C(9)-N(4)-N(3)	108.1(7)	O(1)-Fe(2)-Cl(5)	172.6(2)
C(9)-N(4)-Fe(2)	133.3(6)	N(9)-Fe(2)-Cl(5)	89.2(2)
N(3)-N(4)-Fe(2)	118.5(5)	N(4)-Fe(2)-Cl(5)	90.2(2)
C(10)-N(5)-N(6)	109.7(8)	N(7)-Fe(2)-Cl(5)	93.2(2)
C(12)-N(6)-N(5)	107.0(7)	N(6)-Fe(2)-Cl(5)	91.3(2)
C(12)-N(6)-Fe(2)	134.0(6)	O(1)-Fe(3)-O(2)	81.9(2)
N(5)-N(6)-Fe(2)	118.9(6)	O(1)-Fe(3)-N(11)	141.2(3)
C(16)-N(7)-N(8)	106.4(8)	O(2)-Fe(3)-N(11)	85.5(3)
C(16)-N(7)-Fe(2)	133.3(6)	O(1)-Fe(3)-N(10)	85.5(3)
N(8)-N(7)-Fe(2)	120.1(7)	O(2)-Fe(3)-N(10)	141.9(3)
C(18)-N(8)-N(7)	109.9(9)	N(11)-Fe(3)-N(10)	82.1(3)
C(19)-N(9)-N(10)	107.1(8)	O(1)-Fe(3)-Cl(4)	111.47(19)
C(19)-N(9)-Fe(2)	133.3(7)	O(2)-Fe(3)-Cl(4)	110.33(19)
N(10)-N(9)-Fe(2)	118.8(5)	N(11)-Fe(3)-Cl(4)	107.3(2)
C(21)-N(10)-N(9)	107.6(7)	N(10)-Fe(3)-Cl(4)	107.7(2)
C(21)-N(10)-Fe(3)	132.1(7)	O(1)-Fe(3)-Fe(1)	41.72(16)
N(9)-N(10)-Fe(3)	119.5(6)	O(2)-Fe(3)-Fe(1)	42.00(16)
C(25)-N(11)-N(12)	107.5(8)	N(11)-Fe(3)-Fe(1)	111.2(2)
C(25)-N(11)-Fe(3)	132.7(7)	N(10)-Fe(3)-Fe(1)	111.4(2)
N(12)-N(11)-Fe(3)	119.6(6)	Cl(4)-Fe(3)-Fe(1)	127.64(9)
C(27)-N(12)-N(11)	107.8(8)	O(2)-Fe(4)-N(1)	85.2(3)
C(27)-N(12)-Fe(4)	133.1(7)	O(2)-Fe(4)-N(12)	85.0(3)
N(11)-N(12)-Fe(4)	118.8(6)	N(1)-Fe(4)-N(12)	101.8(3)
C(28)-N(13)-N(14)	109.9(9)	O(2)-Fe(4)-N(15)	95.8(3)
C(30)-N(14)-N(13)	106.6(7)	N(1)-Fe(4)-N(15)	90.8(3)
C(30)-N(14)-Fe(4)	132.4(6)	N(12)-Fe(4)-N(15)	167.3(3)

Table 4. Anisotropic displacement parameters (A^2x 10^3)for kjc0523. The anisotropic
displacement factor exponent takes the form: $-2\square^2[$ h^{2}a^{*2}U^{11} + ... + 2 h k a* b* U^{12}]

	U^{11}	U^{22}	U^{33}	U^{23}	U^{13}	U^{12}
C(1)	29(6)	33(6)	28(8)	3(5)	-6(5)	5(5)
C(2)	38(6)	18(5)	21(7)	-7(5)	-14(5)	-5(4)
C(3)	17(5)	21(6)	36(8)	-8(5)	-3(4)	4(4)
C(4)	14(5)	13(5)	32(7)	-5(4)	-4(4)	-3(4)
C(5)	29(6)	21(5)	35(8)	-6(5)	-6(5)	-6(4)
C(6)	18(5)	48(7)	42(9)	-4(6)	-1(5)	-3(5)
C(7)	21(5)	24(6)	18(6)	-4(4)	4(4)	-2(4)
C(8)	37(6)	32(6)	30(8)	-10(5)	-2(5)	-5(5)
C(9)	39(6)	20(6)	39(9)	2(5)	-3(5)	-7(5)
C(10)	34(6)	29(6)	33(8)	9(5)	7(5)	-2(5)
C(11)	34(6)	40(7)	36(9)	-5(6)	14(5)	6(5)
C(12)	34(6)	16(5)	20(7)	4(4)	7(4)	6(4)
C(13)	33(6)	22(5)	25(7)	-5(4)	-2(4)	0(4)
C(14)	64(8)	30(6)	26(8)	-4(5)	8(6)	0(5)
C(15)	34(6)	22(5)	37(8)	4(5)	0(5)	2(4)
C(16)	17(5)	24(6)	38(8)	9(5)	-12(4)	-8(4)
C(17)	44(7)	26(6)	43(9)	7(5)	-8(6)	-18(5)
C(18)	21(6)	28(6)	49(9)	10(5)	-13(5)	1(5)
C(19)	40(6)	21(6)	40(9)	-1(5)	2(5)	6(5)
C(20)	32(6)	45(7)	26(8)	0(5)	11(5)	17(5)
C(21)	18(5)	21(6)	29(7)	6(5)	-2(4)	3(4)
C(22)	25(5)	34(6)	14(7)	-1(5)	10(4)	2(4)
C(23)	10(5)	52(7)	45(9)	-3(6)	-4(5)	0(5)
C(24)	23(6)	46(7)	36(8)	-11(6)	10(5)	2(5)
C(25)	17(5)	42(6)	15(7)	-7(5)	2(4)	-8(5)
C(26)	20(5)	47(7)	22(7)	-1(5)	14(4)	-4(5)
C(27)	28(6)	43(6)	4(6)	6(5)	4(4)	-5(5)
C(28)	21(5)	33(6)	42(9)	-7(6)	-4(5)	-10(5)
C(29)	38(6)	41(7)	30(8)	-10(6)	-3(5)	-4(5)
C(30)	29(6)	15(5)	21(7)	-2(4)	-9(4)	-3(4)
C(31)	34(5)	12(5)	26(7)	-5(4)	2(5)	-7(4)
C(32)	34(5)	24(5)	22(6)	1(4)	-9(5)	4(5)
C(33)	35(6)	30(6)	35(8)	-8(5)	-1(5)	4(5)
C(34)	14(5)	32(6)	21(7)	5(5)	-3(4)	-2(4)
C(35)	37(6)	33(6)	45(9)	-16(6)	-6(5)	7(5)
C(36)	21(6)	37(7)	56(10)	-15(6)	-1(5)	8(5)
C(37)	35(6)	70(8)	47(10)	-17(7)	-5(6)	0(6)
C(38)	37(7)	40(7)	43(10)	-8(6)	0(6)	1(6)
C(39)	66(9)	52(8)	78(13)	-2(7)	23(8)	-11(7)
C(40)	37(8)	35(7)	66(13)	0(7)	-15(7)	1(6)
C(41)	113(12)	44(9)	72(14)	4(8)	43(10)	6(8)
C(42)	82(10)	38(8)	46(12)	-1(7)	5(7)	4(7)
C(43)	95(11)	55(9)	68(14)	1(9)	11(9)	20(8)
C(44)	69(9)	38(8)	42(12)	9(7)	2(7)	-8(6)
C(45)	95(12)	77(10)	51(13)	-14(8)	-4(8)	-15(9)
C(46)	74(9)	50(8)	49(12)	7(8)	5(8)	7(7)
C(47)	72(10)	112(13)	52(12)	-28(9)	16(8)	7(10)
C(48)	115(14)	58(10)	36(11)	-4(8)	-2(9)	24(10)
C(49)	94(12)	74(11)	133(19)	-28(11)	47(11)	14(9)
C(50)	37(7)	28(7)	86(13)	-3(7)	-10(7)	-3(6)
N(1)	27(5)	19(5)	26(6)	5(4)	-1(4)	4(3)

N(2)	19(4)	19(4)	21(6)	5(4)	2(3)	-2(3)
N(3)	19(4)	16(4)	22(6)	4(4)	-1(3)	-1(3)
N(4)	23(4)	20(4)	16(5)	0(4)	-2(3)	-4(3)
N(5)	22(4)	23(4)	26(6)	8(4)	3(4)	-3(3)
N(6)	25(4)	23(4)	21(6)	0(4)	5(3)	3(3)
N(7)	21(4)	19(4)	26(6)	1(4)	-6(3)	2(3)
N(8)	16(4)	26(5)	49(8)	12(5)	-8(4)	-4(4)
N(9)	30(4)	19(4)	30(6)	4(4)	1(4)	-1(4)
N(10)	22(4)	30(5)	27(6)	-7(4)	5(4)	4(4)
N(11)	24(4)	30(5)	19(6)	1(4)	3(4)	-3(4)
N(12)	22(4)	20(4)	18(6)	-1(4)	0(3)	-7(3)
N(13)	22(4)	27(5)	26(6)	6(4)	-1(4)	-8(4)
N(14)	18(4)	29(5)	29(6)	4(4)	2(4)	-4(3)
N(15)	23(4)	13(4)	17(5)	2(4)	0(3)	2(3)
N(16)	14(4)	22(5)	49(7)	-6(4)	-4(4)	4(3)
N(17)	42(6)	59(7)	64(10)	3(6)	10(6)	3(5)
N(18)	50(7)	53(7)	76(11)	0(7)	5(6)	1(6)
N(19)	86(8)	36(7)	82(12)	15(6)	-13(7)	-28(6)
N(20)	106(10)	54(8)	59(11)	-14(7)	26(8)	-16(7)
N(21)	175(15)	108(11)	50(13)	-16(10)	-13(11)	6(10)
N(22)	134(14)	55(9)	139(17)	23(10)	35(11)	22(9)
N(23)	46(6)	47(6)	70(10)	-4(6)	3(6)	12(5)
Fe(1)	12(1)	18(1)	18(1)	0(1)	1(1)	0(1)
Fe(2)	23(1)	19(1)	20(1)	2(1)	1(1)	2(1)
Fe(3)	14(1)	19(1)	16(1)	-2(1)	1(1)	-2(1)
Fe(4)	20(1)	17(1)	18(1)	1(1)	0(1)	-2(1)
O(1)	13(3)	14(3)	16(4)	-2(2)	-2(3)	-2(2)
O(2)	13(3)	23(3)	16(4)	1(3)	1(3)	2(3)
Cl(3)	19(1)	35(1)	28(2)	-8(1)	9(1)	2(1)
Cl(4)	22(1)	37(2)	29(2)	-5(1)	-8(1)	-3(1)
Cl(5)	40(2)	23(1)	29(2)	5(1)	3(1)	0(1)
Cl(6)	35(1)	29(1)	24(2)	9(1)	-1(1)	-3(1)
O(3)	26(4)	54(5)	32(5)	4(5)	1(3)	6(3)
O(4)	70(7)	78(7)	86(10)	-5(6)	13(6)	-18(5)
C(51)	18(5)	41(6)	37(8)	1(6)	-1(5)	13(5)
C(52)	40(7)	38(7)	44(10)	-13(6)	-12(6)	-0(5)

Table 5. Hydrogen coordinates (x 10^4) and isotropic displacement parameters (A^2x 10^3) for kjc0523.

	x	y	z	U(eq)
H(1)	6403	6616	226	36
H(2)	5495	5694	195	31
H(5A)	5457	4479	372	43
H(5B)	4685	4880	424	43
H(5C)	4790	4217	633	43
H(6A)	4439	4817	1194	54
H(6B)	4465	5503	1007	54
H(6C)	4994	5354	1355	54
H(8)	5654	3563	930	40
H(9)	6641	3258	1393	39
H(10)	5238	4164	2599	38
H(11)	6010	4893	3009	44
H(14A)	7494	4878	3269	60

H(14B)	7030	5524	3204	60
H(14C)	7945	5536	3230	60
H(15A)	7951	6123	2641	46
H(15B)	7042	6064	2590	46
H(15C)	7607	5810	2276	46
H(17)	9050	5013	3077	45
H(18)	9994	4425	2706	39
H(19)	8834	3322	1401	41
H(20)	9803	3672	941	41
H(23A)	10884	5648	1025	54
H(23B)	10884	4987	1241	54
H(23C)	10315	5543	1364	54
H(24A)	9983	4504	425	52
H(24B)	10737	4439	673	52
H(24C)	10621	5050	418	52
H(26)	9810	5814	198	36
H(27)	8766	6616	209	30
H(28)	9878	8318	1207	38
H(29)	9045	8584	1738	44
H(32A)	8112	7212	2144	40
H(32B)	7551	6853	1866	40
H(32C)	7203	7264	2196	40
H(33A)	8076	8425	2160	50
H(33B)	7161	8387	2184	50
H(33C)	7561	8799	1868	50
H(35)	6109	8453	1783	46
H(36)	5264	8195	1261	45
H(37A)	7856	5192	550	76
H(37B)	7753	4553	782	76
H(37C)	7162	4720	461	76
H(39A)	2105	6047	725	98
H(39B)	2838	6389	900	98
H(39C)	2680	5653	980	98
H(41A)	4621	2597	2825	114
H(41B)	5247	2069	2728	114
H(41C)	4421	2049	2537	114
H(43A)	3671	3616	1435	109
H(43B)	4263	3150	1635	109
H(43C)	3404	2920	1556	109
H(45A)	2305	3777	237	111
H(45B)	2905	4336	162	111
H(45C)	2029	4500	252	111
H(47A)	7571	3185	748	118
H(47B)	7184	3256	352	118
H(47C)	7891	2782	409	118
H(49A)	1742	2857	1786	151
H(49B)	1759	3369	1462	151
H(49C)	1162	2793	1448	151

Complex 3j

Table 1. Crystal data and structure refinement.

Identification code	asKJC27	
Empirical formula	C33 H46 Cl5 N15 Ni3 O	
Formula weight	1022.23	
Temperature	150(2) K	
Wavelength	0.71073 A	
Crystal system, space group	Trigonal, R3c	
Unit cell dimensions	a = 14.148(2) A	alpha = 90 deg.
	b = 14.148(2) A	beta = 90 deg.
	c = 37.826(8) A	gamma = 120 deg.
Volume	6557.0(19) A^3	
Z, Calculated density	6, 1.553 Mg/m^3	
Absorption coefficient	1.632 mm^-1	
F(000)	3156	
Crystal size	0.25 x 0.15 x 0.12 mm	
Theta range for data collection	3.30 to 26.96 deg.	
Limiting indices	-18<=h<=18, -15<=k<=15, -46<=l<=35	
Reflections collected / unique	5507 / 2948 [R(int) = 0.0271]	
Completeness to theta =	26.96 98.5 %	
Absorption correction	Multi scan	
Max. and min. transmission	sortav 0.870 and 0.701	
Refinement method	Full-matrix least-squares on F^2	
Data / restraints / parameters	2948 / 7 / 176	
Goodness-of-fit on F^2	1.037	
Final R indices [I>2sigma(I)]	R1 = 0.0324, wR2 = 0.0770	
R indices (all data)	R1 = 0.0351, wR2 = 0.0783	
Absolute structure parameter	0.102(12)	
Largest diff. peak and hole	0.538 and -0.296 e.A^-3	

Table 2. Atomic coordinates (x 10^4) and equivalent isotropic
displacement parameters (A^2 x 10^3) for asKJC27.
U(eq) is defined as one third of the trace of the orthogonalized
Uij tensor.

	x	y	z	U(eq)
Ni(1)	7983(1)	4495(1)	835(1)	21(1)
Cl(1)	8522(1)	3114(1)	826(1)	25(1)
O(1)	6667	3333	1093(1)	22(1)
N(1)	9136(2)	5528(2)	495(1)	26(1)
C(1)	10154(2)	6328(2)	544(1)	28(1)
Cl(2)	6667	3333	332(1)	28(1)
N(2)	8945(2)	5518(2)	144(1)	32(1)
C(2)	10618(2)	6833(3)	221(1)	39(1)
Cl(3)	6667	3333	1900(1)	28(1)
N(3)	8963(2)	5466(2)	1230(1)	23(1)
C(3)	9823(3)	6290(3)	-25(1)	40(1)
N(4)	8558(2)	5514(2)	1552(1)	27(1)
C(4)	10709(2)	6559(2)	903(1)	32(1)

C(5)	11663(3)	7736(3)	916(1)	50(1)
C(6)	11181(2)	5784(3)	952(1)	38(1)
C(7)	9941(2)	6361(2)	1208(1)	29(1)
C(8)	10150(3)	6988(3)	1519(1)	46(1)
C(9)	9246(3)	6410(3)	1727(1)	39(1)
N(5)	12468(16)	7562(17)	2357(4)	223(10)
C(10A)	12216(6)	7248(6)	2503(2)	42(2)
C(10)	12597(10)	7342(11)	2043(3)	103(4)
C(11A)	12090(7)	6805(8)	2799(3)	76(3)
C(11)	12995(12)	7075(13)	1773(3)	120(5)
N(5A)	12205(6)	7576(6)	2197(2)	54(2)

Table 3. Bond lengths [A] and angles [deg] for asKJC27.

Ni(1)-O(1)   2.0143(16)
Ni(1)-N(1)   2.018(2)
Ni(1)-N(3)   2.034(2)
Ni(1)-Cl(1)   2.4266(8)
Ni(1)-Cl(1_2)   2.4664(7)
Ni(1)-Cl(2)   2.5964(9)
Cl(1)-Ni(3)   2.4664(7)
O(1)-Ni(3)   2.0143(16)
O(1)-Ni(1_2)   2.0143(16)
N(1)-C(1)   1.326(3)
N(1)-N(2)   1.355(3)
C(1)-C(2)   1.400(4)
C(1)-C(4)   1.520(4)
Cl(2)-Ni(3)   2.5964(9)
Cl(2)-Ni(1_2)   2.5964(10)
N(2)-C(3)   1.338(4)
C(2)-C(3)   1.365(5)
N(3)-C(7)   1.332(3)
N(3)-N(4)   1.361(3)
N(4)-C(9)   1.326(4)
C(4)-C(7)   1.513(4)
C(4)-C(5)   1.533(4)
C(4)-C(6)   1.553(5)
C(7)-C(8)   1.412(5)
C(8)-C(9)   1.371(5)
N(5)-C(10)   1.264(15)
C(10A)-N(5A)   1.250(9)
C(10A)-C(11A)   1.251(11)
C(10)-C(11)   1.312(13)

O(1)-Ni(1)-N(1)   169.23(11)
O(1)-Ni(1)-N(3)   103.65(10)
N(1)-Ni(1)-N(3)   87.05(9)
O(1)-Ni(1)-Cl(1)   83.381(19)
N(1)-Ni(1)-Cl(1)   96.20(7)
N(3)-Ni(1)-Cl(1)   99.93(7)
O(1)-Ni(1)-Cl(1_2) 82.36(2)
N(1)-Ni(1)-Cl(1_2) 95.97(7)
N(3)-Ni(1)-Cl(1_2) 92.98(7)
Cl(1)-Ni(1)-Cl(1_2) 162.66(2)
O(1)-Ni(1)-Cl(2)   76.12(8)
N(1)-Ni(1)-Cl(2)   93.12(7)
N(3)-Ni(1)-Cl(2)   176.11(7)
Cl(1)-Ni(1)-Cl(2)   83.917(18)
Cl(1_2)-Ni(1)-Cl(2) 83.137(19)
Ni(1)-Cl(1)-Ni(3)   77.24(2)
Ni(1_3)-O(1)-Ni(1) 98.60(10)
Ni(1_3)-O(1)-Ni(1_2) 98.60(10)
Ni(1)-O(1)-Ni(1_2) 98.60(10)
C(1)-N(1)-N(2)   105.8(2)
C(1)-N(1)-Ni(1)   132.0(2)
N(2)-N(1)-Ni(1)   122.22(17)
N(1)-C(1)-C(2)   110.3(3)
N(1)-C(1)-C(4)   122.1(2)
C(2)-C(1)-C(4)   127.4(2)
Ni(3)-Cl(2)-Ni(1)   72.06(3)

Ni(3)-Cl(2)-Ni(1_2) 72.06(3)
Ni(1)-Cl(2)-Ni(1_2) 72.06(3)
C(3)-N(2)-N(1)   111.1(2)
C(3)-C(2)-C(1)   105.3(3)
C(7)-N(3)-N(4)   105.8(2)
C(7)-N(3)-Ni(1)   129.0(2)
N(4)-N(3)-Ni(1)   121.92(16)
N(2)-C(3)-C(2)   107.5(3)
C(9)-N(4)-N(3)   111.6(2)
C(7)-C(4)-C(1)   113.3(2)
C(7)-C(4)-C(5)   109.7(3)
C(1)-C(4)-C(5)   110.0(3)
C(7)-C(4)-C(6)   107.4(2)
C(1)-C(4)-C(6)   108.3(3)
C(5)-C(4)-C(6)   107.9(3)
N(3)-C(7)-C(8)   109.6(3)
N(3)-C(7)-C(4)   122.2(3)
C(8)-C(7)-C(4)   127.9(2)
C(9)-C(8)-C(7)   105.3(3)
N(4)-C(9)-C(8)   107.6(3)
N(5A)-C(10A)-C(11A) 171.6(8)
N(5)-C(10)-C(11)   160.1(18)

Symmetry transformations used to generate
equivalent atoms:
#1 -y+1,x-y,z   #2 -x+y+1,-x+1,z

196

Table 4. Anisotropic displacement parameters (A^2 x 10^3) for asKJC27.
The anisotropic displacement factor exponent takes the form:
-2 pi^2 [h^2 a*^2 U11 + ... + 2 h k a* b* U12]

	U11	U22	U33	U23	U13	U12
Ni(1)	21(1)	21(1)	18(1)	0(1)	2(1)	9(1)
Cl(1)	25(1)	28(1)	26(1)	1(1)	2(1)	15(1)
O(1)	25(1)	25(1)	16(2)	0	0	12(1)
N(1)	31(1)	27(1)	21(1)	5(1)	4(1)	15(1)
C(1)	28(1)	25(1)	32(2)	5(1)	9(1)	14(1)
Cl(2)	32(1)	32(1)	18(1)	0	0	16(1)
N(2)	34(1)	40(1)	20(1)	6(1)	6(1)	18(1)
C(2)	33(1)	40(2)	43(2)	10(1)	15(1)	17(1)
Cl(3)	32(1)	32(1)	19(1)	0	0	16(1)
N(3)	22(1)	27(1)	18(1)	-3(1)	0(1)	12(1)
C(3)	48(2)	44(2)	28(2)	14(1)	18(1)	22(1)
N(4)	24(1)	34(1)	21(1)	-4(1)	4(1)	13(1)
C(4)	23(1)	32(1)	35(2)	-2(1)	6(1)	9(1)
C(5)	33(2)	37(2)	55(2)	0(2)	5(2)	1(1)
C(6)	35(1)	51(2)	37(2)	4(1)	6(1)	28(1)
C(7)	22(1)	26(1)	35(2)	-5(1)	-2(1)	9(1)
C(8)	29(2)	45(2)	49(2)	-22(2)	-1(2)	8(1)
C(9)	34(1)	45(2)	33(2)	-16(1)	1(1)	17(1)

Table 5. Hydrogen coordinates (x 10^4) and isotropic
displacement parameters (A^2 x 10^3) for asKJC27.

	x	y	z	U(eq)
H(2)	8323	5063	40	38
H(2A)	11334	7428	183	47
H(3)	9883	6434	-272	48
H(4)	7919	5013	1634	32
H(5A)	11399	8239	857	74
H(5B)	12223	7825	745	74
H(5C)	11976	7897	1154	74
H(6A)	11497	5885	1189	57
H(6B)	11747	5953	774	57
H(6C)	10595	5026	924	57
H(8)	10781	7667	1572	55
H(9)	9134	6614	1956	46
H(1)	6667	3333	1337(11)	0(9)
H(11A)	11381	6635	2897	114
H(11B)	12672	7304	2959	114
H(11C)	12119	6131	2773	114
H(11D)	13789	7550	1766	180
H(11E)	12676	7163	1554	180
H(11F)	12816	6314	1796	180

Appendix B

Complex 4d

Table 1. Crystal data and structure refinement

Identification code	asKJC02
Empirical formula	C16 H21 Cu F3 N4 O5 S
Formula weight	501.97
Temperature	150(2) K
Wavelength	0.71073 A
Crystal system, space group	orthorhombic, Pnma
Unit cell dimensions	a = 11.264(2) A alpha = 90 deg.
	b = 11.732(2) A beta = 90 deg.
	c = 15.645(3) A gamma = 90 deg.
Volume	2067.5(7) A^3
Z, Calculated density	4, 1.613 Mg/m^3
Absorption coefficient	1.220 mm^-1
F(000)	1028
Crystal size	0.25 x 0.25 x 0.20 mm
Theta range for data collection	3.17 to 27.00 deg.
Limiting indices	-14<=h<=14, -14<=k<=14, -19<=l<=19
Reflections collected / unique	4290 / 2355 [R(int) = 0.0256]
Completeness to theta = 27.00	99.6 %
Max. and min. transmission	sortav 0.791 and 0.674
Refinement method	Full-matrix least-squares on F^2
Data / restraints / parameters	2355 / 0 / 155
Goodness-of-fit on F^2	1.055
Final R indices [I>2sigma(I)]	R1 = 0.0320, wR2 = 0.0759
R indices (all data)	R1 = 0.0402, wR2 = 0.0797
Largest diff. peak and hole	0.464 and -0.404 e.A^-3

Table 2. Atomic coordinates (x 10^4) and equivalent isotropic
displacement parameters (A^2 x 10^3) for asKJC02.
U(eq) is defined as one third of the trace of the orthogonalized
Uij tensor.

	x	y	z	U(eq)
Cu(1)	4718(1)	2500	5828(1)	18(1)
S(1)	7029(1)	2500	4290(1)	23(1)
F(1)	9171(2)	2500	3663(2)	55(1)
O(1)	3990(1)	1323(1)	5166(1)	22(1)
N(1)	5145(1)	1342(1)	6694(1)	21(1)
C(1)	5723(2)	1433(2)	7439(1)	23(1)
F(2)	9014(1)	1587(1)	4843(1)	58(1)
O(2)	6591(2)	2500	5158(1)	28(1)
N(2)	4694(1)	277(1)	6670(1)	24(1)
C(2)	5648(2)	391(2)	7878(2)	33(1)
O(3)	6824(2)	1464(1)	3830(1)	40(1)
C(3)	4981(2)	-308(2)	7366(2)	34(1)
C(4)	6398(3)	2500	7679(2)	23(1)
C(5)	6621(3)	2500	8647(2)	34(1)

C(6)	7598(3)	2500	7201(2)	29(1)
C(7)	3309(2)	1457(2)	4513(1)	20(1)
C(8)	3031(2)	2500	4134(2)	21(1)
C(9)	2740(2)	368(2)	4205(1)	28(1)
C(10)	2269(3)	2500	3328(2)	36(1)
C(11)	8643(3)	2500	4425(2)	33(1)

Table 3. Bond lengths [A] and angles [deg] for asKJC02.

Cu(1)-O(1)	1.9106(13)
Cu(1)-O(1_8)	1.9106(13)
Cu(1)-N(1_8)	1.9783(17)
Cu(1)-N(1)	1.9783(17)
Cu(1)-O(2)	2.356(2)
S(1)-O(3)	1.4316(16)
S(1)-O(3_8)	1.4316(16)
S(1)-O(2)	1.444(2)
S(1)-C(11)	1.830(3)
F(1)-C(11)	1.333(4)
O(1)-C(7)	1.286(2)
N(1)-C(1)	1.340(3)
N(1)-N(2)	1.350(2)
C(1)-C(2)	1.404(3)
C(1)-C(4)	1.512(2)
F(2)-C(11)	1.322(2)
N(2)-C(3)	1.327(3)
C(2)-C(3)	1.371(3)
C(4)-C(1_8)	1.512(2)
C(4)-C(5)	1.535(4)
C(4)-C(6)	1.546(4)
C(7)-C(8)	1.396(2)
C(7)-C(9)	1.509(3)
C(8)-C(7_8)	1.396(2)
C(8)-C(10)	1.525(4)
C(11)-F(2_8)	1.322(2)

O(1)-Cu(1)-O(1_8)	92.53(8)
O(1)-Cu(1)-N(1_8)	166.42(7)
O(1_8)-Cu(1)-N(1_8)	88.82(6)
O(1)-Cu(1)-N(1)	88.82(6)
O(1_8)-Cu(1)-N(1)	166.42(7)
N(1_8)-Cu(1)-N(1)	86.77(10)
O(1)-Cu(1)-O(2)	98.21(6)
O(1_8)-Cu(1)-O(2)	98.21(6)
N(1_8)-Cu(1)-O(2)	94.96(6)
N(1)-Cu(1)-O(2)	94.96(6)
O(3)-S(1)-O(3_8)	116.20(15)
O(3)-S(1)-O(2)	114.72(8)
O(3_8)-S(1)-O(2)	114.72(8)
O(3)-S(1)-C(11)	102.59(9)
O(3_8)-S(1)-C(11)	102.59(9)
O(2)-S(1)-C(11)	103.31(15)
C(7)-O(1)-Cu(1)	126.72(12)
C(1)-N(1)-N(2)	106.30(16)
C(1)-N(1)-Cu(1)	131.27(14)
N(2)-N(1)-Cu(1)	121.69(13)
N(1)-C(1)-C(2)	109.06(18)
N(1)-C(1)-C(4)	121.74(19)
C(2)-C(1)-C(4)	129.1(2)
S(1)-O(2)-Cu(1)	136.38(13)
C(3)-N(2)-N(1)	111.38(17)
C(3)-C(2)-C(1)	105.58(19)

N(2)-C(3)-C(2)	107.65(19)
C(1)-C(4)-C(1_8)	111.8(2)

C(1)-C(4)-C(5)	109.09(16)
C(1_8)-C(4)-C(5)	109.09(16)
C(1)-C(4)-C(6)	108.65(16)
C(1_8)-C(4)-C(6)	108.65(16)
C(5)-C(4)-C(6)	109.5(2)
O(1)-C(7)-C(8)	125.32(18)
O(1)-C(7)-C(9)	113.83(17)
C(8)-C(7)-C(9)	120.74(18)
C(7_8)-C(8)-C(7)	122.5(3)
C(7_8)-C(8)-C(10)	118.55(13)
C(7)-C(8)-C(10)	118.55(13)
F(2_8)-C(11)-F(2)	108.2(3)
F(2_8)-C(11)-F(1)	107.52(18)
F(2)-C(11)-F(1)	107.52(18)
F(2_8)-C(11)-S(1)	111.77(16)
F(2)-C(11)-S(1)	111.77(16)
F(1)-C(11)-S(1)	109.9(2)

Symmetry transformations used to generate equivalent atoms:
#1 x,-y+1/2,z

Table 4. Anisotropic displacement parameters (A^2 x 10^3) for asKJC02.
The anisotropic displacement factor exponent takes the form:
$-2 \pi^2 [h^2 a^{*2} U11 + ... + 2 h k a^* b^* U12]$

	U11	U22	U33	U23	U13	U12
Cu(1)	19(1)	17(1)	18(1)	0	-3(1)	0
S(1)	22(1)	24(1)	23(1)	0	2(1)	0
F(1)	38(1)	67(2)	59(2)	0	27(1)	0
O(1)	25(1)	19(1)	23(1)	0(1)	-6(1)	0(1)
N(1)	20(1)	20(1)	22(1)	0(1)	-1(1)	-1(1)
C(1)	20(1)	25(1)	22(1)	2(1)	-2(1)	1(1)
F(2)	35(1)	55(1)	84(1)	25(1)	-4(1)	13(1)
O(2)	25(1)	36(1)	23(1)	0	5(1)	0
N(2)	26(1)	20(1)	25(1)	4(1)	-4(1)	-4(1)
C(2)	38(1)	35(1)	27(1)	11(1)	-9(1)	-4(1)
O(3)	45(1)	39(1)	38(1)	-15(1)	6(1)	-14(1)
C(3)	39(1)	28(1)	36(1)	11(1)	-3(1)	-6(1)
C(4)	24(1)	26(1)	21(2)	0	-6(1)	0
C(5)	36(2)	41(2)	25(2)	0	-11(1)	0
C(6)	20(1)	34(2)	34(2)	0	-4(1)	0
C(7)	19(1)	22(1)	19(1)	-4(1)	2(1)	0(1)
C(8)	22(1)	23(1)	18(1)	0	-1(1)	0
C(9)	32(1)	21(1)	32(1)	-3(1)	-7(1)	-4(1)
C(10)	40(2)	32(2)	36(2)	0	-18(2)	0
C(11)	24(2)	29(2)	44(2)	0	6(2)	0

Table 5. Hydrogen coordinates (x 10^4) and isotropic
displacement parameters (A^2 x 10^3) for asKJC02.

	x	y	z	U(eq)
H(2)	4263	5	6247	29
H(2A)	5988	209	8416	40
H(3)	4763	-1074	7487	41
H(5A)	5860	2472	8950	51
H(5B)	7048	3195	8808	51
H(5C)	7097	1832	8802	51
H(6A)	7456	2466	6583	44
H(6B)	8066	1836	7377	44
H(6C)	8036	3199	7338	44
H(9A)	3081	-281	4514	42
H(9B)	2887	277	3591	42
H(9C)	1883	400	4309	42

H(10A)	2582	3061	2922	54
H(10B)	1450	2699	3477	54
H(10C)	2286	1741	3067	54

Appendix C

Complex 5a

Table 1. Crystal data and structure refinement

Identification code	kjc0506
Empirical formula	C22 H33 Cl4 N9 Pd2
Formula weight	778.17
Temperature	150(2) K
Wavelength	0.71073 A
Crystal system	Monoclinic
Space group	P 21/n
Unit cell dimensions	a = 12.0350(2) A alpha = 90°.
	b = 12.9330(3) A beta = 102.0490(10)°.
	c = 20.0240(5) A gamma = 90°.
Volume	3048.05(12) Å³
Z	4
Density (calculated)	1.696 Mg/m³
Absorption coefficient	1.559 mm⁻¹
F(000)	1552
Crystal size	0.33 x 0.28 x 0.25 mm³
Theta range for data collection	3.59 to 26.37°.
Index ranges	-15<=h<=15, -13<=k<=16, -21<=l<=25
Reflections collected	19435
Independent reflections	6190 [R(int) = 0.0551]
Completeness to theta = 26.37°	99.6 %
Absorption correction	Semi-empirical from equivalents
Max. and min. transmission	0.6965 and 0.6272
Refinement method	Full-matrix least-squares on F²
Data / restraints / parameters	6190 / 0 / 328
Goodness-of-fit on F²	1.071
Final R indices [I>2sigma(I)]	R1 = 0.0373, wR2 = 0.0783
R indices (all data)	R1 = 0.0487, wR2 = 0.0826
Largest diff. peak and hole	1.044 and -0.890 e.A⁻³

Table 2. Atomic coordinates (x 10⁴) and equivalent isotropic displacement parameters (A²x 10³) for kjc0506. U(eq) is defined as one third of the trace of the orthogonalized U^{ij} tensor.

	x	y	z	U(eq)
C(1)	11254(3)	2961(3)	10567(2)	25(1)
C(2)	11357(3)	3943(3)	10339(2)	23(1)
C(3)	11521(3)	3838(3)	9666(2)	16(1)
C(4)	11775(3)	4653(3)	9181(2)	17(1)
C(5)	11664(4)	5732(3)	9482(2)	26(1)
C(6)	13013(3)	4537(3)	9070(2)	23(1)
C(7)	10998(3)	4521(3)	8464(2)	16(1)
C(8)	10486(4)	5459(3)	8093(2)	23(1)
C(9)	11851(3)	3996(3)	7073(2)	24(1)
C(10)	10668(3)	3608(3)	7018(2)	17(1)
C(11)	9952(3)	3364(3)	6304(2)	22(1)
C(12)	8982(4)	4170(3)	6140(2)	31(1)
C(13)	10651(4)	3424(4)	5748(2)	34(1)
C(14)	9471(3)	2283(3)	6316(2)	17(1)
C(15)	9539(3)	1436(3)	5886(2)	22(1)
C(16)	8947(3)	656(3)	6122(2)	22(1)
C(17)	10388(4)	-1337(4)	8327(3)	36(1)

C(18)	9747(5)	-536(4)	7918(3)	49(1)
C(19)	9738(4)	-2229(3)	6048(3)	29(1)
C(20)	10296(5)	-2872(5)	6605(3)	49(1)
N(1)	11342(3)	2312(3)	10060(2)	21(1)
N(2)	11502(3)	2842(2)	9509(2)	18(1)
N(3)	10910(3)	3614(2)	8199(2)	14(1)
N(4)	10195(3)	3501(2)	7534(2)	15(1)
N(5)	8871(3)	2016(2)	6775(2)	16(1)
N(6)	8566(3)	1021(2)	6656(2)	19(1)
N(7)	10895(4)	-1973(3)	8648(3)	49(1)
N(8)	9300(4)	-1736(3)	5603(2)	37(1)
Pd(1)	11605(1)	2239(1)	8609(1)	15(1)
Pd(2)	8641(1)	2873(1)	7558(1)	15(1)
Cl(1)	12393(1)	786(1)	9149(1)	33(1)
Cl(2)	11761(1)	1547(1)	7575(1)	22(1)
Cl(3)	8321(1)	3964(1)	8405(1)	26(1)
Cl(4)	7008(1)	1984(1)	7564(1)	33(1)
C(22)	11410(4)	-653(4)	10526(3)	35(1)
N(9)	11213(4)	189(4)	10603(3)	52(1)
C(21)	11686(5)	-1719(5)	10427(3)	60(2)

Table 3. Bond lengths [Å] and angles [°] for kjc0506.

C(1)-N(1)	1.339(5)
C(1)-C(2)	1.364(6)
C(1)-H(1)	0.9500
C(2)-C(3)	1.408(6)
C(2)-H(2)	0.9500
C(3)-N(2)	1.325(5)
C(3)-C(4)	1.507(5)
C(4)-C(5)	1.536(5)
C(4)-C(7)	1.551(5)
C(4)-C(6)	1.558(5)
C(5)-H(5A)	0.9800
C(5)-H(5B)	0.9800
C(5)-H(5C)	0.9800
C(6)-H(6A)	0.9800
C(6)-H(6B)	0.9800
C(6)-H(6C)	0.9800
C(7)-N(3)	1.284(5)
C(7)-C(8)	1.487(5)
C(8)-H(8A)	0.9800
C(8)-H(8B)	0.9800
C(8)-H(8C)	0.9800
C(9)-C(10)	1.492(5)
C(9)-H(9A)	0.9800
C(9)-H(9B)	0.9800
C(9)-H(9C)	0.9800
C(10)-N(4)	1.286(5)
C(10)-C(11)	1.540(5)
C(11)-C(14)	1.514(6)
C(11)-C(13)	1.530(6)
C(11)-C(12)	1.549(6)
C(12)-H(12A)	0.9800
C(12)-H(12B)	0.9800
C(12)-H(12C)	0.9800
C(13)-H(13A)	0.9800
C(13)-H(13B)	0.9800
C(13)-H(13C)	0.9800
C(14)-N(5)	1.327(5)
C(14)-C(15)	1.407(5)
C(15)-C(16)	1.374(6)
C(15)-H(15)	0.9500
C(16)-N(6)	1.335(5)
C(16)-H(16)	0.9500
C(17)-N(7)	1.140(6)
C(17)-C(18)	1.440(7)
C(18)-H(18A)	0.9800
C(18)-H(18B)	0.9800
C(18)-H(18C)	0.9800
C(19)-N(8)	1.133(6)
C(19)-C(20)	1.440(7)
C(20)-H(20A)	0.9800
C(20)-H(20B)	0.9800

C(20)-H(20C)	0.9800
N(1)-N(2)	1.346(5)
N(1)-H(1A)	0.8800
N(2)-Pd(1)	1.991(3)
N(3)-N(4)	1.433(4)
N(3)-Pd(1)	2.062(3)
N(4)-Pd(2)	2.050(3)
N(5)-N(6)	1.346(4)
N(5)-Pd(2)	1.987(3)
N(6)-H(6)	0.8800
Pd(1)-Cl(1)	2.2732(10)
Pd(1)-Cl(2)	2.2986(10)
Pd(2)-Cl(4)	2.2781(11)
Pd(2)-Cl(3)	2.3001(10)
C(22)-N(9)	1.131(6)
C(22)-C(21)	1.442(8)
C(21)-H(21A)	0.9800
C(21)-H(21B)	0.9800
C(21)-H(21C)	0.9800
N(1)-C(1)-C(2)	107.6(4)
N(1)-C(1)-H(1)	126.2
C(2)-C(1)-H(1)	126.2
C(1)-C(2)-C(3)	105.8(4)
C(1)-C(2)-H(2)	127.1
C(3)-C(2)-H(2)	127.1
N(2)-C(3)-C(2)	108.7(3)
N(2)-C(3)-C(4)	121.5(3)
C(2)-C(3)-C(4)	129.6(4)
C(3)-C(4)-C(5)	109.6(3)
C(3)-C(4)-C(7)	110.8(3)
C(5)-C(4)-C(7)	112.2(3)
C(3)-C(4)-C(6)	110.7(3)
C(5)-C(4)-C(6)	107.9(3)
C(7)-C(4)-C(6)	105.5(3)
C(4)-C(5)-H(5A)	109.5
C(4)-C(5)-H(5B)	109.5
H(5A)-C(5)-H(5B)	109.5
C(4)-C(5)-H(5C)	109.5
H(5A)-C(5)-H(5C)	109.5
H(5B)-C(5)-H(5C)	109.5
C(4)-C(6)-H(6A)	109.5
C(4)-C(6)-H(6B)	109.5
H(6A)-C(6)-H(6B)	109.5
C(4)-C(6)-H(6C)	109.5
H(6A)-C(6)-H(6C)	109.5
H(6B)-C(6)-H(6C)	109.5
N(3)-C(7)-C(8)	123.3(3)
N(3)-C(7)-C(4)	117.8(3)
C(8)-C(7)-C(4)	118.7(3)
C(7)-C(8)-H(8A)	109.5
C(7)-C(8)-H(8B)	109.5
H(8A)-C(8)-H(8B)	109.5
C(7)-C(8)-H(8C)	109.5
H(8A)-C(8)-H(8C)	109.5
H(8B)-C(8)-H(8C)	109.5

C(10)-C(9)-H(9A)	109.5	C(7)-N(3)-N(4)	117.3(3)
C(10)-C(9)-H(9B)	109.5	C(7)-N(3)-Pd(1)	129.2(3)
H(9A)-C(9)-H(9B)	109.5	N(4)-N(3)-Pd(1)	113.4(2)
C(10)-C(9)-H(9C)	109.5	C(10)-N(4)-N(3)	117.1(3)
H(9A)-C(9)-H(9C)	109.5	C(10)-N(4)-Pd(2)	128.3(3)
H(9B)-C(9)-H(9C)	109.5	N(3)-N(4)-Pd(2)	113.1(2)
N(4)-C(10)-C(9)	123.4(4)	C(14)-N(5)-N(6)	107.2(3)
N(4)-C(10)-C(11)	117.9(3)	C(14)-N(5)-Pd(2)	125.9(3)
C(9)-C(10)-C(11)	118.6(3)	N(6)-N(5)-Pd(2)	126.5(3)
C(14)-C(11)-C(13)	109.2(3)	C(16)-N(6)-N(5)	110.6(3)
C(14)-C(11)-C(10)	108.4(3)	C(16)-N(6)-H(6)	124.7
C(13)-C(11)-C(10)	112.2(3)	N(5)-N(6)-H(6)	124.7
C(14)-C(11)-C(12)	110.5(3)	N(2)-Pd(1)-N(3)	85.74(12)
C(13)-C(11)-C(12)	108.4(4)	N(2)-Pd(1)-Cl(1)	89.55(9)
C(10)-C(11)-C(12)	108.0(3)	N(3)-Pd(1)-Cl(1)	175.20(9)
C(11)-C(12)-H(12A)	109.5	N(2)-Pd(1)-Cl(2)	178.91(10)
C(11)-C(12)-H(12B)	109.5	N(3)-Pd(1)-Cl(2)	94.55(9)
H(12A)-C(12)-H(12B)	109.5	Cl(1)-Pd(1)-Cl(2)	90.15(4)
C(11)-C(12)-H(12C)	109.5	N(5)-Pd(2)-N(4)	85.62(13)
H(12A)-C(12)-H(12C)	109.5	N(5)-Pd(2)-Cl(4)	89.18(9)
H(12B)-C(12)-H(12C)	109.5	N(4)-Pd(2)-Cl(4)	172.99(9)
C(11)-C(13)-H(13A)	109.5	N(5)-Pd(2)-Cl(3)	175.54(10)
C(11)-C(13)-H(13B)	109.5	N(4)-Pd(2)-Cl(3)	93.93(9)
H(13A)-C(13)-H(13B)	109.5	Cl(4)-Pd(2)-Cl(3)	91.62(4)
C(11)-C(13)-H(13C)	109.5	N(9)-C(22)-C(21)	178.8(6)
H(13A)-C(13)-H(13C)	109.5	C(22)-C(21)-H(21A)	109.5
H(13B)-C(13)-H(13C)	109.5	C(22)-C(21)-H(21B)	109.5
N(5)-C(14)-C(15)	109.3(3)	H(21A)-C(21)-H(21B)	109.5
N(5)-C(14)-C(11)	121.1(3)	C(22)-C(21)-H(21C)	109.5
C(15)-C(14)-C(11)	129.6(4)	H(21A)-C(21)-H(21C)	109.5
C(16)-C(15)-C(14)	105.1(4)	H(21B)-C(21)-H(21C)	109.5
C(16)-C(15)-H(15)	127.4		
C(14)-C(15)-H(15)	127.4		
N(6)-C(16)-C(15)	107.8(3)		
N(6)-C(16)-H(16)	126.1		
C(15)-C(16)-H(16)	126.1		
N(7)-C(17)-C(18)	179.6(6)		
C(17)-C(18)-H(18A)	109.5		
C(17)-C(18)-H(18B)	109.5		
H(18A)-C(18)-H(18B)	109.5		
C(17)-C(18)-H(18C)	109.5		
H(18A)-C(18)-H(18C)	109.5		
H(18B)-C(18)-H(18C)	109.5		
N(8)-C(19)-C(20)	178.9(5)		
C(19)-C(20)-H(20A)	109.5		
C(19)-C(20)-H(20B)	109.5		
H(20A)-C(20)-H(20B)	109.5		
C(19)-C(20)-H(20C)	109.5		
H(20A)-C(20)-H(20C)	109.5		
H(20B)-C(20)-H(20C)	109.5		
C(1)-N(1)-N(2)	110.5(3)		
C(1)-N(1)-H(1A)	124.7		
N(2)-N(1)-H(1A)	124.7		
C(3)-N(2)-N(1)	107.4(3)		
C(3)-N(2)-Pd(1)	126.5(3)		
N(1)-N(2)-Pd(1)	126.0(3)		

Symmetry transformations used to generate
equivalent atoms:

Table 4. Anisotropic displacement parameters (Å²x 10³)for kjc0506. The anisotropic displacement factor exponent takes the form: -2□²[h²a*²U¹¹ + ... + 2 h k a* b* U¹²]

	U¹¹	U²²	U³³	U²³	U¹³	U¹²
C(1)	23(2)	35(2)	19(2)	-7(2)	7(2)	1(2)
C(2)	21(2)	26(2)	20(2)	-8(2)	5(2)	-1(2)
C(3)	11(2)	20(2)	17(2)	-3(2)	-1(2)	0(2)
C(4)	14(2)	15(2)	20(2)	-2(2)	-1(2)	0(2)
C(5)	28(2)	17(2)	29(2)	-7(2)	-4(2)	1(2)
C(6)	11(2)	28(2)	27(2)	0(2)	-2(2)	-1(2)
C(7)	12(2)	15(2)	21(2)	0(2)	3(2)	0(2)
C(8)	25(2)	18(2)	23(2)	0(2)	1(2)	1(2)
C(9)	23(2)	26(2)	23(2)	2(2)	7(2)	-5(2)
C(10)	21(2)	12(2)	19(2)	-1(2)	6(2)	-2(2)
C(11)	25(2)	25(2)	17(2)	-2(2)	5(2)	-5(2)
C(12)	38(3)	26(2)	23(2)	4(2)	-8(2)	0(2)
C(13)	46(3)	37(3)	21(2)	-7(2)	12(2)	-18(2)
C(14)	16(2)	22(2)	14(2)	-3(2)	2(2)	-1(2)
C(15)	22(2)	26(2)	17(2)	-7(2)	4(2)	1(2)
C(16)	23(2)	21(2)	22(2)	-10(2)	4(2)	-1(2)
C(17)	33(3)	30(3)	46(3)	8(2)	15(2)	-4(2)
C(18)	50(3)	41(3)	53(4)	18(3)	2(3)	2(3)
C(19)	22(2)	30(2)	37(3)	-8(2)	14(2)	-3(2)
C(20)	39(3)	62(4)	51(4)	17(3)	22(3)	4(3)
N(1)	26(2)	22(2)	15(2)	3(1)	5(1)	-1(2)
N(2)	22(2)	19(2)	13(2)	-1(1)	3(1)	2(1)
N(3)	14(2)	17(2)	10(2)	-2(1)	1(1)	0(1)
N(4)	16(2)	15(2)	12(2)	-2(1)	0(1)	-1(1)
N(5)	17(2)	15(2)	16(2)	-2(1)	3(1)	-2(1)
N(6)	23(2)	15(2)	19(2)	0(1)	2(1)	-4(1)
N(7)	46(3)	37(2)	64(3)	14(2)	11(2)	-2(2)
N(8)	42(2)	35(2)	36(3)	-6(2)	9(2)	4(2)
Pd(1)	18(1)	14(1)	13(1)	-1(1)	4(1)	3(1)
Pd(2)	14(1)	18(1)	14(1)	-3(1)	3(1)	-1(1)
Cl(1)	55(1)	23(1)	22(1)	5(1)	11(1)	19(1)
Cl(2)	29(1)	21(1)	17(1)	-3(1)	6(1)	6(1)
Cl(3)	29(1)	27(1)	26(1)	-10(1)	12(1)	-1(1)
Cl(4)	24(1)	42(1)	30(1)	-13(1)	14(1)	-14(1)

Table 5. Hydrogen coordinates (x 10⁴) and isotropic displacement parameters (Å²x 10³) for kjc0506.

	x	y	z	U(eq)
H(1)	11140	2772	11006	30
H(2)	11325	4568	10583	27
H(5A)	10888	5828	9550	39
H(5B)	11833	6260	9167	39
H(5C)	12201	5795	9922	39
H(6A)	13551	4656	9503	34
H(6B)	13146	5045	8732	34
H(6C)	13119	3838	8905	34

H(8A)	11081	5868	7950	34
H(8B)	10119	5875	8394	34
H(8C)	9919	5251	7689	34
H(9A)	11828	4710	6905	36
H(9B)	12248	3559	6799	36
H(9C)	12253	3976	7552	36
H(12A)	8512	4027	5687	47
H(12B)	9307	4865	6144	47
H(12C)	8512	4127	6484	47
H(13A)	11265	2913	5842	51
H(13B)	10976	4119	5744	51
H(13C)	10160	3280	5303	51
H(15)	9914	1408	5514	26
H(16)	8830	-22	5938	27
H(18A)	10260	-110	7713	74
H(18B)	9371	-103	8206	74
H(18C)	9173	-852	7556	74
H(20A)	9725	-3248	6793	73
H(20B)	10750	-2438	6962	73
H(20C)	10794	-3366	6439	73
H(1A)	11301	1634	10083	25
H(6)	8170	661	6898	23
H(21A)	11145	-2002	10035	90
H(21B)	11643	-2117	10838	90
H(21C)	12457	-1764	10342	90

—

Complex 5b

Table 1. Crystal data and structure refinement

Identification code	kjc0510
Empirical formula	C32 H48 Cl2 Co N12
Formula weight	730.65
Temperature	150(2) K
Wavelength	0.71073 A
Crystal system	Monoclinic
Space group	P 21/c

Unit cell dimensions

$a = 14.9990(2)$ A	alpha = 90°.
$b = 16.9650(3)$ A	beta= 107.369(1)°.
$c = 15.2590(2)$ A	gamma = 90°.

Volume	3705.73(10) A^3
Z	4
Density (calculated)	1.310 Mg/m^3
Absorption coefficient	0.648 mm^{-1}
F(000)	1540
Crystal size	0.20 x 0.15 x 0.15 mm^3
Theta range for data collection	2.93 to 30.05°.
Index ranges	-21<=h<=21. -23<=k<=23. -21<=l<=21
Reflections collected	69146
Independent reflections	10825 [R(int) = 0.0909]
Completeness to theta = 30.05°	99.7 %
Absorption correction	Semi-empirical from equivalents
Max. and min. transmission	0.9091 and 0.8814
Refinement method	Full-matrix least-squares on F^2
Data / restraints / parameters	10825 / 0 / 436
Goodness-of-fit on F^2	1.061
Final R indices [I>2sigma(I)]	R1 = 0.0560, wR2 = 0.1035
R indices (all data)	R1 = 0.0866, wR2 = 0.1131
Largest diff. peak and hole	0.356 and -0.351 e.A^{-3}

Table 2. Atomic coordinates (x 10^4) and equivalent isotropic displacement parameters (A^{2}x 10^3) for kjc0510. U(eq) is defined as one third of the trace of the orthogonalized U^{ij} tensor.

	x	y	z	U(eq)
C(1)	3605(2)	3328(1)	3016(2)	28(1)
C(2)	4022(2)	3587(2)	2364(2)	32(1)
C(3)	3565(1)	4267(1)	1996(1)	25(1)
C(4)	3717(2)	4831(1)	1282(2)	28(1)
C(5)	2911(2)	5422(2)	969(2)	42(1)
C(6)	3781(2)	4345(2)	456(2)	39(1)
C(7)	4628(2)	5280(1)	1724(2)	27(1)
C(8)	4701(2)	5788(2)	2547(2)	50(1)
C(9)	6829(2)	5248(2)	2046(2)	31(1)
C(10)	6803(2)	4378(2)	2144(3)	84(1)
C(11)	7779(2)	5665(2)	2360(2)	32(1)
C(12)	7672(2)	6552(2)	2199(2)	48(1)
C(13)	8423(2)	5324(3)	1837(2)	68(1)
C(14)	8188(1)	5484(1)	3370(2)	26(1)
C(15)	8849(2)	4960(2)	3854(2)	34(1)
C(16)	8876(2)	5044(1)	4774(2)	30(1)
C(17)	309(2)	3176(1)	3148(2)	28(1)

C(18)	-232(2)	2646(2)	3463(2)	32(1)
C(19)	356(2)	2323(1)	4257(2)	26(1)
C(20)	159(2)	1750(1)	4938(2)	27(1)
C(21)	-269(2)	996(1)	4426(2)	41(1)
C(22)	1056(2)	1545(2)	5709(2)	43(1)
C(23)	-524(2)	2160(1)	5362(2)	25(1)
C(24)	-254(2)	2937(2)	5844(2)	34(1)
C(25)	-2605(2)	2538(1)	5158(2)	27(1)
C(26)	-2714(2)	2708(2)	4162(2)	39(1)
C(27)	-3368(2)	2828(1)	5563(2)	32(1)
C(28)	-4267(2)	2361(2)	5112(2)	49(1)
C(29)	-3081(2)	2716(2)	6611(2)	43(1)
C(30)	-3533(2)	3696(1)	5342(2)	28(1)
C(31)	-4240(2)	4105(2)	4740(2)	47(1)
C(32)	-3978(2)	4898(2)	4855(2)	40(1)
N(1)	2922(1)	3814(1)	3053(1)	24(1)
N(2)	2909(1)	4380(1)	2422(1)	23(1)
N(3)	5277(1)	5206(1)	1355(1)	31(1)
N(4)	6096(1)	5652(1)	1716(1)	31(1)
N(5)	7863(1)	5848(1)	3998(1)	26(1)
N(6)	8281(1)	5588(1)	4864(1)	24(1)
N(7)	1184(1)	3188(1)	3703(1)	24(1)
N(8)	1192(1)	2659(1)	4366(1)	25(1)
N(9)	-1304(1)	1821(1)	5263(1)	28(1)
N(10)	-1921(1)	2160(1)	5686(1)	28(1)
N(11)	-2906(1)	4239(1)	5775(1)	26(1)
N(12)	-3167(1)	4981(1)	5491(1)	25(1)
Co(1)	2236(1)	4056(1)	4038(1)	21(1)
Cl(1)	3280(1)	3092(1)	3130(1)	27(1)
Cl(2)	1184(1)	3012(1)	2911(1)	27(1)

Table 3.   Bond lengths [Å] and angles [°] for kjc0510.

C(1)-N(1)	1.329(3)	C(22)-H(22B)	0.9800
C(1)-C(2)	1.395(3)	C(22)-H(22C)	0.9800
C(1)-H(1)	0.9500	C(23)-N(9)	1.272(3)
C(2)-C(3)	1.373(3)	C(23)-C(24)	1.506(3)
C(2)-H(2)	0.9500	C(24)-H(24A)	0.9800
C(3)-N(2)	1.345(3)	C(24)-H(24B)	0.9800
C(3)-C(4)	1.517(3)	C(24)-H(24C)	0.9800
C(4)-C(7)	1.533(3)	C(25)-N(10)	1.273(3)
C(4)-C(6)	1.534(3)	C(25)-C(26)	1.507(3)
C(4)-C(5)	1.534(3)	C(25)-C(27)	1.534(3)
C(5)-H(5A)	0.9800	C(26)-H(26A)	0.9800
C(5)-H(5B)	0.9800	C(26)-H(26B)	0.9800
C(5)-H(5C)	0.9800	C(26)-H(26C)	0.9800
C(6)-H(6A)	0.9800	C(27)-C(30)	1.514(3)
C(6)-H(6B)	0.9800	C(27)-C(28)	1.539(3)
C(6)-H(6C)	0.9800	C(27)-C(29)	1.539(4)
C(7)-N(3)	1.268(3)	C(28)-H(28A)	0.9800
C(7)-C(8)	1.499(3)	C(28)-H(28B)	0.9800
C(8)-H(8A)	0.9800	C(28)-H(28C)	0.9800
C(8)-H(8B)	0.9800	C(29)-H(29A)	0.9800
C(8)-H(8C)	0.9800	C(29)-H(29B)	0.9800
C(9)-N(4)	1.266(3)	C(29)-H(29C)	0.9800
C(9)-C(10)	1.484(4)	C(30)-N(11)	1.341(3)
C(9)-C(11)	1.534(3)	C(30)-C(31)	1.366(3)
C(10)-H(10A)	0.9800	C(31)-C(32)	1.399(4)
C(10)-H(10B)	0.9800	C(31)-H(31)	0.9500
C(10)-H(10C)	0.9800	C(32)-N(12)	1.317(3)
C(11)-C(14)	1.510(3)	C(32)-H(32)	0.9500
C(11)-C(12)	1.526(4)	N(1)-N(2)	1.356(2)
C(11)-C(13)	1.539(3)	N(1)-Co(1)	2.0981(17)
C(12)-H(12A)	0.9800	N(2)-H(2A)	0.8800
C(12)-H(12B)	0.9800	N(3)-N(4)	1.407(3)
C(12)-H(12C)	0.9800	N(5)-N(6)	1.356(2)
C(13)-H(13A)	0.9800	N(5)-H(5)	0.8800
C(13)-H(13B)	0.9800	N(6)-Co(1)	2.1330(18)
C(13)-H(13C)	0.9800	N(7)-N(8)	1.350(2)
C(14)-N(5)	1.347(3)	N(7)-Co(1)	2.1070(18)
C(14)-C(15)	1.372(3)	N(8)-H(8)	0.8800
C(15)-C(16)	1.400(3)	N(9)-N(10)	1.400(2)
C(15)-H(15)	0.9500	N(11)-N(12)	1.351(2)
C(16)-N(6)	1.320(3)	N(11)-H(11)	0.8800
C(16)-H(16)	0.9500	N(12)-Co(1)	2.1299(18)
C(17)-N(7)	1.333(3)	Co(1)-N(12)	2.1299(18)
C(17)-C(18)	1.389(3)	Co(1)-N(6)	2.1330(18)
C(17)-H(17)	0.9500	Co(1)-Cl(1)	2.5344(6)
C(18)-C(19)	1.382(3)	Co(1)-Cl(2)	2.5409(6)
C(18)-H(16)	0.9500		
C(19)-N(8)	1.342(3)	N(1)-C(1)-C(2)	110.6(2)
C(19)-C(20)	1.515(3)	N(1)-C(1)-H(1)	124.7
C(20)-C(23)	1.531(3)	C(2)-C(1)-H(1)	124.7
C(20)-C(21)	1.535(3)	C(3)-C(2)-C(1)	106.3(2)
C(20)-C(22)	1.540(3)	C(3)-C(2)-H(2)	126.9
C(21)-H(21A)	0.9800	C(1)-C(2)-H(2)	126.9
C(21)-H(21B)	0.9800	N(2)-C(3)-C(2)	105.65(19)
C(21)-H(21C)	0.9800	N(2)-C(3)-C(4)	123.1(2)
C(22)-H(22A)	0.9800	C(2)-C(3)-C(4)	131.24(19)

213

C(3)-C(4)-C(7)	107.63(17)	C(15)-C(14)-C(11)	133.6(2)
C(3)-C(4)-C(6)	108.1(2)	C(14)-C(15)-C(16)	105.9(2)
C(7)-C(4)-C(6)	111.24(18)	C(14)-C(15)-H(15)	127.0
C(3)-C(4)-C(5)	111.22(17)	C(16)-C(15)-H(15)	127.0
C(7)-C(4)-C(5)	109.2(2)	N(6)-C(16)-C(15)	111.0(2)
C(6)-C(4)-C(5)	109.4(2)	N(6)-C(16)-H(16)	124.5
C(4)-C(5)-H(5A)	109.5	C(15)-C(16)-H(16)	124.5
C(4)-C(5)-H(5B)	109.5	N(7)-C(17)-C(18)	110.9(2)
H(5A)-C(5)-H(5B)	109.5	N(7)-C(17)-H(17)	124.6
C(4)-C(5)-H(5C)	109.5	C(18)-C(17)-H(17)	124.6
H(5A)-C(5)-H(5C)	109.5	C(19)-C(18)-C(17)	106.0(2)
H(5B)-C(5)-H(5C)	109.5	C(19)-C(18)-H(16)	127.0
C(4)-C(6)-H(6A)	109.5	C(17)-C(18)-H(16)	127.0
C(4)-C(6)-H(6B)	109.5	N(8)-C(19)-C(18)	105.52(19)
H(6A)-C(6)-H(6B)	109.5	N(8)-C(19)-C(20)	123.6(2)
C(4)-C(6)-H(6C)	109.5	C(18)-C(19)-C(20)	130.8(2)
H(6A)-C(6)-H(6C)	109.5	C(19)-C(20)-C(23)	106.87(17)
H(6B)-C(6)-H(6C)	109.5	C(19)-C(20)-C(21)	108.8(2)
N(3)-C(7)-C(8)	123.7(2)	C(23)-C(20)-C(21)	111.30(18)
N(3)-C(7)-C(4)	117.2(2)	C(19)-C(20)-C(22)	111.33(18)
C(8)-C(7)-C(4)	119.11(19)	C(23)-C(20)-C(22)	108.8(2)
C(7)-C(8)-H(8A)	109.5	C(21)-C(20)-C(22)	109.7(2)
C(7)-C(8)-H(8B)	109.5	C(20)-C(21)-H(21A)	109.5
H(8A)-C(8)-H(8B)	109.5	C(20)-C(21)-H(21B)	109.5
C(7)-C(8)-H(8C)	109.5	H(21A)-C(21)-H(21B)	109.5
H(8A)-C(8)-H(8C)	109.5	C(20)-C(21)-H(21C)	109.5
H(8B)-C(8)-H(8C)	109.5	H(21A)-C(21)-H(21C)	109.5
N(4)-C(9)-C(10)	122.2(2)	H(21B)-C(21)-H(21C)	109.5
N(4)-C(9)-C(11)	119.4(2)	C(20)-C(22)-H(22A)	109.5
C(10)-C(9)-C(11)	118.4(2)	C(20)-C(22)-H(22B)	109.5
C(9)-C(10)-H(10A)	109.5	H(22A)-C(22)-H(22B)	109.5
C(9)-C(10)-H(10B)	109.5	C(20)-C(22)-H(22C)	109.5
H(10A)-C(10)-H(10B)	109.5	H(22A)-C(22)-H(22C)	109.5
C(9)-C(10)-H(10C)	109.5	H(22B)-C(22)-H(22C)	109.5
H(10A)-C(10)-H(10C)	109.5	N(9)-C(23)-C(24)	123.9(2)
H(10B)-C(10)-H(10C)	109.5	N(9)-C(23)-C(20)	116.9(2)
C(14)-C(11)-C(12)	110.9(2)	C(24)-C(23)-C(20)	119.27(19)
C(14)-C(11)-C(9)	106.40(18)	C(23)-C(24)-H(24A)	109.5
C(12)-C(11)-C(9)	111.2(2)	C(23)-C(24)-H(24B)	109.5
C(14)-C(11)-C(13)	109.1(2)	H(24A)-C(24)-H(24B)	109.5
C(12)-C(11)-C(13)	109.8(2)	C(23)-C(24)-H(24C)	109.5
C(9)-C(11)-C(13)	109.5(2)	H(24A)-C(24)-H(24C)	109.5
C(11)-C(12)-H(12A)	109.5	H(24B)-C(24)-H(24C)	109.5
C(11)-C(12)-H(12B)	109.5	N(10)-C(25)-C(26)	124.0(2)
H(12A)-C(12)-H(12B)	109.5	N(10)-C(25)-C(27)	117.7(2)
C(11)-C(12)-H(12C)	109.5	C(26)-C(25)-C(27)	118.3(2)
H(12A)-C(12)-H(12C)	109.5	C(25)-C(26)-H(26A)	109.5
H(12B)-C(12)-H(12C)	109.5	C(25)-C(26)-H(26B)	109.5
C(11)-C(13)-H(13A)	109.5	H(26A)-C(26)-H(26B)	109.5
C(11)-C(13)-H(13B)	109.5	C(25)-C(26)-H(26C)	109.5
H(13A)-C(13)-H(13B)	109.5	H(26A)-C(26)-H(26C)	109.5
C(11)-C(13)-H(13C)	109.5	H(26B)-C(26)-H(26C)	109.5
H(13A)-C(13)-H(13C)	109.5	C(30)-C(27)-C(25)	108.33(18)
H(13B)-C(13)-H(13C)	109.5	C(30)-C(27)-C(28)	109.8(2)
N(5)-C(14)-C(15)	105.70(19)	C(25)-C(27)-C(28)	108.3(2)
N(5)-C(14)-C(11)	120.6(2)	C(30)-C(27)-C(29)	109.1(2)

C(25)-C(27)-C(29)	111.6(2)		N(12)-Co(1)-N(6)	82.71(7)
C(28)-C(27)-C(29)	109.7(2)		N(1)-Co(1)-Cl(1)	90.91(5)
C(27)-C(28)-H(28A)	109.5		N(7)-Co(1)-Cl(1)	88.81(5)
C(27)-C(28)-H(28B)	109.5		N(12)-Co(1)-Cl(1)	93.28(5)
H(28A)-C(28)-H(28B)	109.5		N(6)-Co(1)-Cl(1)	87.33(5)
C(27)-C(28)-H(28C)	109.5		N(1)-Co(1)-Cl(2)	88.79(5)
H(28A)-C(28)-H(28C)	109.5		N(7)-Co(1)-Cl(2)	90.77(5)
H(28B)-C(28)-H(28C)	109.5		N(12)-Co(1)-Cl(2)	87.20(5)
C(27)-C(29)-H(29A)	109.5		N(6)-Co(1)-Cl(2)	93.03(5)
C(27)-C(29)-H(29B)	109.5		Cl(1)-Co(1)-Cl(2)	179.43(2)
H(29A)-C(29)-H(29B)	109.5			
C(27)-C(29)-H(29C)	109.5			
H(29A)-C(29)-H(29C)	109.5			
H(29B)-C(29)-H(29C)	109.5			
N(11)-C(30)-C(31)	105.8(2)			
N(11)-C(30)-C(27)	121.0(2)			
C(31)-C(30)-C(27)	133.2(2)			
C(30)-C(31)-C(32)	105.8(2)			
C(30)-C(31)-H(31)	127.1			
C(32)-C(31)-H(31)	127.1			
N(12)-C(32)-C(31)	110.9(2)			
N(12)-C(32)-H(32)	124.5			
C(31)-C(32)-H(32)	124.5			
C(1)-N(1)-N(2)	104.82(17)			
C(1)-N(1)-Co(1)	134.52(15)			
N(2)-N(1)-Co(1)	117.59(14)			
C(3)-N(2)-N(1)	112.65(18)			
C(3)-N(2)-H(2A)	123.7			
N(1)-N(2)-H(2A)	123.7			
C(7)-N(3)-N(4)	117.9(2)			
C(9)-N(4)-N(3)	114.7(2)			
C(14)-N(5)-N(6)	112.63(18)			
C(14)-N(5)-H(5)	123.7			
N(6)-N(5)-H(5)	123.7			
C(16)-N(6)-N(5)	104.81(17)			
C(16)-N(6)-Co(1)	134.06(15)			
N(5)-N(6)-Co(1)	120.24(13)			
C(17)-N(7)-N(8)	104.60(17)			
C(17)-N(7)-Co(1)	133.54(16)			
N(8)-N(7)-Co(1)	116.41(13)			
C(19)-N(8)-N(7)	113.03(18)			
C(19)-N(8)-H(8)	123.5			
N(7)-N(8)-H(8)	123.5			
C(23)-N(9)-N(10)	118.10(19)			
C(25)-N(10)-N(9)	115.81(19)			
C(30)-N(11)-N(12)	112.83(18)			
C(30)-N(11)-H(11)	123.6			
N(12)-N(11)-H(11)	123.6			
C(32)-N(12)-N(11)	104.67(19)			
C(32)-N(12)-Co(1)	134.30(17)			
N(11)-N(12)-Co(1)	120.54(14)			
N(1)-Co(1)-N(7)	100.41(7)			
N(1)-Co(1)-N(12)	88.90(7)			
N(7)-Co(1)-N(12)	170.44(7)			
N(1)-Co(1)-N(6)	171.31(7)			
N(7)-Co(1)-N(6)	88.07(7)			

Symmetry transformations used to generate
equivalent atoms:
#1 -x+1,-y+1,-z+1   #2 -x,-y+1,-z+1

215

Table 4. Anisotropic displacement parameters (A²x 10³)for kjc0510. The anisotropic displacement factor exponent takes the form: $-2\pi^2[\ h^2a^{*2}U^{11} + ... + 2\ h\ k\ a^*\ b^*\ U^{12}\ ]$

	U^{11}	U^{22}	U^{33}	U^{23}	U^{13}	U^{12}
C(1)	28(1)	27(1)	31(1)	-1(1)	11(1)	0(1)
C(2)	29(1)	39(1)	33(1)	2(1)	17(1)	6(1)
C(3)	18(1)	36(1)	21(1)	-1(1)	7(1)	-2(1)
C(4)	21(1)	41(1)	24(1)	4(1)	11(1)	-2(1)
C(5)	30(1)	55(2)	43(2)	22(1)	13(1)	5(1)
C(6)	32(1)	62(2)	23(1)	-6(1)	10(1)	-13(1)
C(7)	27(1)	32(1)	24(1)	4(1)	11(1)	1(1)
C(8)	48(2)	62(2)	49(2)	-22(1)	29(1)	-15(1)
C(9)	27(1)	39(1)	25(1)	-7(1)	7(1)	1(1)
C(10)	52(2)	32(2)	129(3)	-18(2)	-31(2)	5(2)
C(11)	23(1)	52(2)	23(1)	-1(1)	9(1)	-4(1)
C(12)	43(2)	60(2)	33(1)	16(1)	0(1)	-21(1)
C(13)	33(2)	148(4)	24(1)	-3(2)	11(1)	19(2)
C(14)	19(1)	35(1)	24(1)	-4(1)	9(1)	-5(1)
C(15)	30(1)	43(2)	32(1)	-5(1)	12(1)	10(1)
C(16)	28(1)	35(1)	28(1)	4(1)	9(1)	7(1)
C(17)	28(1)	33(1)	24(1)	1(1)	9(1)	-3(1)
C(18)	23(1)	36(1)	36(1)	1(1)	8(1)	-7(1)
C(19)	22(1)	24(1)	34(1)	-1(1)	13(1)	-1(1)
C(20)	22(1)	25(1)	38(1)	7(1)	16(1)	2(1)
C(21)	44(1)	23(1)	68(2)	-5(1)	37(1)	-2(1)
C(22)	30(1)	50(2)	54(2)	26(1)	20(1)	13(1)
C(23)	24(1)	22(1)	29(1)	5(1)	10(1)	2(1)
C(24)	31(1)	33(1)	38(1)	-4(1)	13(1)	-4(1)
C(25)	25(1)	20(1)	39(1)	-5(1)	14(1)	-4(1)
C(26)	38(1)	41(2)	39(1)	-2(1)	12(1)	9(1)
C(27)	26(1)	24(1)	51(2)	-2(1)	21(1)	0(1)
C(28)	30(1)	26(1)	95(2)	-6(1)	25(1)	-4(1)
C(29)	58(2)	30(1)	57(2)	7(1)	40(2)	10(1)
C(30)	25(1)	26(1)	36(1)	-3(1)	14(1)	0(1)
C(31)	31(1)	28(1)	68(2)	-9(1)	-7(1)	0(1)
C(32)	31(1)	29(1)	50(2)	-1(1)	-3(1)	5(1)
N(1)	24(1)	26(1)	23(1)	2(1)	9(1)	-3(1)
N(2)	22(1)	28(1)	23(1)	3(1)	11(1)	1(1)
N(3)	22(1)	45(1)	26(1)	-1(1)	9(1)	-4(1)
N(4)	24(1)	43(1)	26(1)	2(1)	11(1)	-3(1)
N(5)	23(1)	30(1)	24(1)	5(1)	9(1)	5(1)
N(6)	22(1)	30(1)	21(1)	4(1)	7(1)	2(1)
N(7)	26(1)	25(1)	26(1)	3(1)	12(1)	-1(1)
N(8)	23(1)	24(1)	28(1)	3(1)	10(1)	-1(1)
N(9)	24(1)	24(1)	39(1)	1(1)	16(1)	2(1)
N(10)	25(1)	23(1)	41(1)	-1(1)	18(1)	-3(1)
N(11)	24(1)	23(1)	31(1)	3(1)	9(1)	0(1)
N(12)	23(1)	22(1)	31(1)	1(1)	10(1)	0(1)
Co(1)	20(1)	23(1)	21(1)	2(1)	10(1)	-1(1)
Cl(1)	23(1)	30(1)	31(1)	6(1)	11(1)	6(1)
Cl(2)	22(1)	33(1)	27(1)	6(1)	7(1)	3(1)

Table 5. Hydrogen coordinates (x 10^4) and isotropic displacement parameters (A^2x 10^3) for kjc0510.

	x	y	z	U(eq)
H(1)	3784	2869	3382	34
H(2)	4522	3342	2206	39
H(5A)	2323	5136	712	63
H(5B)	3020	5771	499	63
H(5C)	2873	5737	1495	63
H(6A)	4300	3970	654	58
H(6B)	3889	4698	-11	58
H(6C)	3196	4056	196	58
H(8A)	5322	5725	2990	75
H(8B)	4223	5629	2831	75
H(8C)	4606	6341	2356	75
H(10A)	6509	4246	2619	125
H(10B)	7441	4170	2320	125
H(10C)	6441	4145	1559	125
H(12A)	7286	6770	2557	72
H(12B)	7373	6654	1545	72
H(12C)	8290	6801	2391	72
H(13A)	9050	5550	2083	102
H(13B)	8173	5455	1183	102
H(13C)	8457	4750	1910	102
H(15)	9215	4612	3614	41
H(16)	9270	4748	5268	36
H(17)	85	3488	2609	34
H(18)	-875	2530	3188	38
H(21A)	-824	1132	3919	61
H(21B)	-446	639	4850	61
H(21C)	191	737	4182	61
H(22A)	1513	1312	5441	64
H(22B)	909	1166	6131	64
H(22C)	1317	2025	6045	64
H(24A)	-738	3330	5574	51
H(24B)	343	3113	5774	51
H(24C)	-193	2875	6498	51
H(26A)	-2281	3128	4119	59
H(26B)	-3357	2877	3855	59
H(26C)	-2576	2231	3866	59
H(28A)	-4771	2555	5342	73
H(28B)	-4159	1800	5263	73
H(28C)	-4445	2429	4444	73
H(29A)	-2515	3022	6897	65
H(29B)	-2959	2157	6759	65
H(29C)	-3587	2898	6845	65
H(31)	-4794	3893	4329	57
H(32)	-4337	5321	4520	48
H(2A)	2514	4778	2304	28
H(5)	7428	6214	3861	31
H(8)	1693	2547	4823	29
H(11)	-2380	4124	6200	31

Complex 5c

Table 1. Crystal data and structure refinement

Identification code	kjc0512
Empirical formula	C32 H48 Cl2 N12 Ni
Formula weight	730.43
Temperature	150(2) K
Wavelength	0.71073 Å
Crystal system	Monoclinic
Space group	P 21/c

Unit cell dimensions

$a = 14.9750(5)$ Å   alpha $= 90°$.
$b = 16.9410(6)$ Å   beta $= 107.2860(10)°$.
$c = 15.2480(7)$ Å $\sqcup = 90°$.

Volume	3693.6(2) Å^3
Z	4
Density (calculated)	1.314 Mg/m^3
Absorption coefficient	0.710 mm^{-1}
F(000)	1544
Crystal size	0.15 x 0.15 x 0.10 mm^3
Theta range for data collection	3.56 to 26.37°.
Index ranges	-18<=h<=17, -21<=k<=21, -19<=l<=19
Reflections collected	31126
Independent reflections	7489 [R(int) = 0.1049]
Completeness to theta = 26.37°	99.1 %
Absorption correction	Semi-empirical from equivalents
Max. and min. transmission	0.9324 and 0.9009
Refinement method	Full-matrix least-squares on F^2
Data / restraints / parameters	7489 / 0 / 436
Goodness-of-fit on F^2	1.043
Final R indices [I>2sigma(I)]	R1 = 0.0712, wR2 = 0.1227
R indices (all data)	R1 = 0.1238, wR2 = 0.1396
Largest diff. peak and hole	0.480 and -0.411 e.Å^{-3}

Table 2. Atomic coordinates (x 10^4) and equivalent isotropic displacement parameters (A^2x 10^3) for kjc0512. U(eq) is defined as one third of the trace of the orthogonalized U^{ij} tensor.

	x	y	z	U(eq)
C(1)	3559(3)	3325(2)	3017(3)	30(1)
C(2)	3966(3)	3569(3)	2352(3)	35(1)
C(3)	3538(3)	4263(2)	2004(3)	28(1)
C(4)	3697(3)	4819(3)	1286(3)	33(1)
C(5)	2890(3)	5417(3)	966(3)	45(1)
C(6)	3762(3)	4334(3)	464(3)	42(1)
C(7)	4607(3)	5277(2)	1721(3)	30(1)
C(8)	4683(4)	5793(3)	2537(4)	54(1)
C(9)	6812(3)	5212(3)	2059(3)	34(1)
C(10)	6758(4)	4358(3)	2205(5)	92(3)
C(11)	7769(3)	5620(3)	2357(3)	38(1)
C(12)	7687(3)	6506(3)	2181(3)	55(2)
C(13)	8397(3)	5245(4)	1833(4)	77(2)
C(14)	8192(3)	5451(2)	3372(3)	29(1)
C(15)	8854(3)	4938(3)	3865(3)	38(1)
C(16)	8879(3)	5032(3)	4778(3)	32(1)
C(17)	363(3)	3183(3)	3141(3)	31(1)
C(18)	-186(3)	2642(3)	3439(3)	35(1)
C(19)	388(3)	2329(2)	4249(3)	30(1)
C(20)	181(3)	1757(2)	4923(3)	32(1)
C(21)	-238(3)	1000(3)	4408(4)	46(1)
C(22)	1067(3)	1549(3)	5704(4)	49(1)
C(23)	-516(3)	2165(2)	5333(3)	30(1)
C(24)	-249(3)	2939(3)	5819(3)	38(1)
C(25)	-2603(3)	2537(2)	5114(3)	31(1)
C(26)	-2706(3)	2710(3)	4118(3)	42(1)
C(27)	-3377(3)	2821(2)	5513(3)	34(1)
C(28)	-4271(3)	2354(3)	5052(4)	55(2)
C(29)	-3098(3)	2700(3)	6553(4)	48(1)
C(30)	-3544(3)	3688(2)	5304(3)	33(1)
C(31)	-4251(3)	4106(3)	4714(4)	49(1)
C(32)	-3991(3)	4901(3)	4837(3)	42(1)
N(1)	2908(2)	3833(2)	3080(2)	25(1)
N(2)	2904(2)	4398(2)	2451(2)	28(1)
N(3)	5258(2)	5185(2)	1349(2)	36(1)
N(4)	6088(2)	5631(2)	1713(2)	37(1)
N(5)	7858(2)	5819(2)	3997(2)	28(1)
N(6)	8276(2)	5573(2)	4864(2)	25(1)
N(7)	1226(2)	3210(2)	3722(2)	27(1)
N(8)	1222(2)	2682(2)	4379(2)	28(1)
N(9)	-1292(2)	1823(2)	5227(3)	32(1)
N(10)	-1921(2)	2158(2)	5645(3)	31(1)
N(11)	-2914(2)	4234(2)	5739(2)	30(1)
N(12)	-3177(2)	4975(2)	5468(2)	26(1)
Ni(1)	2251(1)	4086(1)	4071(1)	23(1)
Cl(1)	3297(1)	3147(1)	5147(1)	31(1)
Cl(2)	1195(1)	5012(1)	2970(1)	31(1)

Table 3. Bond lengths [Å] and angles [°] for kjc0512.

C(1)-N(1)	1.325(5)
C(1)-C(2)	1.392(6)

C(1)-H(1)	0.9500
C(2)-C(3)	1.370(6)
C(2)-H(2)	0.9500
C(3)-N(2)	1.342(5)
C(3)-C(4)	1.516(6)
C(4)-C(6)	1.526(6)
C(4)-C(7)	1.536(6)
C(4)-C(5)	1.541(6)
C(5)-H(5A)	0.9800
C(5)-H(5B)	0.9800
C(5)-H(5C)	0.9800
C(6)-H(6A)	0.9800
C(6)-H(6B)	0.9800
C(6)-H(6C)	0.9800
C(7)-N(3)	1.274(5)
C(7)-C(8)	1.498(6)
C(8)-H(8A)	0.9800
C(8)-H(8B)	0.9800
C(8)-H(8C)	0.9800
C(9)-N(4)	1.271(5)
C(9)-C(10)	1.470(7)
C(9)-C(11)	1.533(6)
C(10)-H(10A)	0.9800
C(10)-H(10B)	0.9800
C(10)-H(10C)	0.9800
C(11)-C(14)	1.516(6)
C(11)-C(12)	1.522(7)
C(11)-C(13)	1.542(6)
C(12)-H(12A)	0.9800
C(12)-H(12B)	0.9800
C(12)-H(12C)	0.9800
C(13)-H(13A)	0.9800
C(13)-H(13B)	0.9800
C(13)-H(13C)	0.9800
C(14)-N(5)	1.353(5)
C(14)-C(15)	1.363(6)
C(15)-C(16)	1.391(6)
C(15)-H(15)	0.9500
C(16)-N(6)	1.319(5)
C(16)-H(16)	0.9500
C(17)-N(7)	1.333(5)
C(17)-C(18)	1.393(6)
C(17)-H(17)	0.9500
C(18)-C(19)	1.384(6)
C(18)-H(16)	0.9500
C(19)-N(8)	1.345(5)
C(19)-C(20)	1.510(6)
C(20)-C(23)	1.531(6)
C(20)-C(21)	1.537(6)
C(20)-C(22)	1.537(6)
C(21)-H(21A)	0.9800
C(21)-H(21B)	0.9800
C(21)-H(21C)	0.9800
C(22)-H(22A)	0.9800
C(22)-H(22B)	0.9800
C(22)-H(22C)	0.9800

C(23)-N(9)	1.265(5)
C(23)-C(24)	1.502(6)
C(24)-H(24A)	0.9800
C(24)-H(24B)	0.9800
C(24)-H(24C)	0.9800
C(25)-N(10)	1.273(5)
C(25)-C(26)	1.509(6)
C(25)-C(27)	1.538(6)
C(26)-H(26A)	0.9800
C(26)-H(26B)	0.9800
C(26)-H(26C)	0.9800
C(27)-C(30)	1.507(6)

C(27)-C(29)	1.530(7)	H(6A)-C(6)-H(6B)	109.5
C(27)-C(28)	1.535(6)	C(4)-C(6)-H(6C)	109.5
C(28)-H(28A)	0.9800	H(6A)-C(6)-H(6C)	109.5
C(28)-H(28B)	0.9800	H(6B)-C(6)-H(6C)	109.5
C(28)-H(28C)	0.9800	N(3)-C(7)-C(8)	124.2(4)
C(29)-H(29A)	0.9800	N(3)-C(7)-C(4)	116.4(4)
C(29)-H(29B)	0.9800	C(8)-C(7)-C(4)	119.4(4)
C(29)-H(29C)	0.9800	C(7)-C(8)-H(8A)	109.5
C(30)-N(11)	1.347(5)	C(7)-C(8)-H(8B)	109.5
C(30)-C(31)	1.366(6)	H(8A)-C(8)-H(8B)	109.5
C(31)-C(32)	1.399(6)	C(7)-C(8)-H(8C)	109.5
C(31)-H(31)	0.9500	H(8A)-C(8)-H(8C)	109.5
C(32)-N(12)	1.315(5)	H(8B)-C(8)-H(8C)	109.5
C(32)-H(32)	0.9500	N(4)-C(9)-C(10)	122.2(4)
N(1)-N(2)	1.354(4)	N(4)-C(9)-C(11)	118.6(4)
N(1)-Ni(1)	2.078(3)	C(10)-C(9)-C(11)	119.2(4)
N(2)-H(2A)	0.8800	C(9)-C(10)-H(10A)	109.5
N(3)-N(4)	1.419(5)	C(9)-C(10)-H(10B)	109.5
N(5)-N(6)	1.349(4)	H(10A)-C(10)-H(10B)	109.5
N(5)-H(5)	0.8800	C(9)-C(10)-H(10C)	109.5
N(6)-Ni(1)	2.088(3)	H(10A)-C(10)-H(10C)	109.5
N(7)-N(8)	1.344(4)	H(10B)-C(10)-H(10C)	109.5
N(7)-Ni(1)	2.087(3)	C(14)-C(11)-C(12)	110.8(4)
N(8)-H(8)	0.8800	C(14)-C(11)-C(9)	106.7(4)
N(9)-N(10)	1.403(5)	C(12)-C(11)-C(9)	111.9(4)
N(11)-N(12)	1.343(4)	C(14)-C(11)-C(13)	108.4(4)
N(11)-H(11)	0.8800	C(12)-C(11)-C(13)	110.1(4)
N(12)-Ni(1)	2.090(3)	C(9)-C(11)-C(13)	108.7(4)
Ni(1)-N(6)	2.088(3)	C(11)-C(12)-H(12A)	109.5
Ni(1)-N(12)	2.090(3)	C(11)-C(12)-H(12B)	109.5
Ni(1)-Cl(1)	2.4798(11)	H(12A)-C(12)-H(12B)	109.5
Ni(1)-Cl(2)	2.4900(11)	C(11)-C(12)-H(12C)	109.5
		H(12A)-C(12)-H(12C)	109.5
N(1)-C(1)-C(2)	110.6(4)	H(12B)-C(12)-H(12C)	109.5
N(1)-C(1)-H(1)	124.7	C(11)-C(13)-H(13A)	109.5
C(2)-C(1)-H(1)	124.7	C(11)-C(13)-H(13B)	109.5
C(3)-C(2)-C(1)	106.3(4)	H(13A)-C(13)-H(13B)	109.5
C(3)-C(2)-H(2)	126.8	C(11)-C(13)-H(13C)	109.5
C(1)-C(2)-H(2)	126.8	H(13A)-C(13)-H(13C)	109.5
N(2)-C(3)-C(2)	105.6(4)	H(13B)-C(13)-H(13C)	109.5
N(2)-C(3)-C(4)	123.2(4)	N(5)-C(14)-C(15)	105.4(4)
C(2)-C(3)-C(4)	131.1(4)	N(5)-C(14)-C(11)	120.1(4)
C(3)-C(4)-C(6)	108.7(4)	C(15)-C(14)-C(11)	134.3(4)
C(3)-C(4)-C(7)	108.2(3)	C(14)-C(15)-C(16)	106.1(4)
C(6)-C(4)-C(7)	111.2(3)	C(14)-C(15)-H(15)	126.9
C(3)-C(4)-C(5)	111.1(3)	C(16)-C(15)-H(15)	126.9
C(6)-C(4)-C(5)	109.1(4)	N(6)-C(16)-C(15)	111.3(4)
C(7)-C(4)-C(5)	108.5(4)	N(6)-C(16)-H(16)	124.4
C(4)-C(5)-H(5A)	109.5	C(15)-C(16)-H(16)	124.4
C(4)-C(5)-H(5B)	109.5	N(7)-C(17)-C(18)	110.9(4)
H(5A)-C(5)-H(5B)	109.5	N(7)-C(17)-H(17)	124.6
C(4)-C(5)-H(5C)	109.5	C(18)-C(17)-H(17)	124.6
H(5A)-C(5)-H(5C)	109.5	C(19)-C(18)-C(17)	105.8(4)
H(5B)-C(5)-H(5C)	109.5	C(19)-C(18)-H(16)	127.1
C(4)-C(6)-H(6A)	109.5	C(17)-C(18)-H(16)	127.1
C(4)-C(6)-H(6B)	109.5	N(8)-C(19)-C(18)	105.3(4)

N(8)-C(19)-C(20)	123.6(4)	N(11)-C(30)-C(31)	105.1(4)
C(18)-C(19)-C(20)	131.0(4)	N(11)-C(30)-C(27)	121.2(4)
C(19)-C(20)-C(23)	106.9(3)	C(31)-C(30)-C(27)	133.7(4)
C(19)-C(20)-C(21)	108.8(4)	C(30)-C(31)-C(32)	106.3(4)
C(23)-C(20)-C(21)	111.1(3)	C(30)-C(31)-H(31)	126.8
C(19)-C(20)-C(22)	111.7(3)	C(32)-C(31)-H(31)	126.8
C(23)-C(20)-C(22)	108.9(4)	N(12)-C(32)-C(31)	110.5(4)
C(21)-C(20)-C(22)	109.4(4)	N(12)-C(32)-H(32)	124.8
C(20)-C(21)-H(21A)	109.5	C(31)-C(32)-H(32)	124.8
C(20)-C(21)-H(21B)	109.5	C(1)-N(1)-N(2)	104.8(3)
H(21A)-C(21)-H(21B)	109.5	C(1)-N(1)-Ni(1)	134.8(3)
C(20)-C(21)-H(21C)	109.5	N(2)-N(1)-Ni(1)	117.8(2)
H(21A)-C(21)-H(21C)	109.5	C(3)-N(2)-N(1)	112.6(3)
H(21B)-C(21)-H(21C)	109.5	C(3)-N(2)-H(2A)	123.7
C(20)-C(22)-H(22A)	109.5	N(1)-N(2)-H(2A)	123.7
C(20)-C(22)-H(22B)	109.5	C(7)-N(3)-N(4)	117.3(4)
H(22A)-C(22)-H(22B)	109.5	C(9)-N(4)-N(3)	113.9(4)
C(20)-C(22)-H(22C)	109.5	N(6)-N(5)-C(14)	112.7(3)
H(22A)-C(22)-H(22C)	109.5	N(6)-N(5)-H(5)	123.7
H(22B)-C(22)-H(22C)	109.5	C(14)-N(5)-H(5)	123.7
N(9)-C(23)-C(24)	124.2(4)	C(16)-N(6)-N(5)	104.5(3)
N(9)-C(23)-C(20)	117.0(4)	C(16)-N(6)-Ni(1)	134.2(3)
C(24)-C(23)-C(20)	118.8(3)	N(5)-N(6)-Ni(1)	120.2(2)
C(23)-C(24)-H(24A)	109.5	C(17)-N(7)-N(8)	104.7(3)
C(23)-C(24)-H(24B)	109.5	C(17)-N(7)-Ni(1)	133.5(3)
H(24A)-C(24)-H(24B)	109.5	N(8)-N(7)-Ni(1)	116.7(2)
C(23)-C(24)-H(24C)	109.5	N(7)-N(8)-C(19)	113.4(3)
H(24A)-C(24)-H(24C)	109.5	N(7)-N(8)-H(8)	123.3
H(24B)-C(24)-H(24C)	109.5	C(19)-N(8)-H(8)	123.3
N(10)-C(25)-C(26)	124.1(4)	C(23)-N(9)-N(10)	118.2(4)
N(10)-C(25)-C(27)	117.6(4)	C(25)-N(10)-N(9)	115.8(4)
C(26)-C(25)-C(27)	118.3(4)	N(12)-N(11)-C(30)	113.0(3)
C(25)-C(26)-H(26A)	109.5	N(12)-N(11)-H(11)	123.5
C(25)-C(26)-H(26B)	109.5	C(30)-N(11)-H(11)	123.5
H(26A)-C(26)-H(26B)	109.5	C(32)-N(12)-N(11)	105.1(3)
C(25)-C(26)-H(26C)	109.5	C(32)-N(12)-Ni(1)	134.1(3)
H(26A)-C(26)-H(26C)	109.5	N(11)-N(12)-Ni(1)	120.2(2)
H(26B)-C(26)-H(26C)	109.5	N(1)-Ni(1)-N(7)	98.00(13)
C(30)-C(27)-C(29)	109.1(4)	N(1)-Ni(1)-N(6)	173.31(13)
C(30)-C(27)-C(28)	109.9(4)	N(7)-Ni(1)-N(6)	88.57(13)
C(29)-C(27)-C(28)	109.7(4)	N(1)-Ni(1)-N(12)	89.52(12)
C(30)-C(27)-C(25)	108.6(3)	N(7)-Ni(1)-N(12)	172.34(13)
C(29)-C(27)-C(25)	111.2(4)	N(6)-Ni(1)-N(12)	83.95(13)
C(28)-C(27)-C(25)	108.4(4)	N(1)-Ni(1)-Cl(1)	90.37(9)
C(27)-C(28)-H(28A)	109.5	N(7)-Ni(1)-Cl(1)	89.10(10)
C(27)-C(28)-H(28B)	109.5	N(6)-Ni(1)-Cl(1)	88.46(9)
H(28A)-C(28)-H(28B)	109.5	N(12)-Ni(1)-Cl(1)	92.31(9)
C(27)-C(28)-H(28C)	109.5	N(1)-Ni(1)-Cl(2)	89.02(10)
H(28A)-C(28)-H(28C)	109.5	N(7)-Ni(1)-Cl(2)	90.23(10)
H(28B)-C(28)-H(28C)	109.5	N(6)-Ni(1)-Cl(2)	92.23(9)
C(27)-C(29)-H(29A)	109.5	N(12)-Ni(1)-Cl(2)	88.44(9)
C(27)-C(29)-H(29B)	109.5	Cl(1)-Ni(1)-Cl(2)	179.03(4)
H(29A)-C(29)-H(29B)	109.5		
C(27)-C(29)-H(29C)	109.5		
H(29A)-C(29)-H(29C)	109.5	Symmetry transformations used to generate	
H(29B)-C(29)-H(29C)	109.5	equivalent atoms:	

#1 -x+1,-y+1,-z+1   #2 -x,-y+1,-z+1

Table 4.   Anisotropic displacement parameters (Å^2x 10^3)for kjc0512. The anisotropic displacement factor exponent takes the form: $-2\square^2[\ h^2a^{*2}U^{11} + ... + 2\ h\ k\ a^*\ b^*\ U^{12}\ ]$

	U^{11}	U^{22}	U^{33}	U^{23}	U^{13}	U^{12}
C(1)	30(2)	29(2)	33(3)	-1(2)	11(2)	3(2)
C(2)	33(2)	44(3)	35(3)	1(2)	18(2)	5(2)
C(3)	23(2)	39(3)	22(2)	-2(2)	8(2)	-2(2)
C(4)	26(2)	48(3)	29(3)	6(2)	14(2)	-2(2)
C(5)	30(3)	58(3)	49(3)	18(3)	15(2)	1(2)
C(6)	36(3)	65(3)	28(3)	-3(2)	13(2)	-11(2)
C(7)	30(2)	34(2)	28(2)	6(2)	13(2)	1(2)
C(8)	50(3)	68(4)	51(3)	-19(3)	28(3)	-11(3)
C(9)	28(2)	47(3)	26(2)	-9(2)	9(2)	6(2)
C(10)	55(4)	40(3)	143(7)	-17(4)	-28(4)	3(3)
C(11)	26(2)	64(3)	24(2)	-5(2)	10(2)	-3(2)
C(12)	50(3)	74(4)	37(3)	18(3)	5(2)	-24(3)
C(13)	33(3)	173(7)	27(3)	-3(4)	12(2)	22(4)
C(14)	22(2)	38(3)	29(2)	-7(2)	11(2)	-7(2)
C(15)	31(2)	44(3)	39(3)	-8(2)	12(2)	10(2)
C(16)	26(2)	41(3)	29(3)	6(2)	10(2)	5(2)
C(17)	27(2)	38(3)	26(2)	-1(2)	8(2)	-2(2)
C(18)	23(2)	41(3)	38(3)	-1(2)	6(2)	-6(2)
C(19)	27(2)	26(2)	43(3)	-4(2)	19(2)	-1(2)
C(20)	27(2)	26(2)	48(3)	7(2)	19(2)	2(2)
C(21)	52(3)	29(3)	76(4)	3(2)	46(3)	2(2)
C(22)	33(3)	52(3)	65(4)	22(3)	22(2)	14(2)
C(23)	30(2)	27(2)	34(3)	6(2)	12(2)	2(2)
C(24)	31(2)	39(3)	45(3)	-1(2)	12(2)	-3(2)
C(25)	29(2)	18(2)	49(3)	-5(2)	17(2)	-5(2)
C(26)	41(3)	43(3)	44(3)	-3(2)	15(2)	7(2)
C(27)	26(2)	30(2)	50(3)	0(2)	19(2)	2(2)
C(28)	32(3)	28(3)	113(5)	-10(3)	34(3)	-2(2)
C(29)	61(3)	31(3)	69(4)	11(2)	44(3)	12(2)
C(30)	27(2)	31(2)	48(3)	-4(2)	20(2)	-1(2)
C(31)	32(3)	34(3)	69(4)	-10(3)	-3(2)	-1(2)
C(32)	29(3)	31(3)	56(3)	-1(2)	-2(2)	1(2)
N(1)	25(2)	28(2)	26(2)	-1(2)	13(2)	-4(2)
N(2)	27(2)	30(2)	30(2)	4(2)	12(2)	3(2)
N(3)	27(2)	51(2)	31(2)	-1(2)	10(2)	-2(2)
N(4)	29(2)	50(2)	32(2)	2(2)	10(2)	-6(2)
N(5)	26(2)	34(2)	24(2)	5(2)	8(2)	4(2)
N(6)	26(2)	26(2)	25(2)	3(2)	11(2)	2(2)
N(7)	29(2)	26(2)	29(2)	-2(2)	13(2)	-5(2)
N(8)	25(2)	28(2)	33(2)	3(2)	11(2)	-1(2)
N(9)	27(2)	27(2)	47(2)	2(2)	19(2)	2(2)
N(10)	28(2)	25(2)	47(2)	1(2)	20(2)	0(2)
N(11)	25(2)	23(2)	41(2)	4(2)	10(2)	0(2)
N(12)	22(2)	24(2)	35(2)	0(2)	12(2)	-1(1)
Ni(1)	21(1)	26(1)	25(1)	2(1)	11(1)	-1(1)
Cl(1)	26(1)	33(1)	35(1)	5(1)	12(1)	5(1)
Cl(2)	24(1)	38(1)	31(1)	6(1)	9(1)	3(1)

Table 5. Hydrogen coordinates (x 10^4) and isotropic displacement parameters (Å^2x 10^3) for kjc0512.

	x	y	z	U(eq)
H(1)	3725	2859	3376	36
H(2)	4446	3306	2176	42
H(5A)	2300	5133	707	67
H(5B)	3005	5763	496	67
H(5C)	2851	5735	1490	67
H(6A)	4254	3936	669	63
H(6B)	3910	4683	14	63
H(6C)	3162	4072	180	63
H(8A)	5322	5769	2954	80
H(8B)	4244	5609	2859	80
H(8C)	4533	6339	2334	80
H(10A)	6458	4263	2685	137
H(10B)	7390	4135	2395	137
H(10C)	6390	4108	1632	137
H(12A)	7330	6745	2556	83
H(12B)	7367	6602	1530	83
H(12C)	8314	6739	2344	83
H(13A)	9028	5469	2057	116
H(13B)	8136	5354	1175	116
H(13C)	8427	4673	1934	116
H(15)	9223	4587	3632	45
H(16)	9278	4744	5276	38
H(17)	151	3490	2598	37
H(16)	-823	2515	3146	41
H(21A)	-789	1134	3896	70
H(21B)	-420	642	4830	70
H(21C)	229	742	4171	70
H(22A)	1526	1304	5446	73
H(22B)	907	1180	6129	73
H(22C)	1333	2031	6035	73
H(24A)	-739	3330	5559	57
H(24B)	344	3122	5741	57
H(24C)	-178	2872	6475	57
H(26A)	-2268	3128	4078	63
H(26B)	-3347	2882	3809	63
H(26C)	-2569	2231	3820	63
H(28A)	-4783	2550	5270	83
H(28B)	-4166	1793	5208	83
H(28C)	-4436	2419	4384	83
H(29A)	-2530	3003	6845	72
H(29B)	-2980	2139	6694	72
H(29C)	-3605	2881	6787	72
H(31)	-4808	3899	4303	59
H(32)	-4352	5328	4510	50
H(2A)	2528	4809	2347	34
H(5)	7416	6181	3854	33
H(8)	1715	2577	4847	34
H(11)	-2384	4118	6158	36

232